

The Impact of Tumor Necrosis Factor on Osteogenic Differentiation of Human Adipose Tissue-Derived Stem Cells *In Vitro*

Dissertation

zur

Erlangung des akademischen Grades
doctor rerum naturalium (Dr. rer. nat.)
der Mathematisch-Naturwissenschaftlichen Fakultät
der Universität Rostock

vorgelegt von

Achim Salamon, geb. am 26.07.1979 in Berlin-Neukölln,
aus Rostock

Rostock, den 02.03.2012

Universität
Rostock



Traditio et Innovatio



Erstgutachter: Prof. Dr. rer. nat. Dieter G. Weiss
Universität Rostock
Mathematisch-Naturwissenschaftliche Fakultät
Institut für Biowissenschaften
Abteilung Tierphysiologie
Albert-Einstein-Straße 3
18059 Rostock
0381/498-6300
dieter.weiss@uni-rostock.de

Zweitgutachter: PD Dr. rer. nat. et med. habil. Kirsten Peters
Universitätsmedizin Rostock
Arbeitsbereich Zellbiologie
Schillingallee 69
18057 Rostock
0381/494-7757
kirsten.peters@med.uni-rostock.de

Einreichung der Dissertation: 02.03.2012

Eingang der Gutachten: 08.06.2012

Wissenschaftliches Kolloquium: 19.11.2012

Contents

Abbreviations	IV
Zusammenfassung	X
Abstract	XII
1 Introduction	1
1.1 Aim and Motivation	1
1.2 Adipose Tissue-Derived Stem Cells	1
1.2.1 Biological Niche of ASC	1
1.2.2 Differentiation Capabilities of ASC	2
1.2.3 ASC Isolation	3
1.2.4 ASC Culture	4
1.2.5 Summary on ASC <i>in vitro</i>	4
1.3 TNF, its Receptors and Signal Transduction Pathways	4
1.3.1 TNF	4
1.3.2 TNF Receptors and Signaling Pathways	5
1.4 Osteogenic Differentiation <i>in vitro</i>	7
1.4.1 Osteogenic Differentiation Markers <i>in vitro</i>	7
1.4.2 Bone Remodeling	10
1.4.3 Induction of Osteogenic Differentiation <i>in vitro</i>	12
1.5 Experimental Outline	18
2 Materials	20
3 Methods	27
3.1 Isolation and Culture of ASC	27
3.1.1 Isolation of ASC	27
3.1.2 ASC Culture	28
3.1.3 ASC Counting	29
3.1.4 ASC Stimulation Media	29
3.2 <i>In vitro</i> Assays	31
3.2.1 Quantification of Cell Number	31
3.2.2 Quantification of Cellular Metabolic Activity	32
3.2.3 Quantification of RUNX2 DNA-Binding Activity	32
3.2.4 Staining of Active Alkaline Phosphatase for Microscopy	34
3.2.5 Quantification of Alkaline Phosphatase Activity	36

3.2.6	Quantification of Extracellular Matrix Calcium Content	36
3.2.7	Quantification of Secreted Osteoprotegerin	37
3.2.8	Quantification of Cellular Lipid Content	37
3.3	Real-Time RT-PCR	38
3.3.1	RNA Isolation	38
3.3.2	RNA Quantification	38
3.3.3	RNA Electrophoresis	39
3.3.4	Reverse Transcription	39
3.3.5	Real-Time RT PCR	40
3.3.6	Analysis of Real-Time PCR Data	42
3.4	Conventional and Confocal Fluorescence Microscopy	45
3.4.1	Immunofluorescence Staining	45
3.4.2	The Live-Dead Assay	47
3.5	Flow Cytometry	47
3.5.1	Quantification of Cell Surface Antigens	47
3.5.2	Cell Cycle Analysis	48
3.6	Data Analysis and Statistics	50
3.6.1	Data Normalization	50
3.6.2	Data Illustration	51
3.6.3	Statistics	51
4	Results	52
4.1	Expression of TNF Receptors by ASC	52
4.2	Impact of TNF on NF κ B Signaling Pathway Activation in ASC	52
4.3	Impact of TNF on MAPK Signaling Pathway Activation in ASC	54
4.3.1	Analysis of p38 Activation	54
4.3.2	Analysis of AP1 Activation	55
4.3.3	Analysis of ERK Activation	56
4.4	Impact of TNF on ASC Cytoskeletal Organization and Viability	58
4.5	Impact of TNF on ASC Proliferation, Cell Cycle and Metabolic Activity	59
4.5.1	Analysis of Proliferation and Cell Cycle	59
4.5.2	Analysis of Metabolic Activity	60
4.6	Impact of TNF on Osteogenic Differentiation of ASC	61
4.6.1	Analysis of Osteogenic Transcription Factors	61
4.6.2	Analysis of Alkaline Phosphatase Activity	63
4.6.3	Analysis of Extracellular Matrix Calcium Content	65
4.7	Impact of the TNF Concentration on Osteogenic Differentiation of ASC	66
4.8	Impact of the Seeding Density on Osteogenic Differentiation of ASC	67
4.9	Impact of TNF Pre-Treatment on Osteogenic Differentiation of ASC	67
4.10	Impact of Ascorbic Acid and β -Glycerophosphate on Osteogenic Differentiation of TNF-Treated ASC	68
4.11	Impact of TNF on Osteoprotegerin Secretion by ASC	69
4.12	Summary of Results	70

5 Discussion	72
5.1 ASC Express both TNF Receptors	72
5.1.1 TNF Induced the NFκB Pathway in ASC	75
5.1.2 TNF did not Induce the MAPK Pathway in ASC	75
5.1.3 TNF did not Induce Apoptosis in ASC	78
5.2 ASC Proliferation Rate and Cell Cycle	81
5.2.1 TNF Increased ASC Proliferation Rate and Accelerated S Phase Transition .	81
5.2.2 Osteogenic Stimulation Increased ASC Proliferation Rate, but Decelerated S Phase Transition	82
5.2.3 The Role of ZBTB16 in Proliferation and Cell Cycle Regulation	82
5.2.4 The Role of RUNX2 in Proliferation and Cell Cycle Regulation	83
5.2.5 The Role of p38 and AP1 in Proliferation and Cell Cycle Regulation	83
5.2.6 Concluding Remarks on the Regulation of Proliferation and Cell Cycle Progression	84
5.3 The Impact of TNF and Osteogenic Stimulation on ASC Metabolic Activity	85
5.4 Osteogenic Differentiation of ASC <i>in vitro</i>	87
5.4.1 Basal Level Osteogenic Differentiation Occurred in Unstimulated ASC Cul- tures	87
5.4.2 The Impact of TNF on Osteogenic Differentiation of ASC	90
5.5 Summary and Conclusions	98
Bibliography	i
Selbstständigkeitserklärung	xiii
Curriculum Vitae	xiv
Danksagung	xvii

Abbreviations

	Abbreviation	Full Designation
Genes	ADAM17	ADAM metallopeptidase domain 17; formerly: TNF-alpha converting enzyme (TACE)
	ALPL	alkaline phosphatase, liver/bone/kidney
	AKT	v-akt murine thymoma viral oncogene homolog family
	ATF	officially: plasminogen activator, urokinase (PLAU)
	BAX	BCL2-associated X protein
	BCL	B-cell CLL/lymphoma family
	BID	BH3 interacting domain death agonist
	BMP2	bone morphogenetic protein 2
	CAK	CDK-activating kinase family
	CBP	CREB binding protein (officially: CREBBP)
	CDK	cyclin-dependent kinase family
	CFLAR	CASP8 and FADD-like apoptosis regulator
	(c)IAP	(cellular) inhibitor of apoptosis family
	CREB	cAMP responsive element binding protein 1 (officially: CREB1)
	Dkk1	dickkopf 1 homolog (Xenopus laevis)
	EGF	epidermal growth factor
	ERK1	extracellular signal-regulated kinase 1; officially: mitogen-activated protein kinase 3 (MAPK3)
	ERK2	extracellular signal-regulated kinase 2; officially: mitogen-activated protein kinase 1 (MAPK1)
	FAK	focal adhesion kinase family
	FOS	FBJ murine osteosarcoma viral oncogene homolog; formerly: C-FOS or activator protein 1 (AP1)
	FRA2	officially: FOS-like antigen 2 (FOSL2)
	GAPDH	glyceraldehyde-3-phosphate dehydrogenase
	GR	glucocorticoid receptor family
	HAT	histone acetyltransferase family; officially: K(lysine) acetyltransferase (KAT)
	HDAC	histone deacetylase family
	HOX	homeobox gene family
	HSP90	heat shock protein 90 kDa family
	IGF	insulin-like growth factor family
	IκB	nuclear factor of kappa light polypeptide gene enhancer in B-cells inhibitor family
	IKK	inhibitor of κB kinase family; officially: inhibitor of kappa light polypeptide gene enhancer in B-cells kinase (IKBKB)
	IKKK	kinase family upstream of IKK
	IL	interleukin family
	JNK	JUN N-terminal kinase family
	JUN	jun proto-oncogene; formerly: c-Jun or activator protein 1 (AP1)

Abbreviation	Full Designation
M-CSF	macrophage colony-stimulating factor 1 (MCSF); officially: colony stimulating factor 1 (macrophage) (CSF1)
MAPK	mitogen-activated protein kinase family
MEK	MAPK/ERK kinase family; officially: mitogen-activated protein kinase kinase family (MAP2K)
MEKK	MAPK/ERK kinase kinase family; officially: mitogen-activated protein kinase kinase kinase family (MAP3K)
MKK	MAPK/ERK kinase family; officially: mitogen-activated protein kinase kinase family (MAP2K)
Msx2	msh homeobox 2
MYC	v-myc myelocytomatosis viral oncogene homolog (avian)
NANOG	nanog homeobox
NFKB1	nuclear factor of kappa light polypeptide gene enhancer in B-cells 1; formerly: nuclear factor NF-kappa-B p105/p50 subunit (p105, p50)
NFKB2	nuclear factor of kappa light polypeptide gene enhancer in B-cells 2; formerly: nuclear factor NF-kappa-B p100/p52/p49 subunit (p100, p52, p49)
OCN	osteocalcin (OC); officially: bone gamma-carboxyglutamate (gla) protein (BGLAP)
OCT1	octamer-binding transcription factor-1; officially: POU class 2 homeobox 1 (POU2F1)
OPG	osteoprotegerin; officially: tumor necrosis factor receptor superfamily member 11b (TNFRSF11B)
P27KIP1	cyclin-dependent kinase inhibitor 1B (p27, Kip1) (CDKN1B)
p38	p38 MAP kinase; officially: mitogen-activated protein kinase 14 (MAPK14)
PKA	protein kinase A family; officially: protein kinase, cAMP-dependent, catalytic (PRKAC)
PKC	protein kinase C family; officially: PRKC
POU5F1	POU class 5 homeobox 1; formerly: octamer-binding protein 4 (OCT4)
PP1	pyrophosphatase 1; officially: pyrophosphatase (inorganic) 1 (PPA1)
PP2A	protein phosphatase 2A family; officially: protein phosphatase 2, catalytic subunit (PPP2C)
PPARG	peroxisome proliferator-activated receptor gamma
PTH	parathyroid hormone
RAF	RAF proto-oncogene serine/threonine-protein kinase family; officially: v-raf murine sarcoma viral oncogene homolog family
RANK	receptor activator of nuclear factor-kappa B; officially: tumor necrosis factor receptor superfamily member 11a (TNFRSF11A)
RANKL	receptor activator of nuclear factor kappa-B ligand; officially: tumor necrosis factor (ligand) superfamily member 11 (TNFSF11)
RELA	v-rel reticuloendotheliosis viral oncogene homolog A (avian); formerly: nuclear factor NF-kappa-B p65 subunit (p65) or NFKB3
RELB	v-rel reticuloendotheliosis viral oncogene homolog B
RHOA	ras homolog gene family member A
RIP	receptor-interacting protein kinase; officially: receptor (TNFRSF)-interacting serine-threonine kinase 1 (RIPK1)
RNase H	officially: ribonuclease H2 family (RNASEH2)
ROCK	rho-associated, coiled-coil containing protein kinase family

	Abbreviation	Full Designation
	RUNX2	runt-related transcription factor 2; formerly: acute myeloid leukemia 3 protein (AML3) or core-binding factor, runt domain, alpha subunit 1 (CBF-alpha-1)
	Smad	SMA mothers against decapentaplegic family
	Smurf1	SMAD-specific E3 ubiquitin protein ligase 1
	SOST	sclerostin
	STAT	signal transducer and activator of transcription family
	TGFbeta	transforming growth factor beta family
	TNF	tumor necrosis factor; formerly: TNF-alpha or cachectin
	TNFAIP6	tumor necrosis factor alpha-induced protein 6; formerly: tumor necrosis factor-stimulated gene-6 protein (TSG6)
	TNFRSF1A	tumor necrosis factor receptor superfamily member 1A; formerly: TNF receptor 1 (TNFR1)
	TNFRSF1B	tumor necrosis factor receptor superfamily member 1B; formerly: TNF receptor 2 (TNFR2)
	TRADD	TNFRSF1A-associated via death domain
	TRAF2	TNF receptor-associated factor 2
	TRX	thioredoxin (TXN)
	VEGF	vascular endothelial growth factor; officially: VEGFA
	WNT	wingless-type MMTV integration site family
	Wwp1	WW domain containing E3 ubiquitin protein ligase 1
	WWTR1	WW domain containing transcription regulator 1; officially: transcriptional co-activator with PDZ-binding motif (TAZ)
	ZBTB16	zinc finger and BTB domain containing 16; formerly: promyelocytic leukemia zinc finger (PLZF)
Chemicals	AMP	2-amino-2-methyl-1-propanol
	AMPED	2-amino-2-methyl-1,3-propanediol
	Bodipy	boron-dipyrromethene
	Ca	calcium
	CO ₂	carbon dioxide
	ddH ₂ O	double distilled water
	DEPC	diethylpyrocarbonate
	(D)MEM	(Dulbecco's) modified Eagle medium
	(D)PBS	(Dulbecco's) phosphate-buffered saline
	DMSO	dimethyl sulfoxide
	EDTA	ethylenediaminetetraacetic acid
	Fast Red TR	4-chloro-2-methylbenzenediazonium
	Fe ²⁺	ferrous ion
	FITC	fluorescein isothiocyanate
	H ⁺	hydron
	HCl	hydrochloric acid
	HEPES	4-(2-hydroxyethyl)-1-piperazineethanesulfonic acid
	IBMX	3-isobutyl-1-methylxanthine
	Mg	magnesium
	MgCl ₂	magnesium chloride
	MTS	3-(4,5-dimethylthiazol-2-yl)-5-(3-carboxymethoxyphenyl)-2-(4-sulfophenyl)-2H-tetrazolium
	NaCl	sodium chloride
	NaOH	sodium hydroxide
	Naphthol AS-MX phosphate	3-(phosphonoxy)-N-(2,4-xylyl)naphthalene-2-carboxamid
	PE	phycoerythrin
	PES	phenazine ethosulfate
	PFA	paraformaldehyde
	PI	propidium iodide
	PMSF	phenylmethanesulfonylfluorid

	Abbreviation	Full Designation
	pNPP	para-nitrophenyl phosphate
	PVC	polyvinyl chloride
	ROS	radical oxygen species
	TAE	Tris acetate-EDTA
	TBS	Tris-buffered saline
	TCPS	tissue culture polystyrene
	TRIS	tris(hydroxymethyl)aminomethane
	Triton X-100	4-(1,1,3,3-tetramethylbutyl)phenyl-polyethylene glycol
	Tween 20	polyethylene glycol sorbitan monolaurate
Biological Terms	5', 3'	carbon atom positions within a nucleosidic pentose
	A,G,C,T	adenine, guanine, cytosine, thymine
	Ab	antibody
	<i>Ac-Protein</i>	acetylated protein
	AD	activation domain
	ADP	adenosine diphosphate
	ALCL	Anaplastic Large Cell Lymphoma
	AM	acetoxymethylester
	ASC	adipose tissue-derived stem (stromal) cell(s)
	ATP	adenosine-5'-triphosphate
	B cell	lymphocyte formed in the bone marrow
	BSA	bovine serum albumin
	C2C12	myoblast cell line from C3H mice
	CD	cluster of differentiation
	cDNA	complementary DNA
	CHO	epithelial-like ovary cell line from chinese hamster
	D- or L- <i>d-base</i>	spatial configuration of optical isomers deoxyribose-conjugated base (DNA nucleosides)
	DBD	DNA-binding domain
	DNA	deoxyribonucleic acid
	ECM	extracellular matrix
	ESC	embryonic stem cell(s)
	EST	expressed sequence tag
	f-actin	filamentous actin
	FCS	fetal calf serum
	G ₀ , G ₁ and G ₂	gap phases of the cell cycle
	gDNA	genomic DNA
	H+L	heavy and light chain of an immunoglobulin
	HeLa	human cervical adenocarcinoma cell line
	HRP	horseradish peroxidase
	HSC	hematopoietic stem cell(s)
	IgG	immunoglobulin G
	iPS cell	induced pluripotent stem cell
	LAF	liposuction aspirate fluid
	LBD	ligand-binding domain
	MC3T3-E1	pre-osteoblast cell line from calvaria of C57BL/6 mice
	MDSC	muscle-derived stromal cell(s)
	MG-63	human osteosarcoma cell line
	mRNA	messenger RNA
	MSC	mesenchymal stem cell(s)
	NAD(P) ⁺	oxidized form of NAD(P)H
	NAD(P)H	nicotinamide adenine dinucleotide (phosphate) (reduced form)
	<i>P-Protein</i>	phosphorylated form of a protein
	PGE2	prostaglandin E2
	PLA	processed lipoaspirate
	RNA	ribonucleic acid
	RNAi	RNA interference

	Abbreviation	Full Designation
	rRNA	ribosomal RNA
	S	synthesis phase of the cell cycle
	SAOS-2	human osteosarcoma cell line
	SMC	smooth muscle cell(s)
	snRNA	small nuclear RNA
	STRO-1	antibody detecting an antigen expressed on osteogenic precursor cells
	SVF	stromal vascular fraction
	T cell	lymphocyte matured in the thymus
	<i>Taq</i>	<i>Thermus aquaticus</i>
	tRNA	transfer RNA
Technical Terms	ACS	American Chemical Society
	C_t	threshold cycle
	ΔC_t	Delta threshold cycle
	$df(x)/dx$	derivative of f with respect to x
	ΔR_n	background fluorescence-corrected R_n
	ELISA	enzyme-linked immunosorbent assay
	FACS	fluorescence-activated cell sorting
	fwd	forward
	GC	gas chromatography
	HPLC	high-performance liquid chromatography
	ISO	International Organization for Standardization
	LASER	Light Amplification by Stimulated Emission of Radiation
	\LaTeX	Lamport variant of the tau epsilon chi typesetting system
	LB	lysogeny broth (medium)
	NCBI	National Center for Biotechnology Information
	p -value	probability that a statistic test erroneously assumes two datasets to differ significantly
	PCR	polymerase chain reaction
	pH	<i>potentia hydrogenii</i>
	R	reporter signal fluorescence intensity
	rev	reverse
	R_n	normalized reporter signal fluorescence intensity
	RT	reverse transcription
	RT PCR	reverse transcription polymerase chain reaction
	T	variable calculated in the Student's statistics test
	TLC	thin layer chromatography
	TPM	transcripts per million
	U	variable calculated in the Mann-Whitney statistics test
Physical Quantities	l	length
	m	mass
	t	time
	n	amount of substance
	c	concentration
	θ	temperature
	Θ	temperature difference
	V	volume
	U	voltage
	$O.D.$	optical density
	$F.I.$	fluorescence intensity
Physical Units	m	meter
	bp	base pair(s)
	kg	kilogram
	mol	mol

	Abbreviation	Full Designation
	M	molar=mol/l
	g/l	gram per liter
	I.U.	international unit
	%	per cent
	s	second
	min	minute
	h	hour
	d	day
	g	gravitational acceleration of a mass of 1 kg within the earth gravitational field
	°C	degree Celsius
	K	Kelvin
	l	liter
	V	volt
	rpm	rounds per minute
Unit Prefixes	c	centi (10 ⁻²)
	m	milli (10 ⁻³)
	μ	micro (10 ⁻⁶)
	n	nano (10 ⁻⁹)
	p	pico (10 ⁻¹²)
Latin Terms	<i>et al.</i>	<i>et alii</i>
	<i>e.g.</i>	<i>exempli gratia</i>
	<i>i.e.</i>	<i>id est</i>
Greek Terms	α	<i>alpha</i>
	β	<i>beta</i>
	γ	<i>gamma</i>
	δ	<i>delta</i>
	Δ	<i>Delta</i>
	θ	<i>theta</i>
	Θ	<i>Theta</i>
	κ	<i>kappa</i>
	μ	<i>mu</i>
	ο	<i>omicron</i>
English Terms	w/o	without
Other Abbreviations	AA	ascorbic acid
	b-Glycero-P	β-glycerophosphate
	min	minimum
	max	maximum
	<i>nx</i>	<i>n</i> times
	#	number
	AS	adipogenic differentiation stimulating medium
	OS	osteogenic differentiation stimulating medium
	TNF	TNF-supplemented medium

Zusammenfassung

Ziel der vorliegenden Studie war es zu untersuchen, ob eine entzündliche Stimulierung mesenchymaler Stammzellen des Fettgewebes (ASC) durch Medium, welches mit Tumornekrosefaktor (TNF) supplementierte wurde, *in vitro* eine osteogene Differenzierung dieser Zellen bewirkt bzw. unter osteogenen Bedingungen einen Einfluß auf die osteogene Differenzierung dieser Zellen hat.

Die Motivation für diese Untersuchung resultiert aus der bekannten Rolle von TNF als Promotor der Differenzierung und Aktivierung von Osteoklasten *in vitro* und *in vivo*, die in entzündlichen Erkrankungen wie der rheumatoiden Arthritis dazu führt, daß das im Gesunden ausbalancierte System der Osteoblasten-vermittelten Knochenbildung und der Osteoklasten-vermittelten Knochenresorption in Richtung Knochenresorption verschoben wird. Da TNF die osteogene Differenzierung der hämatopoetischen Osteoklastenvorläufer stimuliert, stellte sich die Frage, ob es auch einen Einfluß auf die osteogene Differenzierung der mesenchymalen Osteoblastenvorläufer, zu denen auch ASC zählen, hat.

Zu diesem Zweck untersuchte ich die Proliferation und die osteogene Differenzierung von ASC unter dem Einfluß von TNF *in vitro* im Vergleich zu osteogen stimulierten und unstimulierten Zellen. ASC, die sowohl mit TNF als auch osteogen stimuliert wurden, dienten der Untersuchung eines Effektes von TNF auf die osteogene Differenzierung unter osteogenen Bedingungen.

TNF bindet zwei Rezeptoren, TNFRSF1A und TNFRSF1B. Beide Rezeptoren wurden von ASC exprimiert, TNFRSF1B dabei weitaus schwächer als TNFRSF1A. TNF-Behandlung der ASC veränderte die Expression der Rezeptor-Proteine nicht.

Die TNF-Rezeptoren regulieren drei intrazelluläre Signalwege: Apoptose, den MAP-Kinase- und den NF κ B-Weg. Apoptose wurde in ASC nicht ausgelöst, weder durch TNF noch durch osteogene Stimulation. Der MAP-Kinase-Weg wurde ebenfalls weder durch TNF noch durch osteogene Stimulation reguliert. Nichtsdestrotz waren zwei Mitglieder der MAP-Kinase-Familie, der Transkriptionsfaktor AP1 und die Kinase p38, konstitutiv bis mindestens Tag sieben der Kultur aktiviert. Im Gegensatz zum Apoptose- und MAP-Kinase-Weg wurde der NF κ B-Weg durch TNF, aber nicht durch osteogene Stimulanzien, aktiviert, und Ko-Stimulation mit sowohl TNF als auch osteogenen Stimulanzien bewirkte denselben Effekt wie TNF allein.

TNF erhöhte signifikant die Proliferation der ASC, was auch zutraf für osteogene Stimulation und Ko-Stimulation mit TNF und osteogenen Stimulanzien.

Der Zellzyklus wurde von TNF in entgegengesetzter Weise reguliert wie durch die osteogenen Stimulanzien. Während TNF den Anteil der ASC in der Synthese-Phase des Zellzyklus' signifikant reduzierte, wurde dieser durch osteogene Stimulation signifikant erhöht. Ko-Stimulation der ASC mit sowohl TNF als auch osteogenen Stimulanzien verringerte die Stärke der S-Phasen-Reduktion durch TNF.

Die metabolische Aktivität der ASC verringerte sich im Verlauf der Kultur unter Stimulation

mit TNF zunehmend, während osteogene Stimulation einen starken zwischenzeitlichen Anstieg bewirkte. Ko-Stimulation bewirkte einen ähnlichen zeitlichen Verlauf der metabolischen Aktivität wie TNF allein, aber von Anfang an auf niedrigerem Niveau.

Um herauszufinden, ob TNF einen spezifischen osteogenen Effekt hat, habe ich die Expression und Aktivität einer Reihe osteogener Zeigermoleküle untersucht.

Die Expression des Transkriptionsfaktors *ZBTB16* ist ein früher Marker der osteogenen Differenzierung. *ZBTB16* reguliert Expression und Aktivität des Schlüsseltranskriptionsfaktors der osteogenen Differenzierung, *RUNX2*. Die *ZBTB16*-Expression wurde durch TNF nicht signifikant beeinflusst, durch osteogene Stimulation und Ko-Stimulation mit TNF und osteogenen Substanzen hingegen bis zu 10.000-fach erhöht.

Die Bindung des Transkriptionsfaktors *RUNX2* an die regulatorischen Sequenzen seiner Zielgene wurde durch TNF initial erhöht, nachfolgend aber reduziert, hingegen durch osteogene Stimulation stark erhöht. Ko-Stimulation bewirkte ebenfalls eine initial signifikant verstärkte Bindung, die allerdings schwächer war als unter ausschließlicher osteogener Stimulation und nachfolgend stark reduziert wurde.

Neben diesen Transkriptionsfaktoren als frühen Markern der osteogenen Differenzierung habe ich Expression und Aktivität des Schlüsselenzyms der Kalzifikation der extrazellulären Matrix, der Alkalischen Phosphatase, als einem intermediären Marker untersucht. TNF hatte keinen signifikanten Effekt auf Expression und Aktivität der Alkalischen Phosphatase, wohingegen die osteogene Stimulation beide signifikant erhöhte. Die Ko-Stimulation mit TNF und osteogenen Substanzen erhöhte die Expression und Aktivität der alkalischen Phosphatase in gleichem Maße wie die osteogene Stimulation allein.

Als einen finalen Indikator der osteogenen Differenzierung analysierte ich den Kalziumgehalt der extrazellulären Matrix. TNF hatte hierauf keinen Einfluß, während die osteogene Stimulation ihn signifikant erhöhte. In gleichem Maße galt dies für Ko-Stimulation mit TNF und osteogenen Substanzen.

Demnach induziert TNF nicht die osteogene Differenzierung von ASC als mesenchymalen Osteoblastenvorläuferzellen *in vitro*, was im Gegensatz zu der bekannten, die Differenzierung fördernden Wirkung von TNF auf hämatopoetische Osteoklastenvorläuferzellen *in vitro* und *in vivo* steht. Da TNF unter osteogenen Bedingungen die osteogene Differenzierung von ASC zusätzlich weder inhibierte noch verstärkte, ist der Effekt der Osteolyse der Röhrenknochen in chronisch-entzündlichen Erkrankungen, die charakterisiert sind durch erhöhte Konzentrationen dieses Zytokins, wahrscheinlich hauptsächlich auf den pro-osteoklastogenen Effekt von TNF zurückzuführen.

Auf den ersten Blick paradoxerweise können dieselben entzündlichen Bedingungen, die die Reduktion der Mineraldichte in den Röhrenknochen bewirken, an heterotoper Stelle zu einer Kalzifikation führen. Dieser Umstand wurde bislang hauptsächlich für die Kalzifikation der Vasculatur berichtet. Demnach bewirken chronisch-entzündliche Erkrankungen zusammenfassend ein "Aufweichen" von Hartgewebe und ein "Verhärten" von Weichgewebe.

Die zwei Hauptergebnisse dieser Arbeit verallgemeinernd läßt sich sagen, daß, da TNF *in vitro* nicht die osteogene Differenzierungsfähigkeit der ASC reduzierte, aber ihre Proliferation verstärkte, entzündliche Prozesse *in vivo* als Promotoren der Stammzellerneuerung angesehen werden können, ohne einen Einfluß auf deren Differenzierung zu haben, während andere Umgebungsfaktoren die Differenzierung dieser vergrößerten Stammzellpopulation in das jeweilige Gewebe induzieren. Daher erhöht die entzündliche Aktivierung eines infizierten oder beschädigten Gewebes dessen regeneratives Potential initial, benötigt aber zusätzliche Umgebungssignale, um den Regenerationsprozeß abzuschließen.

Abstract

The present study aimed at finding out whether an inflammatory treatment of mesenchymal stem cells (MSC) from the adipose tissue (adipose tissue-derived stem cells, ASC), as was done by the culture of ASC in tumor necrosis factor- (TNF)-supplemented medium *in vitro*, will direct these cells into osteogenic differentiation or will affect this differentiation pathway under osteogenic conditions.

The rationale for the study came from the well-known role of TNF as a promoter of osteoclast maturation and activity *in vitro* and *in vivo*, which in inflammatory diseases, as e.g. rheumatoid arthritis, shifts the tightly balanced system of osteoblast-mediated bone formation and osteoclast-mediated bone resorption towards bone resorption. Hence, if TNF increases osteogenic differentiation of hematopoietic osteoclast precursors, it may also have an impact on differentiation of mesenchymal osteoblast precursors as ASC.

To this end, I analyzed proliferation and osteogenic differentiation of ASC treated with TNF *in vitro* in comparison to osteogenically stimulated and unstimulated cells. ASC treated with both TNF and osteogenic stimulants were analyzed to elucidate the impact of TNF on osteogenic differentiation under osteogenic conditions.

TNF exerts its cellular effects via two receptors, TNFRSF1A and TNFRSF1B. Both receptors were found to be expressed on ASC, TNFRSF1B being much weaker expressed than TNFRSF1A, and TNF treatment did not change the expression levels of both receptor proteins.

The TNF receptors regulate three signal transduction pathways: apoptosis, the MAP kinase and the NF κ B pathway. Apoptosis was not induced in ASC, irrespective of TNF or osteogenic stimulation. The MAP kinase pathway was also not regulated by TNF or osteogenic stimulation, although two of its members, the kinase p38 and the transcription factor AP1, were found to be constitutively activated at least until day seven of culture. Contrastingly, the NF κ B pathway was strongly induced by TNE, but not by osteogenic stimulants, and it was found to be active also when osteogenic substances were present in addition to TNE.

TNF significantly increased ASC proliferation rates, which was also true for osteogenic stimulation and stimulation with both TNF and osteogenic substances.

Cell cycle data however showed contrasting effects for TNF and osteogenic stimulation. While TNF significantly decreased the portion of ASC within the synthesis phase of the cell cycle, osteogenic substances increased this portion. Treatment with both TNF and osteogenic stimuli yielded a lower decrease of synthesis phase cells as TNF treatment alone.

The temporal course of the metabolic activity of ASC was changed by TNF in direction of a continuous decrease with increasing duration of cell culture, whereas osteogenic stimulation induced a strong intermediate peaking. Treatment with both osteogenic stimulants and TNF yielded a temporal course of metabolic activity resembling that found for TNF alone, but at a lower level of overall metabolic activity.

To elucidate whether TNF has any specific effect on osteogenic differentiation of ASC, I analyzed expression and activity of a variety of osteogenic markers.

As an early hallmark of osteogenic differentiation, expression of the transcription factor *ZBTB16*, an upstream regulator of expression and activity of the osteogenic key transcription factor RUNX2, was analyzed. *ZBTB16* expression was neither significantly increased nor decreased by TNF treatment of ASC, whereas osteogenic stimulation and stimulation with both TNF and osteogenic stimulants yielded a significant and up to 10,000-fold increase in expression of this gene.

Binding of the osteogenic key transcription factor RUNX2 to the regulatory sequence of its target genes was found to be reduced by TNF, but significantly increased in osteogenically stimulated ASC. Co-stimulation with both TNF and osteogenic stimulants also resulted in a significant, though less strong increase in DNA-binding activity of this transcription factor.

Besides these osteogenic transcription factors as early markers of osteogenic differentiation, I analyzed the expression and activity of the key enzyme involved in extracellular matrix calcification, alkaline phosphatase, as an intermediate marker. TNF treatment of ASC had no significant impact on expression and activity of this enzyme, whereas osteogenic stimulation and co-stimulation with TNF and osteogenic stimulants significantly and equally strong increased it.

As a final indicator of osteogenic differentiation, I analyzed the extent of extracellular matrix calcium content. TNF treatment of ASC had no effect on extracellular matrix calcium content, whereas osteogenic stimulation and co-stimulation with TNF and osteogenic stimulants significantly and equally strong increased it.

Thus, treatment of ASC with TNF did not induce osteogenic differentiation of these stem cells *in vitro*. This is in contrast to the well-known differentiation-promoting effect of TNF on osteoclast precursor cells from the hematopoietic lineage. Since TNF did neither increase nor reduce the osteogenic differentiation capacity of ASC in an osteogenic environment *in vitro*, the effect of osteolysis of the long bone observed in chronic inflammatory diseases characterized by increased TNF levels presumably is mainly due to the pro-osteoclastogenic effect of this cytokine *in vivo*.

Seemingly paradoxically, the same inflammatory stimuli that induce osteolysis of the long bone can nevertheless induce calcification at ectopic sites, as was reported primarily for the vasculature via a variety of different pathways. Therefore, chronic inflammatory diseases can be summarized to cause “softening” of hard tissue and simultaneous “hardening” of soft tissue.

Generalizing the two main findings of this study, i.e. the finding that TNF did not impair ASC osteogenic differentiation capability *in vitro*, but increased ASC proliferation rate, inflammatory processes *in vivo* appear to act as a driving force for stem cell self-renewal without affecting their differentiation potential, and environmental factors other than the mediators of inflammation govern subsequent differentiation of this enlarged stem cell pool into the desired tissue. Thus, inflammatory activation of infected or damaged tissue increases its regenerative potential as a starting point, but requires further signals for regeneration to complete.

Chapter 1

Introduction

1.1 Aim and Motivation

The present study aimed at finding out whether an inflammatory treatment of mesenchymal stem cells (MSC) from the adipose tissue (adipose tissue-derived stem cells, ASC), as was done by the culture of ASC in tumor necrosis factor- (TNF)-supplemented medium *in vitro*, will direct these cells into osteogenic differentiation or will affect this differentiation pathway under osteogenic conditions.

The rationale for the study came from the well-known role of TNF as a promoter of osteoclast maturation and activity *in vitro* and *in vivo*, which in inflammatory diseases, as e.g. rheumatoid arthritis, shifts the tightly balanced system of osteoblast-mediated bone formation and osteoclast-mediated bone resorption towards bone resorption [Azuma et al., 2000]. Hence, if TNF increases osteogenic differentiation of hematopoietic osteoclast precursors, it may also have an impact on differentiation of mesenchymal osteoblast precursors as ASC.

1.2 Adipose Tissue-Derived Stem Cells

1.2.1 Biological Niche of ASC

ASC are isolated from the stromal vascular fraction of subcutaneous adipose tissue obtained in large quantity and minimally invasive by liposuction. ASC, as MSC, are adult stem cells which embryonically originate from the mesodermal layer. They are multipotent, i.e. they are able to differentiate into all types of cells belonging to the connective tissue, as e.g. adipocytes, osteoblasts, chondrocytes and myocytes [Zuk et al., 2001]. *In vitro*, ASC express typical MSC markers as cluster of differentiation (CD) 29, CD44, CD105 and CD166, and in primary culture immediately after isolation also STRO-1 antigen [Kalbermatten et al., 2011], a surface protein whose expression was found to be characteristic for that subpopulation of cells from bone marrow aspirates that is able to undergo osteoblastogenesis [Gronthos et al., 1994; Kaneko et al., 2009].

As other types of MSC that were found to be in close contact to blood vessels within their appropriate niche *in vivo* [Crisan et al., 2008; da Silva Meirelles et al., 2008], ASC are also of perivascular origin, express the pericyte marker CD34 and were found to interact with endothelial cells to stabilize vascular networks *in vitro* [Traktuev et al., 2008]. Therefore, the characteristic of CD34 expression shifted from being formerly interpreted as an exclusive feature of

activated hematopoietic precursors towards being nowadays considered as a global marker of vasculature-associated cells [Furness and McNagny, 2006].

1.2.2 Differentiation Capabilities of ASC

Before I go into detail regarding the differentiation capacities of ASC, I have to define the terms used in discussions of stem cell differentiation and which were concisely reviewed by Ratajczak and colleagues [Ratajczak et al., 2008].

Differentiation capacities of cells during development continuously decline from the fertilized egg called zygote to the fully differentiated adult tissue. The zygote is able to differentiate into both all tissues and organs of the developing organism and into the placental tissue governing nutrient supply and exchange of metabolic waste products. Therefore, the zygote is said to be totipotent. Embryonic stem (ES) cells, which are derived from a morula-stage embryo, from the inner cell mass of a blastocyst-stage embryo or from the epiblast cells of a cylinder-stage embryo, can also differentiate into all cells the developing organism will be made of, but have lost the capability to differentiate into placental tissue and therefore are referred to be pluripotent. These pluripotent stem cells can give rise to any of the three embryonic germ layers the embryo is made of, i.e. the ectodermal, the mesodermal and the endodermal layer. Each of the germ layers gives rise to a distinct set of tissues and organs, and stem cells that are able to differentiate into any of these tissues and organs of a distinct germ layer are called multipotent. Stem cells that are able to differentiate only into one distinct tissue or organ of a distinct germ layer are said to be monopotent.

After embryogenesis has completed and the entire organism is formed, cells having reached the end of their lifetime or which were damaged in any way are replaced by adult stem cells differentiating into the cell type of the affected tissue. In case this replacement process occurs by stem cells originating from another embryonic germ layer, this process is called transdifferentiation. Adult stem cells reside in specialized environments of the body which are called “niches” and which have the property to promote self-renewal (proliferation) of the stem cells and preclude their spontaneous differentiation.

Following these definitions, ASC reside to the perivasculature of adipose tissue as their niche and are adult multipotent stem cells, since they were shown to differentiate into all mesenchymal tissues which themselves develop from the mesodermal layer during embryogenesis.

Moreover, there are also reports describing pluripotent differentiation capabilities of ASC. ASC were found to express embryonic stem cell markers as POU5F1 (formerly called OCT4) and NANOG [Kalbermatten et al., 2011], what suggests even broader differentiation capabilities, and indeed, some early indications of a transdifferentiation capability of mesodermal ASC into human ectodermal neuron-like cells [Zuk et al., 2002] were confirmed *in vitro* for rat ASC which differentiated into Schwann cells and contributed to nerve regeneration mostly indirectly by secretion of neurotrophic factors, but hardly by direct differentiation into neural cells [Kalbermatten et al., 2011]. Supportingly, neural pre-differentiation of rat ASC *in vitro* improved their differentiation into glia cells in the healing of a spinal cord injury *in vivo* in comparison to undifferentiated ASC, but did not augment their neuronal differentiation [Arboleda et al., 2011]. Therefore, ASC are currently thought to participate in neuronal regeneration *in vivo* mainly by differentiating into neural stromal cells and by secretion of paracrine factors that recruit other neuronal precursors from their niches.

Besides their neural differentiation capacities, the potency of ASC to differentiate into ectodermal tissues was substantiated by the finding of ASC differentiating into epithelial cells

[Gimble and Bunnell, 2010]. Thus, in addition to their ability to differentiate into mesodermal smooth muscle, cardiac progenitor, endothelial and hepatic cells, these findings underline a broad differentiation capacity of ASC, being able to differentiate not only into different mesenchymal tissues and thus along the mesodermal lineage, but also to transdifferentiate into the ectodermal lineage to participate in neural regeneration. During embryogenesis, this process of epithelial-to-mesenchyme transition is of paramount significance, since neural crest cells in this way give rise to not only ectodermal tissues as neurons, glia cells, endocrine cells and skin melanocytes, but also to mesenchymal cell types as chondrocytes, osteoblasts, myofibroblasts and adipocytes [Douarin et al., 2008].

1.2.3 ASC Isolation

In addition to their broad differentiation capacity, ASC, as compared to bone marrow-derived MSC, offer the advantage of being isolated by minimally invasive means, in large quantity and from mostly young and healthy donors.

The liposuction technique that was used for adipose tissue isolation in this study was based on the subcutaneous application of a sodium chloride solution which is exhausted from the adipose tissue after mechanical agitation. This tumescence-based technique was reported to offer the best results for subsequent stem cell isolation with respect to ASC viability, proliferation rate and osteogenic and chondrogenic differentiation capacity [Oedayrajsingh-Varma et al., 2006]. ASC isolation from directly resected adipose tissue or by ultrasound-based liposuction techniques yielded significantly less viable cells.

The anatomical site the adipose tissue was harvested from was reported to influence ASC yield, the abdominal region yielding significantly more ASC than the hip or thigh region [Jurgens et al., 2008]. However, the differentiation capacity of ASC isolated from these differing sites did not differ. For human bone marrow-derived MSC, osteogenic and chondrogenic as well as adipogenic and myogenic differentiation were reported to be even independent of the donor age [Roura et al., 2006; Fickert et al., 2011], what may also be true for ASC. Therefore, the reduced regenerative potential of elderly people presumably is due to a reduced total number of adult stem cells within their respective niches, but not due to an impaired differentiation capacity of these stem cells. However, the body mass index of the donor individual was reported to negatively correlate with ASC adipogenic differentiation capacity, whereas ASC yield was reported to positively correlate with this parameter [Isakson et al., 2009]. Hence, a lesser adipogenic differentiation capacity *in vivo* is compensated by a higher number of progenitor cells.

The time between liposuctive surgery and isolation of ASC from the adipose tissue should not exceed one day, since increasing storage times of the adipose tissue at room temperature for up to three days was shown to significantly and increasingly reduce ASC yield [Carvalho et al., 2011]. By comparing these results to those obtained in another study [Matsumoto et al., 2007], storage of adipose tissue at 4 °C is not recommended.

Thus, ASC can be isolated from various adipose tissues with varying yield, but unchanged differentiation capacity for subsequent *in vitro* or *in vivo* approaches. Most importantly, the isolation technique needs to be sufficiently gentle to avoid ASC death *in situ*, but rough enough to allow liberation of the adipose tissue from the patient. Currently, tumescence-based systems balance these opposed demands the best.

1.2.4 ASC Culture

ASC have a remarkable long-term genomic stability. Culture of these cells for up to 35 passages was not accompanied by accumulation of genomic aberrations, whereas other primary cells as e.g. chorionic villus cells showed 12 % tetraploidy even after eight passages [Grimes et al., 2009].

Nevertheless, the duration of cell culture, as reflected by the number of passages, affects proliferation and differentiation behaviour. Osteoblast-like cells from bone biopsies yielded highest proliferation rates in the fourth passage and subsequently decreased their proliferation rate as well as their osteogenic differentiation capacity [Pradel et al., 2008], which was confirmed for human bone marrow stromal cells [Rosa and Beloti, 2005]. Therefore, ASC, as other mesenchymal stem cells, should be used as early as possible after isolation and adaptation to *in vitro* conditions. In this study, they were seeded into experimentation exclusively in the fourth passage.

Use of differing serum lots in culture of ASC derived from the same patient can change differentiation capacities of these cells, but no serum substitute so far has been shown to be as reliable as serum with respect to differentiation along the adipogenic, osteogenic and chondrogenic lineage [Lund et al., 2009]. Moreover, not only the particular serum chosen influences ASC differentiation, even the composition of the basal medium does. Alpha-modified Eagle medium (MEM) in the same study was reported to induce stronger proliferation as well as adipogenesis and osteogenesis, but weaker chondrogenesis in ASC than Dulbecco's MEM. Therefore, some media formulations appear to promote distinct differentiation pathways, and no single medium equally well supports all of them. With respect to these inherent limitations, I decided to use the widely-used DMEM in all experiments.

Additionally, use of cryopreserved cells can alter experimental results in comparison to non-cryopreserved cells, but also in dependence on the cryopreservation method used. The osteogenic differentiation capacity of osteoblast-like cells was reported to differ with respect to the cryopreservation method used, the best method being freezing cells in DMEM containing 10 % DMSO without any serum or serum replacement and culturing cells after thawing in DMEM supplemented with autologous serum [Reuther et al., 2006]. However, other cell types may require other freezing conditions. To avoid any impact of cryopreservation on experimental outcome, use of cryopreserved cells was completely avoided in this study.

1.2.5 Summary on ASC *in vitro*

Summarizingly, ASC represent an important population of mesenchymal stem cells. They can be obtained minimally invasive and in large quantity from various adipose tissues, have a differentiation capacity clearly exceeding that of the widely used bone marrow-derived MSC, but do not require higher effort for culture *in vitro*. Therefore, they are a crucial type of adult stem cells for fundamental as well as for translational research.

1.3 TNF, its Receptors and Signal Transduction Pathways

1.3.1 TNF

Tumor necrosis factor (TNF, formerly $\text{TNF}\alpha$) was named after its inductive effect on necrosis of tumors, a condition discovered almost 150 years ago in cancer patients showing spontaneous

tumor regression after acute bacterial infection [Clark, 2007]. In 1975, the excess production of the pro-inflammatory cytokine TNF by bacterial endotoxin-activated macrophages was demonstrated to kill these tumors [Carswell et al., 1975; Helson et al., 1975; Mansell et al., 1975]. However, the molecular identity of TNF was not resolved until 1985 [Pennica et al., 1984; Aggarwal et al., 1985].

TNF is produced predominantly by activated macrophages and T lymphocytes as a plasma membrane-bound pro-protein (“mTNF”) which subsequently undergoes cleavage in its extracellular domain by metalloproteinases to give rise to the shorter soluble form of TNF. Both the membrane bound and the soluble form of TNF are biologically active. The metalloproteinase that cleaves TNF was formerly called TNF α converting enzyme (TACE), but is nowadays officially referred to as ADAM metalloproteinase domain 17 (ADAM17).

TNF is the major cytokine involved in the pathogenesis of chronic inflammatory diseases, and its neutralization has proven to efficiently ameliorate the prognosis of inflammatory diseases as rheumatoid arthritis and Crohn’s disease [Clark, 2007].

1.3.2 TNF Receptors and Signaling Pathways

TNF binds two distinct receptors, TNF receptor 1 (tumor necrosis factor receptor superfamily member 1A, TNFRSF1A) and 2 (tumor necrosis factor receptor superfamily member 1B, TNFRSF1B). Upon binding of a homotrimer of TNF molecules, the TNF receptors that initially were organized as trimers loosely interconnected via their pre-ligand-binding assembly domain (PLAD) form a stable trimeric complex [MacEwan, 2002]. Binding of TNF to the extracellular portion of the receptor results in the release of inhibitory factors bound to the intracellular domains of these transmembrane receptors, and these intracellular domains subsequently recruit a variety of different factors, so-called adaptor proteins, that activate downstream signaling cascades [Wajant and Scheurich, 2011]. Thus, activated TNF receptors do explicitly not have catalytic activity and are regulated through the presence or absence of cytoplasmic inhibitory factors.

The cellular functions first discovered to be regulated by TNFRSF1A were apoptosis, inflammatory response and function of the immune system, but later on also proliferation and differentiation [Chen and Goeddel, 2002]. The major pathways activated upon TNF binding to TNFRSF1A are the nuclear factor of kappa B light chain (NF κ B), mitogen-activated protein kinase (MAPK) and apoptosis pathway.

TNFRSF1B also directly regulates activation of the NF κ B and MAPK pathway, whereas activation of the apoptosis pathway occurs only indirectly via cross-talk with TNFRSF1A signaling [Faustman and Davis, 2010].

Although TNFRSF1A cannot directly activate the NF κ B pathway, it can do so by crosstalking with TNFRSF1B [Bradley, 2008]. *Vice versa*, TNFRSF1B can pass its ligand to TNFRSF1A for activation of apoptosis [Haridas et al., 1998]. Hence, TNF signaling involves not only cross-talk between the signaling pathways regulated by one distinct TNF receptor, but involves also cross-talk between the pathways activated by different TNF receptors. Figure 1.1 on page 6 summarizes these findings and depicts the signal molecules analyzed in ASC to determine activation of a distinct pathway.

TNFRSF1A is expressed on most cell types, whereas TNFRSF1B is largely confined to cells of the hematopoietic lineage and to endothelial cells [Santee and Owen-Schaub, 1996], but was lately reported to be also expressed on diverse neuronal subtypes and mesenchymal stem cells [Faustman and Davis, 2010]. Despite the activation of other non-TNF receptor-regulated,

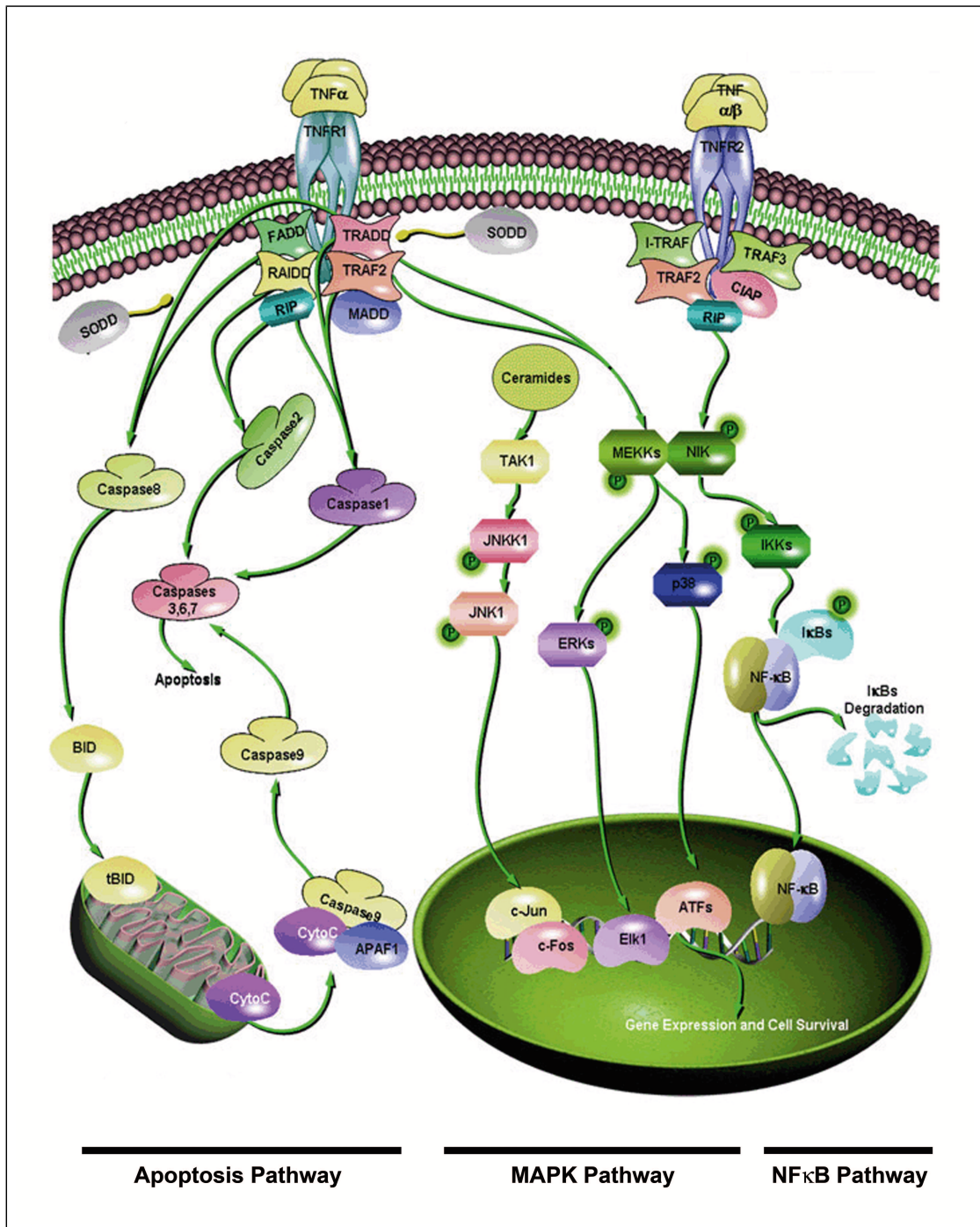


Figure 1.1: TNF receptors and downstream signaling cascades. Binding of TNF to its receptors, designated here as TNFR1 and TNFR2, regulates activation of three distinct signaling pathways: the apoptosis pathway, the MAPK and NF κ B pathway (see left, middle and right part of this illustration, respectively). I analyzed NF κ B activation by assessing translocation of the NF κ B transcription factor subunit p5 to the nucleus. MAPK pathway activation was analyzed by assessing nuclear translocation of the kinases extracellular signal-regulated kinase 1 and 2 (ERK1/2) and p38 as well as by assessing nuclear translocation of the transcription factor activator protein 1 (AP1) subunit cJUN. Activation of the apoptosis pathway was assessed indirectly by analyzing cytoskeletal organization, nuclear envelope integrity and cellular viability. Illustration taken and modified from Pathway Central [SABiosciences, 2011].

but cross-talking intracellular signal transduction pathways, the ratio of the expression of both receptors on a distinct cell type thus determines the outcome of receptor activation by TNF. For ASC, expression of TNF receptors was not analyzed so far.

1.4 Osteogenic Differentiation *in vitro*

1.4.1 Osteogenic Differentiation Markers *in vitro*

Osteogenic differentiation of ASC was analyzed by quantifying the expression of the osteogenic transcription factor zinc finger and BTB domain containing 16 (*ZBTB16*), the DNA-binding activity of the runt-related transcription factor 2 (*RUNX2*), expression and activity of extracellular matrix-mineralizing alkaline phosphatase (*ALPL*) and the calcium content of the extracellular matrix.

The Role of *ZBTB16* in Osteogenic Differentiation

The important role of *ZBTB16* in osteogenic differentiation is highlighted by the severe skeletal defects present in patients suffering from monozygous loss-of-function mutations of the *ZBTB16* gene [Fischer et al., 2008]. In mice, *Zbtb16* regulates limb and axial skeletal patterning by impacting differentiation of limb bud cells through the *Hox* family of genes as well as proliferation and apoptosis through the *Bmp* gene family, in the latter case to give rise to the interdigital separations [Barna et al., 2000].

ZBTB16, the former promyelocytic leukemia zinc finger (*PLZF*), is a transcription factor which was reported to increase transcript and protein activity levels of the osteogenesis key transcription factor *RUNX2* described below and thus indirectly promotes expression of *RUNX2*-targeted genes involved in osteoblastic differentiation of human bone marrow-derived MSC [Ikeda et al., 2005]. When the osteogenic differentiation program is in the course of completing, expression of *ZBTB16* is no longer required and was reported to decline gradually, as was shown for human CD34 positive bone marrow progenitor cells [Reid et al., 1995].

As an early marker of osteogenic differentiation, I quantified expression of the *ZBTB16* gene in ASC following treatment with TNF and in comparison to osteogenic stimulation.

The Role of *RUNX2* in Osteogenic Differentiation

RUNX2 is a transcription factor involved in a large variety of processes in bone development *in vivo*, as is seen in patients suffering from the heterogeneous disease cleidocranial dysplasia that is caused by mutations of the *RUNX2* gene [Otto et al., 2002] (see figure 1.2 on page 8).

RUNX2, formerly known as core binding factor-alpha 1 (*CBFA1*), was shown to upregulate expression of osteopontin, osteocalcin, alkaline phosphatase and collagen 1 and 10 genes during osteogenic differentiation *in vitro* [Komori, 2010]. In rodents, *Runx2* levels are upregulated in the osteoblastic lineage, which is a direct consequence of an increased transcription rate of the gene [Shui et al., 2003] as well as a decreased proteasomal degradation of the protein product through *Bmp2*-induced *Runx2* acetylation in turn precluding *Runx2* ubiquitinylation [Jeon et al., 2006]. In differentiation of human osteoblasts however, *RUNX2* is permanently and constantly expressed, *RUNX2* activity being regulated exclusively post-transcriptionally through the extent of phosphorylation [Shui et al., 2003].

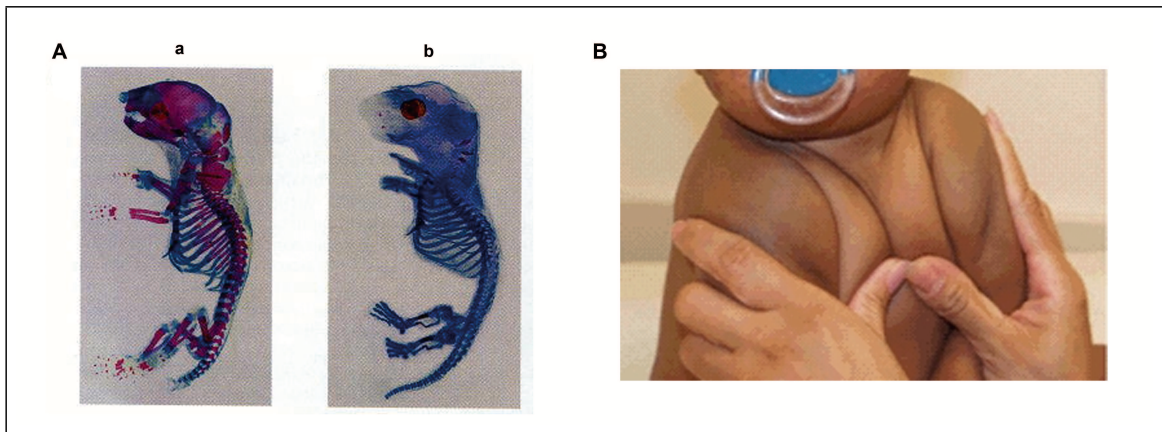


Figure 1.2: The role of *RUNX2* mutations in skeletal development. (A) *Runx2* knockout in mice inhibits chondrocyte to bone transition in the process of endochondral ossification: (a) During skeletal development, mice wild-type for *Runx2* show cartilaginous as well as bony parts of the skeleton, as demonstrated by alcian blue staining and alizarin red staining, respectively. (b) Mice with fully deleted *Runx2* show normal cartilage development, but complete absence of ossification. These mice die shortly after birth. Illustration taken and modified from [Gilbert and National Center for Biotechnology Information (U.S.), 2000]. (B) In humans, the most prominent non-lethal skeletal disease associated with mutations of the *RUNX2* gene is Cleidocranial Dysplasia, a disease characterized by delayed closure of the cranial sutures, hypoplastic or aplastic clavicles and multiple dental abnormalities. The image shows an individual with clavicular hypoplasia resulting in extreme flexibility of shoulder deflection even to the midline. The disease is inherited in an autosomal dominant fashion, but epidemiologically shows a high incidence of *de novo* mutations. Illustration taken from [Roberta et al., 1993 - 2011].

Therefore, I did not analyze *RUNX2* expression, but *RUNX2* binding to the consensus promoter sequence of its target genes as the only reliable measure of active *RUNX2* in the human system and as an early marker of osteogenic differentiation of ASC *in vitro*.

The Role of ALPL in Osteogenic Differentiation

The liver/bone/kidney-specific alkaline phosphatase (ALPL) plays a pivotal role in osteogenesis *in vitro* and *in vivo*. *Alpl*-deficient mice exhibit impaired skeletal calcification [Anderson et al., 2004], which is also true for humans where mutations in the *ALPL* gene were found to be associated with bone diseases as skeletal hypophosphatasia in infants [Baumgartner-Sigl et al., 2007] and age-related bone loss in adults [Goseki-Sone et al., 2005] (see figure 1.3 on page 9).

ALPL plays a role in the process of extracellular matrix mineralization, although the mechanism is still not completely understood. It was discovered that calcification in osteogenic differentiation occurs via the generation of vesicles that bud off from the osteoblast's cytoplasmic membrane [Anderson, 1995]. These so-called matrix vesicles contain a high concentration of calcium and inorganic phosphate ions and make up an appropriate environment for nucleation of hydroxyapatite crystals. When growing, these crystals destroy the matrix vesicle's membrane and grow further using extracellular calcium and phosphate ions, which finally generates the calcified extracellular matrix of bony tissue.

Alkaline phosphatase is localized to the outer surface of the matrix vesicle membrane and degrades inorganic pyrophosphate present in the extracellular matrix, which both reduces the amount of hydroxyapatite formation-inhibiting pyrophosphate and yields free inorganic phosphate [Orimo and Shimada, 2008]. This free inorganic phosphate can then be incorporated



Figure 1.3: The role of *ALPL* mutations in human skeletal diseases. The most prominent skeletal disease caused by mutations of the *ALPL* gene is hypophosphatasia. Hypophosphatasia is characterized by defective mineralization of bone and teeth in the presence of low activity of serum and bone alkaline phosphatase. (A) Radiographic image showing loss of bone surrounding teeth in childhood hypophosphatasia. (B) Pseudofracture in a long bone in adult hypophosphatasia. There are two different inheritance patterns for hypophosphatasia which differ in the age of onset of the disease: Perinatal and infantile hypophosphatasia are inherited in an autosomal recessive fashion, whereas the late onset types of the disease may also be inherited in an autosomal dominant way, depending on the effect the *ALPL* mutation has on the phosphatase's activity. The incidence of *de novo* mutations of *ALPL*, in contrast to *RUNX2*, is low. Illustrations taken and modified from [Roberta et al., 1993 - 2011].

from the extracellular space into the matrix vesicle by type III sodium-phosphate cotransporters. In conjunction with several calcium ion-binding phospholipids and proteins as well as annexins which have the ability to function as calcium ion channels through the matrix vesicle membrane, the calcium and phosphate ion concentration inside the matrix vesicle is raised to facilitate nucleation of hydroxyapatite crystals [Anderson, 1995].

After completion of the nucleation phase, the ALPL-mediated liberation of inorganic phosphate promotes the reaction with free calcium ions to form hydroxyapatite in the extracellular space [Orimo and Shimada, 2008]. Thus, ALPL activity is required for both the initiation and the propagation phase of mineralization.

I analyzed the extent of extracellular matrix calcification as a final parameter of osteogenic differentiation and the expression of the alkaline phosphatase gene and the activity of the gene product as median markers of osteogenic differentiation of ASC.

Proliferation, Cell Cycle and Metabolic Activity

Proliferation, cell cycle and and metabolic activity are basal parameters of living cells that were analyzed in addition to the specific markers of osteogenic differentiation in order to more broadly characterize the changes induced by the differentiation processes.

The increase in cell number, called proliferation, is regulated in a tightly controlled system of cell cycle phases. The cell cycle defines all replicative stages of a cell. It is composed of a DNA synthesis (S) phase and a mitosis (M) phase which are separated from each other by gap (G) phases. Progression of cells through these phases of the cell cycle involves passage through several quality control checkpoints to avoid erroneous reduplication (see figure 1.4 on page 11).

By summing up the time needed for a cell to pass all of the distinct stages of the cell cycle, the duration of one cellular replication can be calculated. Since the individual cells of a population usually pass the cell cycle not in a synchronized fashion, the percentage of all cells of a population that is present in a distinct cell cycle stage directly corresponds to the time needed to pass this stage. Hence, a large percentage of cells in a distinct cell cycle phase reflects slow passage through this stage.

Proliferation, but also differentiation of cells, involves metabolic pathways that break down larger molecules into smaller ones to release energy (catabolism), but also biosynthetic (anabolic) reactions. Therefore, ASC metabolic activity was analyzed in an assay quantifying the cellular capacity for NADH and NADPH generation, these reduced redox equivalents being generated in catabolic reactions as e.g. glycolysis and their generation rate thus reflecting overall cellular metabolic activity.

1.4.2 Bone Remodeling

The bony structures generated during embryogenesis are subject to lifelong remodeling. In this manner, the complete skeleton is replaced every ten years [Novack, 2011]. The process of remodeling is governed by a tightly balanced system of bone matrix-secreting cells (osteoblasts) and bone matrix-resorbing cells (osteoclasts) (see figure 1.5 on page 11).

Regulation of Bone Remodeling

Bone remodeling is regulated via the rate of differentiation of osteoclast and osteoblast precursors as well as via the bone-resorbing and bone-forming activity of the corresponding mature

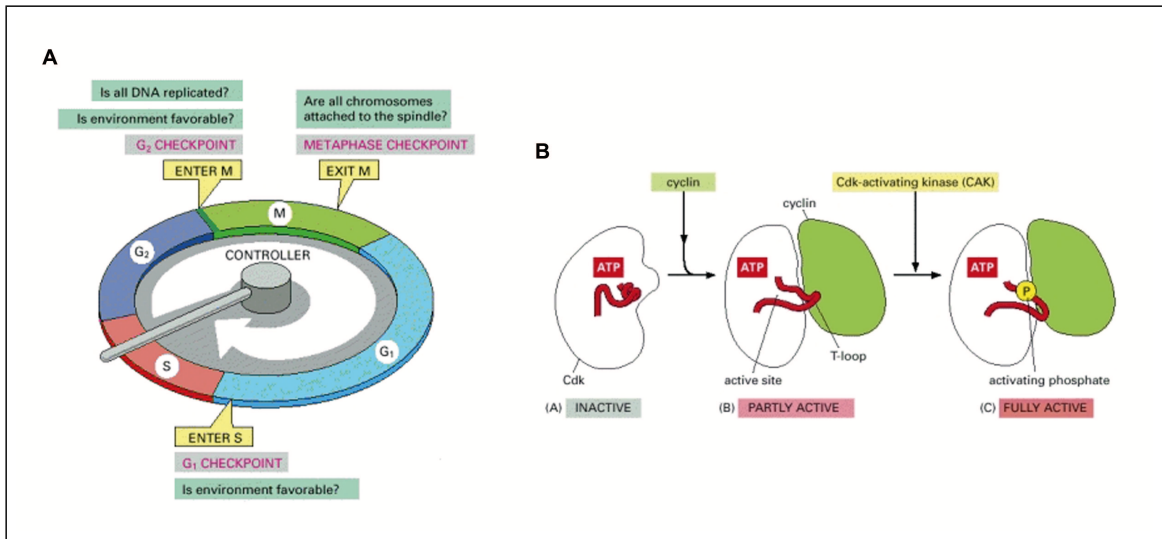


Figure 1.4: Progression and regulation of the cell cycle. (A) Entry into the M phase after DNA replication (G_2 checkpoint), exit from the M phase (metaphase checkpoint) as well as entry into the S phase after mitosis (G_1 checkpoint) are subject to intrinsic cellular quality control: In case DNA synthesis or mitosis did not take place free of errors, error factors are produced that arrest the cell cycle at the corresponding checkpoints until the error is repaired and the error signal disappears. If the error cannot be corrected, the cell is subjected to apoptosis. (B) The factors driving cellular progression through the cell cycle are called cyclins and are regulated by phosphorylation through cyclin-dependent kinases (CDKs). The constitutively expressed CDKs are only active when bound to cyclins. The levels of individual cyclins change due to proteasomal degradation during the cell cycle, what makes the activity of the cyclin-CDK complexes change in a simultaneous manner. By this means, passage through the distinct cell cycle phases is governed. As is illustrated for human CDK2, cyclin-binding to CDK2 makes the CDK2 T-loop to move out of the kinase's active site, which results in partial activation of the enzyme. Full activation occurs upon phosphorylation through CDK-activating kinase (CAK) at the CDK T-loop. Illustrations taken from [Alberts et al., 2002].

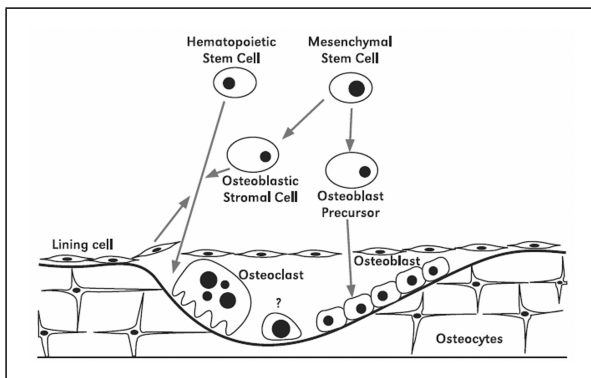


Figure 1.5: The remodeling of bone. Bone is composed of bone matrix-secreting cells (osteoblasts) and matrix-eroding cells (osteoclasts). These cells differentiate from mesenchymal and hematopoietic stem cells, respectively. When osteoblasts become entrapped within the bone matrix, they differentiate into osteocytes. These osteocytes are connected to each other and to the surfacial osteoblasts by channels called *lacunae*. Rupture of a *lacuna* ceases communication and induces osteocytes to secrete signals inducing bone regeneration at the affected site. Resorption of the bone matrix at the affected site usually takes only a few weeks, whereas matrix formation is much slower and takes several months to complete, as multiple layers of new bone are formed by successive waves of osteoblasts. Illustration taken from [Office of the Surgeon General (U.S.), 2004].

cells.

Following the observation that mature monocytes and macrophages are able to differentiate into mature osteoclasts *in vitro* [Udagawa et al., 1990], receptor activator of nuclear factor kappa-B ligand (RANKL, officially designated tumor necrosis factor (ligand) superfamily member 11 (TNFSF11)), was revealed as the driving force of osteoclastogenesis in bone remodeling *in vivo*, *Rankl* knockout mice being found to develop severe osteopetrosis due to a complete lack of osteoclasts [Kong et al., 1999].

Impact of TNF on Bone Remodeling

As RANKL, also TNF was found to induce osteoclastogenesis [Boyce et al., 2010]. Both cytokines induce osteoclastogenesis through activation of the canonical NF κ B pathway signaling through the p65(RELA)-NF κ B1 heterodimer, whereas RANKL also activates the non-canonical NF κ B pathway which signals through p52(RELB)-NF κ B2. As was reported for *Rankl* knockout mice, double knockouts for both the canonical and the non-canonical NF κ B pathway developed severe osteopetrosis due to insufficient osteoclast precursor maturation.

The primary source of RANKL driving osteoclastogenesis *in vivo* is marrow stromal cells [Kitaura et al., 2004], and TNF was found to increase RANKL secretion by these cells [Romas et al., 2002]. Importantly, a high TNF concentration of 50 ng/ml was reported to induce osteoclastogenesis *in vitro* even without RANKL-secreting marrow stromal cells. However, this direct contribution of TNF on osteoclastogenesis *in vivo* has to be questioned, since in chronic inflammatory diseases TNF concentrations were not reported to exceed 50 pg/ml (see page 91 for further details).

In addition to their role in promoting osteoclastogenesis by RANKL secretion, marrow stromal cells were both *in vitro* and *in vivo* reported to secrete a decoy receptor for RANKL, osteoprotegerin (OPG), which inactivates the pro-osteoclastogenic signal by preventing RANKL from binding to RANK on osteoclast precursors [Simonet et al., 1997]. Hence, the ratio of OPG to RANKL determines the outcome on osteoclast maturation rate. TNF and glucocorticoids were reported to decrease the OPG/RANKL ratio, which promotes osteoclastogenesis, whereas TGF β and estrogens increase it [Kearns et al., 2008; Wright et al., 2009]. In line with the increase in osteoclastogenesis by TNF, NF κ B activation in osteoblasts was reported to inhibit osteoblastic bone matrix-secretion activity *in vivo* [Novack, 2011], what substantiates the osteolytic properties of TNF.

The impact of TNF on bone remodeling is summarized in figure 1.6 on page 13.

1.4.3 Induction of Osteogenic Differentiation *in vitro*

Osteogenic differentiation of ASC *in vitro* can be induced by molecules of the transforming growth factor beta (TGF β) superfamily, as e.g. by bone morphogenetic protein 2 (BMP2), but also by glucocorticoids as dexamethasone [Lindroos et al., 2011; Kroeze et al., 2011]. Since BMP2-mediated osteogenic differentiation of ASC is less well described and since there are indications that ASC do not have a functional canonical BMP2 signaling pathway, suggesting that BMP2 may not influence the osteogenic fate of these cells [Zuk et al., 2011], induction of osteogenic differentiation of ASC in this study was done using cell culture medium supplemented with dexamethasone, ascorbic acid and β -glycerophosphate.

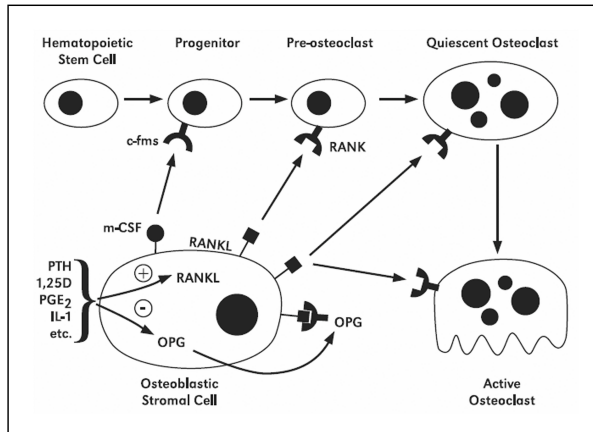


Figure 1.6: The role of TNF in bone remodeling. TNF, as other pro-inflammatory stimuli like IL1, stimulates RANKL expression on the surface of osteoblasts. RANKL binds to a receptor on the surface of osteoclast precursors which is called RANK. This stimulates osteoclast precursors to differentiate into mature osteoclasts, but also increases the resorptive activity of mature osteoclasts. To fast shut down stimulation of osteoclastic differentiation, osteoblasts secrete osteoprotegerin (OPG), a soluble factor binding RANKL and thus preventing it from activating the RANK receptor. Besides IL1, also parathyroid hormone (PTH), 1,25 dihydroxy D (calcitriol, the active form of vitamin D₃) and prostaglandin E2 (PGE2) stimulate RANKL expression by osteoblasts, but also expression of macrophage colony stimulating factor (M-CSF), which induces differentiation of pre-osteoclast precursors into pre-osteoclasts. Thus, the osteoclastic differentiation rate is tightly bound to the number and activity of osteoblasts to balance bone resorption and bone formation. Illustration taken from [Office of the Surgeon General (U.S.), 2004].

The Role of β -Glycerophosphate in Induction of Osteogenic Differentiation

β -Glycerophosphate serves as a source of inorganic phosphate ions after hydrolyzation through phosphatases as alkaline phosphatase [Chung et al., 1992]. In addition, β -glycerophosphate induces ALPL activity in both the initiation and the propagation phase of matrix mineralization [Orimo and Shimada, 2008]. The phosphate ions liberated from β -glycerophosphate react with extracellular calcium ions to form minerals of tricalcium orthophosphate to build up the calcified extracellular matrix of bony tissue. Via this general mechanism, β -glycerophosphate can promote osteogenic differentiation of a broad range of osteoblastic progenitor cells across different species.

The β -glycerophosphate concentration used here was 10 mM, which is in accordance with all publications on osteogenic differentiation of mesenchymal stem cells that were analyzed [Jaiswal et al., 1997; Wang et al., 2006; Hou et al., 2007; Jaeger et al., 2008; Celebi et al., 2010; Liu et al., 2010].

The Role of Ascorbic Acid in Induction of Osteogenic Differentiation

Ascorbic acid is a water-soluble organic compound that cannot be synthesized by humans and is designated as vitamin C. Dietary deficiency in ascorbic acid will result in scurvy, a disease characterized by weakening of the extracellular matrix [Munday, 2003]. The major component of the organic extracellular matrix of connective tissue in general and bone in special is collagen, and ascorbic acid was found to play an important role in the biosynthesis of collagens, as is illustrated in figure 1.7 on page 14.

From these findings, it results that a portion of all active prolyl hydroxylases catalyzes the oxidative decarboxylation of α -ketoglutarate without simultaneously hydroxylating collagen proline residues, which *vice versa* increasingly reduces the portion of active hydroxylases. Connective tissue made from such insufficiently hydroxylated collagen fibers is very weak, since

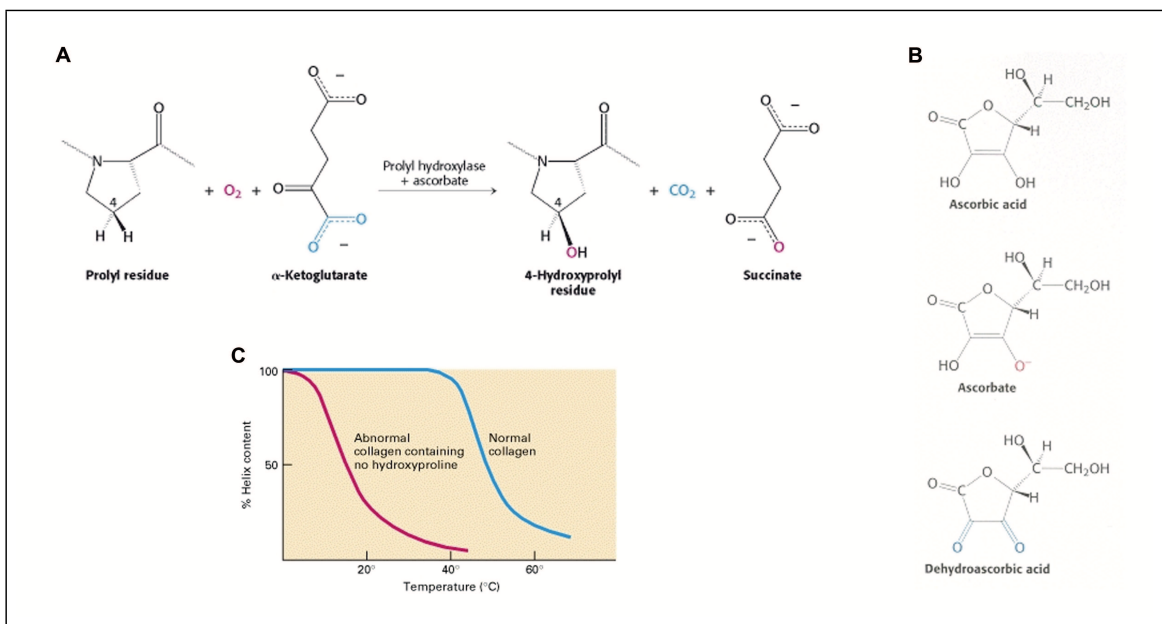


Figure 1.7: The role of ascorbic acid in collagen biosynthesis. In collagen biosynthesis, an enzyme called prolyl hydroxylase catalyzes the transfer of an oxygen atom from molecular oxygen to a collagen proline residue and thus generates hydroxyproline (A). The remaining oxygen atom is transferred to α -ketoglutarate, which subsequently decarboxylates into succinate. Activation of molecular oxygen is assisted by an Fe^{2+} ion in the hydroxylase's active center. However, the enzyme can also convert α -ketoglutarate into succinate without hydroxylating proline, which leaves one oxygen atom in the hydroxylase's catalytic center and thus inactivates it. (B) In order to regenerate the prolyl hydroxylase in that case, the oxidized catalytic center is reduced by ascorbate, which in turn oxidizes ascorbate to dehydroascorbic acid. Illustrations taken from [Berg et al., 2002]. (C) Insufficient hydroxylation of collagen prolines, as a result of dietary ascorbic acid deficiency, reduces the extent of hydrogen bonding within the collagen helices and makes them lose their native conformation even below body temperature. Illustration taken from [Lodish et al., 1999].

hydrogen bonding between collagen fibers is impaired, resulting in increased appearance of skin and blood vessel lesions as well as bone fragility seen in diseases as scurvy and Ehlers-Danlos syndrome.

Ascorbic acid regenerates the inactivated hydroxylases by reducing the ferrous ion in their active center and thereby itself is oxidized [Myllyharju, 2008]. Therefore, it increases overall activity of prolyl hydroxylases and thus the extent of hydroxylation of collagen proline residues to yield the normal strength of connective tissue.

Besides its obvious importance in collagen biosynthesis, the role of ascorbic acid in osteogenic differentiation on the molecular level is hardly characterized. In a broad gene expression analysis, treatment of mouse MC3T3-E1 osteoblast precursor cells with 280 μM ascorbic acid was found to alter the expression of genes involved in the regulation and synthesis of extracellular matrix, cell-matrix and cell-cell interaction, cell cycle progression, cell growth and structure, as well as apoptosis [Carinci et al., 2005]. The results of a gene expression analysis investigating the effect of treatment of the same cell type with both the same ascorbic acid concentration and 10 mM β -glycerophosphate are in line with what was found for ascorbic acid alone: distinct cyclins were down- and anti-proliferative factors were simultaneously upregulated to promote exit from the cell cycle [Beck et al., 2001]. At the same time, matrix-remodeling factors were induced.

Since a change in gene expression does not necessarily translate into a change in protein activity, a high throughput analysis of the kinome, i.e. the entity of kinases, involved in osteogenic differentiation of MC3T3-E1 mouse pre-osteoblasts treated with β -glycerophosphate and 280 μM ascorbic acid substantiated the gene expression data mentioned above and revealed that the process of osteogenic differentiation involves regulation of at least the Mapk and Wnt signaling pathways as well as regulation of the factors Akt, Fak, Pka, Pkc and Vegf [Chaves Neto et al., 2011].

Ascorbic acid treatment of human bone marrow-derived MSC was reported to induce effects on the extent of osteogenic differentiation in dependency of its concentration. Medium containing an ascorbic acid concentration below or equal to 250 μM induced MSC proliferation, whereas higher concentrations decreased proliferation rates and were beneficial for subsequent osteogenic as well as adipogenic differentiation [Choi et al., 2008]. Human ASC cultured in medium containing 250 μM ascorbic acid were also found to increase proliferation rates without inducing osteogenic differentiation [Potdar and D'Souza, 2010]. Moreover, the loss of differentiation potency usually occurring with increasing duration of cell culture was prevented, and multipotency and pluripotency markers as CD34 and *POU5F1* (also designated as *OCT4*), respectively, continued to be expressed for up to four weeks.

Hence, a low concentration of ascorbic acid was found to keep mesenchymal stem cells in an undifferentiated and proliferative state *in vitro*, whereas higher concentrations promoted their differentiation. In this study, ascorbic acid was used at a comparatively high concentration of 1.5 mM to have an inductive effect on promotion of bone-like matrix collagen synthesis and osteogenic differentiation.

The ascorbic acid concentration used was 0.25 g/l, which corresponds to 1.42 mM and lies in the middle of the very broad range of ascorbic acid concentrations used for osteogenic differentiation of MSC, ranging from as little as 0.000284 mM [Wang et al., 2006; Hou et al., 2007] over 0.25 mM [Jaiswal et al., 1997] and 0.8 mM [Liu et al., 2010] to as much as 50 mM [Jaeger et al., 2008] or even 284 mM [Celebi et al., 2010].

The Role of Dexamethasone in Induction of Osteogenic Differentiation

Dexamethasone belongs to the group of artificial glucocorticoids, i.e. it is a synthetic steroid hormone inspired by the naturally occurring steroid hormones cortisol and corticosteron that *in vivo* are produced by the nephric adrenal gland. After freely diffusing over the cell membrane, the hydrophobic glucocorticoid binds its receptor, a transcription factor belonging to the family of nuclear hormone receptors (see figure 1.8 on page 17).

The molecular mechanism of dexamethasone-induced osteogenic differentiation is only partially understood. In primary human osteoblasts derived from trabecular bone explants, dexamethasone was found to increase expression of the osteogenic marker genes *RUNX2* and osteocalcin (*OCN*) [Viereck et al., 2002]. In human endometrial stromal and myometrial smooth muscle cells, dexamethasone significantly increased the expression of the *ZBTB16* gene and its protein product via an AP1-dependent mechanism and also caused nuclear translocalization of the ZBTB16 transcription factor [Fahnenstich et al., 2003]. Expression of *Wwtr1* (earlier designated as *Taz*), a co-activator of *Runx2*, was upregulated by dexamethasone in rat MSC [Hong et al., 2009]. By binding to diverse SMAD molecules, TAZ controls their nuclear translocalization and transcriptional activity and is therefore an important regulator in TGF β -mediated developmental processes [Varelas et al., 2008]. In bovine vascular pericytes, the dexamethasone-promoted osteogenesis was reported to be accompanied not only by upregulation of alkaline phosphatase activity and extracellular matrix calcium content, but also by downregulation of calcification-inhibitor molecules as osteopontin and matrix Gla protein [Kirton et al., 2006].

Dexamethasone-induced osteogenic differentiation was reported to occur most strongly in early cell culture passages [Beloti and Rosa, 2005] and in an exposure time-dependent manner. This effect could be confirmed even after implantation of dexamethasone-treated MSC into immune-deficient mice [Song et al., 2009]. There is evidence that the presence of dexamethasone is only required during the initiation of osteogenic differentiation *in vitro*. Short-term treatment of mouse MC3T3-E1 osteo-progenitor cells with a low concentration of less or equal 0.1 μ M dexamethasone promoted osteogenic differentiation induced by 280 μ M ascorbic acid and 10 mM β -glycerophosphate in a dose-dependent manner, but acted inhibitory in the long run [Park, 2010].

As was stated before for ascorbic acid, dexamethasone also has a concentration-dependent effect on the extent of osteogenic differentiation of MSC. This effect is biphasic, i.e. low dexamethasone concentrations affecting osteogenic differentiation in a way directly opposed to that of high dexamethasone concentrations.

High concentrations of dexamethasone, lying in the range of those applied clinically for treatment of chronic inflammatory diseases and ranging from 10^{-6} to 10^{-7} M, which is 30 times higher than the concentrations of endogenous steroid hormones, were found to decrease expression of the co-activator of *Runx2*, *Taz*, and lowered activity of alkaline phosphatase in rat bone marrow-derived MSC, whereas low concentrations, ranging from 10^{-8} to 10^{-9} M, had the opposite effect on alkaline phosphatase [Hong et al., 2009].

Treatment of mouse osteoblasts with a low concentration of the glucocorticoid corticosterone upregulated the levels of diverse Wnts, whereas a higher concentration lowered them [Mak et al., 2009]. These Wnts are important mediators of osteogenic differentiation and auto-stimulatory keep osteoblasts in a differentiated state, whereas they induce osteogenic differentiation of osteoblast precursors.

In addition to the WNT pathway, glucocorticoids were found to regulate the MAP kinase pathway in a dose-dependent manner. With increasing concentration of the glucocorticoid, the

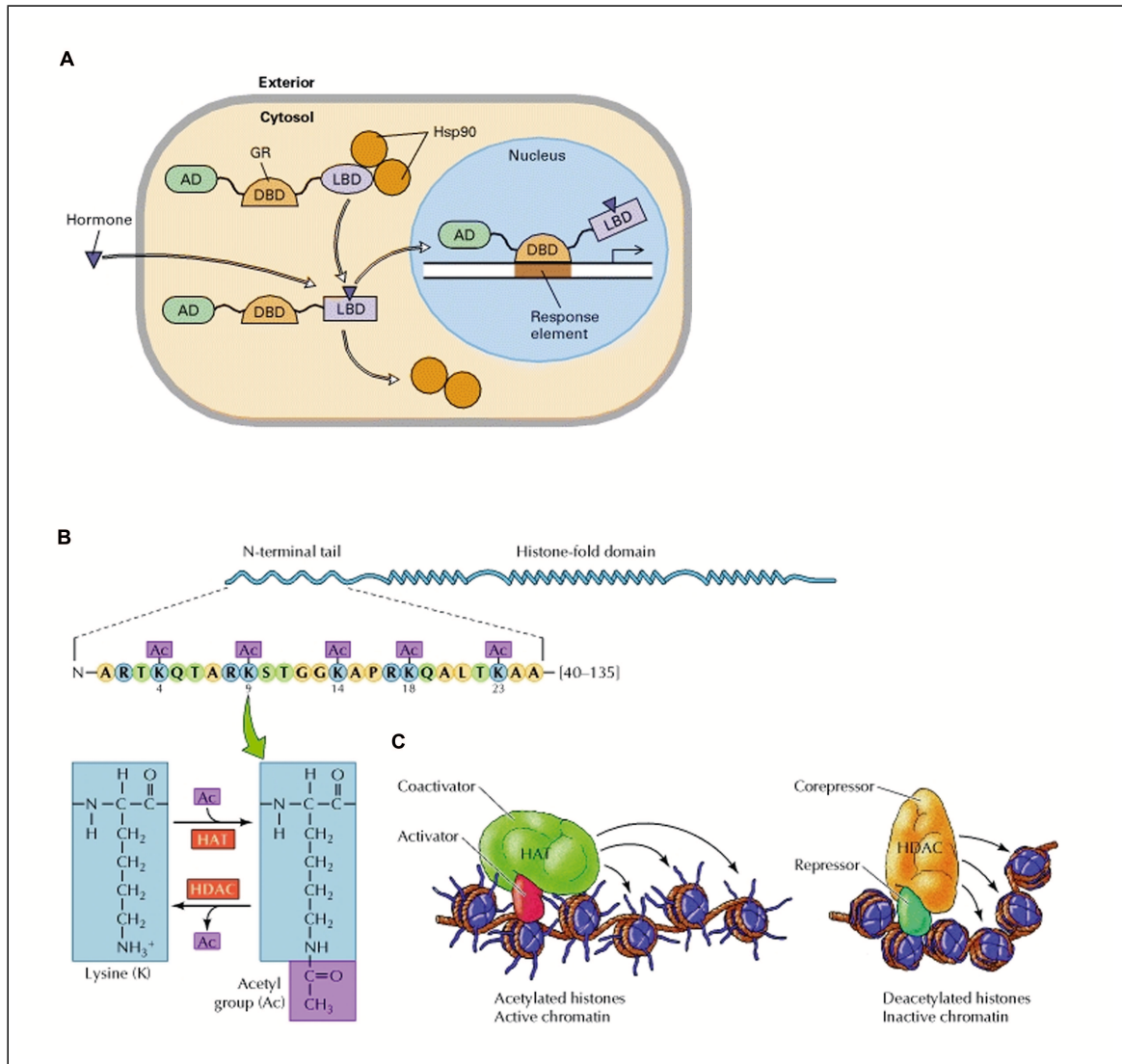


Figure 1.8: The role of glucocorticoids in regulation of gene expression. (A) After diffusing over the cell membrane, the lipophilic glucocorticoid hormone binds its receptor (GR) which, in the absence of hormone, is inactivated by binding of a heat shock protein (Hsp90) to the receptor's ligand-binding domain (LBD). After glucocorticoid-binding, the LBD undergoes a conformational change that enables the heat shock protein to bind, and the glucocorticoid-GR complex translocalizes from the cytoplasm to the nucleus. In the nucleus, the DNA-binding domain (DBD) of the complex binds to glucocorticoid response elements in the promoters of target genes and thus enables the activation domain (AD) to stimulate transcription of target genes. (B) Transcriptional activation by glucocorticoid receptors occurs by recruitment of histone acetyl transferases (HATs) that catalyze the acetylation of lysine residues at the N-terminal tails of histones. Since each acetylation replaces the positive charge of a lysine ammonium group by an uncharged acetyl group, the ionic attraction between the positive charge of the histone and the negative charge of the de-protonated phosphate groups of the DNA backbone diminishes, resulting in de-condensing of the DNA to make it more accessible for transcription factors and the multimeric RNA polymerase transcriptional apparatus. (C) Thus, regulation of histone acetylation is a means for transcriptional activation (by HATs) or repression (by histone de-acetylases, HDACs). Illustrations taken and modified from [Cooper and National Center for Biotechnology Information (U.S.), 2000].

activity of JUN was decreased, and the reduced JUN activity subsequently reduced proliferation of MSC [Carcamo-Orive et al., 2010]. Therefore, a high concentration of dexamethasone of approximately 10^{-6} M promoted adipogenesis of bone marrow-derived MSC, whereas a ten-times lower concentration of 10^{-7} M yielded a much lesser reduction in proliferation and thus a proper biochemical environment for osteogenesis.

In spinal ligament cells *in vitro*, dexamethasone dose-dependently reduced proliferation with increasing concentration, but simultaneously increased alkaline phosphatase activity [Murata et al., 2004]. The same was true for bone marrow-derived MSC [Walsh et al., 2001]. At a 10^{-8} M, the number of alkaline phosphatase-expressing cells and the intensity of expression were increased, whereas expression of the osteo-progenitor marker antigen STRO-1 was reduced. With a dexamethasone concentration increasing over 10^{-7} to 10^{-6} M, the proliferation rate was increasingly reduced, accompanied by an increase in alkaline phosphatase activity.

Even translating a low dose of dexamethasone into the temporal dimension as a short-term treatment confirmed the biphasic action of this synthetic glucocorticoid: Short-term administration of dexamethasone to ascorbic acid- and β -glycerophosphate-treated MC3T3-E1 mouse osteo-progenitor cells promoted their osteogenic differentiation, whereas long-term treatment had a rather inhibitory effect [Park, 2010].

Hence, both high concentrations and long-term treatment with glucocorticoids were found to inhibit osteogenic differentiation *in vitro* and to promote a phenotype of bone resorption *in vivo*, whereas low concentrations *in vitro* promoted osteogenic differentiation of diverse precursor cell types.

It has to be added that such a biphasic behavior on osteogenic differentiation was reported also for other regulators of bone metabolism. Parathyroid hormone (PTH) stimulates bone resorption as well as bone formation, low PTH concentrations resulting in bone formation, and high concentrations stimulating bone resorption *in vivo* [Office of the Surgeon General (U.S.), 2004]. The sex hormone estrogen showed a similar dose-dependent effect on bone metabolism *in vivo*, low concentrations increasing bone formation, but high concentrations leading to closure of the articular growth plates in the adult female. Thus, bone metabolism is regulated in a biphasic fashion by a variety of factors.

The dexamethasone concentration used here was 1 μ M, which lies at the upper end of the concentrations published on osteogenic differentiation of MSC, ranging from 0.01 μ M [Celebi et al., 2010] over 0.1 μ M [Jaiswal et al., 1997; Wang et al., 2006; Hou et al., 2007; Liu et al., 2010] to 1 μ M [Walsh et al., 2001; Murata et al., 2004].

1.5 Experimental Outline

To investigate whether TNF has any specific effect on osteogenic differentiation of ASC, I analyzed expression and activity of a variety of osteogenic markers. As early hallmarks of osteogenic differentiation, expression of the transcription factor *ZBTB16*, an upstream regulator of RUNX2 expression and activity, was analyzed just as DNA binding activity of RUNX2. The transcription factor RUNX2 has a key role in osteogenic differentiation and induces expression of a plethora of genes involved in this differentiation process. I analyzed activation of this factor to bind to the regulatory sequence of its target genes. Besides these osteogenic transcription factors and as later markers of osteogenic differentiation, I analyzed the expression and activity of the key enzyme involved in extracellular matrix calcification, alkaline phosphatase, and the extent of extracellular matrix calcium content.

These analyses were supplemented by the surveillance of more basal cellular parameters as proliferation, cell cycle and metabolic activity. Analysis of the expression of the TNF receptor genes and proteins as well as analysis of activation of the signal transduction pathways downstream of these receptors, i.e. the NF κ B, MAPK and apoptosis pathway, completed this study.

All parameters were investigated for TNF-treated ASC in comparison to osteogenically stimulated and unstimulated ASC. ASC treated with both TNF and osteogenic stimulants were analyzed to elucidate the impact of TNF under osteogenic conditions.

Chapter 2

Materials

The following pages contain the devices, software and consumables used in this work and are organized in a tabulated manner.

Table 2.1: Devices used.

	Device	additional information	Manufacturer	Residence city	country
general laboratory equipment	JL-200	analytical balance	Chyo		
	SONOREX DIGITEC	ultrasound water bath	Carl Roth GmbH + Co. KG	Karlsruhe	Germany
	REAX 2000	test tube shaker	Heidolph Instruments GmbH & Co. KG	Schwabach	Germany
	Unimax	orbital platform shaker with heating module and incubator hood	Heidolph Instruments GmbH & Co. KG	Schwabach	Germany
	BTR5-12V	tube roller mixer	Ratek Instruments Pty. Ltd.	Victoria	Australia
	5417 R and 5810 R	centrifuges	Eppendorf AG	Hamburg	Germany
	Easypet Reference and Research Transferpette S -8 and S -12	pipettes pipettes	Eppendorf AG BRAND GmbH + Co KG	Hamburg Wertheim	Germany Germany
cell culture	CB 150	humidified atmosphere incubator for 37 °C and 5 % CO ₂	BINDER GmbH	Tuttlingen	Germany
	NuncFlow Model Safeflow 1.2	laminar airflow cabinet	Nunc GmbH & Co. KG	Langenselbold	Germany
	VACUSAFE comfort	liquid exhaustion system	INTEGRA Biosciences GmbH	Fernwald	Germany
	Cell Counter Model DT	cell number counter	Schärfe System GmbH	Reutlingen	Germany
microscopes	Axiovert 25 and 40 C	inverse bright-field phase contrast microscopes	Carl Zeiss MicroImaging GmbH	Göttingen	Germany
	Axio Scope.A1 and Axio Observer.Z1	upright and inverse fluorescence microscopes	Carl Zeiss MicroImaging GmbH	Göttingen	Germany
	TCS SP2	inverse confocal fluorescence microscope	Leica Microsystems GmbH	Wetzlar	Germany
	AxioCam ICc1	microscope camera at bright-field microscope	Carl Zeiss MicroImaging GmbH	Göttingen	Germany
	AxioCam MRc and MRm	microscope cameras at upright and inverse fluorescence microscope	Carl Zeiss MicroImaging GmbH	Göttingen	Germany
microplate reader	anthos 2010	filter-based optical density microplate reader	anthos Mikrosysteme GmbH	Krefeld	Germany
	infinite M200	monochromator-based fluorescence, luminescence and optical density microplate reader	Tecan Deutschland GmbH	Crailsheim	Germany
RNA and gene expression	Bosch KN83.1	microwave oven	Carl Roth GmbH + Co. KG	Karlsruhe	Germany
	Sub-Cell Model 96 Complete System	agarose gel electrophoresis unit	Bio-Rad Laboratories GmbH	München	Germany
	ChemiDoc MP System	gel documentation system	Bio-Rad Laboratories GmbH	München	Germany
	NanoDrop ND-1000	spectrophotometer	PEQLAB Biotechnologie GmbH	Erlangen	Germany
	NuncFlow AURA PCR	passive PCR cabinet	Nunc GmbH & Co. KG	Langenselbold	Germany
	MyCycler 7500 Real-Time PCR System	thermal cycler thermal cycler for real-time PCR	Bio-Rad Laboratories GmbH Life Technologies GmbH	München Darmstadt	Germany Germany
flow cytometry	FACSCalibur	flow cytometer	BD Biosciences AG	Heidelberg	Germany
	Flow Supply System	sheath fluid volume extension system for flow cytometer	BD Biosciences AG	Heidelberg	Germany

Table 2.2: Software used.

Software	<i>additional information</i>	Developer	Residence <i>city</i>	<i>country</i>
Windows 7 Professional SP1	operating system	Microsoft Deutschland GmbH	Unterschleißheim	Germany
Mac OS 9.2.2	operating system	Apple Inc.	Cupertino	USA
WinRead 2.36	anthos microplate reader control	anthos Mikrosysteme GmbH	Krefeld	Germany
i-control 1.5	TECAN microplate reader control	Tecan Deutschland GmbH	Crailsheim	Germany
NanoDrop 1000 3.7.1	NanoDrop control	Fisher Scientific GmbH	Schwerte	Germany
Axiovision 40 Rel. 4.8.0.0	bright-field microscope image acquisition	Carl Zeiss MicroImaging GmbH	Göttingen	Germany
Axiovision 40 Rel. 4.8.2.0	fluorescence microscope image acquisition	Carl Zeiss MicroImaging GmbH	Göttingen	Germany
Leica Confocal Software 2.61	confocal fluorescence microscope image acquisition	Leica Microsystems GmbH	Wetzlar	Germany
Volocity Demo 6.0.0	microscope image processing	PerkinElmer Life and Analytical Sciences, Inc.	Rodgau	Germany
Photoshop CS 8.0.1	image processing	Adobe Systems Software Ireland Limited	Dublin	Ireland
Sequence Detection Software 1.4	real-time cycler control and data analysis	Life Technologies GmbH	Darmstadt	Germany
CellQuest Pro 4.0.2	flow cytometer control	BD Biosciences AG	Heidelberg	Germany
FlowJo 7.6.3	flow cytometer data analysis	Tree Star, Inc.	Ashland	USA
SPSS Statistics 19	statistical data analysis	IBM Deutschland GmbH	Ehningen	Germany
SigmaPlot 11	scientific plot generation	Systat Software GmbH	Erkrath	Germany
LibreOffice 3.3.3	open source office package	The Document Foundation	Wiesbaden	Germany
Office Professional Plus 2007	proprietary office package	Microsoft Deutschland GmbH	Unterschleißheim	Germany
TeX Live 2011	TeX distribution	TeX Users Group	Heidelberg	Germany
Ghostsript 9.02	open source postscript package	Artifex Software, Inc.	San Rafael	USA
GSview 4.9	open source postscript viewer	Ghostgum Software Pty Ltd.	Glen Waverley	Australia
TeXnicCenter 1.0 Stable Release Candidate 1	TeX editor	The TeXnicCenter Team		
JabRef 2.6	open source reference manager	The JabRef Team	New York	USA
Endnote X2	proprietary reference manager	Thomson Reuters		

Table 2.3: Consumables used.

	Consumable	additional information	Manufacturer	Residence city	country	catalog #
ASC isolation	CD34 Progenitor Cell Selection System	kit for labeling cells with an CD34 antibody conjugated to a magnetic bead	Life Technologies GmbH	Darmstadt	Germany	113-01D
	DynaMag-15	permanent magnet for holding one 15 ml tube with cell suspension during CD34 ⁺ cell isolation	Life Technologies GmbH	Darmstadt	Germany	123-01D
	metal sieve	stainless steel with wire gauze, 800 µm pore size, 100 mm diameter x 40 mm height, ISO 3310/1	RETSCH GmbH	Haan	Germany	60.106.000800
	Albumin solution from bovine serum (BSA)	35 % in DPBS, sterile-filtered, BioXtra, endotoxin tested, suitable for cell culture	Sigma-Aldrich Chemie GmbH	Taufkirchen	Germany	A7979
	Cell Strainer, 100 µm, yellow	sterile, nylon mesh	BD Biosciences AG	Heidelberg	Germany	352360
	Cell Strainer, 40 µm, blue	sterile, nylon mesh	BD Biosciences AG	Heidelberg	Germany	352340
	Collagenase NB 4	from Clostridium histolyticum, collagenase class I and class II and proteolytic activity	SERVA Electrophoresis GmbH	Heidelberg	Germany	17454
cell counting	CASY clean	liquid system cleaning solution for CASY cell counter	Roche Applied Science	Mannheim	Germany	05651786001
	CASY cups	disposable sample tube for cell suspension in CASY cell counting	Roche Applied Science	Mannheim	Germany	05651794001
	CASY ton	isotonic saline solution for cell suspension in CASY cell counting	Roche Applied Science	Mannheim	Germany	05651808001
cell culture medium	DMEM	high glucose, GlutaMAX, pyruvate, phenol red, w/o HEPES	Life Technologies GmbH	Darmstadt	Germany	31966
	Fetal Calf Serum (FCS)	from South America, virus and mycoplasma tested, health class 1a	PAN Biotech GmbH	Aidenbach	Germany	3302-P281305
	Penicillin-Streptomycin (P/S), liquid	10,000 units/ml	Life Technologies GmbH	Darmstadt	Germany	15140-122
osteogenic stimulants	L-Ascorbic acid	powder, cell culture tested, gamma-irradiated	Sigma-Aldrich Chemie GmbH	Taufkirchen	Germany	A4403
	β-Glycerol phosphate	disodium salt pentahydrate	Sigma-Aldrich Chemie GmbH	Taufkirchen	Germany	50020
	Dexamethasone	powder, BioReagent, suitable for cell culture, ≥ 97 %	Sigma-Aldrich Chemie GmbH	Taufkirchen	Germany	D4902
adipogenic stimulants	3-Isobutyl-1-methylxanthin (IBMX)	≥ 99 % (HPLC), powder	Sigma-Aldrich Chemie GmbH	Taufkirchen	Germany	15879
	Insulin	human, recombinant (expressed in yeast)	Sigma-Aldrich Chemie GmbH	Taufkirchen	Germany	12643
	Indomethacin	≥ 99 % (TLC)	Sigma-Aldrich Chemie GmbH	Taufkirchen	Germany	17378
TNF	Tumor Necrosis Factor (TNF)	human, recombinant (expressed in yeast)	Sigma-Aldrich Chemie GmbH	Taufkirchen	Germany	T0157
other cell culture solutions	Dulbecco's PBS (DPBS, 1x)	without Ca and Mg, sterile, 500 ml	PAA Laboratories GmbH	Cölbe	Germany	H15-002
	Trypsin-EDTA	1x, 0.25 %, with phenol red	Life Technologies GmbH	Darmstadt	Germany	25200
cell culture plasticware	Cell culture multiwell plate, 6 well	sterile, polystyrene	Greiner Bio-One GmbH	Frickenhausen	Germany	657160
	Cell culture multiwell plate, 12 well	sterile, polystyrene	Greiner Bio-One GmbH	Frickenhausen	Germany	665180
	Cell culture multiwell plate, 24 well	sterile, polystyrene	Greiner Bio-One GmbH	Frickenhausen	Germany	662160
	Cell culture multiwell plate, 48 well	sterile, polystyrene	Greiner Bio-One GmbH	Frickenhausen	Germany	677180
	Cell culture plate, 96 well	sterile, polystyrene	Greiner Bio-One GmbH	Frickenhausen	Germany	655180
	Cell culture flask, 25 cm ²	sterile, polystyrene	Greiner Bio-One GmbH	Frickenhausen	Germany	690175
	Cell culture flask, 75 cm ²	sterile, polystyrene	Greiner Bio-One GmbH	Frickenhausen	Germany	658175
	Pipette, 2 ml	sterile, polystyrene	Greiner Bio-One GmbH	Frickenhausen	Germany	710180
	Pipette, 5 ml	sterile, polystyrene	Greiner Bio-One GmbH	Frickenhausen	Germany	606180
	Pipette, 10 ml	sterile, polystyrene	Greiner Bio-One GmbH	Frickenhausen	Germany	607180
Pipette, 25 ml	sterile, polystyrene	Greiner Bio-One GmbH	Frickenhausen	Germany	760180	
cell culture glassware	Fisherbrand Pasteur Pipette	230 mm, glass	Fisher Scientific GmbH	Schwerte	Germany	10786941

Table 2.3: Consumables used.

Consumable	additional information	Manufacturer	Residence city	country	catalog #	
diverse plasticware	Pipette tip, 200 µl, yellow	sterile, polypropylene	SARSTEDT AG & Co.	Nümbrecht	Germany	70.760.002
	Pipette tips, 100 – 1000 µl	sterile, polypropylene	Greiner Bio-One GmbH	Frickenhausen	Germany	686290
	Tube, 12 ml	sterile, polystyrene, conical bottom	Greiner Bio-One GmbH	Frickenhausen	Germany	164161
	Tube, 15 ml	sterile, polypropylene, conical bottom	Greiner Bio-One GmbH	Frickenhausen	Germany	188271
	Tube, 50 ml	sterile, polypropylene, conical bottom	Greiner Bio-One GmbH	Frickenhausen	Germany	227261
	Standard and Safe-Lock reaction tubes	unsterile, polypropylene	Eppendorf AG	Hamburg	Germany	0030.120.xxx
	Microplate, 96 well	for optical density determination	Greiner Bio-One GmbH	Frickenhausen	Germany	655101
	Rotilabo fluid reservoir, 55 ml	unsterile, PVC	Carl Roth GmbH + Co. KG	Karlsruhe	Germany	E830.2
	POLYMER PLUS	Latex examination gloves	Brimon	Hamburg	Germany	11034
	diverse solutions	Aqua ad iniectabilia	ultra pure water	B. Braun Melsungen AG	Melsungen	Germany
Triton X-100		non-ionic detergent	Sigma-Aldrich Chemie GmbH	Taufkirchen	Germany	93420
Tween 20		non-ionic detergent	Sigma-Aldrich Chemie GmbH	Taufkirchen	Germany	P1379
crystal violet assay	Crystal Violet	for microscopy (Bact., Bot., Hist., Vit.), indicator (pH 0.1 - 2.0)	Sigma-Aldrich Chemie GmbH	Taufkirchen	Germany	61135
	Isopropanol	molecular biology grade	SERVA Electrophoresis GmbH	Heidelberg	Germany	39559.02
	Acetic acid	absolute („glacial“)	Merck KGaA	Darmstadt	Germany	100063
ALPL assays	Fast Red Violet	LB Salt, Technical grade	Sigma-Aldrich Chemie GmbH	Taufkirchen	Germany	F3381
	Naphthol AS-MX phosphate	powder, ≥ 99 % (HPLC)	Sigma-Aldrich Chemie GmbH	Taufkirchen	Germany	N4875
	2-Amino-2-methyl-1,3-propanediol (AMPED)	≥ 99 %	Sigma-Aldrich Chemie GmbH	Taufkirchen	Germany	A9754
	Tris Buffered Saline (TBS)	10x solution	Sigma-Aldrich Chemie GmbH	Taufkirchen	Germany	T5912
	4-Nitrophenyl phosphate	para-nitrophenyl phosphate (pNPP) disodium salt hexahydrate	AppliChem GmbH	Darmstadt	Germany	A1442
	Magnesium chloride (MgCl ₂) hexahydrate	Molecular biology grade	AppliChem GmbH	Darmstadt	Germany	A4425
	PMSF	Benzylsulfonyl fluoride, Phenylmethanesulfonyl fluoride	AppliChem GmbH	Darmstadt	Germany	A0999
Sodium hydroxide (NaOH) standard solution	2 M	Sigma-Aldrich Chemie GmbH	Taufkirchen	Germany	3525	
ECM mineralisation assay	o-Cresolphthalein Complexone	indicator (for complexometry)	Sigma-Aldrich Chemie GmbH	Taufkirchen	Germany	64000
	2-Amino-2-methyl-1-propanol (AMP)	purum, ≥ 97.0 % (GC)	Sigma-Aldrich Chemie GmbH	Taufkirchen	Germany	08580
	8-Hydroxyquinoline	ACS reagent, 99 %	Sigma-Aldrich Chemie GmbH	Taufkirchen	Germany	252565
	Hydrochloric acid (HCl)	36.5 - 38.0 %, BioReagent, for molecular biology	Sigma-Aldrich Chemie GmbH	Taufkirchen	Germany	H1758
RUNX2 assay	Nuclear Extract Kit	isolation of total nuclear protein	Active Motif	La Hulpe	Belgium	40010
	TransAM AML-3/Runx2	Transcription Factor ELISA Kit	Active Motif	La Hulpe	Belgium	44496
	Cell scraper	with thin, flexible 2-position blades	SARSTEDT AG & Co.	Nümbrecht	Germany	831832
OPG-ELISA	Nunc-Immuno Plates, 96-well	unsterile, polystyrene, MaxiSorp, flat bottom	Nunc GmbH & Co. KG	Langenselbold	Germany	456537
	human OPG/TNFRSF11B	DuoSet ELISA Development kit	R&D Systems GmbH	Wiesbaden-Nordenstadt	Germany	DY805
	Wash Buffer	for ELISA	R&D Systems GmbH	Wiesbaden-Nordenstadt	Germany	WA126
	Reagent Diluent	for ELISA	R&D Systems GmbH	Wiesbaden-Nordenstadt	Germany	DY995
	Substrate Solution	for ELISA	R&D Systems GmbH	Wiesbaden-Nordenstadt	Germany	DY999
	Stop Solution	for ELISA	R&D Systems GmbH	Wiesbaden-Nordenstadt	Germany	DY994
other assays	BODIPY 493/503	fluorescent stain for neutral lipids and other nonpolar lipids	Life Technologies GmbH	Darmstadt	Germany	D-3922

Table 2.3: Consumables used.

Consumable	additional information	Manufacturer	Residence city	country	catalog #	
	Sodium chloride (NaCl) solution	for molecular biology, 5 M	Sigma-Aldrich Chemie GmbH	Taufkirchen	Germany	S5150
	CellTiter 96 AQueous One Solution	Cell Proliferation (MTS) Assay	PROMEGA GmbH	Mannheim	Germany	G3581
	660 nm Protein Assay	for total soluble protein quantification	Fisher Scientific GmbH	Schwerte	Germany	22662
RNA isolation	Safe Seal Tips Professional Line	filter tips certified free of RNase, DNase, human DNA and PCR inhibitors	Biozym Scientific GmbH	Hessisch Oldendorf	Germany	7700xx
	RNase-ExitusPlus	RNase decontamination solution	AppliChem GmbH	Darmstadt	Germany	A7153
	innuPREP RNA Mini Kit	total RNA isolation kit	Analytik Jena AG	Jena	Germany	845-KS-2040250
	QIAshredder	cell-lysate homogenizer	QIAGEN GmbH	Hilden	Germany	79654
	Ethanol	absolute, gradient grade	Merck KGaA	Darmstadt	Germany	111727
	Water for molecular biology	DEPC-treated, sterile and autoclaved	Carl Roth GmbH + Co. KG	Karlsruhe	Germany	T143.1
RNA electrophoresis	Agarose	For routine use	Sigma-Aldrich Chemie GmbH	Taufkirchen	Germany	A9539
	Tris Acetate-EDTA (TAE) buffer	DNase- and RNase-free, 10x concentrate	Sigma-Aldrich Chemie GmbH	Taufkirchen	Germany	T4038
	Ethidium bromide solution	BioReagent, for molecular biology, 10 mg/ml in H ₂ O	Sigma-Aldrich Chemie GmbH	Taufkirchen	Germany	E1510
	Gel Loading Solution	All-purpose, for native agarose	Life Technologies GmbH	Darmstadt	Germany	AM8556
real-time RT PCR	QuantiTect Rev. Transcription Kit	for cDNA synthesis in real-time two-step RT-PCR	QIAGEN GmbH	Hilden	Germany	205311
	Multiply PCR Plates	96 well, polypropylene	SARSTEDT AG & Co.	Nümbrecht	Germany	721.979.202
	MicroAmp Optical Adhesive Film	optically-clear adhesive film to seal microplates in (real-time) PCR	Life Technologies GmbH	Darmstadt	Germany	4311971
	Power SYBR Green PCR Master Mix	for real-time PCR	Life Technologies GmbH	Darmstadt	Germany	4368708
immunofluorescence	Paraformaldehyde (PFA)	reagent grade, crystalline	Sigma-Aldrich Chemie GmbH	Taufkirchen	Germany	P6148
	Ultra pure bovine serum albumin (BSA)	for immune fluorescence	New England Biolabs GmbH	Frankfurt am Main	Germany	9998
	µ-Slide 8 well	ibiTreat, tissue culture treated	ibidi GmbH	Martinsried	Germany	80826
	Fluoromount-G	fluorescence mounting medium	eBioscience	Frankfurt am Main	Germany	00-4958-02
antibodies	anti-human Lamin A/C	clone 4C11, mouse monoclonal Ab	New England Biolabs GmbH	Frankfurt am Main	Germany	4777
	anti-human NF-κB p65	rabbit polyclonal Ab	New England Biolabs GmbH	Frankfurt am Main	Germany	3987
	anti-human Phospho-c-Jun	rabbit polyclonal Ab	New England Biolabs GmbH	Frankfurt am Main	Germany	9261
	anti-human Phospho-p44/42 MAPK (Erk1/2)	clone D13.14.4E, rabbit monoclonal Ab	New England Biolabs GmbH	Frankfurt am Main	Germany	4370
	anti-human Phospho-p38 MAPK	clone 3D7, rabbit monoclonal Ab	New England Biolabs GmbH	Frankfurt am Main	Germany	9215
	goat anti-rabbit IgG (H+L)	Alexa Fluor 555 F(ab') ₂ fragment, 2 mg/ml	Life Technologies GmbH	Darmstadt	Germany	A-21430
	goat anti-mouse IgG (H+L)	Alexa Fluor 647 F(ab') ₂ fragment, 2 mg/ml	Life Technologies GmbH	Darmstadt	Germany	A-21237
	anti-human TNF receptor 1	clone 16803, mouse monoclonal Ab, isotype IgG1, PE-labeled	R&D Systems GmbH	Wiesbaden-Nordenstadt	Germany	FAB225P
	anti-human TNF receptor 2	clone 80M2, mouse monoclonal Ab, isotype IgG1, FITC-labeled	Biozol Diagnostica Vertrieb GmbH	Eching	Germany	K0040-4
	anti-human CD14	clone 61D3, mouse monoclonal Ab, isotype IgG1, PE-labeled	eBioscience	Frankfurt am Main	Germany	12-0149
	anti-human CD31	clone HC1/6, mouse monoclonal Ab, isotype IgG1, FITC-labeled	Millipore GmbH	Schwalbach/Ts.	Germany	CBL468F
	anti-human CD68	clone Y1/82A, mouse monoclonal Ab, isotype IgG2a, FITC-labeled	eBioscience	Frankfurt am Main	Germany	11-0689
anti-human IgG1	mouse isotype control W3/25, PE-labeled	Acris Antibodies GmbH	Herford	Germany	SM10R	
non-antibody-mediated staining	SYTOX Blue	nucleic acid stain, 5 mM solution in DMSO	Life Technologies GmbH	Darmstadt	Germany	S11348
	Alexa Fluor 594 Phalloidin	actin cytoskeleton stain	Life Technologies GmbH	Darmstadt	Germany	A12381
	Propidium iodide	dead cell nucleic acid stain, 1.0 mg/ml, solution in water	Life Technologies GmbH	Darmstadt	Germany	P3566
	Calcein, AM	live cell stain	Biomol GmbH	Hamburg	Germany	ABD-22002
Flow Cytometry	Round-Bottom Tube	FACS tube w/o cap, unsterile, polystyrene	BD Biosciences AG	Heidelberg	Germany	352008

Table 2.3: Consumables used.

Consumable	additional information	Manufacturer	Residence city	country	catalog #
BD FACSTFlow Sheath Fluid	isotonic saline solution for cell suspension in flow cytometry	BD Biosciences AG	Heidelberg	Germany	342003
BD FACS Clean Solution	sodium hypochlorite and hydroxide containing solution for cleaning the flow cytometer liquid system	BD Biosciences AG	Heidelberg	Germany	340345
BD FACSRinse Solution	sodium azide containing salt solution for rinsing the flow cytometer liquid system after cleaning	BD Biosciences AG	Heidelberg	Germany	340346
PI/RNase Staining Buffer	for staining of cells for flow cytometric cell cycle analysis	BD Biosciences AG	Heidelberg	Germany	550825

Chapter 3

Methods

3.1 Isolation and Culture of ASC

ASC were isolated from adipose tissue obtained from healthy patients having undergone liposuction. The predominant part of the patients was female and aged between 20 and 40 years. The most prominent site of subcutaneous tissue harvesting was the abdominal and the hip region. Figure 3.1 on page 28 gives an overview on the procedure of ASC isolation from adipose tissue obtained by tumescence-based liposuction. Detailed isolation protocols are given below.

3.1.1 Isolation of ASC

The stromal vascular fraction was obtained by collagenase digestion of the adipose tissue of the patient's processed lipoaspirate. The procedure refers to protocols published before by e.g. Patricia Zuk [Zuk et al., 2001]:

1. wash adipose tissue 3x with PBS and transfer 30 ml of tissue to a 50 ml tube
2. add 10 ml of a mixture of Collagenase I and II (6 mg/ml or 0.6 Wunsch units/ml in PBS) to adipose tissue
3. incubate shaking at 100 rpm and 37 °C for 60 min
4. transfer tissue via a 100 µm mesh filter to a new 50 ml tube
5. centrifuge for 10 min at 400 g and room temperature
6. carefully discard supernatant and resuspend pellet in 10 ml PBS (10 % FCS)
7. transfer resuspended cells to new 50 ml tube and centrifuge for 10 min at 400 g and room temperature
8. resuspend pellet in 12 ml DMEM (10 % FCS, 1 % penicillin/streptomycin) and transfer to 75 cm² cell culture flask
9. incubate untouched for 24 h at 37 °C, 5 % CO₂ in a humidified atmosphere

From this primary culture, ASC were isolated via their characteristic expression of CD34 surface antigen by applying a magnetic bead-based cell sorting system. The protocol for doing so was established in our group:

1. add 40 µl CD34 Dynabeads to 7 ml PBS (0.1 % BSA), mount to magnet, discard supernatant, demount tube from magnet and add 4 ml DMEM (10 % FCS, 1 % penicillin/streptomycin)
2. wash cells 2x with PBS

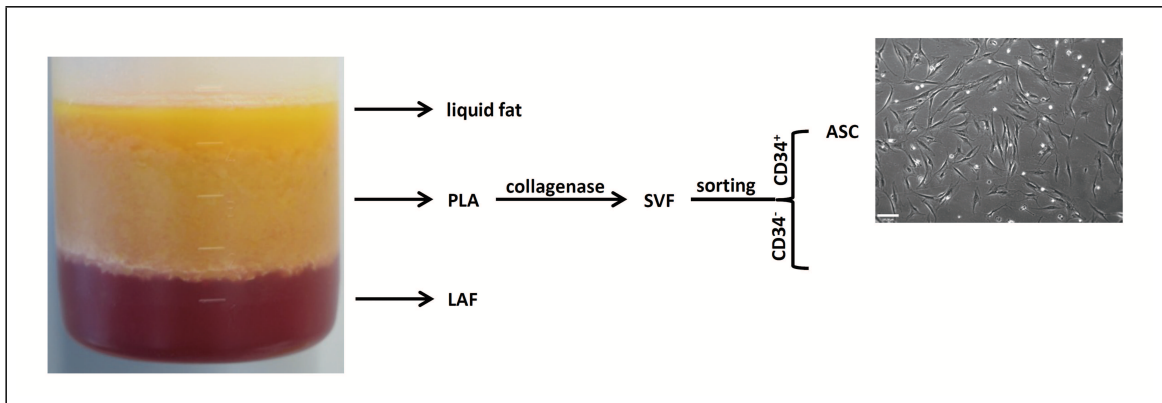


Figure 3.1: Isolation of ASC from adipose tissue. ASC were isolated from processed lipoaspirate (PLA), the non-fluid fraction of tissue obtained following liposuction. The fluid fraction containing liposuction aspirate fluid cells (LAF) was discarded. The PLA was digested by collagenase treatment and thus yielded the stromal vascular fraction (SVF). From this fraction, ASC were purified as the CD34⁺ and plastic-adherent subpopulation. The scale bar corresponds to 120 μm .

3. add 3 ml Dynabead suspension to cells, distribute homogeneously by gently moving flask and incubate for 5 – 10 min at 37 °C, 5 % CO₂ in a humidified atmosphere until beads are bound to cell surface
4. wash cells 2x with PBS, add 1 ml 0.25 % Trypsin and distribute homogeneously by gently moving flask
5. incubate for 5 – 10 min at 37 °C, 5 % CO₂ in a humidified atmosphere until cells are detached
6. resuspend cells in 7 ml PBS (10 % FCS) and transfer to 15 ml tube
7. incubate cells for 10 min at 4 °C on a tube roller mixer
8. transfer cells via a 40 μm mesh filter to a new 15 ml tube
9. mount tube to magnet, discard supernatant, demount tube from magnet and resuspend cells in 7 ml PBS (0.1 % BSA)
10. incubate cells for 10 min at 4 °C on a tube roller mixer
11. mount tube to magnet, discard supernatant, demount tube from magnet and resuspend CD34⁺ cells in 12 ml DMEM (10 % FCS, 1 % penicillin/streptomycin)

This yields the first ASC passage.

3.1.2 ASC Culture

ASC were cultured until 90 % confluency was reached and then passaged into new flasks at an area ratio of one to three, i.e. 75 cm² of 90 % confluent ASC were detached using Trypsin, resuspended in 36 ml DMEM (10 % FCS, 1 % penicillin/streptomycin) and aliquoted into three new 75 cm² flasks at a volume of 12 ml cell suspension each. This was done until passage three was reached. Each passage took three to four days. Passage four was seeding of cells into experimentation. The absence of contaminating monocytes/macrophages and endothelial cells in this culture of primary cells was confirmed by flow cytometry proving the absence of CD14/CD68⁺ and CD31⁺ cells, respectively.

To ascertain the same degree of gas exchange for all formats of cell culture vessels, the height of the medium column over the cell layer was kept constant in relation to the cell culture area, taking 100 μl of medium for each well of a 96-well plate as a reference.

3.1.3 ASC Counting

Unless otherwise noted, ASC were seeded into experimentation at 20,000 cells/cm² growth area. Determination of the cell number was done using electrical current exclusion and pulse area analysis in a CASY system. The principle of this method is described in figure 3.2 on page 30.

Cell counting was done according to the manufacturer's instructions as detailed below:

1. add 100 μ l cell suspension to 10 ml CASY ton in CASY cup
2. perform measurement in appropriate program
3. note viable cells per ml and discard CASY cup with cell solution
4. clean 3x and measure 3x using CASY ton:
 - if less than 100 counts per ml: device is sufficiently cleaned
 - if more than 100 counts per ml: wash again using a new CASY cup with CASYton

3.1.4 ASC Stimulation Media

After seeding, cells were cultured until confluency was reached, which took two to three days. Renewal of the cell culture medium was done every second day. At confluency, culture with distinct stimulation media began, termed day zero, and took up to 28 days.

The differentiation media were termed as follows: US indicates medium without differentiation factors used for the unstimulated ASC control cultures, OS indicates osteogenic differentiation stimulating medium, AS adipogenic differentiation stimulating medium, and TNF TNF-supplemented medium. These media contained the following factors at the indicated concentrations:

	US	OS	TNF	OS+TNF	AS
DMEM, high glucose, GlutaMAX-I	⊕	⊕	⊕	⊕	⊕
FCS	10 %	10 %	10 %	10 %	10 %
penicillin/streptomycin	1 %	1 %	1 %	1 %	1 %
ascorbic acid		0.25 g/l		0.25 g/l	
dexamethasone		1 μ M		1 μ M	1 μ M
β-glycerophosphate		10 mM		10 mM	
TNF			30 IU/ml	30 IU/ml	
IBMX					500 μ M
indomethacin					200 μ M
insulin					10 μ M

These concentrations were chosen in accordance with the current literature published for osteogenic and adipogenic differentiation of mesenchymal stem cells.

The medium for the unstimulated ASC control cultures was supplemented with 10 % FCS, since serum replacements so far failed to support stem cell differentiation equally well as fetal calf serum did [Lund et al., 2009]. In addition, 1 % penicillin/streptomycin, corresponding to 100 units per ml and 100 μ g per ml, respectively, was added to the medium to suppress a possible microbial contamination of the primary tissue.

For osteogenic differentiation, this cell culture medium was supplemented with β -glycerophosphate, ascorbic acid and dexamethasone. The β -glycerophosphate concentration used here was 10 mM, which is in accordance with all publications invoked [Jaiswal et al., 1997; Wang et al., 2006; Hou et al., 2007; Jaeger et al., 2008; Celebi et al., 2010; Liu et al., 2010]. The ascorbic acid concentration used was 0.25 g/l, which corresponds to 1.42 mM. This concentration lies in the middle of the very broad range of ascorbic acid concentrations used for osteogenic differentiation of MSC, ranging from as little as

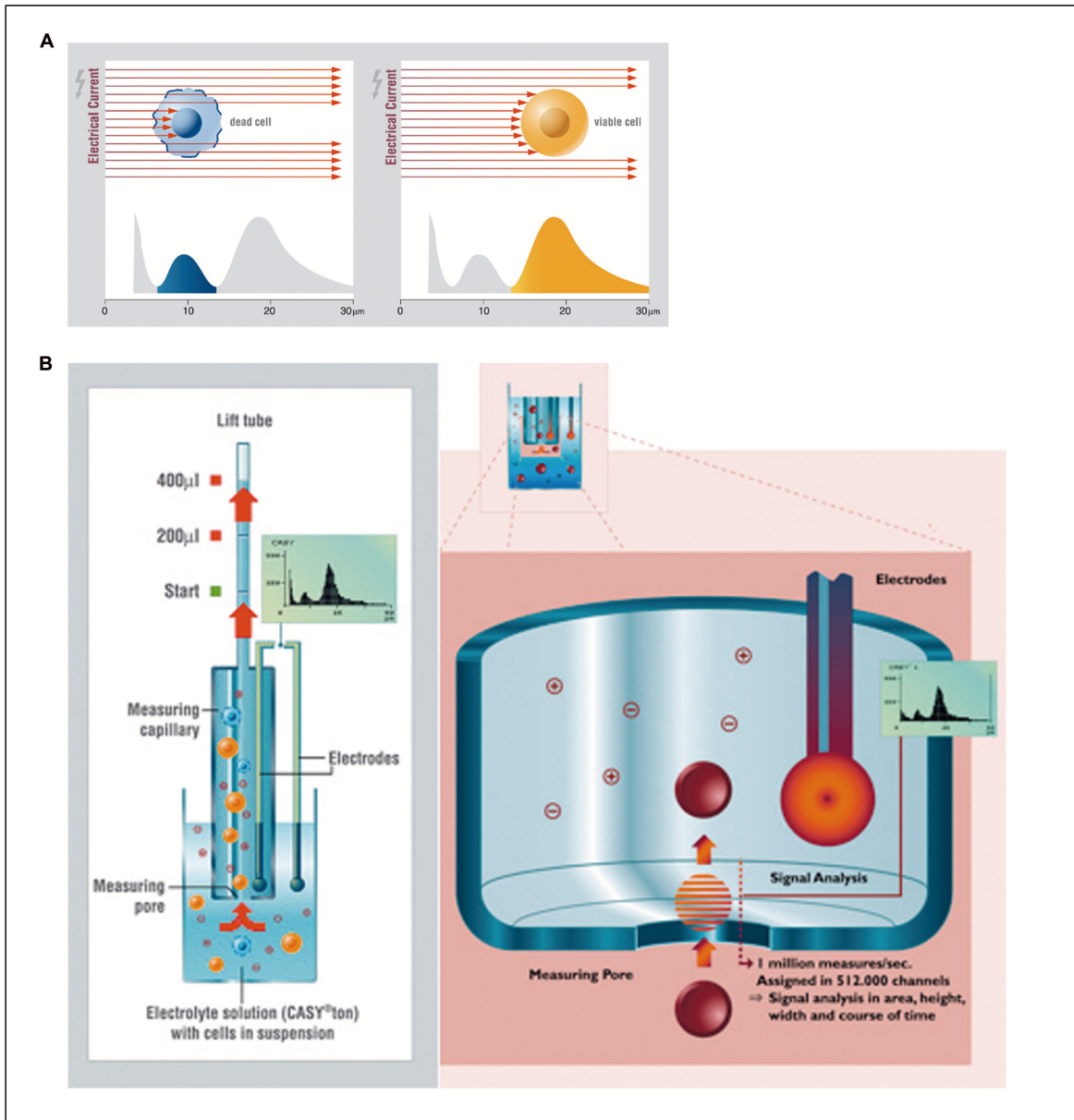


Figure 3.2: The principle of cell counting by electrical current exclusion and pulse area analysis. (A) A cell suspension in an electrolyte is exposed to a low voltage field, and the electrical current flowing through the suspension is quantified as each cell passes the detector. Due to its intact membrane, a viable cell will act as an electric insulator and thus reduce the current conduction by the electrolyte (see subfigure on the right). This reduction in current conduction will be much less if a dead cell passes the detector, since only its intact nucleus will act as an insulator (see subfigure on the left). Therefore, cell viability and size can be deduced as a function of the magnitude of the electrical current flow through the electrolyte, which is called electrical current exclusion. (B) Applying this measurement with a frequency of one million per second, up to several hundred measurements are made per cell, and the complete process of cell passing through the detector is monitored. This results in a gaussian signal generated by each cell, this signal first increasing when the cell is in process of entering the detector, then peaking when it is completely inside, and subsequently decreasing when the cell is leaving the detector. Thus, the width of each pulse is analyzed, which is therefore called pulse area analysis. This high frequency analysis gives an accurate signal for each cell and thus for the entire cell population investigated. Illustrations taken from [Roche Diagnostics, 2010].

0.000284 mM [Wang et al., 2006; Hou et al., 2007] over 0.25 mM [Jaiswal et al., 1997] and 0.8 mM [Liu et al., 2010] to as much as 50 mM [Jaeger et al., 2008] or even 284 mM [Celebi et al., 2010]. The dexamethasone concentration used was 1 μ M, which lies at the upper end of the concentrations published, ranging from 0.01 μ M [Celebi et al., 2010] over 0.1 μ M [Jaiswal et al., 1997; Wang et al., 2006; Hou et al., 2007; Liu et al., 2010] to 1 μ M [Walsh et al., 2001; Murata et al., 2004].

For adipogenic differentiation, mixtures of cell culture medium with dexamethasone, 3-isobutyl-1-methylxanthin (IBMX), indomethacin and insulin are commonly used. The dexamethasone concentration used here was 1 μ M, which is in accordance with the uppermost portion of the literature published [Wu et al., 1995; Giri et al., 2006; Celebi et al., 2010; Liu et al., 2010] and close to the 0.5 μ M used in another study [Smith et al., 1988]. Thus, the dexamethasone concentration used was identical for osteogenic and adipogenic stimulation. The IBMX concentration used here was 500 μ M and is identical to the single concentration published so far [Smith et al., 1988; Wu et al., 1995; Kelly and Gimble, 1998; Giri et al., 2006; Celebi et al., 2010; Liu et al., 2010]. The indomethacin concentration used was 200 μ M, corresponding to 0.2 mM and lying in the middle of what was published before, these concentrations ranging from 0.06 mM [Kelly and Gimble, 1998] over 0.1 mM [Lehmann et al., 1997; Liu et al., 2010] to 10 mM [Celebi et al., 2010]. The insulin concentration used was 10 μ M and lies at the upper end of the concentration range published, ranging from 0.172 μ M [Wu et al., 1995; Liu et al., 2010] over 0.2 μ M [Lehmann et al., 1997] to 1.7 μ M [Giri et al., 2006] and 2 μ M [Smith et al., 1988]. Only under serum-free conditions, an insulin concentration of 1 nM was sufficient to induce adipogenic differentiation [Sorisky, 1999]. Since the maximum activating effect of insulin on glycerol-3-phosphate dehydrogenase, an enzyme downstream of the insulin-binding IGF receptors, lies between 1 and 10 μ M, I decided to use the 10 μ M concentration.

The TNF concentration used was 30 international units per ml medium, which corresponds to a mass concentration of 300 pg/ml. *In vivo*, even lower TNF concentrations around 50 pg/ml are biologically active and were so far not reported to have been exceeded (see page 91).

3.2 *In vitro* Assays

3.2.1 Quantification of Cell Number

The basic dye crystal violet, also called hexamethylpararosaniline chloride or gentian violet, is positively charged under physiologic conditions and thus binds negatively charged cellular macromolecules, most of which being DNA, via ionic attraction [Noeske, 1966]. This binding occurs in a linear fashion and therefore is well applicable to indirectly determine cell numbers by quantifying the dye intensity [Gillies et al., 1986].

On the basis of a protocol published previously [van Kooten et al., 1999], crystal violet staining was done in 96-well plates according to the following protocol:

1. wash cells 2x with PBS
2. fix cells for 10 min in 100 μ l 2-Propanol
3. permeabilize cells by washing 3x with PBS (0.05 % Tween 20)
4. add 50 μ l crystal violet (0.1 % in PBS) and incubate shaking for 20 min at room temperature
5. wash 3x with ddH₂O
6. dissolve bound crystal violet in 100 μ l acetic acid (33 %)
7. transfer 70 μ l of solution to an optical plate
8. quantify optical density in microplate reader at 600 nm

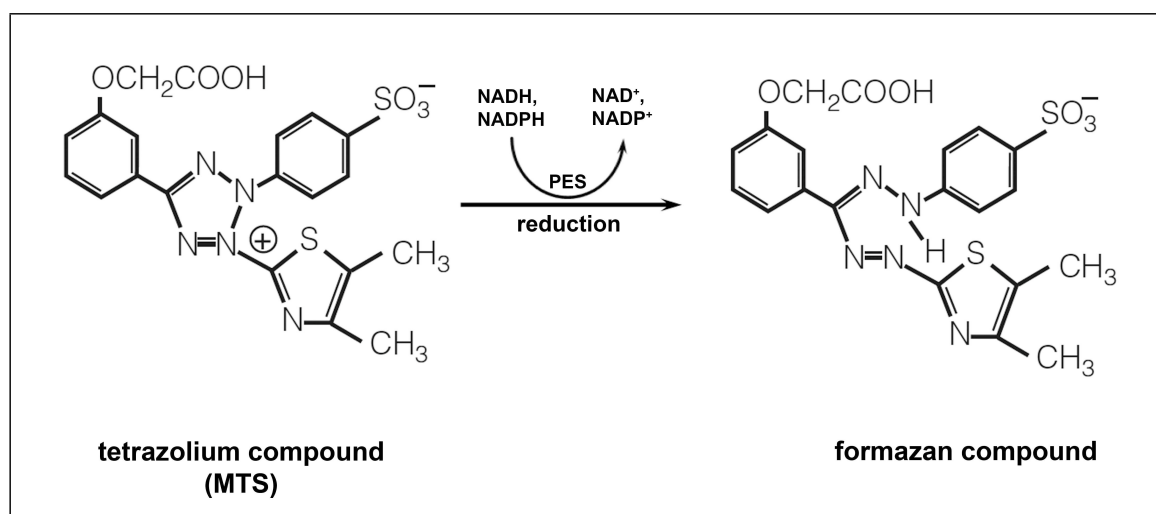


Figure 3.3: The principle of the metabolic activity assay. The tetrazolium compound MTS is reduced into a differently colored formazan salt by electron transfer from the reduced reduction equivalents NADH or NADPH via the electron coupling reagent phenazine ethosulfate (PES) to MTS, leaving NADH and NADPH in their oxidized state NAD^+ and NADP^+ in the cytoplasm. Illustration taken and modified from [Promega, 2009].

3.2.2 Quantification of Cellular Metabolic Activity

Upon transfer of electrons from NADH or NADPH via a coupling reagent to MTS, the tetrazolium dye MTS is reduced into a differently colored, soluble formazan salt [Berridge et al., 2005] (see figure 3.3 on page 32). Thus, quantification of the amount of formazan salt generated in a given time indirectly reflects the amount of reduced reduction equivalents generated in a cell in that time and can therefore be used to determine the cellular metabolic activity.

Staining was done in 96-well plates according to the manufacturer's instructions as detailed below:

1. thaw MTS reagent at 37°C in the water bath
2. prepare a master mix containing $100\ \mu\text{l}$ medium plus $20\ \mu\text{l}$ MTS reagent per well
3. exchange supernatant of cultured cells in test plate with $100\ \mu\text{l}$ MTS master mix
4. incubate for 60 min at 37°C , 5 % CO_2 in a humidified atmosphere
5. transfer $70\ \mu\text{l}$ supernatant to an optical plate
6. quantify optical density in microplate reader at 490 nm (reference wavelength for background correction 650 nm)

3.2.3 Quantification of RUNX2 DNA-Binding Activity

DNA-binding activity of the osteogenic key transcription factor RUNX2 was assayed in an ELISA-based system (see figure 3.4 on page 33).

The assay was done in accordance with the manufacturer's instructions, required however a substantial deal of improvement regarding the isolation of nuclear proteins. The final protocol used is detailed below:

- Prepare nuclear envelope:
 1. wash cells once in ice-cold PBS containing Phosphatase Inhibitors

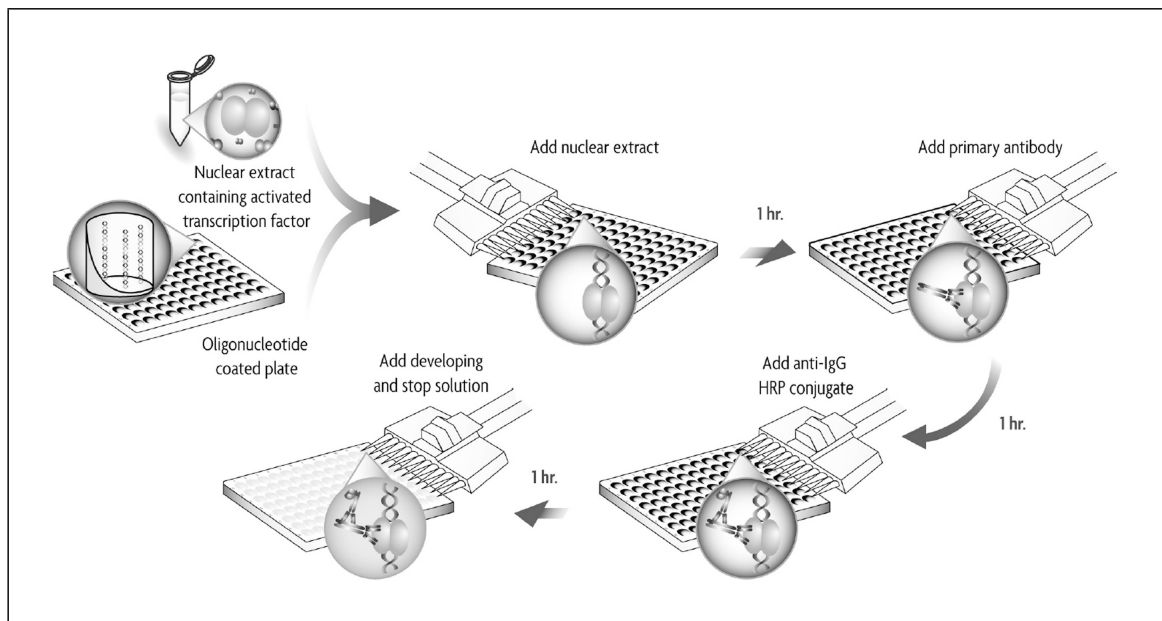


Figure 3.4: The principle of the RUNX2 DNA binding assay. An oligonucleotide with the consensus binding sequence of RUNX2-regulated genes (5'-AACCACA-3') is immobilized to the wells of a 96-well test plate. A nuclear extract is then applied to the wells, and in case it contains activated RUNX2, the transcription factor will bind its target sequence. Via a primary and secondary antibody in a typical ELISA-based setting, RUNX2 is detected and quantified. Illustration taken from [Active Motif, 2010].

2. scrape cells from the cell culture surface in 6 ml ice-cold PBS containing Phosphatase Inhibitors
 3. transfer cells to pre-chilled tube and centrifuge at 500 g and 4 °C for 5 min
 4. resuspend cell pellet in 500 μ l 1X Hypotonic Buffer at 4 °C by pipetting up and down
 5. incubate resuspended cells on ice for 30 min
 6. add 25 μ l Detergent and vortex for 10 s at highest force
 7. centrifuge lysed cells at 14,000 g and 4 °C for 30 s and discard supernatant (cytoplasmic fraction)
- Lyse nuclear envelope:
 1. freeze pellet (nuclear fraction) for 30 min at -80 °C and subsequently thaw it on ice
 2. add 50 μ l Complete Lysis Buffer, resuspend pellet by pipetting up and down and vortex at highest force for at least 10 s
 3. incubate shaking on ice at 150 rpm for 30 min, vortex at highest force for 30 s and incubate in the ultrasonic water bath for 30 s
 4. centrifuge for 10 min at 14,000 g and 4 °C, transfer supernatant (nuclear proteins) to a pre-chilled tube, and discard pellet (nuclear fragments)
 5. aliquot nuclear proteins and store at -80 °C until use
 - Quantify nuclear proteins:
 1. add 28 μ l 660 nm Protein Assay Solution to 2 μ l sample or Complete Lysis Buffer as blank
 2. vortex and incubate at least for 5 min at room temperature
 3. quantify optical density on a spectrophotometer at 660 nm

4. calculate nuclear protein concentration in accordance with BSA standard
- Quantify activated, DNA-binding RUNX2:
 1. add 30 μl Complete Binding Buffer to each test well of the plate (add 2 μl (30 pmol) wild type or mutated consensus oligonucleotide to specificity control wells)
 2. add 20 μl nuclear extract (containing 2 – 20 μg nuclear protein) per test well (5 μg SAOS-2 extract (2 μl extract in 18 μl Complete Lysis Buffer) for positive control, 20 μl Complete Lysis Buffer for negative control)
 3. seal wells with adhesive foil and incubate shaking at 100 rpm for 1 h at room temperature
 4. wash 3x with 200 μl 1X Washing Buffer per well and carefully aspirate wells in the last step
 5. add 100 μl RUNX2 antibody per well (pre-diluted 1:1000 in 1X Antibody Binding Buffer)
 6. seal wells and incubate for 1 h at room temperature
 7. wash 3x with 200 μl 1X Washing Buffer per well and carefully aspirate wells in the last step
 8. add 100 μl HRP-conjugated secondary antibody per well (pre-diluted 1:1000 in 1X Antibody Binding Buffer)
 9. seal wells and incubate for 1 h at room temperature
 10. wash 4x with 200 μl 1X Washing Buffer per well and carefully aspirate wells in the last step
 11. add 100 μl Developing Solution per well and incubate 2 – 10 min at room temperature in the dark
 12. add 100 μl Stop Solution per well and incubate maximally 5 min
 13. quantify optical density in microplate reader at 450 nm (background at 655 nm)

3.2.4 Staining of Active Alkaline Phosphatase for Microscopy

Alkaline phosphatase (ALPL) catalyzes the hydrolysis of naphthol AS-MX phosphate in the presence of the coupling reagent nuclear fast red [Hasselgren, 1978]. This coupling reagent is a diazonium salt which traps the hydrolyzed phosphatase substrate [Talbot et al., 1993], initially via ionic interaction, but finally by formation of a stable adduct of red color [Cox and Singer, 1999] (see figure 3.5 on page 35).

Staining of active alkaline phosphatase for visualization by phase-contrast microscopy was done in 12-well plates according to the following protocol previously established in this department:

1. wash cells 2x with PBS
2. fix cells for 10 min at room temperature in 4 % PFA pre-warmed to 37 °C
3. wash fixed cells 2x with PBS
4. add a solution of 0.03 % Naphthol AS-MX phosphate and 0.03 % Fast Red Violet in 20 mM AMPED and incubate for 10 min at room temperature
5. wash stained cells 2x with PBS
 - *optional: wash 2x with ddH₂O and coverslip cells in mounting medium*
6. perform bright-field phase-contrast microscopy

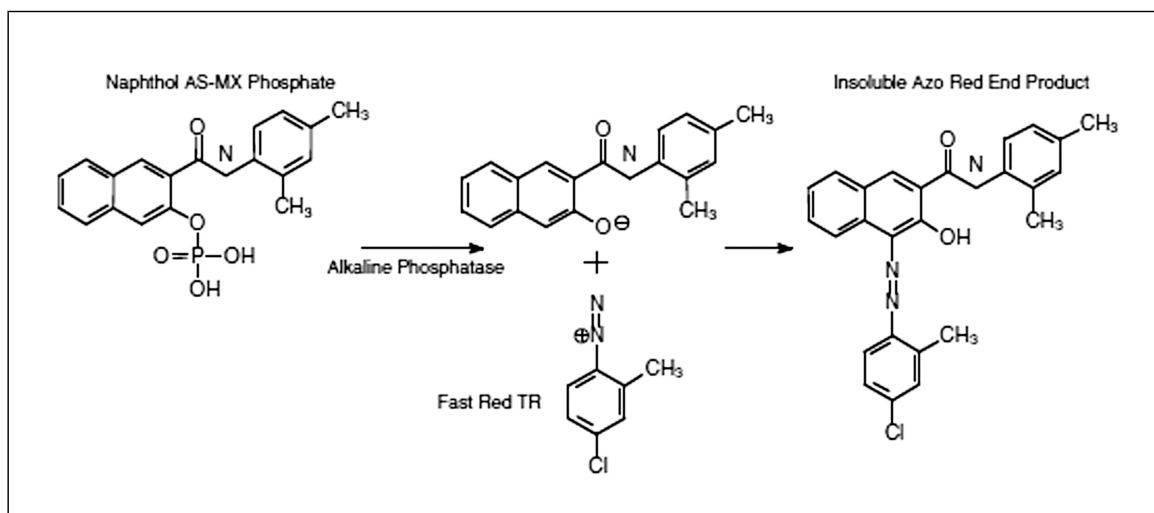


Figure 3.5: The principle of active alkaline phosphatase staining for microscopy. Staining of active alkaline phosphatase relies on the phosphatase-driven hydrolysis of the substrate AS-MX phosphate which subsequently forms a stable, insoluble adduct with the diazonium dye nuclear fast red. Illustration taken from [Sigma-Aldrich, 2008].

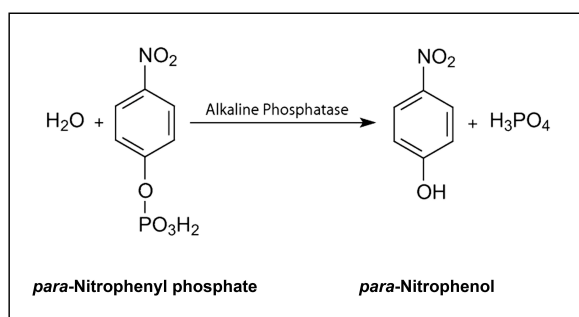


Figure 3.6: The principle of alkaline phosphatase staining for activity quantification. Alkaline phosphatase catalyzes the hydrolysis of *para*-nitrophenyl phosphate into *para*-nitrophenol, a water-soluble product of yellow color. Illustration taken and modified from [Sigma-Aldrich, 2008].

3.2.5 Quantification of Alkaline Phosphatase Activity

Alkaline phosphatase (ALPL) catalyzes the hydrolysis of an arylphosphate residue of its synthetic substrate *para*-nitrophenyl phosphate (pNPP) into the colored product *para*-nitrophenol [Montalibet et al., 2005] (see figure 3.6 on page 35). Thus, by quantification of the optical density of the colored product generated in a given time, the ALPL activity can indirectly be determined. In an extending application of this finding as e.g. in Western blotting, quantitative antigen detection is indirectly done by following the pNPP conversion of an antibody-ALPL conjugate [Voller et al., 1976].

Quantification of alkaline phosphatase activity was done in 96-well plates according to the following self-established protocol:

1. wash cells 2x with TBS
2. add 50 μ l cell lysis buffer (1 % Tween 20 and 100 μ M PMSF in ddH₂O) and incubate for 10 min at room temperature
3. add 200 μ l ALPL substrate solution (10 mM pNPP, 100 mM AMPED and 5 mM MgCl₂ in ddH₂O) and incubate for 60 min at 37 °C, 5 % CO₂ in a humidified atmosphere
4. add 85 μ l NaOH (2 M) to end ALPL activity
5. transfer 100 μ l supernatant to an optical plate
6. quantify optical density in microplate reader at 405 nm

3.2.6 Quantification of Extracellular Matrix Calcium Content

In a largely unknown complexation mechanism, *ortho*-cresolphthalein complexon in solution binds the divalent cations strontium, barium, magnesium and calcium and thereby develops a violet color whose intensity is proportional to the concentration of the ions present. In order to quantify only the concentration of calcium ions in solution, all other ions present have to be masked. For magnesium ions, this is accomplished by adding the chelating agent 8-hydroxy chinoline [Sarkar and Chauhan, 1967]. Strontium and barium ions *in vitro* are, if it all, only present in traces.

Initially, procedures for calcium quantification in serum samples were developed and optimized [Moorehead and Biggs, 1974; Morin, 1974] and subsequently adapted for quantification of extracellular matrix calcium [Proudfoot et al., 2000]. These methods involve acidic liberation of calcium ions from the extracellular matrix and subsequent complexation under alkaline conditions.

Quantification of extracellular matrix calcium content was done in 96-well plates according to the following self-established protocol:

1. wash cells 2x with PBS
2. fix cells for 10 min at room temperature in 4 % PFA pre-warmed to 37 °C
3. wash fixed cells 2x with ddH₂O
4. add 100 μ l cresolphthalein buffer (0.1 mg/ml *ortho*-cresolphthalein complexon, 1 mg/ml 8-hydroxy chinolin and 6 % of 37 % HCl in ddH₂O) and incubate for 5 min at room temperature
5. add 100 μ l AMP buffer (15 % AMP in ddH₂O, pH=10.7) and incubate 15 min at room temperature
6. transfer 100 μ l supernatant to an optical plate
7. quantify optical density in microplate reader at 580 nm

3.2.7 Quantification of Secreted Osteoprotegerin

The concentration of ASC-secreted osteoprotegerin (OPG) in the cell culture supernatant was determined by enzyme-linked immunosorbent assay (ELISA) in a kit-based system in 96-well plates and in accordance with the manufacturer's instructions as detailed below:

1. add 100 μ l Capture Antibody (pre-diluted to 2 μ g/ml in PBS) per well of an immunoplate, seal plate with adhesive foil and incubate at room temperature over night
2. wash each well 3x with 200 μ l Wash Buffer (carefully aspirate wells in the last step)
3. for blocking, add 300 μ l Reagent Diluent per well and incubate for at least 1 h at room temperature
4. wash each well 3x with 200 μ l Wash Buffer (carefully aspirate wells in the last step)
5. add 100 μ l of samples (pre-diluted 1:20 in Reagent Diluent) and Standard Samples per well, seal plate with adhesive foil and incubate at room temperature for 2 h
6. wash each well 3x with 200 μ l Wash Buffer (carefully aspirate wells in the last step)
7. add 100 μ l Detection Antibody (pre-diluted to 200 ng/ml in Reagent Diluent) per well, seal plate with adhesive foil and incubate at room temperature for 2 h
8. wash each well 3x with 200 μ l Wash Buffer (carefully aspirate wells in the last step)
9. add 100 μ l Streptavidin-HRP per well, close plate using the lid and incubate for 20 min at room temperature in the dark
10. wash each well 3x with 200 μ l Wash Buffer (carefully aspirate wells in the last step)
11. add 100 μ l Substrate Solution per well and incubate for 20 min at room temperature in the dark
12. add 50 μ l Stop Solution per well and manually and gently agitate plate
13. quantify optical density in microplate reader at 450 nm (background at 540 or 570 nm)
14. calculate OPG concentration in accordance with OPG standard

3.2.8 Quantification of Cellular Lipid Content

Boron-dipyrromethene (Bodipy) dyes are lipophilic compounds that dissolve well in cellular neutral lipids, most of which being triglycerides, that build the core of lipid droplets and that are surrounded by a monolayer of phospholipids [Spandl et al., 2009]. The Bodipy dyes fluoresce upon excitation, the unmodified form used here being excited at 480 nm and emitting a green fluorescence at 503 nm. Thus, the intensity of the fluorescence emitted by the Bodipy stain is proportional to the total amount of lipid stored within a cell.

Quantification of cellular lipid content was done in 96-well plates according to the following self-established protocol:

1. wash cells 2x with PBS
2. fix cells for 30 min at room temperature in 100 μ l 4 % PFA pre-warmed to 37 °C
3. wash cells 3x with PBS
4. add 100 μ l Bodipy solution (1 μ g/ml in 150 mM NaCl)
5. incubate for 10 min at room temperature in the dark
6. wash cells 2x with PBS and 3x with ddH₂O
7. quantify fluorescence intensity in microplate reader at 515 nm (excitation at 480 nm)

3.3 Real-Time RT-PCR

3.3.1 RNA Isolation

Isolation of total RNA from ASC cultured in 6-well plates was done using a kit-based system and in accordance with the manufacturer's instructions as detailed below:

- Cell lysis:
 1. discard medium and incubate cells in 350 μ l Lysis Buffer RL for 2 min at room temperature
 2. lyse cells by manually shaking the plate and by pipetting lysis buffer over cell layer, and incubate for further 3 min
 3. load lysed cells onto QIAshredder column and centrifuge for 1 min and 4 °C at maximum speed
- DNA removal:
 1. load filtrate onto Spin Filter D in 2 ml Receiver Tube and centrifuge at 10,000 g and 4 °C for 2 min
- RNA retention:
 1. discard Spin Filter D (with DNA bound to it) and add 350 μ l of 70 % ethanol to the filtrate
 2. mix ethanol and filtrate by pipetting up and down and transfer solution onto a Spin Filter R in 2 ml Receiver Tube
 3. centrifuge at 10,000 g und 4 °C für 2 min and transfer Filter to new Receiver Tube
- RNA washing:
 1. add 500 μ l Wash Buffer HS, centrifuge at 10,000 g and 4 °C for 1 min and transfer Filter to new 2 ml Receiver Tube
 2. add 700 μ l Wash Buffer LS, centrifuge at 10,000 g and 4 °C for 1 min and transfer Filter to new 2 ml Receiver Tube
 3. centrifuge at 10,000 g and 4 °C for 3 min and transfer Filter to new 2 ml Receiver Tube
- RNA elution:
 1. add 80 μ l RNase-free water, incubate for 5 min at room temperature and centrifuge at 6,000 g for 1 min
 2. aliquot eluted RNA and store at -80 °C until use

3.3.2 RNA Quantification

Quantification of the amount of isolated total RNA within the samples was done using a spectrophotometer measuring the optical density of the sample at different wavelengths ranging from ultraviolet to visible light. In this setting, the optical density at 260 nm reflects the concentration of RNA in the sample, whereas the optical density at other wavelengths can be used to determine potential contaminants within the RNA sample: proteins exhibit an absorption maximum at 280 nm, contaminants containing peptide bonds or aromatic compounds absorb maximally at 230 nm, and particulates in solution absorb maximally at 325 nm [Gallagher and Desjardins, 2008]. Thus, on a calibrated photometer, the concentration of the RNA as well as that of contaminants can accurately be determined.

The RNA concentration was determined according to the instructions of the spectrophotometer manufacturer as detailed below:

1. load 2 μ l sample to the NanoDrop spectrophotometer (use RNase-free water as blank)
2. quantify the RNA concentration using the NanoDrop Software and the RNA40 program

3.3.3 RNA Electrophoresis

In order to check the integrity of the isolated RNA, especially with regard to RNase-driven RNA degradation, a non-denaturing agarose gel electrophoresis was done for all samples.

Under heating, the polysaccharide agarose dissolves in an aqueous buffer and forms a gel after cooling down to room temperature. This gel consists of agarose fibers building a meshwork of variable pore size, the pore size depending on the agarose concentration used. The higher the agarose concentration of the gel, the smaller the pores. By applying a voltage field, macromolecules are forced to migrate through the gel and will be retarded in dependence of both their own charge to mass ratio and the pore size of the gel. Thus, by casting a gel of high agarose concentration and small pore size, large macromolecules will be largely hindered from migrating through the gel, whereas small ones will well be able to migrate through it, having a migration rate inversely proportional to their size. Visualization of nucleic acids as RNA separated in that manner is usually done by staining with intercalating dyes such as ethidium bromide that are added to the agarose gel during the casting process.

Agarose gel electrophoresis was done according to the following protocol established during my diploma thesis:

1. add 1 % agarose powder to 1x TAE buffer
2. boil suspension in microwave oven to dissolve agarose
3. add ethidium bromide solution at 0.1 µg/ml to agarose solution
4. pour agarose solution into agarose gel electrophoresis tray and wait for the gel to set at room temperature
5. transfer the agarose gel electrophoresis tray to the electrophoresis chamber filled with fresh 1x TAE buffer
6. load RNA samples pre-mixed with loading buffer to the gel pockets
7. run gel at 8 V/cm gel length for 1 h
8. document gel using the gel documentation system

The integrity of the total RNA isolated from the ASC was then evaluated visually by confirming the presence of all RNA species usually present in a cell, i.e. by confirming the presence of RNAs of largely different size as messenger RNA (mRNA), transfer RNA (tRNA), small nuclear RNA (snRNA) and other non-coding RNAs, but most obviously by the prominent bands of the ribosomal RNA (rRNA) present in the small and the large ribosomal subunit. In case of RNase-driven RNA degradation, weakening of the rRNA bands can be observed first, followed by the continuous vanishing of all RNA species.

3.3.4 Reverse Transcription

After isolation of the entire RNA species present in ASC, the mRNA transcripts of genomic DNA were transcribed into complementary DNA (cDNA) in an *in vitro* process of reverse transcription (RT) (see figure 3.7 on page 40).

This reverse transcription was done in a kit-based system according to the manufacturer's instructions as detailed below:

- Removal of genomic DNA:
 1. add 2 µl gDNA Wipeout Buffer (7x) to 12 µl total RNA (maximally 1 µg)
 2. incubate at 42 °C for 2 min, then at 4 °C
- Reverse Transcription:
 1. add 1 µl Quantiscript RT, 4 µl Quantiscript RT Buffer (5x) and 1 µl RT Primer Mix per reaction

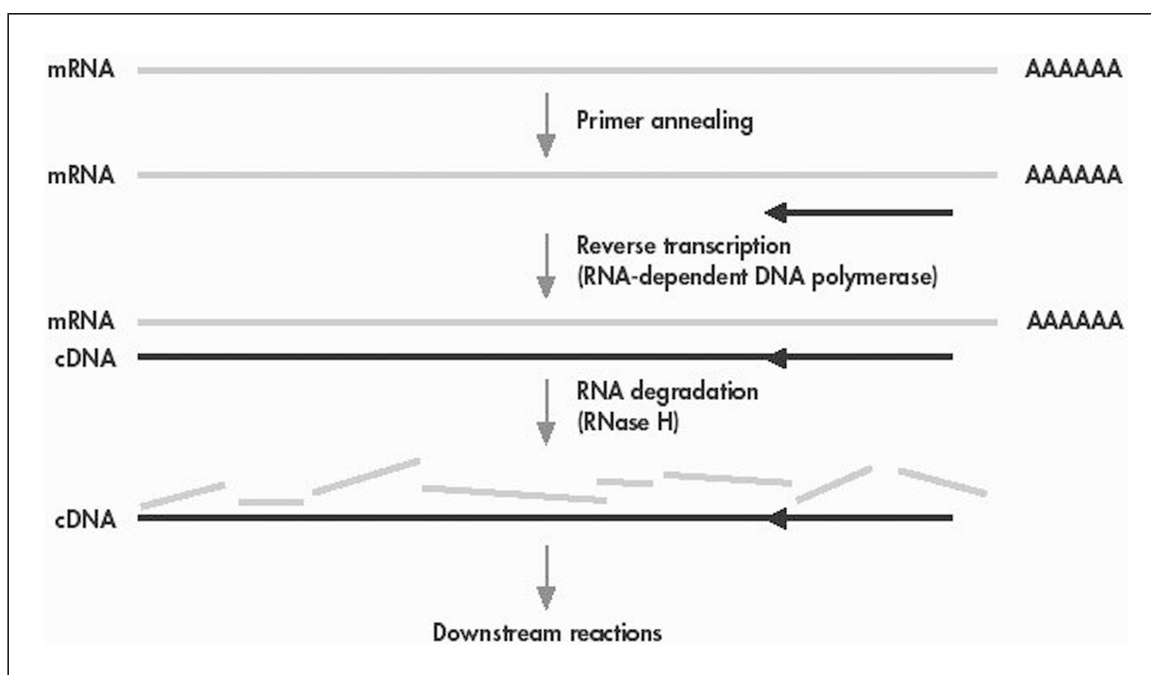


Figure 3.7: The process of reverse transcription. Based on hybridization of oligo-dT primers to poly-A tails and random primers to random sites of the mRNA, the reverse transcriptase catalyzes RNA-dependent DNA polymerization and thus yields a population of double-stranded mRNA-cDNA hybrids. Upon presence of these hybrids, the hybrid-dependent exoribonuclease activity of the reverse transcriptase degrades the mRNA strand and leaves a population of single-stranded cDNAs. Illustration taken from [QIAGEN, 2005].

2. incubate at 42 °C for 30 min (reverse transcription), then at 95 °C for 3 min (reverse transcriptase denaturation)
3. store cDNA at 4 °C for short term or at -20 °C for long term

3.3.5 Real-Time RT PCR

To quantify the number of mRNAs of a certain gene and thus the expression of this gene, real-time PCR was done following reverse transcription of all mRNAs (real-time RT PCR). To avoid amplification of genomic DNA sequences in real-time RT PCR, at least one primer of a primer pair was designed to bind a sequence spanning from one exon to an adjacent one (see figure 3.8 on page 41).

These cDNA-specific primers were designed via the web interfaces of the Primer3 engine [Rozen and Skaletsky, 2000] found at

<http://frodo.wi.mit.edu/primer3/input.htm>

and

<http://www.ncbi.nlm.nih.gov/tools/primer-blast/>.

Melting temperatures were set to maximally deviate one Kelvin from 60 °C, and the 3'-end of the primers was defined to contain at least one guanine (G) or cytosine (C) residue to establish a stable G-C pairing at this critical site.

The sequences of the primers used were as follows (sequences of exon-exon boundaries are indicated in uppercase, fwd (forward) and rev (reverse) indicate the corresponding primer):

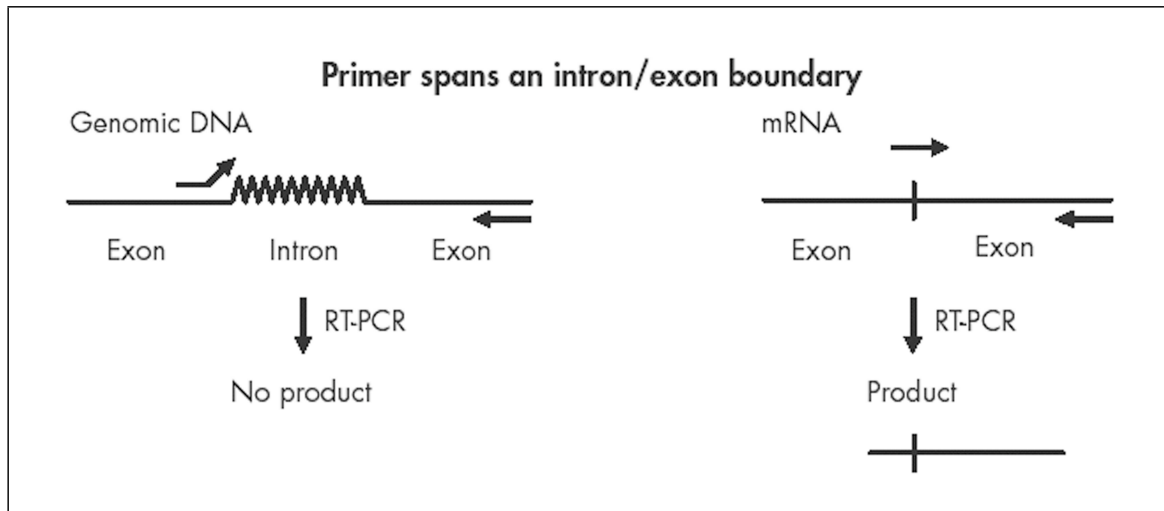


Figure 3.8: Designing of cDNA-specific primers. By designing primers to span an exon-intron boundary, amplification of genomic DNA is precluded. The 3'-end of the left primer in the illustration on the left is complementary to an adjacent exon the 5'-end of this primer is complementary to. Therefore, it cannot hybridize to the genomic sequence of the corresponding gene and amplification of genomic DNA will not occur. However, the primer will be well able to hybridize to the cDNA made from the spliced mRNA, as is illustrated on the right, resulting in the generation of a PCR product during thermal cycling. Illustration taken and modified from [QIAGEN, 2005].

Primer	Sequence (5'–3')	Amplicon size (bp)
GAPDH (fwd)	ctctgctcctcctgttcgac	112
GAPDH (rev)	acgaccaaaTCcgttgactc	
TNFRSF1A (fwd)	actgaggactcaGGcaccac	165
TNFRSF1A (rev)	aagctcccCCtcttttcag	
TNFRSF1B (fwd)	cagtgcggttgacagaagg	116
TNFRSF1B (rev)	caccaggggaagaaTCtgag	
ZBTB16 (fwd)	ggtcgagcttctgataacg	237
ZBTB16 (rev)	gccatgtcagtGCCagtatg	
ALPL (fwd)	cattgtgaccaccagagag	173
ALPL (rev)	ccatgatcaCGtcaatgtcc	

The reaction mixture for PCR of cDNA was set up according to the following protocol:

Order	Substance (concentration)	Volume per reaction	Final concentration
1	add Master Mix (2x)	10 μ l	1x
2	add primers (12 μ M each)	0.5 μ l (= 6 pmol) each	300 nM
3	<i>homogenize gently</i>		
4	<i>aliquot to wells</i>		
5	add cDNA (max. 100 ng)	9 μ l	

Thermal cycling was then done according to the following temperature profile:

- 95 °C for 10 min (initial denaturation and FastStart *Taq* polymerase activation)

- Thermal cycling (40x):
 1. 95 °C for 15 s (template denaturation)
 2. 60 °C for 1 min (primer annealing and extension)
- Melting curve analysis:
 1. 95 °C for 15 s (template denaturation)
 2. 60 °C for 1 min
 3. heat samples at 1 K/s
 4. 95 °C for 15 s
- room temperature (until analysis)

In the first cycle of this thermal cycling program, all single-stranded cDNAs targeted by a primer are complemented, which doubles the number of temperature-denatured single-stranded cDNAs for the next replication round and thus yields a linear increase of their number. Exponential amplification of the cDNAs then begins with the second cycle.

Each of the PCR products generated during thermal cycling in this manner had to be tested for specificity, since fluorescence-based detection of nucleic acids, as was done here using SYBR Green, will stain both specific *and* unspecific PCR products, the latter occurring e.g. from amplification of primer dimers. In real-time PCR, testing for PCR product specificity is done via analysis of the melting behavior of the PCR products in a sample (see figure 3.9 on page 43).

3.3.6 Analysis of Real-Time PCR Data

In real-time PCR, the expression of a certain gene is determined indirectly as that cycle the fluorescence signal of the amplification product of this gene's transcript significantly exceeds the background noise. For determination of this threshold cycle C_t , two parameters have to be defined: the threshold level and the baseline cycles.

The baseline cycles are those cycles within which there is no significant change in the fluorescence signal emitted by the fluorescent dye intercalated into the PCR product or emitted by the negative control samples containing no template. Thus, the reporter fluorescence intensity R found within these cycles defines the background fluorescence intensity. Based on the detector signal, the baseline cycles were determined automatically by the software.

Since increasing the quantity of reporter dye in the master mix will, as long as stain saturation is not reached, increase the quantity of fluorescence emission from the PCR product without an increase in the amount of PCR product, the reporter fluorescence signal intensity R has to be put into relation to the fluorescence intensity of a non-intercalating, so-called "passive" reference dye contained in the master mix at a constant concentration. This yields the normalized reporter signal R_n which thus can be put as

$$R_n \equiv \frac{\text{reporter dye fluorescence intensity}}{\text{reference dye fluorescence intensity}}.$$

Within the baseline cycles, R_n will not change. However, in the growth phase following these cycles, R_n will increase with increasing number of PCR products. Thus, by subtracting the R_n obtained during the baseline cycles or for the negative control samples from the R_n obtained for the template-containing samples in the growth phase, one gets a reliable measure of the magnitude of the PCR product signal generated under the given PCR conditions. This background fluorescence-corrected R_n can thus be put as

$$R_{n \text{ sample}} - R_{n \text{ baseline}} \equiv \Delta R_n.$$

With increasing number of PCR cycles and thus increasing number of PCR products, ΔR_n will increase, until the depleting reagents of the master mix start to limit the PCR or the fluorescence emission.

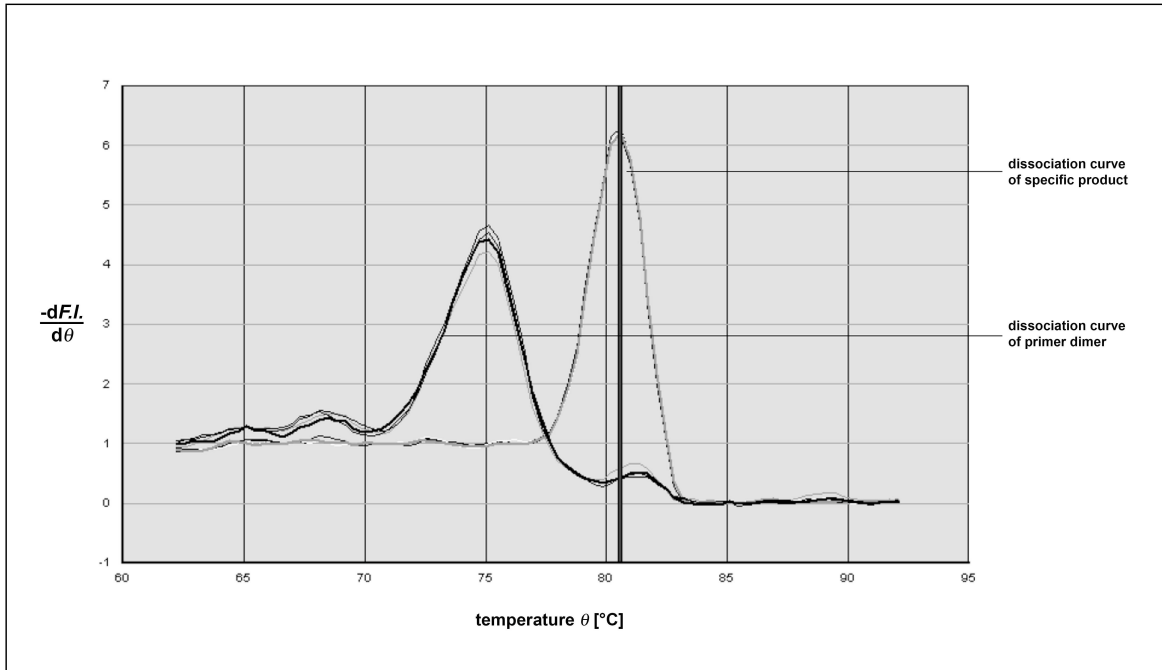


Figure 3.9: Testing of PCR product specificity in real-time PCR. In order to find unspecific PCR products as e.g. primer dimers, melting curve analysis was done. By increasing the temperature θ of a PCR product in solution and stained with an intercalating dye, the fluorescence intensity FI , emitted by this PCR product will continuously decrease as a consequence of increasing melting of the double-stranded PCR product. Since the melting process shows a biphasic behavior, initially accelerating with increasing temperature, but then proceeding increasingly slower with increasing temperature, the derivation of $-FI$ by θ will peak at the temperature of fastest melting. This temperature is characteristic for the length and composition of the PCR product, the melting temperature increasing with length and G/C content of the PCR product. Since there are two peaks in this diagram, two PCR products have been generated, the smaller of which being an unspecific product of primer dimer amplification. Illustration taken and modified from [Applied Biosystems, 2006].

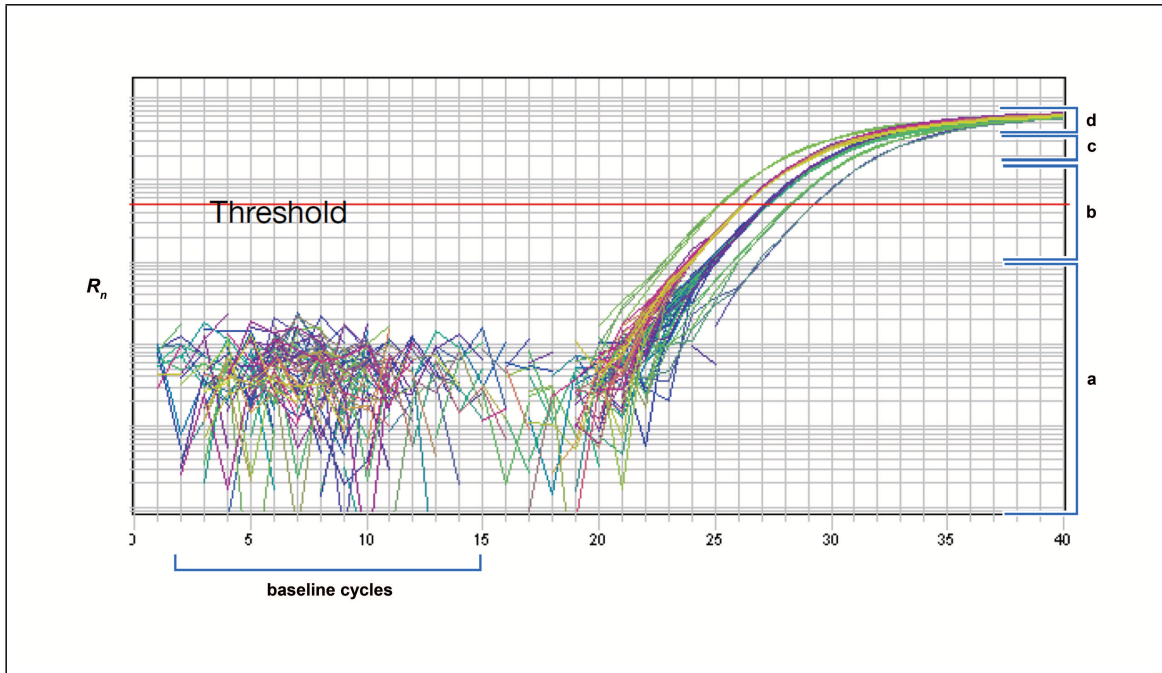


Figure 3.10: Baseline cycles, threshold level and amplification plots in real-time PCR. The baseline cycles define all cycles in which the normalized fluorescence signal intensity R_n does not correlate with the ongoing cDNA amplification. Thus, these cycles define the background fluorescence intensity (a) (see all cycles below cycle 15 in this illustration). When R_n raises above the background level, the exponential growth (b) of the PCR product number in this logarithmic depiction becomes apparent as a linear function of R_n in dependence of the cycle number. When PCR substrates become limiting, the PCR product number, and thus R_n , will grow no longer exponentially, but linearly (c), and finally will reach a plateau phase (d) in which no further amplification occurs. Illustration taken and modified from [Applied Biosystems, 2006].

Within this context, the threshold defines a level of ΔR_n that is intermediate between the baseline level R_n and the saturation level R_n and thus defines a reliable level of reporter fluorescence intensity. In the experimental settings used here, ΔR_n was manually set to be 0.1. In this setting, the threshold level for all reactions exactly corresponded to the middle of the exponential growth phase in the amplification plot. Figure 3.10 on page 44 illustrates a typical amplification plot and baseline cycles and threshold level.

Having baseline cycles and threshold level defined, the expression level of a gene can be calculated from the number of cycles that were needed to raise R_n to the threshold level. This defines the threshold cycle C_t of that sample. The higher the C_t , the more replication rounds were needed to raise the transcript signal above the background level and the lesser the number of transcripts present in that sample. Since each PCR cycle will ideally double the amount of PCR product present, the

$$\text{expression of gene } x = 2^{-C_t \text{ gene } x}.$$

To determine the expression level of a certain gene, it has to be put into relation to a constant representing the amount of RNA put into the PCR, for input of a larger amount of RNA will lower the C_t of the investigated gene and thus misleadingly will result in calculation of a higher expression level of that gene. Under the experimental conditions used here, such a gene with unregulated, so-called housekeeping expression was glyceraldehyde-3-phosphate dehydrogenase (*GAPDH*).

Thus, the fraction

$$\frac{\text{expression of gene } x}{\text{expression of housekeeping gene}} = \frac{2^{-C_t \text{ gene } x}}{2^{-C_t \text{ GAPDH}}} = 2^{-C_t \text{ gene } x + C_t \text{ GAPDH}}$$

delivers the absolute expression of the investigated gene independent from the amount of RNA used for PCR.

With

$$\Delta C_t \equiv C_t \text{ gene } x - C_t \text{ housekeeping gene},$$

it follows that

$$2^{-C_t \text{ gene } x + C_t \text{ GAPDH}} = 2^{-(C_t \text{ gene } x - C_t \text{ GAPDH})} = 2^{-\Delta C_t}.$$

Therefore, the absolute expression of a specific gene can shortly be put as

$$\text{absolute expression of gene } x = 2^{-\Delta C_t}.$$

Statistical evaluation of the expression data was then done on basis of differences in the ΔC_t values and cannot be done on basis of differences in $2^{-\Delta C_t}$, since $2^{-\Delta C_t}$ transfers the *de facto* measured data from a linear scale (C_t values) to an exponential scale ($2^{-\Delta C_t}$ values). Therefore, significance testing of real-time PCR data has to invoke C_t -based data and is recommended to be done by non-parametric significance tests as the Mann-Whitney U test [Yuan et al., 2006], for real-time data, as most biological data, are unlikely to follow a normal distribution (see page 51 for further details).

3.4 Conventional and Confocal Fluorescence Microscopy

Fluorescence microscopy was used to assess expression and localization of signal transduction proteins in ASC as well as to analyze ASC viability. Due to the inherent advantages of confocal fluorescence microscopy over conventional, non-confocal fluorescence microscopy, immunofluorescence analyses were done on a confocal microscope, whereas live-dead staining could sufficiently well, but much faster be done on a non-confocal microscope. Figure 3.11 on page 46 illustrates the basis of conventional and confocal microscopy and underlines the differences between them.

3.4.1 Immunofluorescence Staining

Immunofluorescence staining for confocal microscopy was done in chamber slides according to the following self-established protocol based on recommendations given by the antibody-producing company Cell Signaling Technology [Cell Signaling Technology, 2011]:

1. wash cells in PBS
2. fix cells for 15 min at room temperature in 500 μ l 4 % PFA pre-warmed to 37 °C
3. wash fixed cells 3x with PBS and incubate for 1 h at room temperature in blocking buffer (5 % goat serum and 0.3 % Triton X-100 in PBS)
4. discard blocking buffer and add primary antibody in antibody dilution buffer (1 % IgG-free BSA and 0.3 % Triton X-100 in PBS)
5. incubate at 4 °C over night
6. wash cells 3x with PBS and add secondary antibody in antibody dilution buffer
7. incubate for 1 h at room temperature in the dark
8. wash cells with PBS and 2x with aqua ad iniectabilia
9. embed cells in mounting medium for fluorescence microscopy

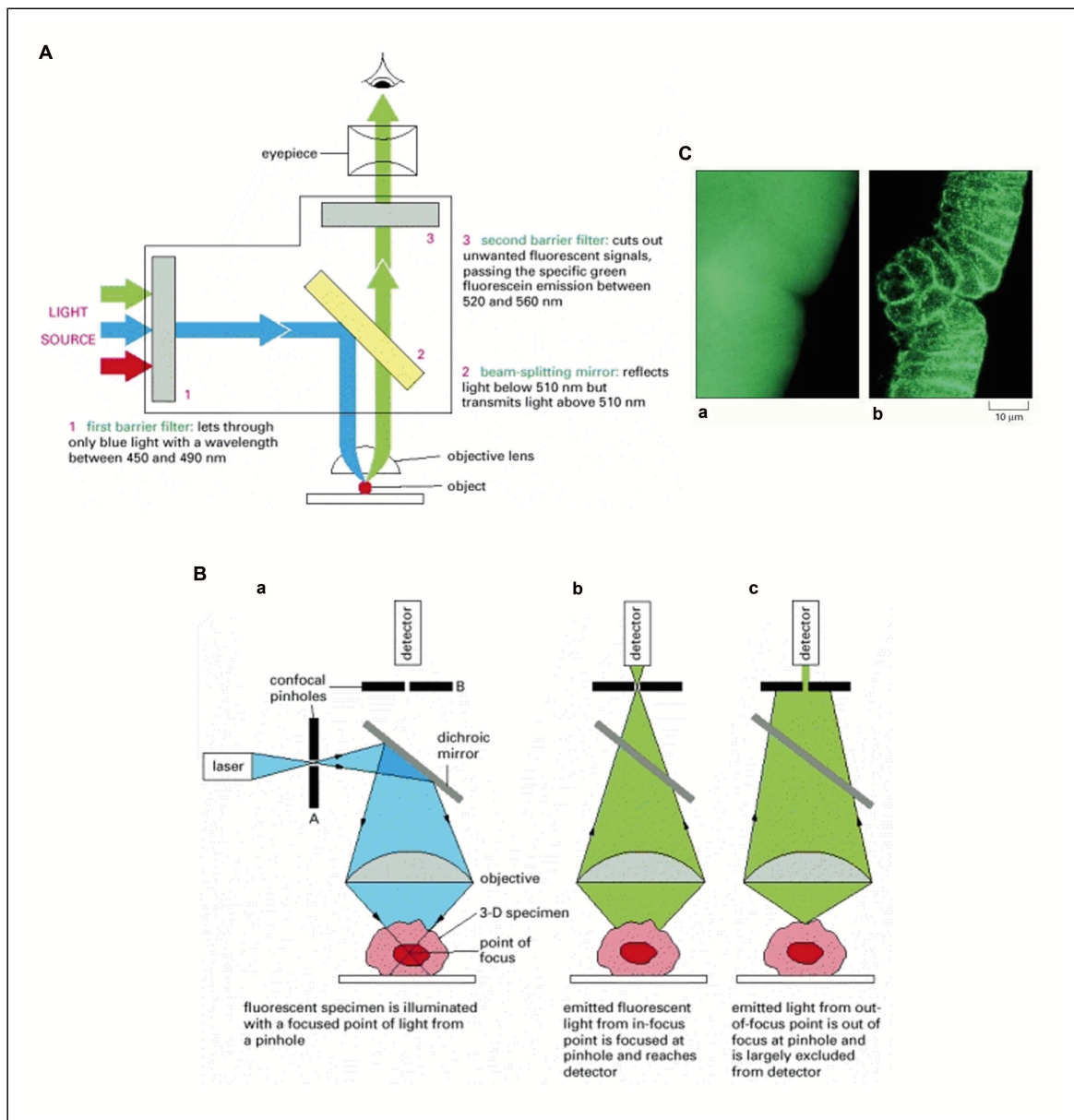


Figure 3.11: The principle of conventional, non-confocal and confocal fluorescence microscopy. (A) In conventional, non-confocal fluorescence microscopy, the light emitted by a high pressure mercury vapor lamp is first barrier filtered for the desired excitation wavelength and then reflected to the specimen by a dichroic mirror. The light emitted by the specimen, which is of longer wavelength as the excitation light, is not reflected by the mirror and passes through a second barrier filter to the ocular or a camera. (B) In confocal microscopy, the monochromatic excitation light of a LASER passes through a pinhole and thus illuminates the specimen in a focussed fashion (a). Light emitted by the specimen in this focus plane is focussed by the objective to pass through a second pinhole and to the detector (b), whereas light emitted from specimen portions out of excitation focus will not focus to the detector pinhole and thus will not reach the detector (c). (C) In large three-dimensional specimens as this *Drosophila* embryo stained for actin, non-confocal microscopy suffers from diffuse images due to the detection of light above and below the focus plane (a). In confocal microscopy, this light does not pass the detector pinhole and thus will not contribute to the image (b). By varying the excitation focus plane, optical sections of the entire specimen can be done and subsequently be computationally post-processed into three-dimensional images. Illustrations taken and modified from [Alberts et al., 2002].

3.4.2 The Live-Dead Assay

Visualization of live and dead ASC was done in conventional, non-confocal microscopy by fluorescence staining with calcein AM and propidium iodide. The acetoxymethyl- (AM)-functionalized form of calcein, calcein AM, is non-fluorescent and uncharged, which allows it to permeate the cell membrane. Inside living cells, active nonspecific esterases hydrolyze the acetoxymethyl group from the calcein backbone and thus allow calcium binding by calcein, which results in emission of green fluorescence light. Calcein shows a low degree of cytotoxicity, which requires microscopy to be done fast in order to avoid false positive results for dead cells. Propidium iodide is an intercalating nucleic acid stain which, due to its polarity, cannot permeate the cell membrane and thus stains only cells with defect membranes commonly considered to be damaged or dead.

The Live-Dead Assay was done in chamber slides according to the following protocol established in our group:

1. add propidium iodide at 500 nM and calcein AM at 1 μ M to cell culture medium to prepare staining medium
2. exchange the medium of cells in culture with this staining medium and incubate for 10 min at 37 $^{\circ}$ C, 5 % CO₂ in a humidified atmosphere
3. replace the staining medium by standard cell culture medium and quickly microscope cells:
 - calcein: excitation at 496 nm, emission at 516 nm
 - propidium iodide: excitation at 535 nm, emission at 617 nm

3.5 Flow Cytometry

By flow cytometry, the expression of TNF receptors and the distribution of ASC within the distinct cell cycle phases was quantified. In contrast to fluorescence microscopy, flow cytometry facilitates the fast and precise quantification of fluorescence properties of a cell, but gives no visual result. Therefore, it is well-suited for quantification of cellular properties in statistical analyses.

The principle of the flow cytometry technique and its difference to fluorescence-activated cell sorting (FACS) is illustrated in figure 3.12 on page 48.

3.5.1 Quantification of Cell Surface Antigens

Staining of surface proteins for flow cytometry is based on immunofluorescence, but avoids cell fixation and undesired modification of antigens due to the fixation process. To preclude internalization of surfacial antigens and to diminish a decline in cellular viability, cells have to be kept on ice over the entire staining procedure, and centrifuging must not exceed an acceleration of 400 g. To determine the level of unspecific binding of the antibodies used for staining of a specific antigen, control stainings with antibodies derived from the same host species and being of identical isotype as the antibody directed against the specific epitope, but being directed against an antigen not expressed in the target species, were done. These antibodies are referred to as “isotype controls” and allow not only for the determination of unspecific staining of an antibody due to non-antigen-binding-domain-mediated protein-protein interactions, but also for the determination of the extent of autofluorescence emitted by the cells to be stained. In case there is no unspecific staining, the fluorescence intensity emitted by isotope control-stained cells will be the same as that of unstained cells.

Quantification of cell surface antigens was done according to the following self-established protocol:

- Harvest ASC:
 1. wash cells 2x with PBS
 2. add 0.25 % Trypsin and incubate for 5 min at 37 $^{\circ}$ C and 5 % CO₂ in a humidified atmosphere

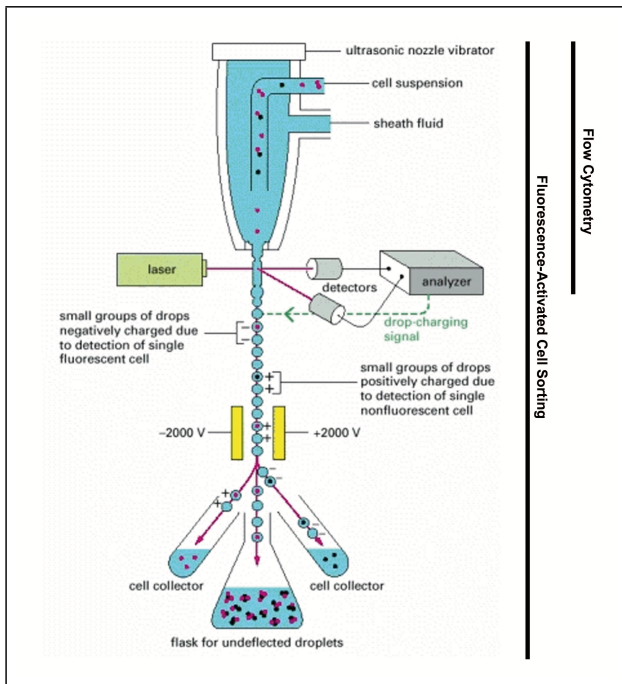


Figure 3.12: The principle of flow cytometry and fluorescence-activated cell sorting (FACS). In Flow Cytometry, fluorescence properties of cells are quantified on the single-cell level. A suspension of cells is stained for a specific marker, incorporated into a stream of sheath fluid and exposed to laser irradiation. Those cells that express the specific marker fluoresce upon irradiation. The fluorescence emission and its intensity are detected for each cell by a detector. In fluorescence-activated cell sorting (FACS), the cell-bearing stream of sheath fluid is broken into droplets by an ultrasonication mechanism, each droplet containing maximally one cell. Those droplets that contain a cell expressing the marker under investigation are polarized to have a distinct charge, whereas those that do not are polarized exactly oppositely. Empty droplets remain uncharged. The oppositely charged droplets are deflected into opposed directions in an electric field and thus are collected in different tubes. Illustration taken and modified from [Alberts et al., 2002].

3. resuspend detached cells in ice-cold PBS (5 % FCS)
 4. wash cells 2x with ice-cold PBS (1 % BSA) and resuspend them therein
- Stain cell surface antigens:
 1. aliquot cells to FACS tubes on ice at 100,000 cells and 100 μ l PBS (1 % BSA) per tube
 2. add primary, directly labeled antibody
 3. incubate on ice for 60 min in the dark
 4. wash cells 2x in ice-cold PBS (1 % BSA) and resuspend them in 200 μ l ice-cold PBS
 5. store cells on ice until flow cytometry (avoid long-term storage)

For analysis of the level of expression of a specific antigen, its median fluorescence intensity, as measured by the fluorescence signal generated by the dye-conjugated specific antibody, was normalized to the median fluorescence intensity of unstained cells. These normalized fluorescence intensities of specific antigens were then compared either to identically normalized isotype stainings in order to judge the significance of antigen expression or compared to other treatment groups to determine significant differences in antigen expression between them. For further details on significance testing see page 51.

3.5.2 Cell Cycle Analysis

By quantifying the fluorescence intensity of a cell nucleus following fluorescent nucleic acid staining, the amount of DNA present in that cell can be determined using flow cytometry. This allows for exact quantification of the distribution of a population of cells within the distinct cell cycle phases (see figure 3.13 on page 49).

Due to the linear relationship between DNA amount and fluorescence intensity emitted, two G_1 cells which simultaneously pass the detector will erroneously be detected as one G_2 cell. To avoid such erroneous enlargement of the G_2 population, the width of the fluorescence peak generated by a cell passing the detector has to be analyzed: A single cell (singlet) passing the detector will have a gaussian profile of fluorescence intensity emission, first increasing when entering the detector, then peaking when being

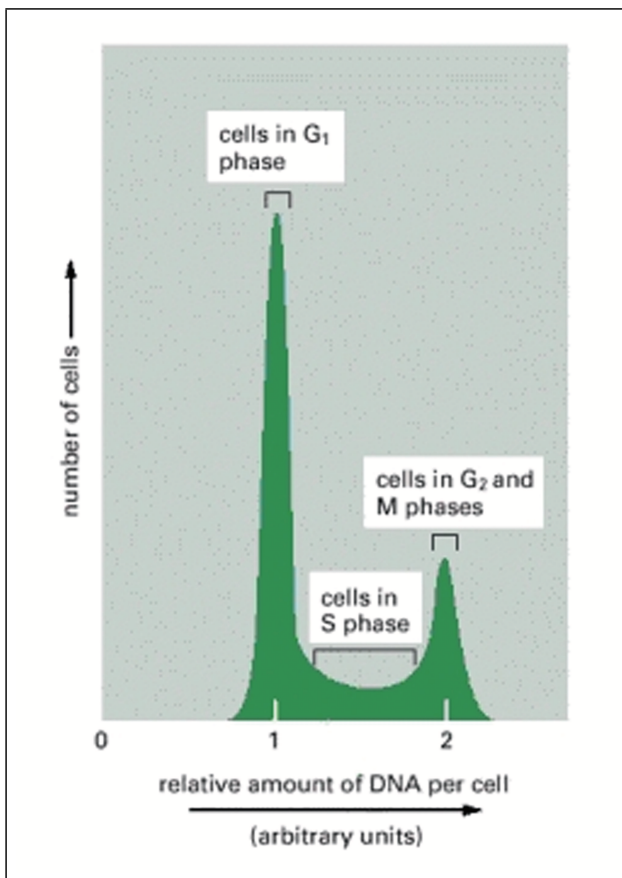


Figure 3.13: The principle of cell cycle analysis by flow cytometry. Upon staining of nuclear DNA with an intercalating fluorescent dye, the intensity of the fluorescent dye can be used as a signal which is directly proportional to the amount of DNA in that cell. Those cells that have a diploid set of chromosomes, i.e. cells in the first gap phase (G_1) of the cell cycle, will fluoresce half as intense as cells having replicated their entire genome once and being in G_2 or mitosis (M) phase. The nuclear fluorescence intensity of cells in the process of DNA synthesis (S phase) will lie intermediate between G_1 and G_2 phase cells. Here, the number of cells in G_1 is greater than the number of cells in G_2 and M phase, which means that cell passage through G_1 takes longer than passage through G_2 and M. Illustration taken from [Alberts et al., 2002].

completely inside, and finally decreasing again when leaving the detector. When two cells (a doublet) pass the detector, the fluorescence intensity generated by the first cell will decrease already when the fluorescence intensity of the second cell still increases. Thus, the width of the fluorescence peak becomes greater, and this greater width can be used as a measure to exclude doublets and even higher orders of cell aggregates from cell cycle analysis.

Nuclear DNA staining for cell cycle analysis by flow cytometry was done according to the manufacturer's instructions as detailed below:

- Harvest ASC:
 1. wash cells 2x with PBS
 2. add 0.25 % Trypsin and incubate for 5 min at 37 °C and 5 % CO₂ in a humidified atmosphere
 3. resuspend detached cells in ice-cold PBS (5 % FCS)
 4. wash cells 2x with ice-cold PBS and resuspend them in ice-cold PBS
- Stain nuclear DNA:
 1. add cell suspension drop-wise to 3 ml ice-cold 70 % ethanol in a FACS tube under vortexing
 2. incubate cells for 45 min on ice
 3. wash cells 2x in PBS, centrifuging at 2,000 g
 4. resuspend cells in RNase-containing propidium iodide staining solution at 10⁶ cells per 500 µl solution
 5. incubate for 30 min in the dark at 37 °C
 6. transfer tubes on ice and perform flow cytometry

The result of this analysis is a graph representing the number of cells as a function of the nuclear fluorescence intensity, i.e. a graph that depicts how many cells exhibit a distinct nuclear fluorescence intensity and thus how many cells contain a distinct amount of nuclear DNA (see figure 3.13 on page 49 for an example). In order to determine the percentage of cells within a distinct cell cycle phase on basis of such a graphic representation, an algorithm has to be used that fits the experimental data to a concrete mathematical model defining begin, course and end of each cell cycle phase. This algorithm can subsequently be used to calculate the number or percentage of cells within a distinct cell cycle phase. I used the Watson algorithm which fits the experimental data to meet the simple assumptions that data are normally distributed and that a G₁ peak is present [Watson et al., 1987]. In contrast to all other assays used in this work, normal distribution of the experimental data obtained can be assumed, since the number of observations in flow cytometry is extremely high and usually exceeds the number of 10,000 by far, whereas most other biological assays are done only in triplicate.

3.6 Data Analysis and Statistics

3.6.1 Data Normalization

To facilitate statistical data analysis, all metrical data obtained in the *in vitro* assays were subjected to normalization. To this end, all data obtained for a certain parameter, as e.g. alkaline phosphatase activity, and for a certain individual, i.e. the adipose tissue donor, were collected, and the minimum (x_{\min}) and maximum (x_{\max}) value for all treatment conditions and time points analyzed in this individual was determined. The position of a distinct value x obtained for this parameter and individual with respect to the extremes x_{\min} and x_{\max} was then represented as

$$x_{\text{norm}} \equiv \frac{x - x_{\min}}{x_{\max} - x_{\min}}.$$

This operation scales all values obtained for a certain individual and parameter to a range from zero (the lowest value measured, $x = x_{\min}$) to one (the highest value measured, $x = x_{\max}$). This yields a set of normalized data for each individual and parameter analyzed.

In order to allow for the representation of one parameter in relation to another, as as e.g. alkaline phosphatase activity in relation to the cell number, the metrical data obtained for the first parameter and individual were divided by the metrical data obtained for the second parameter of the same individual. Then, data normalization was done as described before.

In case both parameters to be related to each other were determined in different individuals, the median value of the metrical data obtained for the first parameter, as e.g. alkaline phosphatase activity, at a distinct experimental condition in a variety of individuals was determined and then divided by the median value of the metrical data obtained for the second parameter, as e.g. the cell number, at the same experimental condition in a variety of individuals. Then, data normalization was done as described before. In contrast to the procedure described in the last paragraph, this yields only one set of normalized data for each parameter analyzed, and intra-individual differences cannot be depicted.

3.6.2 Data Illustration

Data are mostly presented as box plots. The solid box of such a plot represents 50 % of the measured values that assemble around a central value called median and that is indicated by a horizontal line. The box ranges from the 25th to the 75th percentile, i.e. that 25 % of the measured values lay below the lower border of the box and 25 % of them lay above the upper border of the box. Error bars starting below and above the box indicate the 5th and 95th percentile and are called whiskers.

3.6.3 Statistics

Since the data obtained for the parameters analyzed were in virtually all cases not normally distributed, i.e. they did not deviate to the same extent above *and* below a central mean, testing for significance in the difference between two datasets had to be done by non-parametric significance tests. These tests, in contrast to parametric significance tests as e.g. the Student's *T*, do not assume a specific, usually normal distribution of the dataset. The non-parametric significance test applied here is the Mann-Whitney *U* test. The level of significance was set to a *p*-value of lower or equal 0.05 ($p \leq 0.05$), i.e. the probability that the significance test failed and erroneously indicated a significant difference between two datasets that *de facto* arose from pure chance is five percent.

Chapter 4

Results

4.1 Expression of TNF Receptors by ASC

TNF binds two distinct surfacial receptors officially designated TNFRSF1A and TNFRSF1B. By real-time RT PCR and flow cytometry, I confirmed that mesenchymal stem cells derived from the adipose tissue express these receptors.

On both the RNA and protein level, TNFRSF1A was much stronger expressed than TNFRSF1B (compare figures 4.1 and 4.2 on the pages 53 and 53, respectively). With increasing duration of ASC culture, expression of both receptor genes showed a tendency of being up-regulated, which however was significant only for *TNFRSF1A* (see figure 4.1). TNF stimulation showed a tendency of increasing the expression of both receptor genes, which was significant for expression of *TNFRSF1B*, but not for *TNFRSF1A* (see figure 4.1).

On the protein level, this tendency was not confirmed (see figure 4.2). Furthermore, TNFRSF1A showed a tendency of being reduced by TNF treatment of ASC, though not significantly. Despite the weak expression level of TNFRSF1B, TNF receptor protein expression was strong enough to significantly escape the background fluorescence level defined by the isotype control.

4.2 Impact of TNF on NF κ B Signaling Pathway Activation in ASC

Upon binding its surfacial receptors, TNF can induce three distinct signaling axes: the NF κ B pathway, the MAPK pathway and the apoptosis pathway.

A potential activating effect of TNF on the NF κ B pathway was analyzed by staining the p65 subunit of the NF κ B transcription factor. p65, also designated as RELA, heterodimerizes with NF κ B1 to form the most abundant transcription factor variant of the NF κ B family [Pruitt et al., 2009]. In case TNF activates the NF κ B pathway, translocation of NF κ B – and thus also of its subunit p65 – from the cytoplasm to the nucleus will occur.

And indeed, even after only one hour of stimulation, transduction of the TNF signal from the extracellular space to the nucleus was observed (see figure 4.3 on page 54). NF κ B activation was also present at later time points and at least until the end of observation after one week (data not shown). In contrast to TNF, neither osteogenically stimulated nor unstimulated ASC showed NF κ B activation, whereas under co-treatment of ASC with both TNF and osteogenic stimulants, NF κ B activation was also observed. Hence, TNF acted as a strong activator of the

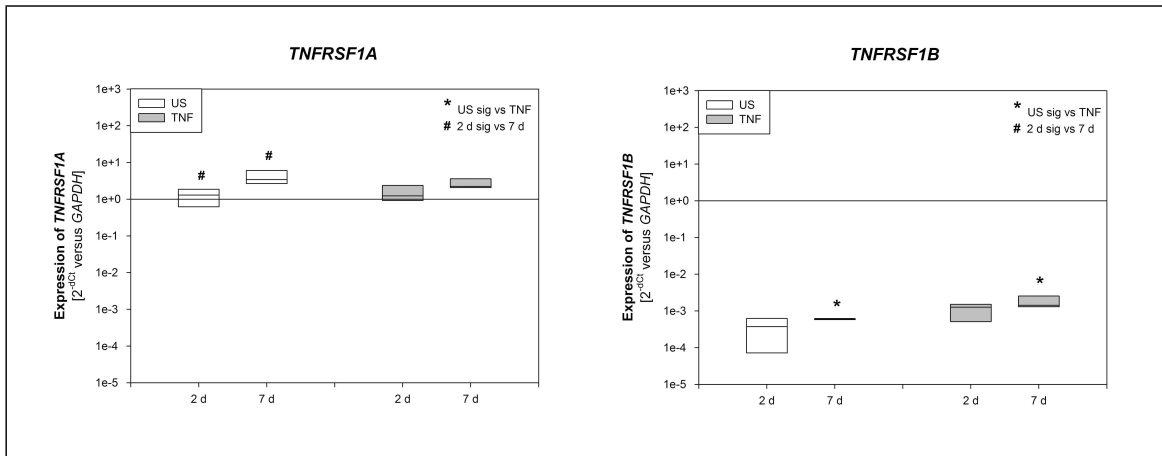


Figure 4.1: Expression of TNF receptor genes by ASC. Absolute expression levels of TNF receptor genes 1 and 2, designated as *TNFRSF1A* and *TNFRSF1B*, were determined by real-time RT PCR, and data were normalized to the expression of the housekeeping gene *GAPDH*. The level of significance was set to a p -value of less or equal 0.05 and determined applying the non-parametric Mann-Whitney U test. US: unstimulated ASC. TNF: TNF-stimulated ASC.

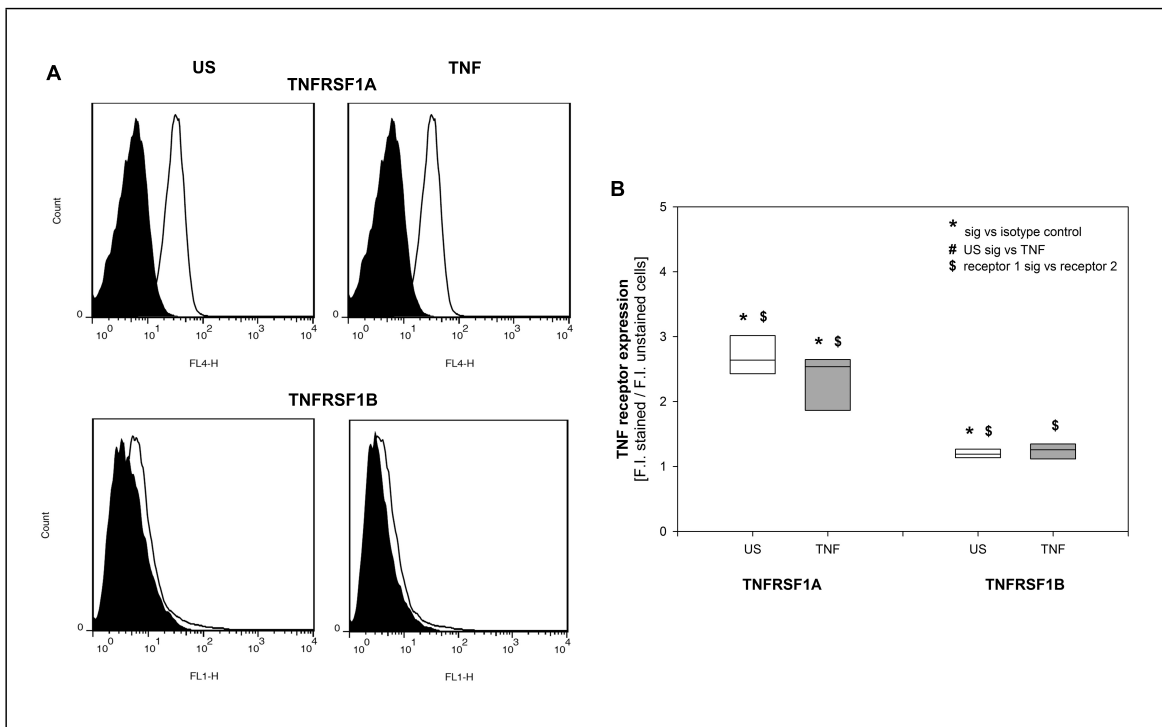


Figure 4.2: Expression of TNF receptor proteins by ASC. In (A), the protein expression level of *TNFRSF1A* and *TNFRSF1B* after one week of stimulation was analyzed by flow cytometry and is displayed for one individual as a histogram overlay of stained (unfilled histogram) and unstained (filled histogram) ASC. Subfigure (B) displays a flow cytometric expression analysis of multiple individual stem cell donors. Data quantification was done by normalizing the fluorescence intensity (F.I.) of the specific receptor staining to the F.I. of unstained ASC. Significance of the absolute expression levels of the receptor proteins was determined by comparing the normalized F.I. of the specific receptor staining to the F.I. of isotype control stainings normalized to unstained ASC. The level of significance was set to a p -value of less or equal 0.05 and determined applying the non-parametric Mann-Whitney U test. US: unstimulated ASC. TNF: TNF-stimulated ASC.

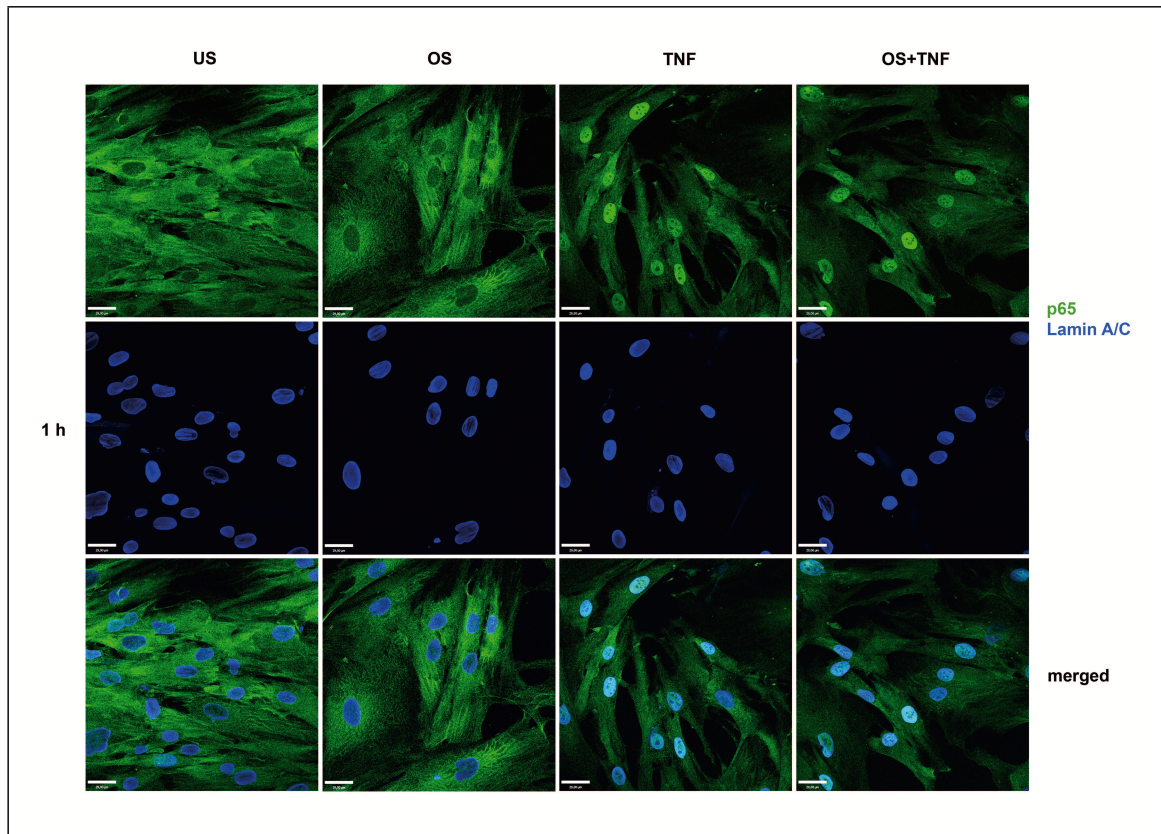


Figure 4.3: Impact of TNF on activation of the NF κ B pathway in ASC. By confocal microscopy, the translocation of NF κ B after one hour of stimulation with TNF was visualized in ASC by staining with a primary antibody directed against the p65 subunit of this heterodimeric transcription factor. Nuclei were co-stained using a primary antibody directed against the nuclear envelope protein dimer lamin A/C. All primary antibodies were visualized by fluorescently labeled secondary antibodies directed against the host species of the primary antibody. All images were captured at identical magnification, the scale bar corresponding to 29 μ m. US: unstimulated ASC. OS: osteogenically stimulated ASC. TNF: TNF-stimulated ASC.

NF κ B pathway in ASC.

4.3 Impact of TNF on MAPK Signaling Pathway Activation in ASC

As was done for the NF κ B pathway, a potential activating effect of TNF on the MAP kinase pathway was analyzed by observation of nuclear translocation of activated transcription factors and kinases. As is summarized in figure 1.1 on page 6, the MAPK pathway comprises three distinct signaling axes that transduce extracellular signals via the transcription factor AP1 and the MAP kinases ERK and p38.

4.3.1 Analysis of p38 Activation

p38 is a member of the MAP kinase family and is designated as MAPK14. Upon activation through phosphorylation by upstream kinases, p38 translocalizes to the nucleus to regulate the

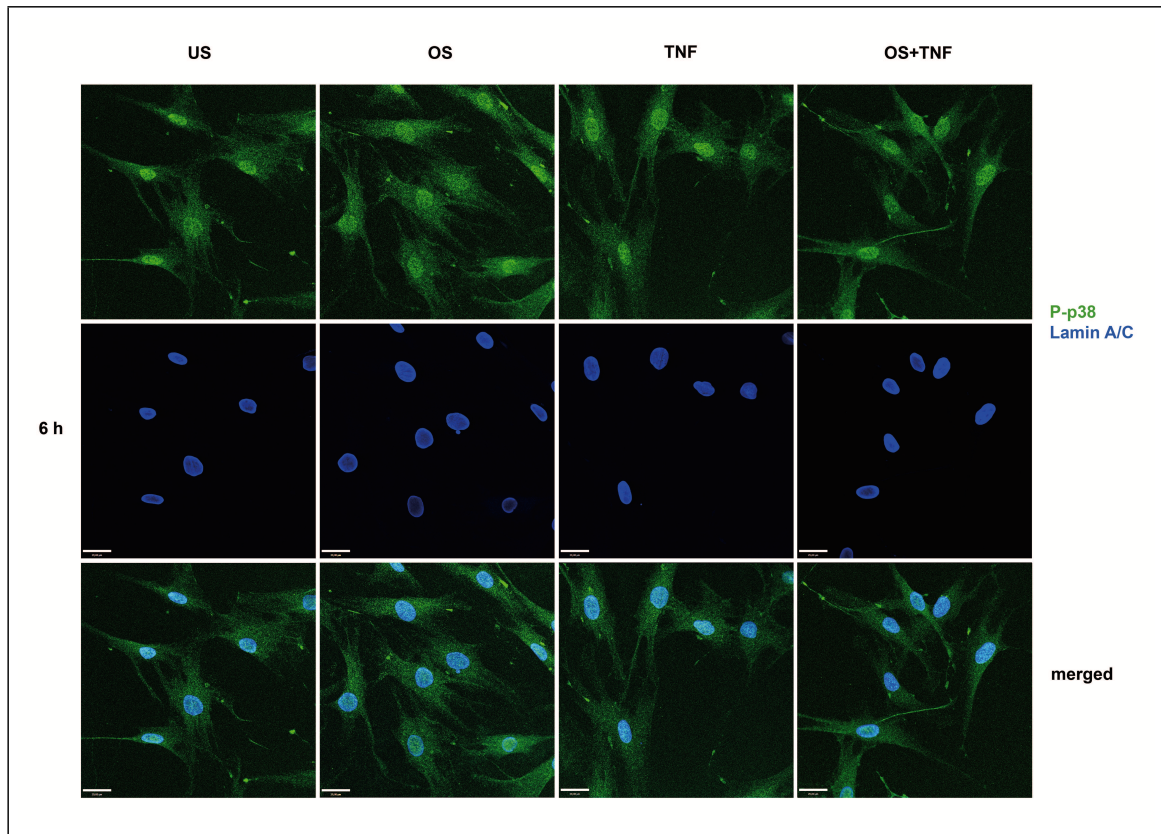


Figure 4.4: Impact of TNF on activation of the MAPK pathway kinase p38 in ASC. By confocal microscopy, active p38 was detected by staining for the phosphorylated and thus activated form of this MAP kinase, designated as P-p38. Nuclei were co-stained using a primary antibody directed against the nuclear envelope protein dimer lamin A/C. All primary antibodies were visualized by fluorescently labeled secondary antibodies directed against the host species of the primary antibody. All images were captured at identical magnification, the scale bar corresponding to 29 μm . US: unstimulated ASC. OS: osteogenically stimulated ASC. TNF: TNF-stimulated ASC.

activity of a variety of transcription factors by phosphorylation [Bradham and McClay, 2006]. Thus, by staining the phosphorylated form of p38, translocation and thus activation of this transcription factor was analyzed.

Active p38 was found under any stimulatory condition after six hours of stimulation (see figure 4.4 on page 55), but also at earlier and later time points for up to one week (data not shown). Thus, the specific stimuli applied did not have any regulatory impact on p38 activation.

4.3.2 Analysis of AP1 Activation

Activator protein 1 (AP1) is a dimeric transcription factor present either as a homodimer consisting of two identical JUN family member subunits or as a heterodimer consisting of one JUN family member and one FOS or ATF family member [Karamouzis et al., 2007]. Activation of AP1 occurs through phosphorylation of the JUN transactivation domain by JUN N-terminal kinases (JNKs), which themselves are activated by upstream JNK kinases. Upon activation, JNKs translocate to the nucleus to activate JUN by phosphorylation. Thus, by staining of the phosphorylated form of cJUN, translocation and activation of the AP1 transcription factor was

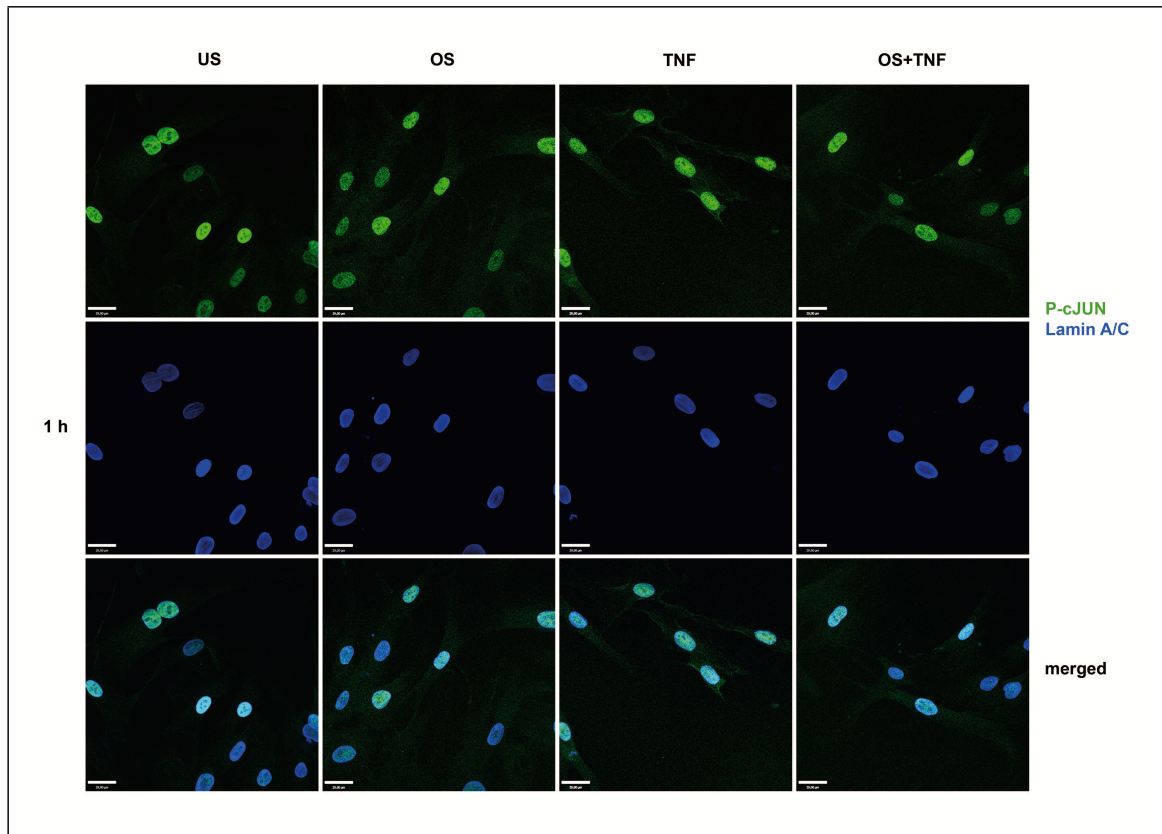


Figure 4.5: Impact of TNF on activation of the MAPK pathway transcription factor AP1 in ASC. By confocal microscopy, active AP1 was detected by staining for the phosphorylated and thus activated transactivation domain of its subunit cJUN, designated as P-cJUN. Nuclei were co-stained using a primary antibody directed against the nuclear envelope protein dimer lamin A/C. All primary antibodies were visualized by fluorescently labeled secondary antibodies directed against the host species of the primary antibody. All images were captured at identical magnification, the scale bar corresponding to 29 μm . US: unstimulated ASC. OS: osteogenically stimulated ASC. TNF: TNF-stimulated ASC.

analyzed.

Active AP1 was found under any stimulatory condition after one hour of stimulation (see figure 4.5 on page 56), but also at later time points for up to one week (data not shown). Thus, the specific stimuli applied did not have any regulatory impact on AP1 activation.

4.3.3 Analysis of ERK Activation

Extracellular signal-regulated kinases (ERKs), which are also called mitogen-activated protein kinases (MAPKs), regulate nuclear transcription factors by phosphorylation. ERKs themselves are activated by phosphorylation through upstream kinases [Pruitt et al., 2009]. Thus, by staining the phosphorylated form of a domain homolog for both ERK1 and ERK2, translocation and activation of these kinases was analyzed.

Active ERK1 and ERK2 was found under no stimulatory condition after one hour of stimulation (see figure 4.6 on page 57), but also not at later time points for up to one week (data not shown). Thus, the specific stimuli applied did not have any regulatory impact on the activation of ERK1 and ERK2.

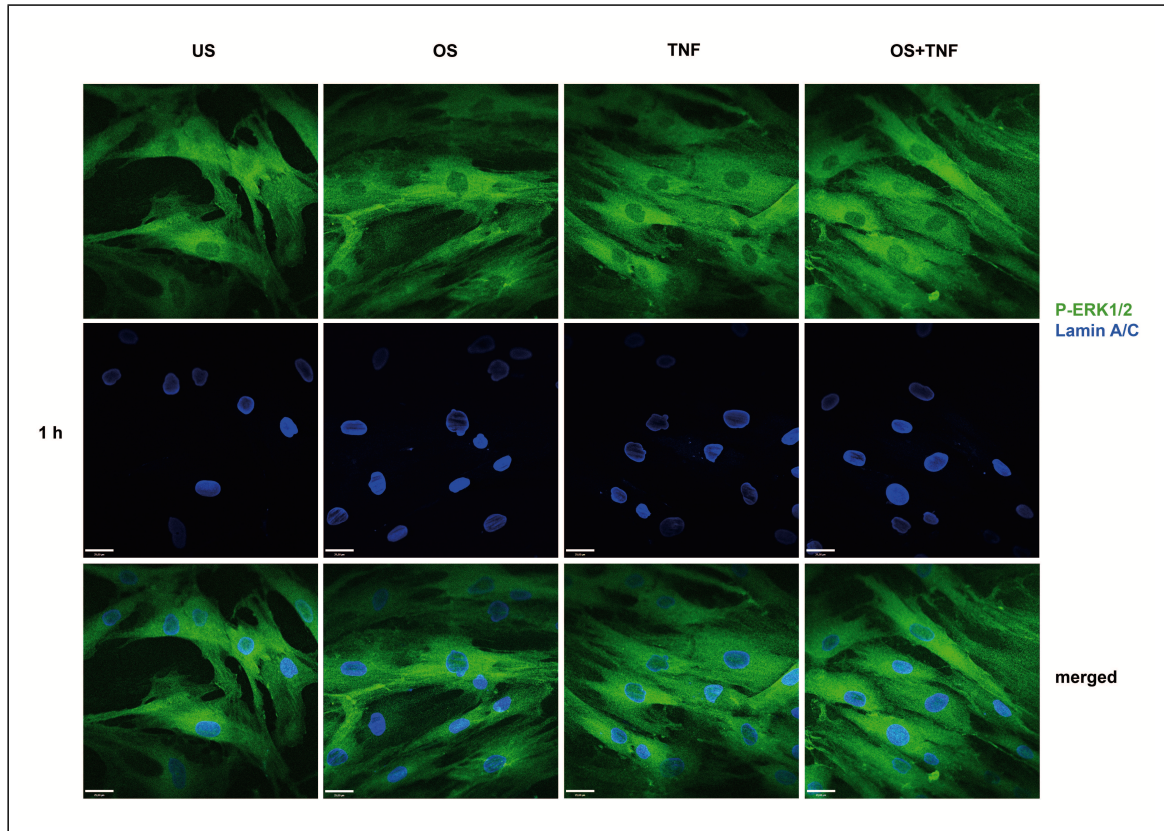


Figure 4.6: Impact of TNF on activation of the MAPK pathway kinases ERK1 and ERK2 in ASC. By confocal microscopy, active ERK1 and ERK2 was detected by staining for the phosphorylated and thus activated form of a domain homolog in both kinases, designated as P-ERK1/2. Nuclei were co-stained using a primary antibody directed against the nuclear envelope protein dimer lamin A/C. All primary antibodies were visualized by fluorescently labeled secondary antibodies directed against the host species of the primary antibody. All images were captured at identical magnification, the scale bar corresponding to 29 μm . US: unstimulated ASC. OS: osteogenically stimulated ASC. TNF: TNF-stimulated ASC.

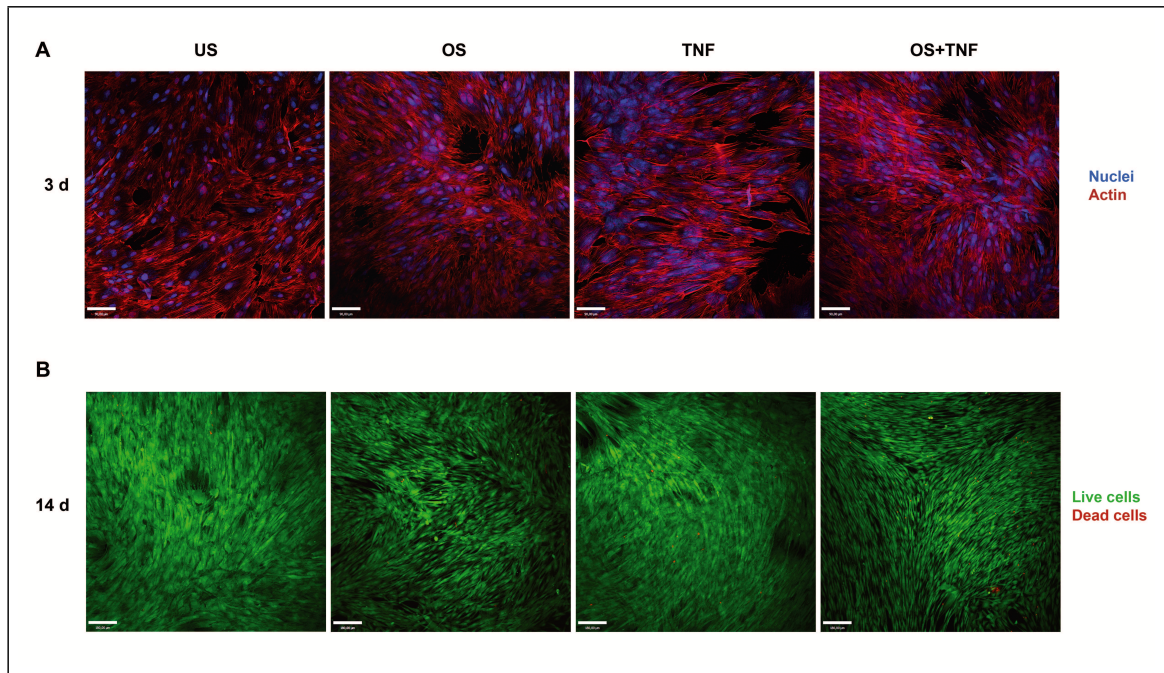


Figure 4.7: Effect of TNF on cytoskeletal organization and viability of ASC. Organization of the f-actin cytoskeleton after three days of stimulation was visualized by confocal microscopy (A), whereas viability of ASC after 14 days of stimulation was visualized by non-confocal fluorescence microscopy (B). In (A), actin staining was done with phalloidin conjugated to a fluorescent dye, whereas nuclei staining was with SYTOX Blue. The scale bar corresponds to 90 μm . In (B), live cell staining was with calcein acetoxymethyl ester, and dead cell staining was with propidium iodide. The scale bar corresponds to 180 μm . US: unstimulated ASC. OS: osteogenically stimulated ASC. TNF: TNF-stimulated ASC.

4.4 Impact of TNF on ASC Cytoskeletal Organization and Viability

In addition to the NF κ B and MAPK pathway, TNF can potentially exhibit an activating effect on the apoptosis pathway in ASC was analyzed. Since changes in the cytoskeletal organization are early hallmarks of apoptosis, I analyzed both the organization of filamentous actin (f-actin) in ASC after three days of stimulation and ASC viability as a late parameter after 14 days of stimulation.

Both actin organization and ASC viability were unchanged, irrespective of the applied stimulus (see figure 4.7 on page 58). Hence, TNF as well as osteogenic treatment of ASC did not induce apoptosis in these cells. Contrastingly, both types of stimulation increased ASC proliferation rates, since the number of cells per image, as judged by the number of nuclei, in both cases was clearly higher than in the corresponding unstimulated controls.

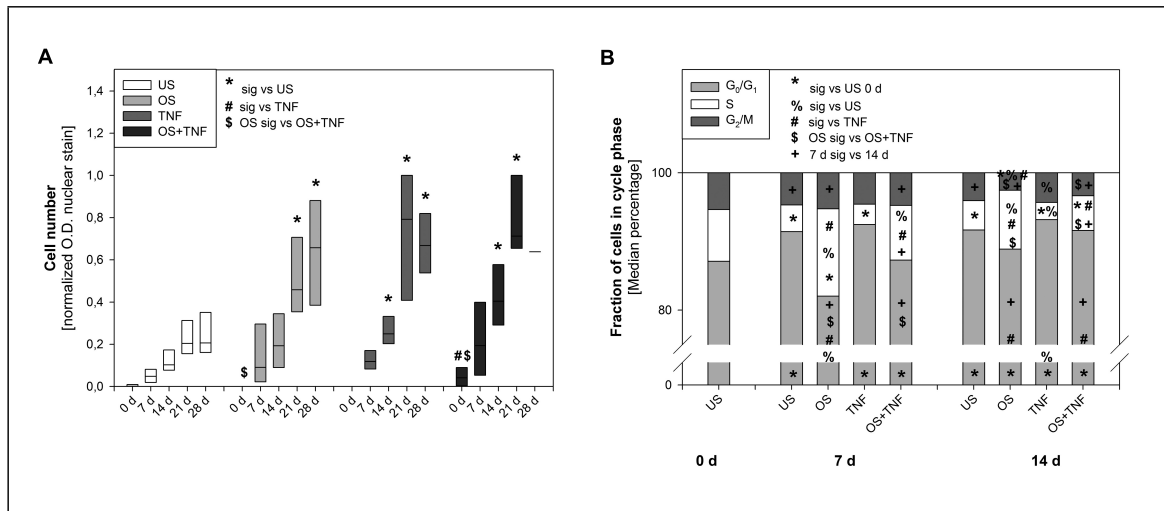


Figure 4.8: Effect of TNF on proliferation and cell cycle of ASC. In (A), the ASC number was determined indirectly by quantifying the optical density (O.D.) of the DNA-staining agent crystal violet. In (B), the percentage of ASC in the different cell cycle phases was assessed by nuclear staining with propidium iodide and subsequent cell cycle analysis on a flow cytometer. The level of significance was set to a p -value of less or equal 0.05 and determined applying the non-parametric Mann-Whitney U test. US: unstimulated ASC. OS: osteogenically stimulated ASC. TNF: TNF-stimulated ASC.

4.5 Impact of TNF on ASC Proliferation, Cell Cycle and Metabolic Activity

4.5.1 Analysis of Proliferation and Cell Cycle

The proliferation-inducing effect of TNF-treatment on ASC proliferation indicated by the greater number of cells seen in figure 4.7 on page 58 could subsequently be confirmed by quantification of cell numbers for up to four weeks in a large number of individuals.

While cell numbers of unstimulated ASC increased comparatively slowly and rather linearly, treatment with TNF or osteogenic substances yielded exponential trends (see figure 4.8A on page 59). From two weeks on, the number of TNF-treated ASC was significantly higher than that of the unstimulated ASC at the same point of time. Osteogenic stimulation also led to an increase in proliferation rate that was significant beginning from three weeks after start of stimulation, while it was significant beginning from two weeks when ASC were co-stimulated with TNF and osteogenic compounds.

Cell cycle analysis by flow cytometry revealed a differing impact of TNF and osteogenic treatment of ASC on the distribution of cells within the three cell cycle phases G_0/G_1 (gap phase of cellular quiescence and gap phase before DNA replication, respectively), S (DNA synthesis) and G_2/M (gap and mitosis phase after DNA replication, respectively).

Under TNF-treatment, the proliferative increase seen for cell numbers in subfigure 4.8A was accompanied by a significant reduction of the portion of cells being into the S phase of the cell cycle (see figure 4.8B). Simultaneously, the portion of cells being into the G_0/G_1 and G_2/M phase increased significantly. For osteogenic stimulation, exactly the opposite was true: Significantly more cells were detected in the S phase, at the expense of cells being into the G_0/G_1 and G_2/M phase. When ASC were co-treated with both TNF and osteogenic substances,

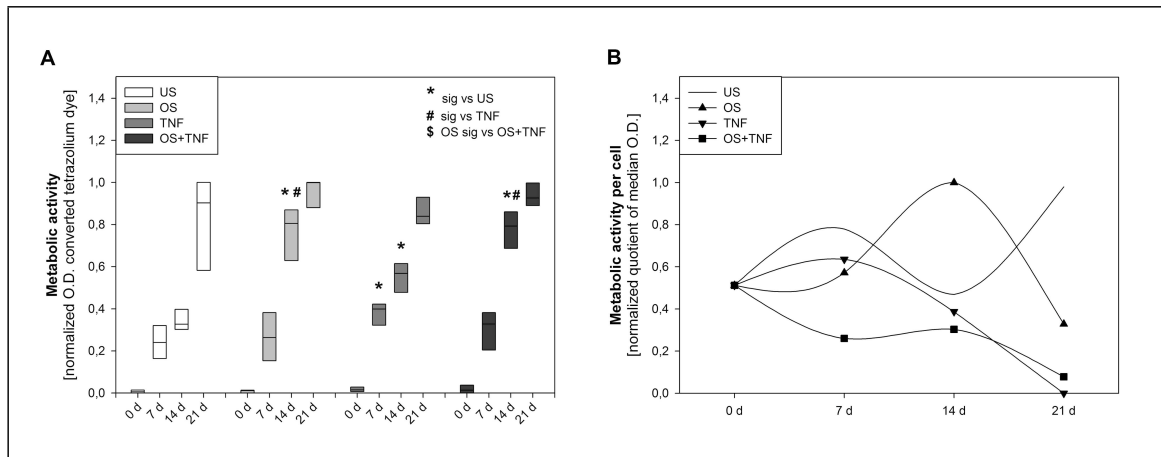


Figure 4.9: Effect of TNF on metabolic activity of ASC. In (A), the metabolic activity of ASC was determined indirectly by quantifying the optical density (O.D.) of the NADH-mediated conversion of the tetrazolium salt MTS into a formazan salt. To determine the metabolic activity per cell as illustrated in (B), the metabolic activity of the MTS assay in subfigure (A) was put into relation to the cell number determined indirectly by quantifying the O.D. of the DNA staining agent crystal violet at the corresponding experimental condition. The level of significance was set to a p -value of less or equal 0.05 and determined applying the non-parametric Mann-Whitney U test. US: unstimulated ASC. OS: osteogenically stimulated ASC. TNF: TNF-stimulated ASC.

the opposed actions of the single substances on ASC cell cycle added to give rise to a cell cycle distribution that lay exactly intermediate. In comparison to osteogenic treatment alone, the TNF and osteogenically co-treated ASC showed a significant increase in the portion of G_0/G_1 and G_2/M phase cells, whereas the portion of cells being into the S phase was significantly reduced.

Interestingly, the duration of cell culture also affected the cell cycle distribution of ASC, but in a different manner as both TNF and osteogenic stimuli. With increasing time of ASC culture, the portion of cells in G_0/G_1 increased, while the portion of cells being into the S and G_2/M phase decreased. Contrastingly, the specific stimuli always altered the portion of S phase cells in one direction and the portion of gap phase cells in the other. These concerted changes therefore, as a reflection of the specific reaction of ASC to a specific stimulus, can well be distinguished from the temporal changes in ASC cell cycle distribution.

4.5.2 Analysis of Metabolic Activity

To shed more light on the processes going on on the proliferation and cell cycle level, global analysis of ASC metabolic activity was done. Under all treatment conditions, the metabolic activity increased strongly with time over the three weeks of observation (see figure 4.9A on page 60). After two weeks of stimulation, all kinds of treatment resulted in a significant increase of metabolic activity in comparison to the unstimulated cells. Additionally, the metabolic activity of ASC that were osteogenically stimulated or co-treated with TNF and osteogenic stimuli was significantly increased compared to those ASC that were treated with TNF alone.

To get not only an idea about the changes of metabolic activity of the entire ASC culture, but also of the change in metabolic activity per cell, I normalized the metabolic activity data shown in subfigure 4.9A to the corresponding cell numbers shown in subfigure 4.8A. In the unstimu-

lated ASC, the metabolic activity per cell showed a sigmoidal shape: it increased during the first week of culture, declined to the starting value around the second week of culture and subsequently increased very strongly until the end of observation after three weeks of culture (see figure 4.9B). For the TNF-treated ASC, the metabolic activity per cell showed a weak tendency of increasing also during the first week of culture, but subsequently declined continuously until the end of observation.

Interestingly, osteogenic stimulation also led to a sigmoidal shape of metabolic activity per cell, but exactly inversely to that observed for the unstimulated ASC: After an initial decline at day seven of culture, the metabolic activity per cell strongly increased to peak at day 14 and subsequently declined to end in the range of the value observed at day zero. Co-treatment with TNF and osteogenic substances induced a stronger initial reduction of metabolic activity than osteogenic treatment alone, and the metabolic activity was reduced a second time at the end of observation after three weeks of ASC culture. Hence, TNF supplementation to osteogenic medium reduced the peaking of metabolic activity observed for solely osteogenically treated ASC at day 14, but ended with the typical decrease that was found for both single treatments.

Thus, both TNF and osteogenic substances increased proliferation rates of ASC, which however resulted from a differing regulation of the cell cycle. Additionally, the temporal course of metabolic activity per cell differed greatly from that of osteogenically stimulated ASC. Therefore, these analyses imply that the increase in proliferation rate observed for both TNF and osteogenic treatment is accomplished through differing cellular processes.

4.6 Impact of TNF on Osteogenic Differentiation of ASC

To gather a comprehensive insight into a putative role of TNF in regulation of osteogenic differentiation of ASC, the differentiation process was analyzed in a variety of functional and non-functional assays addressing numerous osteogenic marker genes and proteins ranging from transcription factors involved in early osteogenesis-inducing steps over enzymes facilitating extracellular matrix mineralization to finally the determination of the extracellular matrix calcium content.

4.6.1 Analysis of Osteogenic Transcription Factors

Representing a very early marker of the osteogenic differentiation pathway, the expression of *ZBTB16*, a zinc finger transcription factor regulating transcription of the osteogenesis key player gene *RUNX2*, was analyzed by real-time RT PCR.

In unstimulated ASC, *ZBTB16* expression showed a tendency to peak around day seven of cell culture and to decline subsequently, an effect that however was characterized by a large variance (see figure 4.10A on page 62). Under TNF-treatment, the expression level of *ZBTB16* was also strongly variable between individuals and showed a tendency of hitting the bottom around day 14 of culture. However, the expression level did never differ significantly from the level found for the unstimulated cells.

Contrastingly, *ZBTB16* expression in osteogenically stimulated ASC increased significantly and by a factor of approximately 10,000 over the unstimulated control cells. In addition, it was significantly higher than observed for the TNF-treated ASC and exhibited a much narrower distribution of intra-individual variances in expression level. In ASC co-treated with TNF and osteogenic stimuli, the *ZBTB16* expression profile closely resembled that found for osteogenic

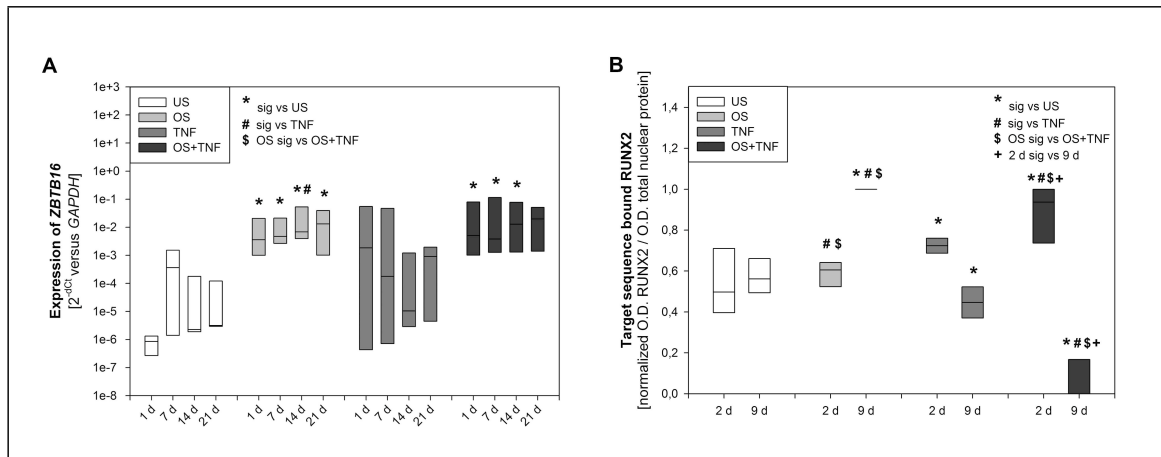


Figure 4.10: Effect of TNF on expression of the osteogenic transcription factor *ZBTB16* and on *RUNX2* DNA-binding activity. In (A), the expression level of the zinc finger and BTB domain containing 16 gene (*ZBTB16*) was analyzed by real-time RT PCR and put into relation to the expression of the housekeeping gene glyceraldehyde-3-phosphate dehydrogenase (*GAPDH*). In (B), nuclear target DNA sequence-bound *RUNX2* was determined colorimetrically in an enzyme-linked immunosorbent assay (ELISA) and put into relation to the optical density (O.D.) of total nuclear protein. The level of significance was set to a p -value of less or equal 0.05 and determined applying the non-parametric Mann-Whitney U test. US: unstimulated ASC. OS: osteogenically stimulated ASC. TNF: TNF-stimulated ASC.

stimulation alone. Again, a very narrow variance in expression level was observed between the individuals analyzed.

Since TNF did not increase *ZBTB16* expression significantly, while osteogenic stimulation of ASC did, and since both kinds of ASC stimulation resulted in a significantly different *ZBTB16* expression profile, the result of the expression analysis of this osteogenesis-related transcription factor denies an inductive effect of TNF on osteogenic differentiation of ASC. Additionally, TNF treatment of ASC under osteogenic stimulation did neither increase nor decrease expression of this transcription factor and thus apparently did not influence osteogenic differentiation.

Activation of the *ZBTB16* downstream target *RUNX2* was analyzed in a functional assay. Upon osteogenic stimulation, runt-related transcription factor 2 (*RUNX2*, also known as core-binding factor subunit alpha-1, CBF-alpha-1) is activated by phosphorylation and translocalizes to the nucleus. There, it activates transcription of genes involved in osteogenic differentiation. If TNF treatment would induce osteogenic differentiation of ASC, activated *RUNX2* would be found bound to the consensus binding sequence in the promoter region of its target genes. In the assay used, the amount of activated *RUNX2* bound to an oligonucleotide representing this consensus binding sequence was measured.

In the unstimulated ASC, activated DNA-bound *RUNX2* was found at a medium extent which remained unchanged by the time of ASC culture (see figure 4.10B on page 62). TNF treatment of ASC induced a small, though significant increase in initial *RUNX2* activity after two days of treatment, which, however, strongly declined after nine days of ASC exposure to TNF. Contrastingly, osteogenic stimulation, starting from the medium *RUNX2* activities that were found also for the unstimulated and TNF-treated ASC after two days, strongly and significantly increased *RUNX2* activity after nine days of stimulation. Co-treatment of ASC with both TNF and osteogenic stimuli yielded this strong increase in *RUNX2* activity already after two days of treatment and ended at the low activity found for TNF treatment alone. Thus, TNF treatment of ASC under osteogenic

stimulation did not preclude the strong peaking of RUNX2 DNA-binding activity, but accelerated its onset, whereas TNF treatment alone was not able to induce the peaking of RUNX2 activity found under osteogenic conditions.

Therefore, a potential inductive or repressive effect of TNF treatment on osteogenic differentiation of ASC is denied by both the result of the gene expression analysis (*ZBTB16*) and by the result of the functional, gene-regulatory analysis (*RUNX2*).

4.6.2 Analysis of Alkaline Phosphatase Activity

The process of extracellular matrix calcification involves activation of the bone-expressed variant of the enzyme alkaline phosphatase, which is designated ALPL. An overview staining of this osteogenic marker for bright-field phase contrast microscopy after 21 days of ASC culture revealed that alkaline phosphatase activity in the TNF-treated ASC raised over the level of the untreated cells, which interestingly showed some islets of alkaline phosphatase-positive cells (see figure 4.11A on page 64). However, alkaline phosphatase activity in both cases was clearly lower than observed for the osteogenically stimulated cells. The intensity of the staining was the highest in the co-stimulated cells, indicating an additive effect of both stimulants. Thus, osteogenic stimulation of ASC strongly increased the activity of alkaline phosphatase, and TNF treatment also showed a tendency of driving cells into osteogenic differentiation, though to a lesser extent.

In order to facilitate a statistically representative analysis of a quantitative measure as alkaline phosphatase activity, assessment of this parameter in fully quantifiable assays and employing a large number of individuals was done.

Real-time RT PCR-based analysis of the expression of the *ALPL* gene revealed a tendency of a time-dependent increase in the expression of this gene for TNF-treated ASC, which however was true also for the unstimulated control cells (see figure 4.11B on page 64). Contrastingly, the osteogenically stimulated ASC showed a much stronger increase in *ALPL* expression as compared to the unstimulated, but also TNF-treated ASC, which was significant at almost any time point of analysis. Co-treatment with TNF and osteogenic stimuli resulted in an expression pattern similar to that obtained for osteogenic stimulation alone.

In order to confirm that the results obtained for the gene expression level hold true also for the protein level, I analyzed the activity of alkaline phosphatase in a substrate conversion assay. The experimental outcome was very similar to what was seen on the RNA level: TNF-treated ASC showed a tendency of a time-dependent increase in alkaline phosphatase activity, which however was also true for the control cells and which was not significant at any point of time (see figure 4.11C on page 64). Only the osteogenically or co-stimulated ASC exhibited a reliable and significant increase in the activity of this enzyme for all time points analyzed when being compared to the untreated ASC, but mostly also when being compared to the TNF-treated ASC.

To exclude the possibility that the increased alkaline phosphatase activity observed following osteogenic stimulation of ASC was the result of the increased cell number under this condition, the median activity determined for each experimental condition was put into relation to the median cell number at that condition. These analyses delivered exactly the same result as before: Beginning from one week after start of osteogenic stimulation, ASC strongly increased alkaline phosphatase activity per cell (see figure 4.11D on page 64). This was not observed for TNF-treated or unstimulated ASC. Co-treatment of ASC with both TNF and osteogenic stimuli resulted in a similar increase of alkaline phosphatase activity per cell as osteogenic stimulation alone, beginning to be significant one week after start of stimulation.

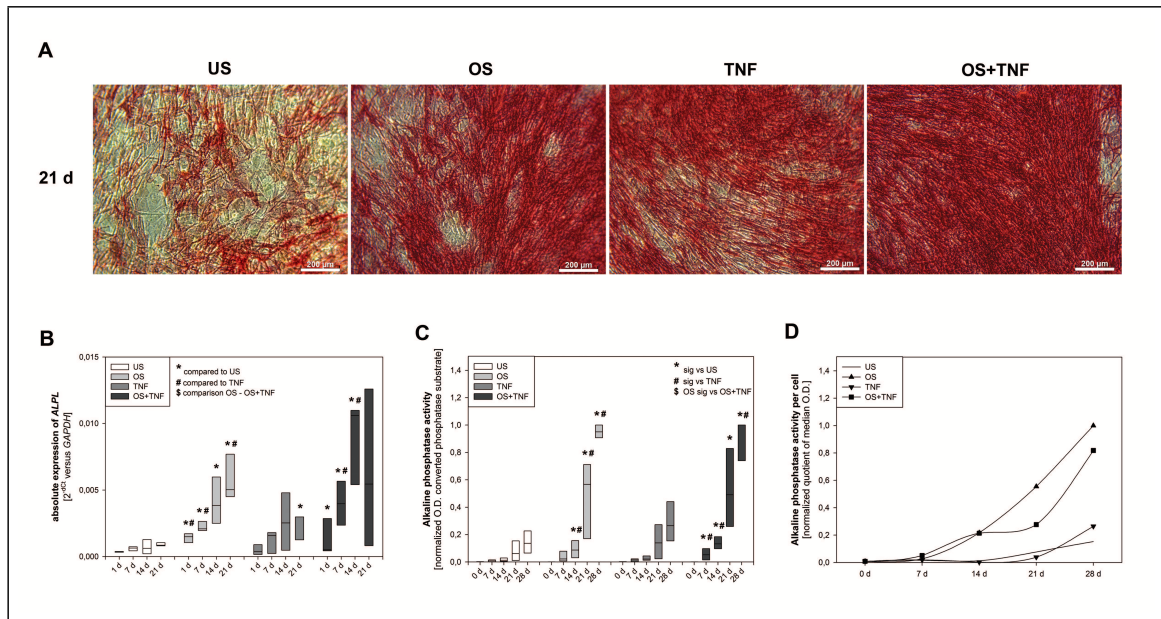


Figure 4.11: Effect of TNF on alkaline phosphatase activity of ASC. Subfigure (A) displays a bright-field phase contrast microscopic image acquired after stimulation of ASC for 21 days and after staining for active alkaline phosphatase with Fast Red Violet and Naphthol AS-MX phosphate. The scale bar corresponds to 200 μm . In (B), the expression level of the alkaline phosphatase gene *ALPL* was analyzed by real-time RT PCR and put into relation to the expression level of the housekeeping gene glyceraldehyde-3-phosphate dehydrogenase (*GAPDH*). In (C), the activity of alkaline phosphatase was determined indirectly by quantifying the optical density (O.D.) of the converted phosphatase substrate para-nitrophenyl phosphate (pNPP). In (D), the alkaline phosphatase activity, as displayed in subfigure (C), was put into relation to the cell number determined indirectly by quantifying the O.D. of the DNA-staining agent crystal violet at the corresponding experimental condition. The level of significance was set to a p -value of less or equal 0.05 and determined applying the non-parametric Mann-Whitney U test. US: unstimulated ASC. OS: osteogenically stimulated ASC. TNF: TNF-stimulated ASC.

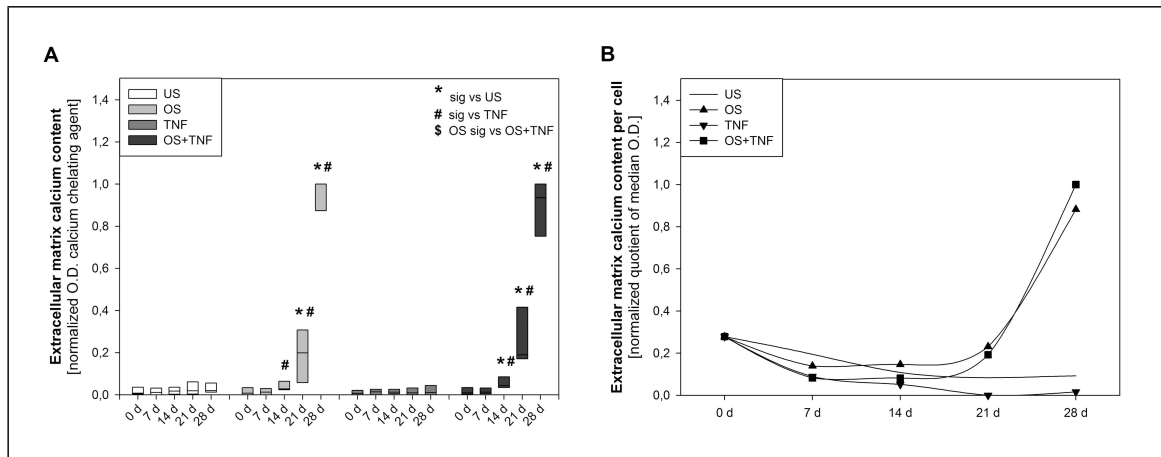


Figure 4.12: Effect of TNF on extracellular matrix calcium content of ASC. In (A), the calcium content of the extracellular matrix was determined indirectly by quantifying the optical density (O.D.) of the calcium-chelating agent ortho-kresolphthalein. In (B), the calcium content, as displayed in (A), was put into relation to the cell number determined indirectly by quantifying the O.D. of the DNA-staining agent crystal violet at the corresponding experimental condition. The level of significance was set to a p -value of less or equal 0.05 and determined applying the non-parametric Mann-Whitney U test. US: unstimulated ASC. OS: osteogenically stimulated ASC. TNF: TNF-stimulated ASC.

Thus, all statistically evaluable metrical analyses of alkaline phosphatase activity match in their basic outcome, namely the finding that there is no indication for an osteogenic effect of TNF on ASC *in vitro*, but also not for an inhibitory effect of TNF under osteogenic conditions.

4.6.3 Analysis of Extracellular Matrix Calcium Content

Calcification of the extracellular matrix of ASC, as a reliable functional and late hallmark of osteogenic differentiation, was absent in unstimulated and TNF-treated ASC (see figure 4.12A on page 65). Contrastingly, the osteogenically stimulated ASC, beginning with day 21 of stimulation, showed a significantly increased matrix calcium content as compared to the unstimulated ASC and beginning with day 14 also in comparison to the TNF-treated ASC. When ASC were co-treated with TNF and osteogenic stimuli, a significant difference was observed for both comparison groups.

Again, I additionally analyzed the extracellular calcium content as a function of the cell number, and the results that were obtained are very similar to what was found for alkaline phosphatase activity before. The unstimulated and TNF-treated ASC both showed a slightly decreasing extracellular calcium content per cell with time (see figure 4.12B), an effect that is likely to have occurred from increasing cell numbers at constant background levels of extracellular matrix calcium. Again, the osteogenically stimulated ASC began to strongly increase their extracellular calcium content beginning from day 21, and they did so equally strong as those ASC that were co-treated with TNF and osteogenic stimuli.

Therefore, the analysis of extracellular matrix calcification also argues against an inductive impact of TNF on osteogenic differentiation of ASC as well as against an impact of TNF on osteogenic differentiation when osteogenic stimulants were present. All marker genes or proteins of osteogenic differentiation analyzed, either acting at a very early (*ZBTB16* expression), early (RUNX2 DNA-binding activity), middle (alkaline phosphatase activity) or late stage of differ-

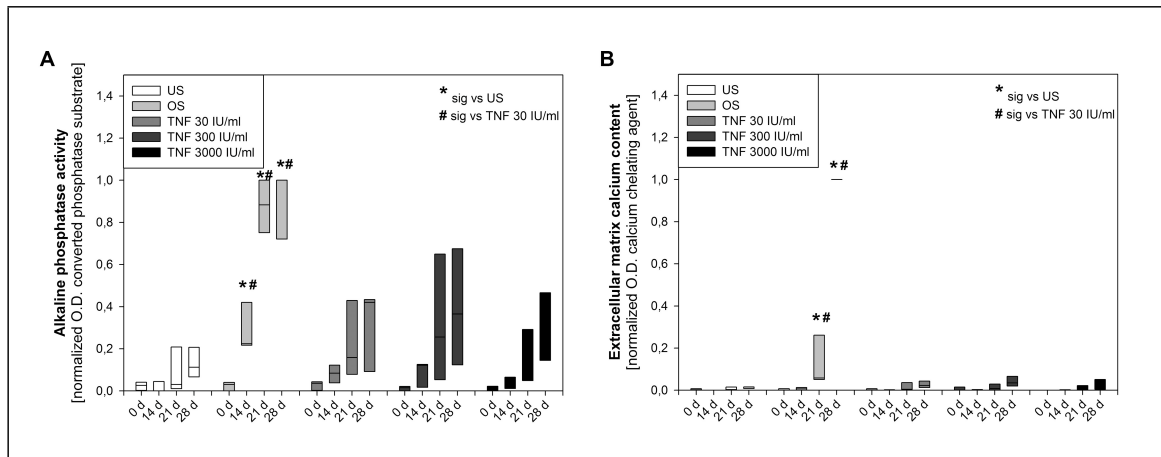


Figure 4.13: Effect of the TNF concentration on osteogenic differentiation of ASC. In (A), the activity of alkaline phosphatase was determined indirectly by quantifying the optical density (O.D.) of the converted phosphatase substrate para-nitrophenyl phosphate (pNPP). In (B), the calcium content of the extracellular matrix was determined indirectly by quantifying the O.D. of the calcium-chelating agent ortho-kresolphthalein. The level of significance was set to a p -value of less or equal 0.05 and determined applying the non-parametric Mann-Whitney U test. US: unstimulated ASC. OS: osteogenically stimulated ASC. TNF: TNF-stimulated ASC. I.U.: international unit.

entiation (extracellular matrix calcification), contradict a potential effect of TNF on osteogenic differentiation of ASC *in vitro*. In addition, they do also not give any indication for an inhibitory or promotive impact of TNF on osteogenic differentiation of ASC when osteogenic stimulants were present simultaneously.

4.7 Impact of the TNF Concentration on Osteogenic Differentiation of ASC

To reveal a potential dose-dependent effect of TNF on osteogenic differentiation of ASC, TNF concentrations ranging from 30 to 3,000 international units (I.U.) TNF per milliliter cell culture medium were used. It turned out that, irrespective of the TNF concentration applied, pro-inflammatory stimulation of ASC did neither induce any significant increase in alkaline phosphatase activity nor calcification of the extracellular matrix (see subfigures 4.13A and B, respectively, on page 66). Solely osteogenic stimulation raised alkaline phosphatase activity and matrix calcium content significantly over the level of the unstimulated controls. Supportingly, both markers of osteogenic differentiation were significantly lower in TNF-treated than in osteogenically stimulated ASC, and there were no significant differences between the different TNF concentrations.

Thus, the inability of TNF to induce osteogenic differentiation of ASC was not due to a dose-dependent effect, but rather reveals an intrinsic inability of this pro-inflammatory cytokine to induce an osteogenic differentiation program in ASC *in vitro* at whatever concentration analyzed. Since the amount of TNF secreted by ASC themselves was in the range of few picograms per ml medium (data not shown) and thus at the lower detection limit of current enzyme-linked immunosorbent assay-based approaches, a potential autocrine effect of TNF on ASC can be excluded. Noteworthy, ASC viability was not reduced even by the highest TNF concentration used,

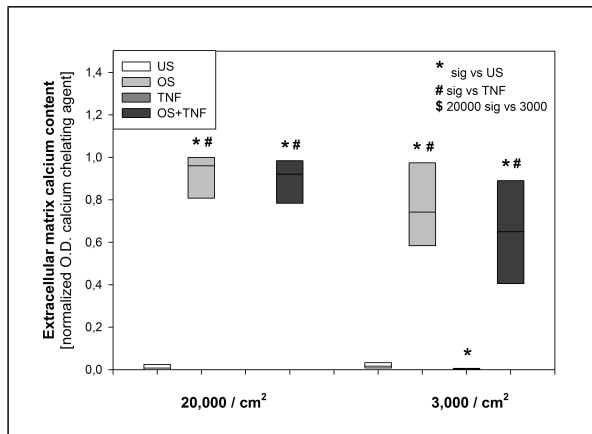


Figure 4.14: Effect of the cell seeding density on osteogenic differentiation of ASC. ASC were seeded at 3,000 and 20,000 cells per square centimeter, respectively. After 28 days of stimulation, osteogenic differentiation was analyzed. The calcium content of the extracellular matrix was determined indirectly by quantifying the optical density (O.D.) of the calcium-chelating agent orthokresolphthalein. The level of significance was set to a p -value of less or equal 0.05 and determined applying the non-parametric Mann-Whitney U test. US: unstimulated ASC. OS: osteogenically stimulated ASC. TNF: TNF-stimulated ASC.

as can be deduced from the active alkaline phosphatase found even under these conditions and after 28 days.

4.8 Impact of the Seeding Density on Osteogenic Differentiation of ASC

In addition to the concentration of TNF, the seeding density of ASC could potentially affect their osteogenic differentiation capacity. Therefore, I compared osteogenic differentiation of ASC seeded at a low density of 3,000 cells per square centimeter to a nearly confluent culture seeded at 20,000 cells per square centimeter, which was the default density in all experiments.

It turned out that there was no significant difference in the extent of osteogenic differentiation between those ASC that were seeded at low or standard density. The activity of alkaline phosphatase (data not shown) and the extracellular matrix calcium content did not show any significant differences after 28 days of stimulation (see figure 4.14 on page 67). Additionally, the number of ASC was virtually identical after 28 days, irrespective of the initial seeding density (data not shown).

Hence, osteogenic differentiation of ASC *in vitro* was not affected by the degree of confluence at the beginning of stimulation. Even at low seeding densities, ASC differentiated osteogenically and to the same extent as observed at nearly confluent seeding density, and TNF had no impact on this differentiation pathway at either seeding density.

4.9 Impact of TNF Pre-Treatment on Osteogenic Differentiation of ASC

Since neither the concentration of TNF nor the seeding density of ASC indicated an impact of TNF on osteogenic differentiation of ASC when TNF was present for the entire duration of cell culture, I analyzed the ability of ASC to differentiate osteogenically after having treated them only for three days with TNF. Subsequently, cells were stimulated osteogenically as before. As ASC are derived from the adipose tissue and are able to differentiate into adipocytes, adipogenic differentiation of ASC was analyzed in addition.

Neither osteogenic nor adipogenic differentiation of ASC was affected when cells were pre-treated with TNF, since alkaline phosphatase activity and cellular lipid content did not differ

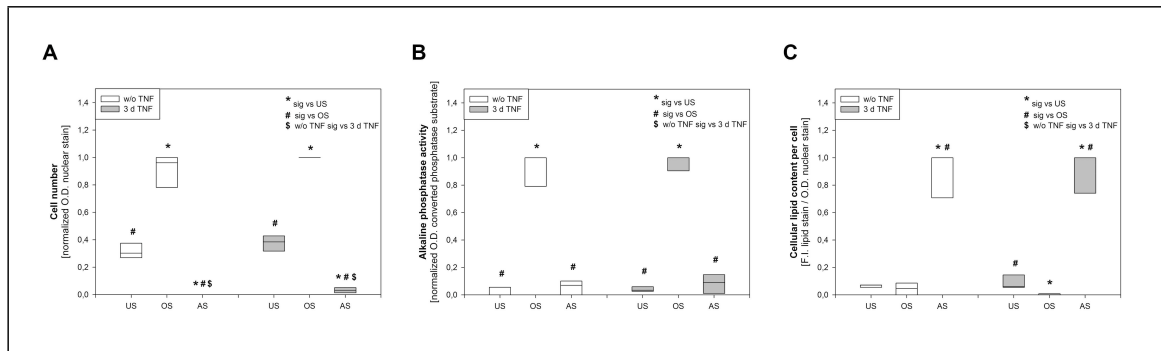


Figure 4.15: Effect of TNF pre-treatment on osteogenic and adipogenic differentiation of ASC. ASC were treated for three days with TNF and subsequently exposed to osteogenic and adipogenic stimulants for 14 days. In (A), the ASC number was determined indirectly by quantifying the optical density (O.D.) of the DNA-staining agent crystal violet. In (B), the activity of alkaline phosphatase was determined indirectly by quantifying the O.D. of the converted phosphatase substrate para-nitrophenyl phosphate (pNPP). In (C), the cellular lipid content was determined indirectly by quantifying the fluorescence intensity (F.I.) of the lipophilic dye boron-dipyrromethene (also called BODIPY), which subsequently was put into relation to the number of cells at the corresponding experimental condition, as determined indirectly by quantifying the O.D. of the DNA-staining agent crystal violet. The level of significance was set to a p -value of less or equal 0.05 and determined applying the non-parametric Mann-Whitney U test. US: unstimulated ASC. OS: osteogenically stimulated ASC. TNF: TNF-stimulated ASC. AS: adipogenically stimulated ASC.

significantly between the TNF pre-treated and the non-treated ASC (see subfigures 4.15B and C on page 68). Alkaline phosphatase activity raised significantly only for the osteogenically stimulated ASC, whereas cellular lipid content increased significantly only for the adipogenically stimulated ASC. In addition, ASC number increased significantly only for the osteogenically stimulated cells, whereas the adipogenically stimulated ASC showed a significant reduction of cell number in comparison to the unstimulated, slowly proliferating ASC, an observation that resulted from the stagnation of proliferation with beginning of adipogenic stimulation (see subfigure 4.15A). Again, there were no considerable and significant differences between the TNF pre-treated and the non-treated ASC.

Hence, neither osteogenic nor adipogenic differentiation of ASC was found to be affected by short-term pre-treatment of cells with TNF, which was true also for the continuous exposure of these cells to the cytokine. Therefore, the duration of TNF exposure had no impact on osteogenic differentiation of ASC *in vitro*.

4.10 Impact of Ascorbic Acid and β -Glycerophosphate on Osteogenic Differentiation of TNF-Treated ASC

Osteogenic stimulation of ASC was done with ascorbic acid, β -glycerophosphate and dexamethasone. Since TNF and the synthetic glucocorticoid dexamethasone are involved in regulation of partially overlapping pathways [Adcock, 2001], I tested whether supplementation of TNF-containing medium with ascorbic acid and β -glycerophosphate induces osteogenic differentiation of ASC.

It turned out that also in conjunction with ascorbic acid and β -glycerophosphate, TNF was not able to induce osteogenic differentiation of ASC. The extracellular calcium content of ASC cultures that were treated with TNF, ascorbic acid and β -glycerophosphate was at no time point

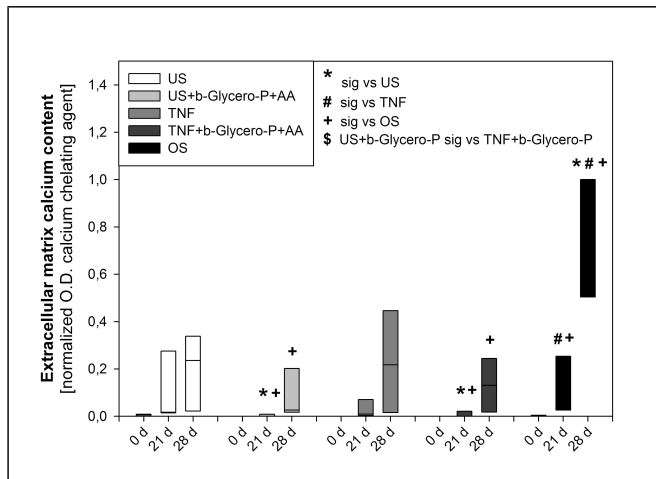


Figure 4.16: Effect of ascorbic acid and β -glycerophosphate on osteogenic differentiation of TNF-treated ASC. The calcium content of the extracellular matrix was determined indirectly by quantifying the optical density (O.D.) of the calcium-chelating agent ortho-kresolphthalein. The level of significance was set to a p -value of less or equal 0.05 and determined applying the non-parametric Mann-Whitney U test. US: unstimulated ASC. OS: osteogenically stimulated ASC. TNF: TNF-stimulated ASC. b-Glycero-P+AA: β -Glycerophosphate and Ascorbic Acid.

of analysis significantly higher than that of the unstimulated ASC, which contrastingly was true for the osteogenically stimulated ASC (see figure 4.16 on page 69). Supportingly, the extracellular matrix calcium content in ASC treated with TNF, ascorbic acid and β -glycerophosphate was significantly lower than in the osteogenically stimulated ASC, and there was no significant difference between ASC treated with either unsupplemented medium, medium supplemented with ascorbic acid and β -glycerophosphate, medium supplemented with TNF or medium supplemented with TNF and ascorbic acid and β -glycerophosphate.

This analysis therefore does not only extend the previous findings that TNF has no impact on osteogenic differentiation of ASC at either concentration, ASC seeding density or TNF exposure time analyzed, but underlines that the osteopromotive compounds ascorbic acid and β -glycerophosphate are not sufficient to induce osteogenic differentiation in ASC *in vitro*, either in presence or absence of TNF. Therefore, TNF cannot be considered to be at least a weak stimulus for osteogenic differentiation of ASC. Moreover, the synthetic glucocorticoid dexamethasone is strictly required for this differentiation pathway to succeed in these cells.

4.11 Impact of TNF on Osteoprotegerin Secretion by ASC

Since TNF treatment of ASC did not influence osteogenic differentiation of these cells *in vitro*, I analyzed whether it has an impact on osteogenic differentiation of other cells via paracrine mechanisms. To this end, secretion of osteoprotegerin (OPG), a factor acting as a decoy receptor for the major osteoclast differentiation-inducing factor RANKL, being involved in balancing the extent of osteoclast-mediated bone resorptive activity to the osteoblast-mediated bone-forming activity *in vivo*, was quantified in an enzyme-linked immunosorbent assay (ELISA).

Under all treatment conditions, OPG secretion increased time-dependently, an effect that was significant for both osteogenic treatment groups (see figure 4.17 on page 70). Following TNF treatment, OPG secretion by ASC was strongly, though not significantly, increased. Contrastingly, osteogenic stimulation yielded a significant reduction in OPG secretion as compared to the TNF-treated ASC. In the ASC treated with both TNF and osteogenic stimulants, OPG secretion was significantly higher than observed for osteogenic stimulation alone, indicating that the OPG secretion-increasing effect of TNF outweighed the OPG secretion-reducing effect of osteogenic stimulation.

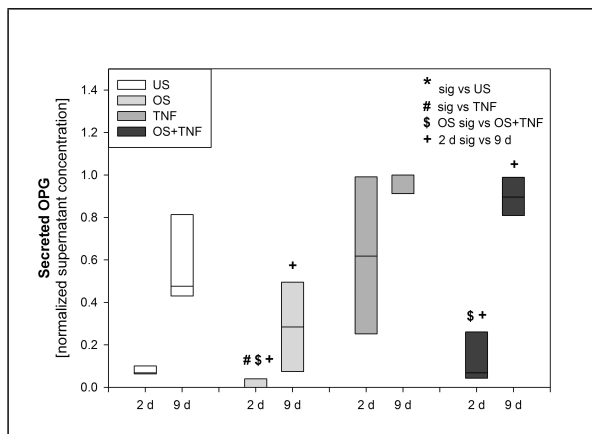


Figure 4.17: Effect of TNF on osteoprotegerin (OPG) secretion by ASC. The OPG concentration in ASC supernatants was determined indirectly in an enzyme-linked immunosorbent assay (ELISA). The level of significance was set to a p -value of less or equal 0.05 and determined applying the non-parametric Mann-Whitney U test. US: unstimulated ASC. OS: osteogenically stimulated ASC. TNF: TNF-stimulated ASC.

Thus, TNF was found to increase OPG secretion by ASC *in vitro*, while osteogenic stimulation reduced secretion of this decoy receptor for the osteoclast differentiation-promoting factor RANKL. Taking only these actions on ASC into account, these findings *in vivo* would translate into a reduction of osteoclast maturation rates by TNF and an increase of osteoclastogenesis for osteogenic conditions, illustrating that TNF exerted directly opposed effects on ASC as compared to osteogenic stimulation.

4.12 Summary of Results

Summarizing the main results presented above, I found that TNF did not induce osteogenic differentiation of ASC, since the results obtained in the analyses of osteogenic markers are the same for TNF-treated and unstimulated ASC *and* at the same time different for TNF-treated and osteogenically stimulated ASC (see table 4.1 on page 71). Most of these osteogenic markers remained unchanged when TNF was added to osteogenic stimulants, with exception of the RUNX2 DNA-binding activity, which increased earlier, but was reduced later as compared to the osteogenically stimulated ASC. Hence, TNF did neither induce osteogenic differentiation of ASC nor have a considerable promotive or reductive impact on this differentiation pathway in ASC *in vitro*.

In contrast to the osteogenic markers, the parameters cell cycle progression, metabolic activity, NF κ B pathway activity and secretion of the osteoclast differentiation-inhibiting factor osteoprotegerin (OPG) by ASC changed by TNF treatment in comparison to unstimulated conditions, but *also* in comparison to osteogenically stimulated ASC *and* to ASC treated with both TNF and osteogenic stimulants. These parameters can help elucidating mechanistic differences in the cellular reactions following TNF-mediated pro-inflammatory treatment of ASC and treatment with stimulants inducing osteogenic differentiation of these cells.

Contrastingly, ASC proliferation rate is not an informative marker, since it was changed in the same direction by all experimental conditions.

TNF receptor expression, ASC f-actin organization and viability as well as nuclear translocation of the activated transcription factor AP1 and the MAP kinases ERK1/2 and p38 were not affected by any stimulatory condition and thus are not regulated by them. However, the constitutive activation of AP1 and p38 can help to explain observations that were made for all ASC treatment groups.

Table 4.1: Summary on the impact of TNF on osteogenic differentiation of ASC. Results are grouped in accordance to the context they belong to. = indicates equal findings for the corresponding parameter, Δ indicates differing findings. US: unstimulated ASC. OS: osteogenically stimulated ASC. TNF: TNF-stimulated ASC.

effect on ...	US	OS	TNF	OS+TNF	TNF vs. US	TNF vs. OS	OS vs. OS+TNF
TNF receptor 1 and 2 expression	temporally increased	not determined	temporally increased	not determined	=	not applicable	not applicable
actin organization and viability	no effect	no effect	no effect	no effect	=	=	=
NF κ B pathway	inactive	inactive	activated	activated	Δ	Δ	Δ
MAPK pathway: AP1	active	active	active	active	=	=	=
MAPK pathway: ERK1/2	inactive	inactive	inactive	inactive	=	=	=
MAPK pathway: p38	active	active	active	active	=	=	=
proliferation rate	default	strong	strong	strong	Δ	=	=
cell cycle	default	increased portion of S phase cells, but decreased portion of neighboring G phases cells	reduced portion of S phase cells, but increased portion of neighboring G phases cells	intermediate between phenotype in TNF and OS	Δ	Δ	Δ
temporal course of metabolic activity	initially increased, intermediately decreased, lately strongly increased	early decreased, intermediately strongly increased, lately decreased	continuously decreased	early and lately decreased	Δ	Δ	Δ
ZBTB16 expression	largely constant	strongly increased	largely constant	strongly increased	=	Δ	=
RUNX2 DNA-binding activity	largely constant	initially and temporally increased	temporally decreased	initially increased, but temporally decreased	Δ	Δ	Δ
alkaline phosphatase expression and activity	temporally increased	very strongly temporally increased	temporally increased	very strongly temporally increased	=	Δ	=
extracellular matrix calcium content	largely constant	strongly temporally increased	largely constant	strongly temporally increased	=	Δ	=
OPG secretion	temporally increased	temporally increased, but overall reduced	very strongly overall and temporally increased	strongly overall and temporally increased	Δ	Δ	Δ

Chapter 5

Discussion

5.1 ASC Express both TNF Receptors

TNF can bind two distinct receptors, TNFRSF1A and TNFRSF1B [Aggarwal et al., 1985]. I found both TNF receptors to be expressed on ASC, TNFRSF1A being expressed much stronger than TNFRSF1B (see figures 4.1 and 4.2 on pages 53 and 53, respectively). This finding fits well to expression data for cells derived from related tissues and developmental stages which can be retrieved in public databases. According to the latest annotation of expressed sequence tags in the UniGene Database of the National Center for Biotechnology Information (NCBI), *TNFRSF1A*, the gene encoding TNF receptor 1, is expressed in almost any tissue and throughout all developmental stages, whereas transcripts of *TNFRSF1B*, encoding TNF receptor 2, are found only at fetal and adult stage and are much more restricted to distinct tissues, including adipose and connective tissue, but not bone marrow e.g. (see figures 5.1A and B on page 73). The overall level of *TNFRSF1B* transcripts is annotated to be much lower than that of *TNFRSF1A*.

Protein expression data for both receptors were also retrieved *in silico* using the Human Protein Atlas. The protein data largely confirmed the data obtained for the transcripts, with exception of TNF receptor 2 which is referenced to be present also in cells of the bone marrow (see figure 5.2 on page 74). Hence, both receptors are expressed in most cell types and tissues, and although expression data for TNF receptors were so far not published for ASC, the expression pattern found goes well together with what is known about related cells and tissues.

I found an influence of TNF on the expression of the TNF receptors, precisely a significant upregulation of the expression of the receptor 2 gene and an insignificant downregulation of the receptor 1 protein. This is in accordance with previous findings revealing TNFRSF1A being either not regulated or partially downregulated after TNF treatment, whereas TNFRSF1B was upregulated [Bradley, 2008]. Both findings fit well to the promoter structure of the corresponding receptor-encoding genes: the *TNFRSF1A* promoter resembles those of housekeeping genes, explaining its constitutive expression, whereas the *TNFRSF1B* promoter has a non-housekeeping structure and provides binding sites for e.g. the signal transducers nuclear factor of kappa light polypeptide gene enhancer in B-cells (NF κ B) and the jun proto-oncogene (JUN, also known as cJUN or activator protein 1, AP1) [Bradley, 2008], which is a member of the mitogen-activated protein kinase (MAPK) pathway family. Both NF κ B and JUN are activated by TNF, which implies a positive feedback loop for the *TNFRSF1B* regulation: the more TNF is present, the more receptor will be expressed, as was observed for ASC on the RNA level.

The upregulation of *TNFRSF1B* expression may have been stronger if pro-TNF would have

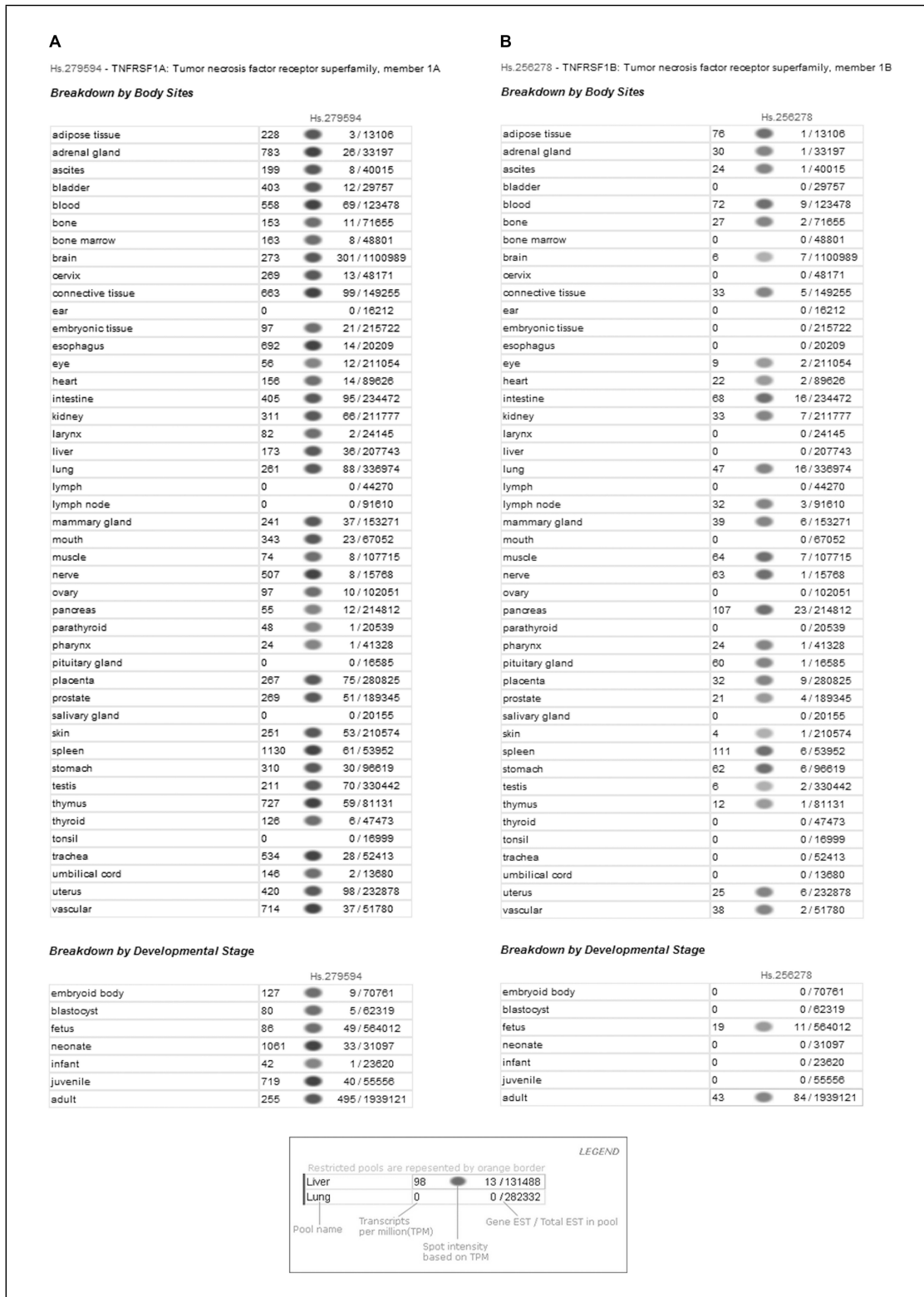


Figure 5.1: Expression of TNF receptor genes in various tissues and developmental stages. (A) Abundance of Expressed Sequence Tags (ESTs) of the TNF receptor 1 gene *TNFRSF1A* and (B) of the TNF receptor 2 gene *TNFRSF1B*. Expression data were retrieved from the NCBI UniGene Database [Wheeler et al., 2005].

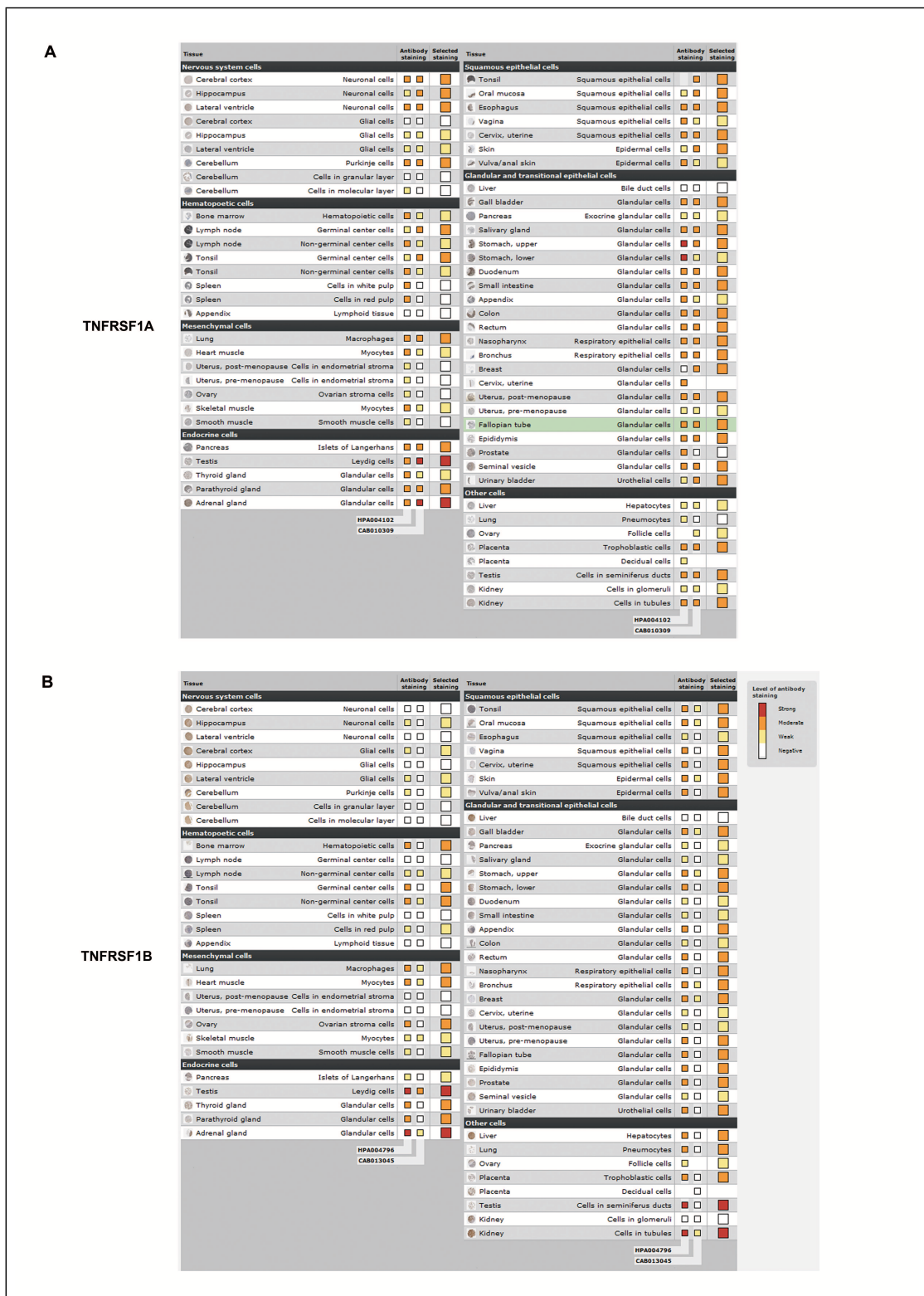


Figure 5.2: Expression of TNF receptor proteins in various tissues. (A) Expression of TNF receptor 1 (TNFRSF1A) and (B) TNF receptor 2 (TNFRSF1B), respectively, as judged by the intensity of the corresponding immunostaining. Expression data were retrieved from the Human Protein Atlas [Berglund et al., 2008].

been used. Pro-TNF is the membrane-bound precursor of TNF (also designated “mTNF”) which is cleaved into soluble TNF by ADAM 17, a member of the metalloproteinase family. In contrast to TNFRSF1A, TNFRSF1B has only low affinity to the soluble form of TNF, but high affinity to the membrane-bound form [Grell et al., 1995]. Therefore, the membrane-bound TNF type may have yielded a higher upregulation of the gene encoding TNFRSF1B.

The low expression level of TNFRSF1B in comparison to TNFRSF1A does not necessarily diminish its biological action, since TNFRSF1B can pass its ligand to the highly expressed TNFRSF1A and thereby potentiate TNFRSF1A-mediated signaling [Haridas et al., 1998]. To inactivate the highly expressed TNFRSF1A, it is shedded from the cell surface by metalloproteinase-mediated cleavage to yield a soluble, but inactive form [Bradley, 2008].

Thus, as both TNF receptors were found to be expressed by ASC, the effect of TNF binding to them was investigated. The best characterized effect of TNF receptor activation known so far is activation of the NF κ B and MAPK signal transduction pathways as well as induction of apoptosis (see figure 1.1 on page 6).

5.1.1 TNF Induced the NF κ B Pathway in ASC

The NF κ B pathway is involved in regulation of almost any cellular process, as e.g. inflammation, immunity, proliferation, differentiation and apoptosis [Oeckinghaus and Ghosh, 2009]. I found that TNF activated the NF κ B pathway in ASC (see figure 4.3 on page 54), and this activation lasted at least until day seven of stimulation. In the NF κ B pathway, ligand-binding to the receptor is transduced into gene expression via a hierarchical system of kinases that activate the transcription factor NF κ B (see figure 5.3 on page 76).

The non-finding of NF κ B activation in unstimulated ASC underlines the correctness of the non-finding of TNF secretion by ASC in an ELISA-based approach (data not shown): If the lower limit for TNF detection would have been too low and TNF would not have been detected for that reason, although it was secreted by ASC, an activating effect of TNF on NF κ B translocation in unstimulated, but also in osteogenically stimulated ASC must have been observed – which obviously was not the case.

5.1.2 TNF did not Induce the MAPK Pathway in ASC

The MAPK pathway is involved in regulation of various cellular processes such as proliferation, differentiation and apoptosis [Raman et al., 2007]. It consists of three signaling axes that can be activated independently of each other (see figure 5.4 on page 77).

While the ERK signaling axis was inactive at all experimental conditions, the p38 and AP1 axis were not.

p38 was Constitutively Active in ASC

The MAP kinase p38 is involved in regulation of cell proliferation and cancer, differentiation and response to stress [Krens et al., 2006; Bradham and McClay, 2006]. I found it to be constitutively activated in ASC, at least until day seven of cell culture (see text and figure 4.4 on page 55).

In order to find a potential function of this constitutively activated kinase on ASC, one has to take into account all cellular reactions that were driven into the same direction for either culture condition applied. One such parameter was the basal level of osteogenic differentiation that was seen even in the unstimulated ASC cultures. Supportingly, p38 activity was reported to be

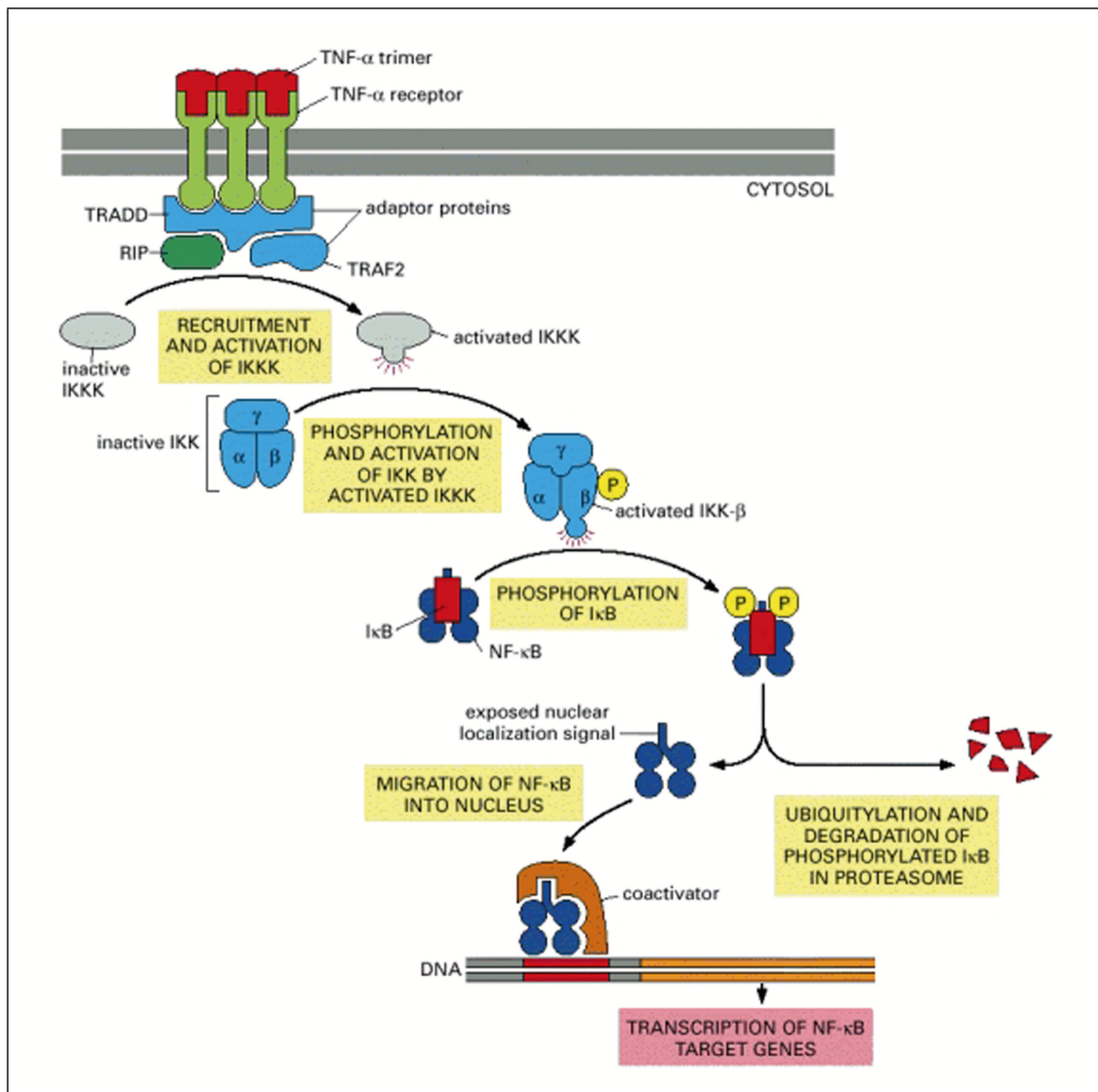


Figure 5.3: Schematic representation of TNF-induced activation of the NF κ B pathway. Binding of a TNF homotrimer to its homotrimeric receptors induces a rearrangement of the clustered cytoplasmic receptor domains. This rearrangement activates the receptor-bound adaptor proteins TNF-associated death-domain protein (TRADD) and TNF-receptor-associated factor 2 (TRAF2) as well as the kinase receptor-interacting protein kinase (RIP). By subsequent activation of inhibitor of kappa B (κ B) kinase kinase kinase (IKKK) and κ B kinase kinase (IKK), κ B is phosphorylated, which drives its ubiquitinylation and proteasomal degradation. Dissociation of κ B from NF κ B makes the nuclear localization signal of NF κ B accessible. This drives the transport of NF κ B into the nucleus, where it regulates expression of its target genes possessing κ B binding sites. Contrastingly to κ B, phosphorylation activates NF κ B by increasing its DNA-binding and transcriptional activity [Naumann and Scheidereit, 1994]. The transcription factor NF κ B is a heterodimer consisting of an NF κ B1 (p50) or NF κ B2 subunit on the one hand and a REL, RELA (p65) or RELB subunit on the other, the p50-p65 heterodimer being the most abundant form of NF κ B. Illustration taken from [Alberts et al., 2002].

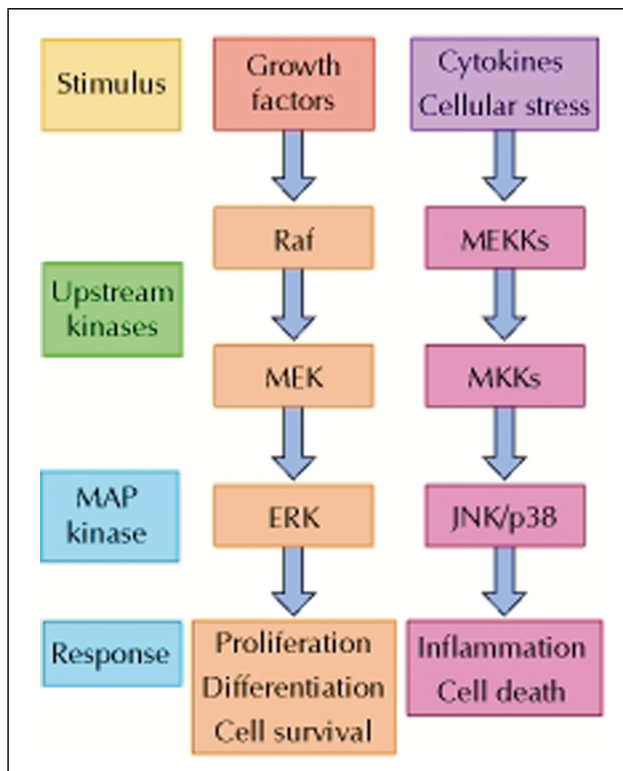


Figure 5.4: Schematic representation of the MAPK pathway. Via a hierarchical system of mitogen-activated protein kinases (MAPK), the MAP kinase pathway transduces extracellular signals into intracellular changes of gene expression. These signals are transduced to the nucleus via three routes, one involving the kinase extracellular signal-regulated kinase (ERK) which activates proliferation, differentiation and survival, whereas the others involve the kinases JUN N-terminal kinase (JNK) and p38 and generally lead to inflammation and cell death. JNK activates a transcription factor called activator protein 1 (AP1) whose activity was analyzed instead of that of JNK. Illustration taken from [Cooper and National Center for Biotechnology Information (U.S.), 2000].

indispensable for skeletal development in mammals. *p38* knockout mice exhibited significantly reduced bone mass, defective osteoblast differentiation, clavicular hypoplasia and incomplete fontanelle closure, the latter features reminding of the human disease phenotype observed in cleidocranial dysplasia caused by *RUNX2* mutations [Greenblatt et al., 2010]. Mechanistically, these mice failed in phosphorylating Runx2 to facilitate its association with transcriptional co-activator CREB binding protein to induce transcription of Runx2 target genes.

TNF was found to induce phosphorylation and thus activation of the α -isoform of p38 which is specific to osteoclasts and osteoclast precursors and drives their maturation into osteoclasts [Boehm et al., 2009]. By osteoclast-specific deletion of *p38 α* in mice, TNF-induced arthritic bone loss was precluded locally as well as systemically, which raises the hope that specific pharmacological inactivation of *p38 α* in human osteoarthritic patients could augment disease progression.

Hence, an important role of the p38 pathway in osteoclastogenesis is much more closely characterized than its role in osteoblastogenesis. The role of its constitutive activation in ASC during culture thus remains elusive.

AP1 was Constitutively Active in ASC

AP1 is involved in the regulation of cell growth and proliferation, differentiation and apoptosis [Krens et al., 2006]. The transcription factor is active as a dimer, the most abundant form being composed of one JUN and one FOS subunit. Activation of the JUN subunit occurs through phosphorylation of its N-terminal transactivation domain by JUN N-terminal kinases (JNKs).

Since I observed nuclear translocalization of the phosphorylated and activated AP1 subunit cJUN in all ASC cultures irrespective of the stimulus added to the cell culture medium and at least until day seven of culture (see figure 4.5 on page 56), the considerations made before for

the p38 activation also suggest a role for AP1 in the basal level of osteogenic differentiation found for all ASC cultures.

Indeed, AP1 was reported to be a promoter of osteogenic differentiation and to be induced by bone anabolic agents as e.g. vitamin D₃ [Wagner, 2002; Wagner and Nebreda, 2009]. Jun-Fos is the most abundant AP1 heterodimer found in the early stages of osteoblastogenesis and is successively replaced by JunD-Fra2 at the mineralization stage. Supportingly, JNK activation was reported to be essentially required for later stages of osteogenic differentiation, since it was found to be required for osteocalcin and bone sialoprotein gene expression, but not for the expression of the alkaline phosphatase, osteopontin or *Runx2* genes in mouse MC3T3-E1 pre-osteoblasts [Matsuguchi et al., 2009].

Mice overexpressing *Fra2*, the AP1 subunit present at late stages of osteogenic differentiation, were reported to develop an osteosclerotic bone phenotype [Wagner, 2002], and *Fra2* knockout resulted in incomplete osteoblastic differentiation [Bozec et al., 2010]. Moreover, the osteocalcin and collagen 1 α 2 genes *in vitro* were revealed as direct targets of Fra2-AP1.

Since JNKs are activated themselves in response to extracellular stimuli as e.g. growth factors [Raman et al., 2007], the observed constitutive AP1 activation – and also the p38 activation – may have been due to growth factors present in the fetal calf serum added to the medium. Serum-supplemented medium without any adipogenic factors was shown to induce adipogenic differentiation of human bone marrow-derived MSC via the ERK pathway [Wu et al., 2010]. Thus, the serum-supplemented medium may also have been the stimulus for AP1 and p38 activation and the basal level of osteogenic differentiation observed for ASC under all treatment conditions.

5.1.3 TNF did not Induce Apoptosis in ASC

The effect of TNF receptor activation on apoptosis of ASC was analyzed via surveillance of changes in the actin cytoskeleton and nuclear lamin structure as well as via surveillance of changes in the subsuming parameter cellular viability.

Analysis of Cytoskeletal Organization

An early hallmark of ongoing apoptotic processes can be seen in fundamental structural changes in cytoskeletal organization. These remodeling processes are very obvious in confluent cultures of human endothelial cells, TNF inducing re-organization of the prominent circumferentially distributed filamentous actin fibers into elongated, cell-spanning stress fibers [Peters et al., 2008; Millan et al., 2010]. Human synovial fibroblasts, also developing from mesodermal mesenchyme, but having a more ASC-like phenotype, lack ostentatious circumferential actin, but clearly increase their stress fiber number and thickness in response to TNF [Vasilopoulos et al., 2007]. Contrastingly, TNF-treated smooth muscle cells completely depolymerize their actin stress fibers to increase their motility, a prerequisite in the pathogenesis of atherosclerosis [Jovinge et al., 1997].

TNF-treated ASC did not show any change of their actin structure, neither in direction of the stress fiber type nor in direction of depolymerization (see figure 4.7A on page 58). Therefore, the analysis of ASC cytoskeletal organization does not give any early indication for ongoing apoptotic processes.

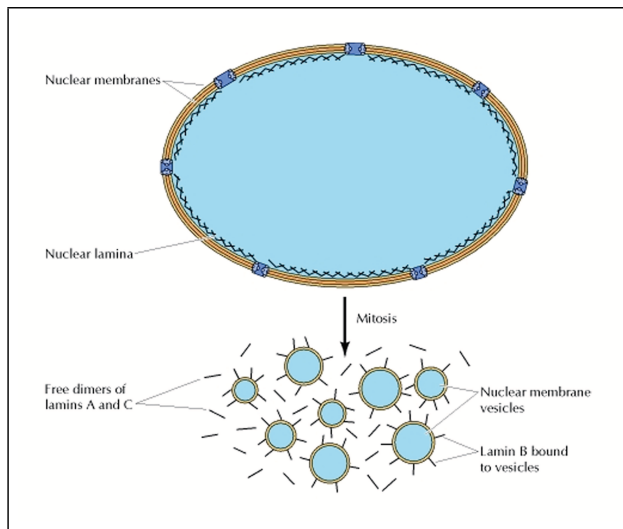


Figure 5.5: Changes in nuclear lamin organization during mitosis. Nuclear DNA is enveloped by a nuclear membrane whose inner surface is connected to a network of nuclear lamin filaments, whereas the outer membrane confines the nucleus from the cytoplasm. Inner and outer membrane define a luminal space continuous to the endoplasmic reticulum and interrupted by nuclear pore complexes. During mitosis and apoptosis, the membrane fragments into vesicles that remain associated with B-type lamins, whereas A-type lamins dissociate from it and are released to the cytoplasm as free dimers with B-type lamins. During apoptosis, DNA is subsequently cleaved by nucleases, which is not the case for mitosis. Illustration taken from [Cooper and National Center for Biotechnology Information (U.S.), 2000].

Analysis of Nuclear Envelope Integrity

In addition to the cytoskeletal organization, apoptotic processes will affect the integrity of the nuclear envelope and thus the organization of lamins which constitute one of the major envelope components (see figure 5.5 on page 79).

Lamins serve as mandatory structural anchors for transcription factors within the nuclear membrane, which was confirmed for the retinoblastoma protein whose transcriptional repressive function depends on lamin A/C binding, and for OCT1 which co-localizes with lamin B to suppress expression of an aging-dependent collagenase gene in fibroblast precursors [Imai et al., 1997]. During apoptosis, caspase-mediated cleavage of lamins acts as a signal activating nucleases for subsequent DNA cleavage [Cohen et al., 2001]. Thus, desintegration of the lamin filaments is a well-suited indicator of ongoing apoptosis before cell viability is seriously impaired.

Since I did not find any indications for breakdown of lamin filaments after up to one week of TNF treatment (see e.g. figure 4.4 on page 55 for a microscopic image captured after six hours of stimulation), a putative apoptosis-inducing effect of TNF, but also of osteogenic stimulation, on ASC can be neglected.

Analysis of Cell Viability

Supporting the results obtained from actin and lamin staining, a check of the cellular viability as a terminal indicator of apoptotic processes revealed that even after two weeks of TNF treatment, hardly any cell in culture was dead (see figure 4.7B on page 58). Even after four weeks of stimulation with TNF concentrations increased by a factor of up to 100, ASC viability was not impaired, as can be judged indirectly by the still detectable activity of alkaline phosphatase (see figure 4.13A on page 66), an enzyme whose activity decreases to 10 % within three days under physiologic conditions within a cell and when no activated alkaline phosphatase is replenished [Fukunaka et al., 2011].

Since ZBTB16 acts as a pro-apoptotic factor [Barna et al., 2000], its high expression during osteogenic differentiation (see figure 4.10A on page 62) is putatively cytotoxic. The fact that I did not observe any obvious decrease in ASC viability during osteogenic differentiation thus

may be attributed to ZBTB16's additional role as a repressor of apoptosis: it represses the expression of the central apoptotic pathway member *BID*, which consequently precludes cleavage of BID to truncated BID (tBID) and thus finally precludes the release of cytochrome c from the mitochondria [Parrado et al., 2004].

The NF κ B Pathway in Apoptosis

A potential mechanistic explanation for the observation that ASC did not undergo apoptosis following treatment with the potentially pro-apoptotic cytokine TNF, which was shown to induce apoptosis in endothelial cells [Sato et al., 1986] or mature human osteoblasts [Tsuboi et al., 1999], but not in most other primary cells [Clark et al., 2005], may be given through the NF κ B-driven expression of genes encoding proteins belonging to the family of cellular inhibitors of apoptosis (c-IAPs). These c-IAPs prevent assembly of the TNFRSF1A-associated death signaling complex and additionally upregulate pro-survival NF κ B signaling pathways [Varfolomeev and Vucic, 2008].

Part of the pro-apoptotic action of TNF may also be compensated by expression of TNF decoy receptors by ASC, as is done e.g. by osteoblasts [Bu et al., 2003]. These receptors lack the intracellular death domain needed for activation of apoptosis signaling and thus indirectly shift the balance between survival and apoptosis towards survival.

While TNFRSF1A has an intracellular TNF receptor-associated death domain (TRADD) enabling it to directly activate a distinct caspase without moderation of TRAFs, TNFRSF1B needs TRAF2 with other co-factors to accomplish this. Therefore, a role of TNFRSF1B in apoptosis was initially underestimated. Later it turned out that TNFRSF1B is well able to activate not only the NF κ B and MAPK pathways, but also to induce apoptosis [Haridas et al., 1998]. Thus, it is the delicate balance in the extent of caspase activation on the one hand and NF κ B activation on the other that determines death or survival of a cell [Aggarwal, 2003].

Although both TNF receptors can in principal activate all the signaling pathways described above, they do so with differing efficiency, making the net effect of TNF receptor activation depending on the expression ratio of both receptors and the abundance of the ligands binding them, as each ligand activates only distinct pathways. Therefore, the main effect that TNF exerts on ASC apparently is activation of the pro-survival NF κ B, but not the apoptosis pathway.

The MAPK Pathway in Apoptosis

The activation of JUN, which was found for all ASC cultures irrespective of their stimulation, indicates an active JNK. Since JNK activates transcription factors of the family of signal transducers and activators of transcription (STAT) which increase expression of *BCL2*, a gene encoding a protein of the B-cell lymphoma (BCL) family, the MAPK pathway is directly involved in regulation of apoptosis. By binding the outer mitochondrial membrane, BCL2 prevents the swelling process observed in mitochondria at early stages of apoptosis [Janeway et al., 2001]. Thus, cytochrome c leakage and the activation of caspases are precluded and apoptosis will not occur.

However, active JNKs also activate other BCL members as e.g. BCL2-associated X protein (BAX) and BH3 interacting domain death agonist (BID), the latter being active only as cleaved (truncated) form tBID [Wagner and Nebreda, 2009]. Both promote the release of cytochrome c from the mitochondria and therefore are pro-apoptotic factors.

Hence, JNK activate both pro- and anti-apoptotic BCL family members, and the activity of a distinct JNK family member and the simultaneous activity of other cross-talking pathways determines the net effect on apoptosis. Since I did not observe any apoptotic events in ASC in response to either stimulus, the activation of JUN may thus have resulted in increased expression of anti-apoptotic BCL members.

5.2 ASC Proliferation Rate and Cell Cycle

5.2.1 TNF Increased ASC Proliferation Rate and Accelerated S Phase Transition

TNF-treated ASC showed increased proliferation rates, and this increase in proliferation rate was accompanied by a decreased portion of cells being into the synthesis (S) phase of the cell cycle (see figure 4.8 on page 59). Simultaneously, an increased portion of cells was into the neighboring gap phases G_0/G_1 and G_2/M .

An increased proliferation rate means that passage through the entire cell cycle needs shorter time. Under such highly proliferative conditions, a smaller fraction of cells in a distinct cell cycle phase thus means that this phase is passed faster than another phase consisting of a larger fraction of cells. For the TNF-treated ASC showing a reduced S phase fraction and a concomitantly increased fraction of cells within the G phases, these considerations mean that the increase in proliferation rate observed is accomplished by faster passage of ASC through the S phase. To promote faster passage of ASC through the S phase, either the entry into the S phase or the exit from it has to be accelerated. Since S to G_2 transition is not subject to cell cycle regulation, but G_1 to S transition is, G_1 to S transition needs to be accelerated in order to facilitate the faster passage through the S phase and the increased proliferation rate observed for TNF-treated ASC. And indeed, such an impact of TNF on G_1 to S transition was reported in a number of studies.

G_1 to S transition is a cell cycle checkpoint under control of the cyclin E-CDK2 complex. In different mouse and human embryonic and adult cells, G_1 to S transition was reported to be regulated by NF κ B-mediated activation of the cyclin D-CDK4 complex, which itself is an upstream regulator of cyclin E-CDK2 [Hinz et al., 1999]. Cyclin D1 associates with CDK4 or CDK6 to promote G_1 to S transition by phosphorylating and thus activating the retinoblastoma protein [Dahlman et al., 2009]. In mouse embryonic fibroblasts, p65 was found to associate with the cyclin D1 complex to stabilize and decrease its degradation. Shutdown of the p65 signal and thus reduction of the abundance of the cyclin D1 complex hampers G_1 to S transition and in that manner is thought to facilitate cell cycle exit and differentiation, which in case of these mouse embryonic fibroblasts was skeletal differentiation. Thus, this mechanism of NF κ B-mediated stabilization of the cyclin D1 complex may also be true for the increase in proliferation rate observed for TNF-treated ASC.

In supportance of the role of NF κ B as a promoter of proliferation, this pathway was found to increase proliferation in a human T-cell line by transcriptional upregulation of one of the major proto-oncogenes, *MYC* [Duyao et al., 1990]. In tumor cells from patients suffering from Hodgkin's lymphomas and breast cancer, NF κ B was found to be constitutively active, and anti-cancer treatment in these patients is done by NF κ B inhibition through anti-inflammatory agents as e.g. corticosteroids [Bours et al., 2000].

Thus, TNF-mediated upregulation of NF κ B was multiply reported to be associated with the

observation of increased proliferation throughout the literature. Since TNF treatment of ASC, either in the presence or absence of osteogenic stimuli, induced p65 translocation into the nucleus, and since TNF-treated ASC differed significantly regarding the progression through the cell cycle compared to the osteogenically stimulated ASC, this effect might have been a consequence of the p65 activation.

5.2.2 Osteogenic Stimulation Increased ASC Proliferation Rate, but Decelerated S Phase Transition

Osteogenic stimulation of ASC, as TNF treatment, resulted in a strongly increased proliferation rate. However, the simultaneously observed distribution within the different cell cycle phases in these ASC was exactly the opposite of what was found for the TNF-treated ones: The portion of ASC in the S phase was significantly increased, whereas the portion of ASC in the surrounding gap phases was reduced (see figure 4.8 on page 59).

As mentioned above, an increased portion of cells within a specific cycle phase indicates that passage of this phase occurs more slowly as compared to the others. Slower passage of ASC through the S phase can be the consequence of either a limited entry or exit rate into it. Since S to G₂ transition is not subject to cell cycle regulation, G₁ to S transition needs to be decelerated in order to facilitate the slower passage through the S phase that was observed for osteogenically stimulated ASC.

5.2.3 The Role of ZBTB16 in Proliferation and Cell Cycle Regulation

The findings stated before may be well explained by the strongly increased expression of the zinc finger and BTB domain containing 16 gene (*ZBTB16*), formerly called promyelocytic leukemia zinc finger (*PLZF*), during osteogenic stimulation of ASC (see figure 4.10A on page 62). This gene encodes a transcription factor involved in the regulation of cell cycle progression and osteogenic differentiation. *ZBTB16* decelerates cell cycle progression at the G₁ to S checkpoint [Costoya et al., 2008]. Following the considerations made before for TNF-treated ASC, this would have a directly opposed effect on ASC cell cycle progression as was found for TNF treatment and thus would result in an increased portion of cells within the S phase.

Substantiating this role of *ZBTB16* on cell cycle regulation, the transcription factor was found to be negatively regulated through phosphorylation by cyclin E-CDK2, the main kinase involved in G₁ to S transition, by triggering its ubiquitinylation and subsequent proteasomal degradation [Costoya et al., 2008]. Hence, the changes in ASC cell cycle during osteogenic differentiation may be due to the upregulated expression of *ZBTB16*. A further mechanistic explanation of the action of *ZBTB16* on the cell cycle comes from the finding that this transcription factor represses the prominent proto-oncogene *MYC* on the transcriptional level [McConnell et al., 2003] as well as on the post-translational level by downregulation of the MAPK pathway. This subsequently reduces *MYC* activation by phosphorylation through ERK [Shi and Vogt, 2009]. Both the direct action of *ZBTB16* on cell cycle progression and the indirect, *MYC*-mediated action of this transcription factor give an explanation for why *ZBTB16* loss-of-function mutations were first described in distinct cancer types as acute promyelocytic leukemia.

5.2.4 The Role of RUNX2 in Proliferation and Cell Cycle Regulation

DNA-binding activity of runt-related transcription factor 2 (RUNX2) was strongly increased during osteogenic stimulation of ASC, but reduced following TNF treatment and following TNF treatment under osteogenic conditions (see figure 4.10B on page 62).

As the osteogenic marker ZBTB16, RUNX2 was found to have not only a role in osteogenic differentiation, but also in regulation of cell cycle progression. RNAi-based *RUNX2* knock down in hMSC resulted in an increase in proliferation rate and cyclin A and B protein levels [Ghali et al., 2010]. Moreover, RUNX2 was shown to promote cell cycle exit at G₁ via induction of P27KIP1 in terminally differentiating osteoblasts, whereas G₁ exit and osteoblastic differentiation were not observed in cancer cells of the osteosarcoma type [Thomas et al., 2004]. G₁ exit will necessarily result in reduced G₁ to S transition. Altogether, these findings assign RUNX2 an anti-proliferative role in cell cycle progression and underline that exit from the cell cycle and entrance into a non-proliferative, quiescent state occur simultaneously and can be considered to be a prerequisite for osteogenic differentiation to be accomplished.

The balance between proliferating and differentiating cells in the course of osteogenic differentiation and cell cycle exit at the terminal differentiation stage is regulated via the phosphorylation degree of RUNX2 and the activity of telomerase. RUNX2, when hyperphosphorylated by cyclin B-CDK1, activates primarily mitotic genes, whereas RUNX2 dephosphorylation by phosphatases PP1 and PP2A shifts its activity towards driving expression of osteoblastic genes [Rajgopal et al., 2007]. Telomerase activity in bone marrow-derived stromal cells was found to induce, alongside with some osteogenic genes, expression of cyclins D and E and thereby facilitated G₁ to S transition to yield the increase in proliferation rate typical for early stages of osteogenic differentiation [Gronthos et al., 2003].

Thus, both ZBTB16 and RUNX2, whose expression and activity was increased during osteogenic differentiation of ASC, were numerously reported to be negative regulators of G₁ to S transition to promote stem cell exit from the proliferative state and entry into the differentiating state.

5.2.5 The Role of p38 and AP1 in Proliferation and Cell Cycle Regulation

The constitutive activation of the MAP kinase p38 and the transcription factor AP1 observed in all ASC treatment groups irrespective of their distinct stimulation was discussed above to possibly have promoted the basal level of osteogenic differentiation found in all ASC treatment groups (see page 75 for further details). In addition, both MAP kinase signal transduction pathway members were reported to play a role in regulation of proliferation.

Activation of TACE, the enzyme catalyzing the processing of the membrane-bound TNF precursor into soluble, mature TNF, by inflammatory stimuli through p38 activation was reported to result in the release of TGF family ligands that subsequently lead to activation of pro-proliferative EGF receptor signaling in CHO-derived cells *in vitro* [Xu and Derynck, 2010]. Additionally, constitutive activation of AP1 was reported to be found in all tumor cells from patients with classical Hodgkin's lymphomas and Anaplastic Large Cell Lymphomas (ALCL), AP1 in these cells stimulating proliferation by upregulating expression of cyclin D2 [Mathas et al., 2002].

Thus, the constitutive activation of p38 and AP1 may also have supported proliferation of ASC as was observed to at least a basal level for all cells in culture.

5.2.6 Concluding Remarks on the Regulation of Proliferation and Cell Cycle Progression

Hence, osteogenic differentiation is regulated via the opposed activity of cyclins D and E on the one hand and ZBTB16 and RUNX2 on the other. Initially, cyclin D-CDK4 and cyclin E-CDK2 promote the fast G_1 to S transition needed for increased proliferation at early stages of osteogenic differentiation. Then, the more active products of the *ZBTB16* and *RUNX2* genes are present with ongoing osteogenic differentiation, the more they exert their inhibitory effect on G_1 to S transition to slow down proliferation and to allow for cell cycle exit and terminal osteoblastic differentiation. Remaining bound to DNA even during mitosis, RUNX2 is involved in keeping expression of lineage-specific genes upright after differentiation has taken place and thus acts as a cell fate-determining transcription factor [Young et al., 2007], which gives an explanation for the gene's constitutive expression and its complex regulation through multiple degrees of phosphorylation. In supportance with the inhibition of cell cycle progression during osteogenic differentiation, ascorbic acid, a common compound in osteogenic differentiation mixtures, in HeLa cells was found to transiently block G_1 to S and G_2 to M transition [Thomas et al., 2005].

The findings for *ZBTB16* expression and RUNX2 DNA-binding activity bring proliferation and differentiation into a common context and underline that proliferation continuously diminishes when differentiation proceeds. If G_1 to S transition is increasingly hampered in the progress of osteogenic differentiation of ASC, but cells still showed high proliferation rates even after four weeks of osteogenic stimulation, how can these opposed observations then be explained?

As was stated in the results section, TNF treatment of ASC, in contrast to osteogenic stimulation, did not result in osteogenic differentiation of these cells and additionally decreased the S phase portion of ASC, but had identical impact on cellular proliferation by strongly increasing it. In generalizing this finding of a small S phase portion of cells, as observed for TNF treatment of ASC, as an indicator of proliferation, but not of differentiation, one can assume that the osteogenically differentiating cells, showing a significantly larger S phase portion, but *also* high proliferation rates, consist of at least two sub-populations: A fast proliferating sub-population characterized by a small S phase portion and a slowly proliferating, but differentiating sub-population exhibiting a large S phase portion. As cell cycle analysis necessarily gives the summary of both sub-populations and shows a significantly increased overall S portion of cells, these considerations imply that in osteogenic differentiation of ASC, the fast proliferating sub-population is comparatively small, but proliferates fast enough to sustain the larger sub-population of differentiating cells. If that would be true, TNF treatment would reduce the increase in S phase cells in osteogenically stimulated ASC – and that is exactly what was observed when ASC were co-treated with TNF and osteogenic stimulants.

Following this assumption, osteogenic differentiation, although characterized by the simultaneous occurrence of differentiation and proliferation, is not accomplished by a single population of precursor cells that both proliferate *and* differentiate, but rather by two distinct sub-populations that are assigned to either the one function *or* the other. In supportance of this hypothesis that a cell cannot differentiate and proliferate at the same time, NF κ B-driven activation of cyclin D1 expression was reported to clearly increase proliferation, but to inhibit myogenesis [Guttridge et al., 1999]. Consequently, NF κ B activity and subsequent cyclin D1 expression was gradually shut down in the developing myoblast.

A probable way how such a co-culture of two different cell types, one proliferating and one differentiating, can develop from a culture of indistinguishable precursors is the mode of asymmetric cell division that was found for hematopoietic stem cells [Giebel and Bruns, 2008]

and for neural stem cells [Farkas and Huttner, 2008]. In such asymmetric divisions, one cell will differentiate, whereas the other exactly reduplicates to self-renew and keep the pool of stem cells upright. A well accepted explanation for how such asymmetric cell divisions can take place is that differentiation factors are inherited inequally during mitosis, which drives the fates of the progeny into different directions. In addition, postmitotic decisions due to interactions between the two daughter cells are discussed.

These asymmetric cell divisions would explain why islets of alkaline phosphatase-positive cells are present in osteogenically stimulated cultures, whereas other islets consist of alkaline phosphatase-negative cells. However, publications demonstrating asymmetric cell divisions in differentiation of mesenchymal stem cells are so far not available, though this mode of cell division is likely, since these cells share the same niche with hematopoietic stem cells *in vivo* and, at least for ASC, were reported to be able to differentiate along the entire hematopoietic lineage [Corre et al., 2006].

5.3 The Impact of TNF and Osteogenic Stimulation on ASC Metabolic Activity

Comparatively little is known regarding changes in the metabolic activity of stem cells during differentiation. When being calculated down to the single cell level, osteogenic stimulation of ASC initially led to a reduction of metabolic activity after one week of culture, followed by a strong peak after two weeks and a final decline to the starting levels after three weeks of culture (see figure 4.9B on page 60). Contrastingly, TNF treatment of ASC led to a continuously decreasing metabolic activity over the three weeks of experimentation. When cells were co-treated with both stimulants, the metabolic activity-reducing effect of TNF outweighed the activity-increasing effect of osteogenic stimulants and thus showed no peaking at day 14, but subsequently a hardly unchanged and decreasing activity profile to the end of observation after 21 days.

Cellular metabolic activity was analyzed by following the reduction of a tetrazolium compound into a formazan dye [Berridge and Tan, 1993]. Reduction of the tetrazolium compound MTS is driven by direct electron transfer from NAD(P)H to MTS via the electron coupling reagent PES. Like tests of the ATP/ADP ratio indicate the energy status of cells, the MTS assay indicates how many electrons can be transferred from NAD(P)H to MTS in a given time and therefore is a measure of the overall cellular metabolic activity (see figure 5.6 on page 86).

Since a high NAD(P)H/NAD(P)⁺ ratio results from NAD(P)H generation in catabolic reactions as e.g. glycolysis, high tetrazolium conversion rates reflect a high catabolic activity, more specifically a high respiratory activity in case of MTS [Berridge et al., 2005]. When comparing osteogenically stimulated with unstimulated ASC, the observed increase of MTS conversion per cell may thus reflect the switching-on of glycolysis and oxidative phosphorylation. This assumption is substantiated by the outcome of a recent analysis of the metabolism of ASC that was done in our group and that revealed an increased activity of the glycolytic enzyme glucose-6-phosphate dehydrogenase and the citric acid cycle enzyme NADP⁺-specific isocitrate dehydrogenase under osteogenic stimulation of ASC (Juliane Meyer, unpublished results).

These observations of an increasingly oxidative metabolism fit well to what is nowadays considered as a common hallmark of reduced “stemness” and increased degree of differentiation [Rehman, 2010]. Interestingly, this metabolic adaptation finds its fingerprint also at the organellar level, since mitochondria number increases during differentiation of precursors. Con-

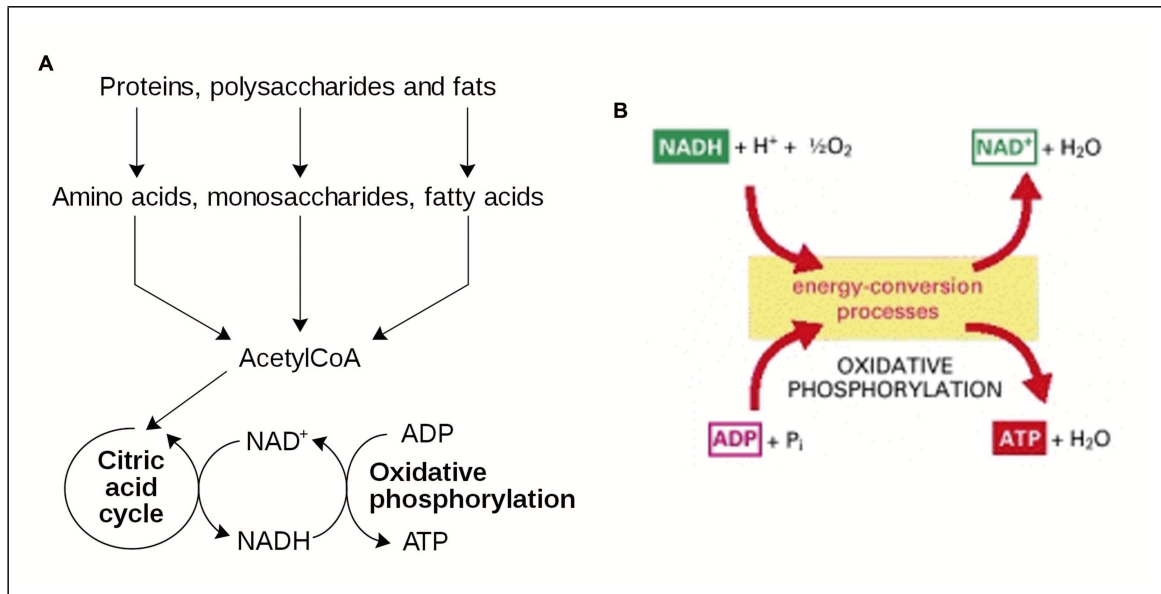


Figure 5.6: Cellular metabolism and the reduction equivalents and energy-rich compounds produced therein. (A) The reduction equivalent NAD^+ is reduced to $\text{NADH} + \text{H}^+$ by catabolic pathways, mainly the citric acid cycle. In the electron transport chain, $\text{NADH} + \text{H}^+$ is oxidized to NAD^+ , yielding the energy-rich compound ATP. Illustration taken from [Wikipedia, 2011]. (B) Thus, NAD^+ regeneration and ATP production are functionally coupled processes, a high ATP/ADP ratio corresponding to a high NADH/NAD^+ ratio. Illustration taken from [Alberts et al., 2002].

sequently, the hypoxic conditions of the stem cell niches *in vivo* in contrast to the mostly well oxygen-supplied compartments of mature differentiated cells are thought to be responsible for keeping stem cells in an undifferentiated state.

The importance of the redox state of cellular metabolism on differentiation of precursor cells is not only represented by the fact that extracellular differentiation factors affect the intracellular redox state, but more strikingly by the finding that the direct change of the redox state by pro- and antioxidant drugs induces the same outcome on differentiation as these factors, as was reported for rat neuronal progenitor cells [Noble et al., 2003]. Pharmacological antagonists of the redox effects induced by extrinsic signaling molecules also antagonized their effects on self-renewal and differentiation. The more oxidized differentiating cells were found to show a stronger response to inducers of differentiation or cell death, but to respond less to inducers of proliferation or survival, whereas the opposite was true for less differentiated neuronal cells [Noble et al., 2005].

These generalized changes of cellular redox state appear to also be true for ASC. In bone marrow-derived and umbilical cord-derived MSC, the increased number of mitochondria and the switch of metabolic activity towards a stronger respiratory, oxidative phenotype was accompanied e.g. by an increased oxygen consumption after 14 days of osteogenic stimulation [Pietilae et al., 2011] and by a shift in the redox potential in direction of oxidation [Imhoff and Hansen, 2011].

Consistently with the increasingly oxidative metabolic phenotype of differentiating cells, the amount of ATP per cell was shown to increase with differentiation degree from embryonic over induced pluripotent stem (iPS) cells to differentiated cells, and lactate concentration inversely decreased [Varum et al., 2011]. The increase in ATP generation is associated with an increase in

generation of radical oxygen species (ROS), which was reported to be a stimulus for differentiation: ROS activate the MAPK pathway which is involved in many differentiation programs, and they reduce the stability of transcription factors associated with keeping cells in an undifferentiated state, as e.g. OCT4 having higher transcriptional activity when bound to the antioxidant thioredoxin (TRX) [Ogasawara and Zhang, 2009].

A recent study revealed a global relationship between the oxidative level of diverse cellular metabolites and cellular differentiation. During differentiation of mouse and human embryonic stem cells, the portion of unsaturated metabolites continuously decreased due to oxidation reactions [Yanes et al., 2010]. During these oxidation reactions, the intracellular concentration of the reducing agent ascorbic acid peaked, whereas the concentration of the reduced form of glutathione dipped simultaneously, both indicating the switching-on of cellular reactions directed against the oxidative stress occurring. After differentiation took place, concentrations of both redox agents returned to the values found before differentiation. Hence, increasing the differentiation degree of cells increases their oxidative level, and reduced, unsaturated compounds are simultaneously used up. Supportingly, the oxidized metabolites generated during differentiation reactions in that study were reported to be able to induce neurogenic and cardiogenic differentiation of the embryonic stem cells used.

Therefore, one can state that cellular differentiation in general is functionally coupled to an oxidative metabolic phenotype, in special to a peaking in ascorbic acid concentration. By supplying progenitor cells with ascorbic acid, the ascorbic acid concentration is artificially raised as it is during differentiation which may therefore act as a signal forcing cells into differentiation, and all additional factors and the physical environment present then influence which path of differentiation is taken.

The complete lack of the prominent peaking of metabolic activity found for osteogenic stimulation, but not for TNF treatment, indicates significant differences in the regulation of the cellular redox system by these differing stimuli and thus may be responsible for the lack of osteogenic differentiation of TNF-treated ASC. In the ASC co-treated with both TNF and osteogenic stimulants, the peaking of metabolic activity after 14 days was considerably less pronounced, but obviously strong enough to support osteogenic differentiation as found in that ASC treatment group.

5.4 Osteogenic Differentiation of ASC *in vitro*

5.4.1 Basal Level Osteogenic Differentiation Occurred in Unstimulated ASC Cultures

Before I go into detail on the impact of TNF as a putative inducer of osteogenic differentiation of ASC, it is noteworthy to underline that not only in the osteogenically stimulated ASC, but also in those ASC cultures kept in cell culture medium without osteogenic stimulants, osteogenic differentiation was observed to a certain, though in comparison to osteogenically stimulated ASC much lesser extent.

There is a variety of factors that may have caused such spontaneous osteogenic differentiation of ASC. In general, differentiation of stem cells is regulated by the concerted action of three environmental parameters: by both soluble factors and by membrane-bound factors during direct cellular interaction with other cells, and by interaction with the extracellular environment, i.e. its physical and chemical properties.

Impact of Soluble Factors

Besides basal nutrients for cellular metabolism as glucose and sodium pyruvate, inorganic salt ions, diverse amino acids and vitamins, Dulbecco's Modified Eagle Medium (DMEM) used for ASC culture contains two soluble factors that play a role in the process of osteogenic differentiation: the red-colored pH indicator phenol red and fetal calf serum.

Fetal calf serum was reported to positively regulate osteogenic differentiation of stem cells. It was reported to spontaneously induce chondrogenic differentiation of bone marrow-derived MSC while simultaneously reducing expression of mesenchymal stem cell markers in a dose-dependent fashion [Yokoyama et al., 2008]. With exception of the skull which is formed by direct differentiation of mesenchymal stem cells into bone in a process called intramembranous ossification, all developmental processes of bone formation *in vivo* involve the intermediate formation of cartilage which subsequently is replaced by bone, a process called endochondral ossification. Therefore, by inducing chondrogenic differentiation of MSC *in vitro*, fetal calf serum itself may initiate ossification of these cells via the endochondral differentiation pathway.

Supportingly, the extent of proliferation and osteogenic, adipogenic and chondrogenic differentiation of bone marrow- and adipose tissue-derived stem cells, as induced by standard stimuli, was reported to decrease with decreasing fetal calf serum concentration [Lund et al., 2009]. Since the MAPK pathway is involved in regulation of various differentiation pathways, the constitutive activation of the MAP kinase p38 and the transcription factor AP1 that was found in ASC under unstimulated conditions (see page 75) may be mediated by fetal calf serum and thus gives a potential mechanistic explanation for the basal level of osteogenic differentiation found under all conditions *in vitro*.

In addition to the osteogenesis-promoting action of fetal calf serum, phenol red was shown to have a supportive effect on osteogenic differentiation induced by different bone anabolic stimuli in rat bone marrow stromal cells, but also being reported not to be able to induce osteogenic differentiation on its own, and the permissive effect of phenol red on osteogenic differentiation is thought to be due to additional lipophilic impurities present in the phenol red charge [Still et al., 2003]. The lipophilic nature of phenol red suggests that it acts via nuclear receptors as e.g. the estrogen receptor, and supportingly, SAOS cells cultured in phenol red-free medium irreversibly lost their estrogen receptor [Nasir and Speirs, 1997].

The estrogen receptor was shown to be involved in bone formation *in vivo* through activation of nitric oxide signaling. No bone formation occurred in nitric oxide synthase knockout mice, and nitroglycerin, which auto-decomposes into nitric oxide, enhanced osteoblastic differentiation of human bone marrow-derived MSC [Huang et al., 2008]. Therefore, nitroglycerin is a promising candidate in osteoporosis treatment in estrogen-deficient, post-menopausal women, since it lacks the adverse side effects of estrogen-replacement therapy as increased breast and endometrial cancer rates and is recognized as safe from its long use in treatment of cardiovascular disease.

Impact of Environmental Properties

In addition to soluble factors present in the cell culture medium, physical and chemical characteristics of the growth substrate, which here was standard tissue culture polystyrene (TCPS), also affect stem cell differentiation. Besides the bare chemical properties of a surface, i.e. its coverage with distinct functional groups or even whole factors as fibronectin, the surface charge, elasticity and nanotopography of the growth substrate strongly impact the proliferation, migra-

tion and differentiation behavior of stem cells seeded onto them.

TCPS, as compared to the cell adhesion substrates from extracellular matrices present in the body, is a hard material having an elasticity similar to that of bone. Thus, it is prone to induce osteogenic differentiation of MSC instead of other differentiation pathways as e.g. adipogenesis or myogenesis, the corresponding extracellular matrices exhibiting much higher elasticities. Strikingly, the low elasticity of the rigid fibrotic tissue generated during wound healing by scar formation within a soft tissue environment having a much higher elasticity was observed to facilitate adhesion of stem cells onto it and thus is thought to act as a homing signal for stem cells in a process of directed migration and adhesion called durotaxis [Discher et al., 2009]. However, this less elastic, more bone-like environment preferentially makes the MSC differentiate into osteoblasts to drive ectopic calcification of fibrotic scar tissue.

Hence, the soluble factors phenol red and fetal calf serum contained in the cell culture medium as well as the cell culture substrate tissue culture polystyrene with its bone matrix-like elasticity were reported to induce osteogenic differentiation of mesenchymal stem cells *in vitro*.

The mechanism the cell senses the mechanic properties of its environment largely depends, as far as is known, on growth substrate-forced changes of cell shape. During differentiation of MSC, cell shape changes in dependency on the differentiation pathway taken: differentiation into osteoblasts results in a flat, well-spread phenotype that allows the osteoblast to maximize mineral deposition into its environment, whereas adipogenic differentiation results in the roundly-shaped adipocyte phenotype with only limited adherence to the surface, but maximized capacity for lipid storage. *Vice versa* forcing bone marrow-derived MSC into these differing cell shapes was reported to result in differentiation of the undifferentiated cells into the mature cells of the corresponding phenotype [McBeath et al., 2004]. The phenotype-shaping force in this study was applied by varying the cell seeding density, a low plating density allowing the cells to spread into a flattened phenotype, whereas a high seeding density allowed only a roundly shaped phenotype. The signal of the actual cell shape adopted was found to be transduced into changed actin cytoskeleton structure and tension via the RHOA-RHOA kinase (ROCK) signaling pathway: Activation of ROCK lead to an increase in cytoskeletal stress fibers and tension and finally to osteogenic differentiation, even if adipogenic differentiation factors were present or the cell phenotype was rounded, whereas the opposite was true for constitutive inactivation of ROCK. Thus, the ROCK-mediated regulation of actin stress fiber generation and the resulting change in cellular mechanical tension and phenotype provides an important system regulating osteogenic and adipogenic differentiation in a way that was even found to be superordinated to common soluble differentiation factors. Consistently, Rhoa activation and increased actin tension in murine MSC were shown to preclude adipogenic and chondrogenic differentiation, but not osteogenic differentiation [Arnsdorf et al., 2009].

The cell shape is also a critical factor for differentiation into other cell types, as was reported for the differentiation of bone marrow-derived MSC into smooth muscle cells and chondrocytes: TGF β 3-treated MSC allowed to spread and flatten differentiated into smooth muscle cells, whereas those kept on micropatterned surfaces preventing spreading differentiated into chondrocytes [Gao et al., 2010]. For these differentiation pathways, the activity of the RHOA-ROCK system remained hardly changed, whereas the activity of AKT1 for MSC on the SMC differentiation pathway was strongly increased and resulted in upregulation of N-cadherin.

Varying the cell seeding density in three-dimensional culture *in vitro* also was reported to affect differentiation and proliferation of cells, as was analyzed for cell types as e.g. the osteosarcoma cell line MG-63. These cells proliferated more strongly when seeded at lower density in three dimensional culture, whereas expression of osteogenic markers decreased to either side

around an optimum [Bitar et al., 2008]. For human MSC in three-dimensional micro-mass culture, expression of chondrogenic markers was the stronger the higher the seeding density was [Hui et al., 2008], an observation that is thought to be the consequence of forcing cells into a condensation step-like aggregate as found during embryonic chondrogenesis.

Therefore, mechanical cues in the environment of stem cells have a considerable impact on their differentiation behaviour and play a long-time underestimated, though at least equally important role as the soluble differentiation factors commonly applied in approaches characterizing differentiation of the plethora of different stem cell types. These mechanical properties of the environment, in contrast to soluble factors, are steadily present and thus are a potent driver of stem cell differentiation as well as of keeping differentiated cells in a differentiated state *in vitro* and *in vivo*.

Impact of the Stem Cell Type

In addition to these environmental parameters affecting stem cell differentiation, these cells differ intrinsically which makes each of the differing stem cell types preferentially follow a distinct route of differentiation. Osteogenically stimulated human bone marrow-derived MSC e.g. showed a much faster increase in alkaline phosphatase activity and earlier onset of extracellular matrix calcification than ASC, but also exhibited a constitutive activation of osteogenic genes alkaline phosphatase, collagen type I, osteocalcin and osteonectin [Frank et al., 2002]. These indications of a higher osteogenic and chondrogenic potential of bone marrow-derived MSC in comparison to ASC were independently confirmed [Im et al., 2005; Glass et al., 2011]. Concludingly, bone marrow-derived MSC, in comparison to ASC, are likely to exhibit a higher basal degree of osteogenic differentiation in an environment mechanically promoting osteogenic differentiation. This stronger degree of osteogenic differentiation is apparently coupled to a higher background degree of differentiation, which may keep the ratio between signal (induced differentiation) and noise (background differentiation) at a constant level for the diverse stem cell types existing.

5.4.2 The Impact of TNF on Osteogenic Differentiation of ASC

TNF had no Impact on *ZBTB16* Expression in ASC

ZBTB16 is involved in osteogenic differentiation by increasing *RUNX2* transcript level and protein activity and thereby was shown to indirectly induce osteoblastic differentiation of human bone marrow-derived MSC via activation of *RUNX2* and thus *RUNX2*-targeted genes [Ikeda et al., 2005]. Interestingly, *ZBTB16* expression in human endometrial stromal cells and myometrial smooth muscle cells exposed to the synthetic glucocorticoid dexamethasone was found to be increased [Fahnenstich et al., 2003], but was not increased in BMP2-driven osteogenic differentiation of human bone marrow-derived MSC [Ikeda et al., 2005]. Since both BMP2 and dexamethasone activate *RUNX2*, dexamethasone-induced *ZBTB16* expression activates *RUNX2* in a BMP2-independent manner.

Expression of the *ZBTB16* gene in ASC remained unaffected by TNF treatment, but increased strongly following osteogenic stimulation (see figure 4.10A on page 62). Addition of TNF to the osteogenic stimulants did also not alter the expression profile of *ZBTB16*. Thus, the *ZBTB16* expression profile gives no indications for a TNF-induced or TNF-inhibited osteogenic differentiation program in ASC *in vitro*.

TNF had no Initial Impact on RUNX2 DNA-Binding Activity in ASC

The DNA-binding activity of RUNX2 was found to be significantly and time-dependently increased following osteogenic stimulation of ASC, but was initially unaffected and later on decreased by TNF treatment as compared to the unstimulated cells showing hardly changed RUNX2 activity over culture time (see figure 4.10B on page 62). Interestingly, the contrasting RUNX2 activity profiles obtained for TNF treatment and osteogenic stimulation in the co-treated ASC gave rise to a RUNX2 activity profile consisting of the characteristic features of both single treatments: the RUNX2 activity peaking characteristic for osteogenic stimulation, but observed earlier in the co-treated ASC, and the significant late-stage decrease in RUNX2 activity characteristic for TNF-treated ASC. Since ASC co-treated with both TNF and osteogenic stimulants showed an unchanged extent of osteogenic differentiation as compared to the osteogenically stimulated ASC, this earlier peaking of RUNX2 activity, although necessarily followed by an earlier shutdown of RUNX2 activity, did not hamper the osteogenic differentiation program to be induced in ASC. Therefore, the peaking of RUNX2 activity, irrespective of its time point, obviously is the key requirement for osteogenic differentiation to be induced.

Remarkably, the variance of RUNX2 activity in unstimulated ASC was higher after two days of culture than after nine days. This elevated initial variance may indicate that ASC differentiation fate under this condition is less defined than one week later.

Thus, the RUNX2 DNA-binding activity gives also no indications for a TNF-induced or TNF-inhibited osteogenic differentiation program in ASC *in vitro*.

TNF had no Impact on ALPL Activity and Mineralization of ASC

TNF treatment did not increase neither expression nor activity of alkaline phosphatase (ALPL) in ASC, whereas osteogenic stimulation clearly did (see figure 4.11 on page 64). Since not only ALPL activity was not induced in TNF-treated ASC, but also mineralization of the extracellular matrix did not occur (see figure 4.12 on page 65), an inductive effect of TNF on osteogenic differentiation of ASC can clearly be denied. In addition, there were no indications for an impact of TNF on osteogenic differentiation of ASC, neither reductive nor promotive, when osteogenic stimulation was done simultaneously.

TNF had no Dose-Dependent Effect on Osteogenic Differentiation of ASC

A potential dose-dependent effect of TNF on osteogenic differentiation of ASC was analyzed by treatment of ASC with TNF concentrations ranging from 30 to 3,000 international units per milliliter medium. However, an inductive effect of TNF on osteogenic differentiation was still not observed even at the highest concentration (see figure 4.13 on page 66).

In healthy individuals, the serum TNF concentration is extremely low and mostly falls below the detection limit of current methods. In patients with chronic spinal cord injury, the serum TNF concentration raised to approximately 30 pg/ml, whereas no TNF was detectable in serum of healthy individuals [Hayes et al., 2002]. In patients suffering from coronary artery disease, a disease associated with elevated serum TNF levels, the TNF concentration was increased to 1.59 pg/ml, whereas healthy controls again fell below the detection limit [Safranow et al., 2009]. Patients suffering from hemorrhagic fever with renal syndrome showed a mean serum TNF concentration of 10 pg/ml [Saksida et al., 2011]. Interestingly, exposure to tobacco smoke was found to positively correlate in a dose-dependent manner with serum TNF levels, TNF serum

levels in the non-smokers group being found as low as 5 pg/ml, whereas it was up to 50 pg/ml in the smokers group [Petrescu et al., 2010]. Thus, the highest concentrations of TNF found in inflammatory processes *in vivo* are in the range of 50 pg/ml.

In comparison to these biologically active TNF serum levels, even the lowest TNF concentration used for ASC treatment was considerably high: 30 international units of TNF per milliliter medium correspond to a TNF concentration of 0.3 ng/ml or 300 pg/ml, and 3,000 international units per milliliter medium accordingly correspond to 30,000 pg/ml. Therefore, the absence of an osteogenic effect of TNF on ASC can obviously not be due to a too low dosage.

Inversely to increasing the concentration of TNF applied to ASC, the cell seeding density was reduced to increase the TNF dose per cell. This approach however did not alter the experimental outcome: Largely reducing the cell seeding density from 20,000 cells per cm² to 3,000 cells per cm² did also not result in osteogenic differentiation of TNF-treated ASC, whereas osteogenic differentiation in the osteogenically stimulated ASC still occurred (see figure 4.14 on page 67). In addition, this finding underlines that a reduction in the initial seeding density had also no beneficial effect on the extent of osteogenic marker expression, a finding that was reported earlier for bone marrow-derived MSC whose matrix calcium deposition was significantly reduced when being seeded at 3,000 cells per cm² versus 5,000 cells per cm² [Jaiswal et al., 1997].

Thus, a limited dose of TNF as a cause for the absence of osteogenic differentiation of ASC can be excluded. Since even addition of the osteogenesis-supporting factors ascorbic acid and β -glycerophosphate, which besides dexamethasone were present in the osteogenic stimulation mixture, did also not result in osteogenic differentiation of ASC (see figure 4.16 on page 69), and since ASC pre-treatment with TNF *before* osteogenic and adipogenic differentiation were induced also did not affect these differentiation pathways (see figure 4.15 on page 68), the cytokine TNF can clearly be stated to be neither able to induce nor to inhibit osteogenic differentiation of ASC *in vitro*.

TNF Increased OPG Secretion by ASC

Osteoprotegerin is a decoy receptor and thus inactivator of the osteoclast differentiation-promoting factor receptor activator of nuclear factor kappa-B ligand RANKL [Simonet et al., 1997]. *Opg* knockout mice were reported to have high bone turnover rates and severe osteoporosis due to high osteoclast activity [Wright et al., 2009]. In contrast to their phenotype of systemic bone loss, they developed ectopic calcification in the vascular system [Bucay et al., 1998]. *cFos* knockout mice were reported to develop osteopetrosis, since this AP1 subunit is an essential mediator of RANKL-induced osteoclastogenesis [Wagner, 2002].

OPG secretion by ASC, either in the presence or absence of osteogenic stimulants, was significantly increased following TNF treatment (see figure 4.17 on page 70), which matches to the observations made for murine bone marrow-derived MSC [Zhu et al., 2009], but also for human endothelial and smooth muscle cells [Cohen et al., 2007]. The TNF-induced increase in secretion of this anti-osteoclastogenic factor in ASC suggests that ASC may counteract inflammatory bone loss *in vivo*. However, since the outcome of inflammatory bone diseases nevertheless is a gradual decrease in bone mineral density, the osteoclastogenic effect of TNF *in vivo* must exceed the anti-osteoclastogenic effect exerted by the increased OPG secretion by these stromal cells by far.

Under osteogenic stimulation however, OPG secretion by ASC was reduced, what *in vivo* would result in increased osteoclastogenesis and thus higher bone turnover rates. In the context of the higher osteoblast precursor differentiation rate and osteoblast activity in an osteogenic

environment, this adaptation appears to be reasonable.

TNF and Osteogenic Differentiation in the Literature

In order to classify the absence of an impact of TNF on osteogenic differentiation of ASC *in vitro*, the current literature on the impact of TNF on osteogenic differentiation of mesenchymal stem cells in general will have to be reviewed. In accordance with the outcome of these studies, these reports can be subdivided into a group of reports of an inhibitory impact of TNF on osteogenic differentiation and a group of reports of no inhibitory impact of TNF on osteogenic differentiation *in vitro* or *in vivo*. A putative inductive effect of TNF without additional osteogenic stimulants was so far not analyzed.

Studies Reporting an Inhibitory Effect of TNF on Osteogenic Differentiation *in vivo*

Transgenic mice overexpressing TNF suffer from osteoarthritis, a chronic inflammatory disease associated with joint inflammation and bone loss [Zhao et al., 2011]. Bone marrow-derived MSC isolated from these mice showed significantly reduced alkaline phosphatase activity and expression of other osteoblast marker genes. The molecular origin was found in overexpression of *Wwp1*, an ubiquitin ligase which ubiquitinylates the MAPK transcription factor AP1 and thus drives its proteasomal degradation. *Wwp1* knockdown could rescue the disease phenotype.

In patients suffering from multiple myelomas, an inflammatory disease that is accompanied by elevated serum TNF levels and severe bone loss, the expression of the *WWTR1* gene and protein was found to be significantly reduced [Li et al., 2007]. As stated earlier, *WWTR1* is a transcriptional co-activator of the osteogenic key transcription factor *RUNX2*, and neutralization of TNF partially restored the osteogenic potential of bone marrow cells isolated from these patients.

In a study using a murine model of osteoarthritis, administration of osteoprotegerin and antibodies against TNF supportingly significantly decreased bone loss [Saidenberg-Kermanac'h et al., 2004]. In the treatment of human rheumatoid arthritis, the monoclonal TNF antibodies infliximab and etanercept are used [Taylor, 2001]. Clinical use of the monoclonal RANKL antibody denusomab further underlines the importance of the TNF-regulated RANKL/RANK/OPG system in bone homeostasis [Wright et al., 2009], TNF promoting bone resorption by increasing osteoclast maturation from their hematopoietic precursors both directly, but also indirectly by increasing secretion of the osteoclast precursor differentiation-promoting factor RANKL by osteoblasts and other bone stromal cells [Nanes, 2003]. Thus, the overall balance between bone formation and bone resorption is shifted towards a resorptive phenotype of bone metabolism *in vivo*.

RANK activation via RANKL induces not only osteoclastogenesis, but also enhances T cell maturation, which links regulation of the immune system to regulation of bone metabolism [Kim et al., 1999]. Additionally, activated T cells at sites of inflammation express RANKL to activate dendritic cells, but in that manner also induce differentiation of osteoclast precursors to mature osteoclasts [Wong et al., 1999]. This gives direct evidence of how inflammatory conditions promote bone resorption *in vivo*.

Supporting the osteolytic role of TNF *in vivo*, mice deficient for the TNF receptor 1 gene were reported to exhibit increased expression of bone markers and increased amounts of cartilage and bone formed in the process of endochondral ossification [Lukic et al., 2005], and mice deficient for TNF and TNF receptor 1 exhibited increased bone mass [Cho et al., 2010]. TNF-induced inhibition of osteoblast differentiation was shown to be mediated by TNF receptor 1 in mice

[Gilbert et al., 2005]. In this model, TNF inhibited the expression of bone-matrix proteins, IGF1 and the parathyroid hormone receptor by mature osteoblasts, but stimulated the expression of osteoclastogenic signals and inhibited differentiation of new osteoblasts from precursors.

Studies Reporting an Inhibitory Effect of TNF on Osteogenic Differentiation *in vitro* TNF treatment of murine bone marrow-derived MSC was reported to reduce expression of osteogenic markers as alkaline phosphatase, $\alpha 1$ type 1 collagen, Runx2 and osterix, and cells subsequently failed to differentiate into osteoblasts [Lacey et al., 2009]. TNF was reported to inhibit osteogenic differentiation of osteoblast precursors rat fetal calvarial cells and mouse MC3T3 cells, but not to affect their viability [Gilbert et al., 2000]. TNF treatment of rat bone marrow-derived MSC stimulated osteogenically with dexamethasone and then seeded onto biodegradable electrospun poly-3-caprolactone scaffolds *per se* supporting osteogenic differentiation resulted in a dose-dependent decrease of alkaline phosphatase activity [Mountziaris et al., 2010].

In murine MC3T3-E1 osteoblast precursor cells, TNF was found to inhibit BMP2-induced alkaline phosphatase activation and subsequent osteogenic differentiation [Nakase et al., 1997]. The inhibitory effect of TNF on TGF β signal transduction in C2C12 mouse pluripotent mesenchymal precursor cells was found to result from a decreased phosphorylation and thus activation of BMP signal transducing Smads 1, 5 and 8 as well as from an increased expression of the inhibitory Smad6, which all in all resulted in decreased expression of the Runx2 and osteocalcin genes [Mukai et al., 2007]. In diverse mouse cell culture systems, Smad6 was reported to bind to and activate the ubiquitin ligase Smurf1, which in turn ubiquitinylates Runx2 to drive proteasomal degradation of this osteogenic key transcription factor [Shen et al., 2006]. In addition, Smad6 was reported to recruit histone deacetylases to activated, promoter-bound glucocorticoid receptors to silence expression of their target genes [Ichijo et al., 2005]. This general mechanism may also apply for other Smad6-regulated transcription factors to mediate the inhibitory effect of TNF on osteogenic differentiation. Interestingly, the inhibitory action of TNF on TGF β signaling was reported to depend on activation of the MAPK pathway member MAPK8, since blockade of MAPK8 action by a specific inhibitor precluded the TNF-mediated decrease in Smad1,5,8 phosphorylation and increased expression of the gene encoding the inhibitory Smad6 [Mukai et al., 2007]. This indicates that the inhibitory effect of TNF on osteogenic differentiation is exerted indirectly by activation of the MAPK pathway which in turn represses the TGF β signaling pathway.

Another mechanistic explanation for a direct inhibitory effect of TNF on osteogenic differentiation involves activation of the NF κ B pathway and comes from the finding that the p65 subunit of the TNF-activated NF κ B dimer binds to the vitamin D receptor. This inhibits recruitment of steroid co-activator 1 to this receptor and in rat osteosarcoma cells was shown to in turn preclude induction of transcription from the osteocalcin promoter [Lu et al., 2004].

TNF was also found to inhibit osteogenic differentiation driven by the WNT pathway. Dickkopf homolog 1, an antagonist of nuclear accumulation of WNT pathway key signal transducer beta catenin, was found to be induced under inflammatory conditions as in diseases as osteoarthritis that are characterized by increased chondrocyte apoptosis rates [Weng et al., 2009]. Neutralization of Dickkopf homolog 1 did not only ameliorate loss of chondrocytes in osteoarthritis, but also loss of bone in a mouse model [Heiland et al., 2010] that develops arthritis due to overexpression of a human TNF transgene [Keffer et al., 1991].

These findings underline the importance of the WNT signaling pathway for osteogenesis *in*

vivo and *in vitro* and illustrate how TNF-mediated induction of the WNT antagonist Dickkopf homolog 1 results in the directly opposed pathogenesis of bone resorption. Further evidence for a Janus-faced relationship between inflammation and osteogenesis in the Wnt context comes from the recent finding that the RUNX2 agonist Wnt3a is able to post-transcriptionally inhibit TNF-mediated induction of Il6 secretion by mouse osteoblast-like MC3T3-E1 cells [Natsume et al., 2011].

Further evidence for an inhibitory action of TNF on osteogenic differentiation comes from functional studies on tumor necrosis factor alpha-induced protein 6 (TNFAIP6, formerly called TNF-stimulated gene 6, TSG6). *TNFAIP6* encodes a factor which is hardly expressed in unstimulated cells, but which is strongly upregulated by pro-inflammatory cytokines as TNF and IL1 as well as in inflammatory diseases as e.g. rheumatoid arthritis [Milner and Day, 2003]. TNFAIP6 is involved in extracellular matrix remodeling by catalyzing the transfer of heavy chains from chondroitin sulfate onto newly synthesized hyaluronan, a process that is crucial in cartilaginous extracellular matrix biosynthesis [Sanggaard et al., 2008], but also in oocytogenesis [Varki et al., 2009]. *Tnfaip6* knockout in mice results in erroneous ovulation and female infertility. Thus, TNFAIP6 is an important factor both in developmental as well as in inflammatory matrix remodeling.

In osteogenic differentiation of human bone marrow-derived MSC, *TNFAIP6* expression is significantly downregulated, and overexpression of *TNFAIP6* was found to inhibit osteogenic differentiation induced by osteogenic chemicals as well as by BMP2 [Inoue et al., 2006]. TNFAIP6 was found to directly bind to and repress BMP2-binding to its receptor [Tsukahara et al., 2006], which gives evidence for a direct inhibitory action of TNF on osteogenic differentiation. Since TNFAIP6 also binds to and increases the activity of the serin protease inhibitor inter-alpha-trypsin inhibitor, it indirectly reduces the activity of proteases involved in matrix remodeling during osteogenic differentiation. Thus, the TNF-driven upregulation of *TNFAIP6* expression impairs osteogenic differentiation on multiple levels.

In mature dells, TNF was not only reported to activate osteoclast-precursor mobilisation and differentiation, but also to directly inhibit the bone matrix-secreting activity of mature osteoblasts [Nanes, 2003; Tat et al., 2004; Datta et al., 2008].

A mechanistic explanation comes from the finding that expression and transactivation activity of the vitamin D receptor are repressed through protein-protein interactions with TNF-activated NF κ B signaling pathway members. In addition, TNF treatment of rat bone marrow-derived MSC was reported to increase secretion of matrix metalloproteinases 2 and 9 *in vitro*, which suggests an unusual catabolic role for osteoblasts in bone remodeling *in vivo* [Ben David et al., 2008]. TNF induced sclerostin (*SOST*) expression via the ERK1/2 MAPK pathway in human adult primary osteoblasts [Vincent et al., 2009], sclerostin being an antagonist of BMP-induced osteogenesis, and loss-of-function mutations of sclerostin cause a disease phenotype of progressive bone overgrowth.

Hence, TNF is numerously reported to act as an inhibitor of osteogenic differentiation both *in vitro* and *in vivo*. Contrastingly, TNF treatment of ASC did not reduce the extent of their osteogenic differentiation. Nevertheless, there is a number of studies that support this finding both *in vitro* and *in vivo*.

Studies Reporting No Inhibitory Effect of TNF on Osteogenic Differentiation *in vitro*

Bone marrow-derived MSC were reported to show increased expression of the *BMP2*, *RUNX2*, *ALPL* and osterix gene and to also show stronger extracellular matrix mineralization following

TNF stimulation under osteogenic conditions induced by ascorbic acid and β -glycerophosphate [Hess et al., 2009]. The increased expression of osteogenic markers was assigned to the TNF-mediated activation of the NF κ B pathway, and a constitutively active version of the NF κ B-inducing kinase IKK2 increased expression of the above-mentioned osteogenic markers. However, blocking of the NF κ B pathway by expression of an IKK substrate that cannot be phosphorylated by this kinase and therefore dominantly suppresses NF κ B activity did not interfere with osteogenic differentiation, which questions the biological relevance of the NF κ B pathway for osteogenic differentiation of bone marrow-derived MSC. Additionally, the predominant portion of osteogenic markers in this study was investigated only at the gene expression, but not at the protein level, and the extracellular matrix calcium content was not put into relation to the simultaneously increased cell number under TNF treatment. Nevertheless, these results show that TNF is not able to abrogate the osteogenic stimulus in bone marrow-derived MSC *in vitro*, a finding that was confirmed also for ASC [Crop et al., 2010; Cho et al., 2010].

Studies Reporting No Inhibitory Effect of TNF on Osteogenic Differentiation *in vivo*

Treating muscle-derived stromal cells (MDSC) with TNF before implanting them into a bone fracture in mice significantly increased osteogenic differentiation and fracture healing [Glass et al., 2011]. The same was true when TNF was directly applied to the fracture site. Since TNF-treated MDSC showed significantly increased migratory activity and since supernatants from tibial bone fragments induced osteogenic differentiation of these cells *in vitro*, the combinatorial effect of the differentiation-inducing environment and the migration-inducing pro-inflammatory stimulus are thought to concert the improved fracture healing observed *in vivo*. This hypothesis was substantiated by the outcome of an earlier study reporting impaired bone formation in both the process of endochondral and intramembranous ossification in a mouse model knocked out for both TNF receptors and thus being insensitive to TNF [Gerstenfeld et al., 2001].

Moreover, TNFAIP6, the factor whose expression just was discussed to be upregulated by inflammatory cytokines as TNF, but needs to be downregulated for osteogenic differentiation to succeed, may, due to its inhibitory action on proteases, also have a protective function against inflammatory osteolysis *in vivo*. Supportingly, TNFAIP6 was found to inhibit RANKL-induced osteoclast activation [Mahoney et al., 2008]. Besides its general anti-inflammatory action as inhibitor of neutrophil migration and reducer of plasmin activity, *TNFAIP6* expression by the inflammatory stimulated cells therefore provides an autocrine feedback inhibition loop to limit inflammatory bone erosion [Mahoney et al., 2011]. Thus, TNFAIP6 participates both in regulation of osteoblastogenesis and osteoclastogenesis, and TNF can exert both anti- and pro-osteogenic effects through it.

In diseases associated with low-grade vascular inflammation, as e.g. diabetes, the upregulated TNF levels in mice were found to induce BMP2-mediated osteogenic differentiation to finally lead to ectopic arterial calcification [Shao et al., 2005, 2006]. Mechanistically, Bmp2 was found to induce the transcription factor *Msx2*, and a multipotential mouse embryonic mesodermal cell line transduced to constitutively express *Msx2* was found to upregulate expression of Wnt agonists *Wnt3a* and *Wnt7a* and to downregulate Wnt antagonist *Dkk1*. This resulted in nuclear translocation of Wnt key transcription factor beta catenin to activate alkaline phosphatase in a Runx2-dependent manner and thus to lead to matrix mineralization. Interestingly, even conditioned medium from these constitutively *Msx2* expressing cells induced osteogenic differentiation of untransduced cells via the same mechanism of Wnt activation *in vitro*, which suggests a paracrine mechanism of vascular calcification *in vivo*.

This finding that elevated serum TNF levels indirectly induce Wnt signaling in arterial was reproduced in aortic myofibroblasts *in vitro* and resulted in increased arterial calcification *in vivo* [Al-Aly et al., 2007]. This mechanism of TNF-mediated vascular calcification was found to apply also for chronic kidney disease *in vivo* [Al-Aly, 2008] and thus may reflect a common mechanism of inflammation-mediated ectopic mineralisation *in vivo*. Thus, inflammatory cytokines regulate osteogenic differentiation of vascular cells, which occurs both in direction of osteoblasts and osteoclasts and generates an active bone metabolism resembling that of trabecular bone tissues [Abedin et al., 2004]. Hence, inflammation and ectopic, cardiovascular calcification are numerous reported to be associated.

Additionally, cardiovascular calcification, atherosclerosis and chronic renal disease are associated with osteoporosis, and recent work in mice has demonstrated that arterial and aortic calcification inversely correlate with osteoporotic bone remodeling, i.e. that with ongoing inflammation-mediated osteolysis of hard cortical and trabecular bone tissue, new bone is ectopically generated in vascular soft tissues [Hjortnaes et al., 2010]. Thus, the disease state of systemic inflammation leads to both the common effect of monocyte/macrophage activation, but inflammatory activation of these cells subsequently leads to opposed effects, i.e. to osteolysis in the long bone and to osteogenic differentiation in arteries and valves. Supportingly, mice exhibiting high bone turnover rates due to knockout of the osteoprotegerin gene were reported to suffer from ectopic calcification [Bucay et al., 1998].

Besides TNF, the calcium and phosphate ions liberated in the osteolytic reactions in the long bone directly contribute to ectopic calcification and subsequently to increased local cytokine levels, since basic calcium phosphate was reported to be internalized into vacuoles by monocytes/macrophages, which elicits an inflammatory stimulus resulting in the secretion of pro-inflammatory cytokines as TNF [Nadra et al., 2005]. This colorfully illustrates the vicious cycle of inflammatory bone remodeling.

Interestingly, TNF in mature osteoblasts and MG-63 cells was found to increase alkaline phosphatase activity even in an RUNX2-independent mechanism involving inhibition of the adipogenic transcription factor PPAR γ , and inhibition of prostaglandin synthesis abolished calcification [Lencel et al., 2011]. In human mesenchymal stem cells, TNF inhibited RUNX2, osteocalcin and collagen expression, but increased alkaline phosphatase activity and mineralization and thus induced an incomplete program of osteogenic differentiation [Ding et al., 2009]. These findings allow two important conclusions. On the one hand, they link the onset of ectopic calcification to the suppression of adipogenic differentiation, a hypothesis that is substantiated by the fact that patients treated with serum lipid-lowering statins show reduced cardiovascular calcification rates [Hjortnaes et al., 2010]. On the other hand, these findings emphasize that ectopic calcification does not necessarily require osteogenic differentiation of stem cells, since it can also take place if a pre-existing collagen network is calcified by mature osteoblast-like cells. Moreover, the mechanical properties of this extracellular environment can act as an inducer of ectopic calcification, since vascular tunica lesion-healing in Peyronie's disease is not only accompanied by the deposition of abnormal amounts of fibrotic tissue, but also by osteogenic differentiation of mesenchymal stem cells residing in the pericytal region and thus in contact to this fibrotic tissue [Vernet et al., 2005].

Hence, systemic inflammation, via a variety of pathways, leads to the apparent, though explainable paradox of simultaneous osteolysis in long bone and calcification at ectopic sites and therefore can be summarized to cause "softening" of hard tissue and "hardening" of soft tissue.

Concluding Remarks on the Impact of TNF on Osteogenic Differentiation *in vitro* and *in vivo* Although a pro-inflammatory stimulus as TNF on its own was not able to induce osteogenic differentiation of multipotent progenitor cells as ASC *in vitro*, it increased their proliferation rate and thus their number. If the inflamed tissue simultaneously provides stimuli that promote osteogenic differentiation, there will be a significantly higher number of progenitor cells that can undergo osteogenic differentiation. This mechanism will then indirectly lead to the establishment of ectopic calcification observed in the cardiovascular system under chronic inflammatory conditions *in vivo*.

5.5 Summary and Conclusions

Summarizingly, both TNF receptors were found to be expressed on ASC, though at strikingly different intensity. As was reported for most cell types, TNFRSF1A was found to be much stronger expressed than TNFRSF1B, the latter being formerly thought to be confined to immune cells, but in recent times being published to be expressed on an increasing number of other cell types.

Upon binding of TNF to its receptors, these receptors can activate three distinct signal transduction pathways: The apoptosis pathway, the MAP kinase pathway and the NF κ B pathway. TNF induced the NF κ B, but not the apoptosis pathway, whereas the MAP kinase p38 and the MAPK transcription factor AP1 were found to be constitutively active in ASC. Osteogenic stimulation had no impact on these signaling pathways.

Thus, although other cell types as endothelial cells, synovial fibroblasts or smooth muscle cells are highly susceptible to TNF-induced apoptosis, ASC were not. This may have been the consequence of the activated NF κ B pathway and the activated MAP kinase transcription factor AP1, the former being generalized to have pro-survival properties and the latter being known to activate expression of anti-apoptotic genes of the B cell lymphoma family.

TNF significantly increased ASC proliferation rates and accelerated their passage through the S phase of the cell cycle. This effect may have been the consequence of a promoted transition through the G₁ to S checkpoint of the cell cycle. This transition was reported to be regulated by activation of the NF κ B pathway which itself increases activity of distinct cyclins and the prominent proto-oncogene MYC.

Osteogenically stimulated ASC also showed increased proliferation rates, but decelerated passage through the S phase. Slower S phase passage may have been the consequence of the increased expression of *ZBTB16*, a transcription factor reported to suppress activity of cyclins involved in G₁ to S transition and found to decrease expression of MYC. In addition, osteogenic stimulation of ASC increased DNA-binding activity of RUNX2, the osteogenic key transcription factor that was reported to promote cell cycle exit from G₁ to G₀ in order to facilitate differentiation. Although increased expression and DNA-binding activity of these osteogenic transcription factors easily explain the induction of an osteogenic differentiation program in ASC, the high proliferation rates observed simultaneously are not. For hematopoietic and neural stem cells, differentiation is known to occur in a process of asymmetric cell division, one daughter cell differentiating and the other self-renewing to keep the pool of stem cells upright. Since ASC were reported to be able to undergo the full hematopoietic differentiation program and since bone marrow-derived MSC even share the same niche with HSC, this mode of differentiation appears to be possible, though not explicitly demonstrated for ASC in special and MSC in general.

Osteogenic stimulation of ASC was found to result in an intermediate increase in metabolic activity that was absent in the TNF-treated cells, and a simultaneous study revealed an increas-

ingly glycolysis- and citric acid cycle-driven metabolism during osteogenic differentiation of ASC. Therefore, this differentiation pathway coincides with an increasingly oxidative metabolism, which nowadays is considered to be a general hallmark of ongoing differentiation processes and interestingly was also shown to inversely induce differentiation of stem cells.

Treatment of ASC with TNF did not induce osteogenic differentiation of these stem cells *in vitro*. This is in contrast to the well-known differentiation-promoting effect of TNF on osteoclastic precursor cells from the hematopoietic lineage. Since TNF did neither increase nor reduce the osteogenic differentiation capacity of ASC in an osteogenic environment *in vitro*, the effect of osteolysis of the long bone observed in chronic inflammatory diseases presumably is mainly due to the pro-osteoclastogenic effect of this cytokine *in vivo*.

Seemingly paradoxically, the same inflammatory stimuli that induce osteolysis of the long bone induce calcification at ectopic sites, primarily the vasculature, via a variety of different pathways. Therefore, chronic inflammatory diseases can be summarized to cause “softening” of hard tissue and simultaneous “hardening” of soft tissue.

Generalizing the main finding of this study, i.e. the finding that TNF did not impair ASC osteogenic differentiation capability, but increased ASC proliferation rate, inflammatory processes *in vivo* appear to act as a driving force for stem cell self-renewal without affecting their differentiation potential, and factors other than the mediators of inflammation govern subsequent differentiation of this enlarged stem cell pool into the desired tissue. Thus, inflammatory activation of infected or damaged tissue increases its regenerative potential as a starting point, but requires further signals for regeneration to complete.

Bibliography

- Abedin M, Tintut Y, Demer LL. Vascular calcification: mechanisms and clinical ramifications. *Arterioscler Thromb Vasc Biol* **24(7)**:1161–70, 2004.
- Active Motif. *TransAM AML-3/Runx2 Transcription Factor Assay Kits*, a1 edn., 2010.
- Adcock IM. Glucocorticoid-regulated transcription factors. *Pulm Pharmacol Ther* **14(3)**:211–9, 2001.
- Aggarwal BB. Signalling pathways of the TNF superfamily: a double-edged sword. *Nat Rev Immunol* **3(9)**:745–56, 2003.
- Aggarwal BB, Eessalu TE, Hass PE. Characterization of receptors for human tumour necrosis factor and their regulation by gamma-interferon. *Nature* **318(6047)**:665–7, 1985.
- Al-Aly Z. Arterial calcification: a tumor necrosis factor-alpha mediated vascular Wnt-opathy. *Transl Res* **151(5)**:233–9, 2008.
- Al-Aly Z, Shao JS, Lai CF, Huang E, Cai J, Behrmann A, Cheng SL, Towler DA. Aortic Msx2-Wnt calcification cascade is regulated by TNF-alpha-dependent signals in diabetic Ldlr^{-/-} mice. *Arterioscler Thromb Vasc Biol* **27(12)**:2589–96, 2007.
- Alberts B, Johnson A, Lewis J, Raff M, Roberts K, Walter P, National Center for Biotechnology Information (US). *Molecular Biology of the Cell* (Garland Science), 4th edn., 2002.
- Anderson HC. Molecular biology of matrix vesicles. *Clin Orthop Relat Res* **314**:266–280, 1995.
- Anderson HC, Sipe JB, Hesse L, Dhanyamraju R, Atti E, Camacho NP, Millan JL. Impaired calcification around matrix vesicles of growth plate and bone in alkaline phosphatase-deficient mice. *Am J Pathol* **164(3)**:841–7, 2004.
- Applied Biosystems. *Power SYBR Green PCR Master Mix and RT-PCR*, c edn., 2006.
- Arboleda D, Forostyak S, Jendelova P, Marekova D, Amemori T, Pivonkova H, Masinova K, Sykova E. Transplantation of Predifferentiated Adipose-Derived Stromal Cells for the Treatment of Spinal Cord Injury. *Cell Mol Neurobiol* 2011.
- Arnsdorf EJ, Tummala P, Kwon RY, Jacobs CR. Mechanically induced osteogenic differentiation—the role of RhoA, ROCKII and cytoskeletal dynamics. *J Cell Sci* **122(Pt 4)**:546–553, 2009.
- Azuma Y, Kaji K, Katogi R, Takeshita S, Kudo A. Tumor necrosis factor-alpha induces differentiation of and bone resorption by osteoclasts. *J Biol Chem* **275(7)**:4858–64, 2000.
- Barna M, Hawe N, Niswander L, Pandolfi PP. Plzf regulates limb and axial skeletal patterning. *Nat Genet* **25(2)**:166–72, 2000.
- Baumgartner-Sigl S, Haberlandt E, Mumm S, Scholl-Burgi S, Sergi C, Ryan L, Ericson KL, Whyte MB, Hogler W. Pyridoxine-responsive seizures as the first symptom of infantile hypophosphatasia caused by two novel missense mutations (c.677T>C, p.M226T; c.1112C>T, p.T371I) of the tissue-nonspecific alkaline phosphatase gene. *Bone* **40(6)**:1655–61, 2007.
- Beck J G R, Zerler B, Moran E. Gene array analysis of osteoblast differentiation. *Cell Growth Differ* **12(2)**:61–83, 2001.
- Beloti MM, Rosa AL. Osteoblast differentiation of human bone marrow cells under continuous and discontinuous treatment with dexamethasone. *Braz Dent J* **16(2)**:156–61, 2005.
- Ben David D, Reznick AZ, Srouji S, Livne E. Exposure to pro-inflammatory cytokines upregulates MMP-9 synthesis by mesenchymal stem cells-derived osteoprogenitors. *Histochem Cell Biol* **129(5)**:589–97, 2008.
- Berg JM, Tymoczko JL, Stryer L, National Center for Biotechnology Information (US). *Biochemistry* (W. H. Freeman and Company), 5th edn., 2002.

- Berglund L, Bjorling E, Oksvold P, Fagerberg L, Asplund A, Szigartyo CA, Persson A, Ottosson J, Wernerus H, Nilsson P, Lundberg E, Sivertsson A, Navani S, Wester K, Kampf C, Hober S, Ponten F, Uhlen M. A genecentric Human Protein Atlas for expression profiles based on antibodies. *Mol Cell Proteomics* **7(10)**:2019–27, 2008.
- Berridge MV, Herst PM, Tan AS. Tetrazolium dyes as tools in cell biology: new insights into their cellular reduction. *Biotechnol Annu Rev* **11**:127–52, 2005.
- Berridge MV, Tan AS. Characterization of the cellular reduction of 3-(4,5-dimethylthiazol-2-yl)-2,5-diphenyltetrazolium bromide (MTT): subcellular localization, substrate dependence, and involvement of mitochondrial electron transport in MTT reduction. *Arch Biochem Biophys* **303(2)**:474–82, 1993.
- Bitar M, Brown RA, Salih V, Kidane AG, Knowles JC, Nazhat SN. Effect of cell density on osteoblastic differentiation and matrix degradation of biomimetic dense collagen scaffolds. *Biomacromolecules* **9(1)**:129–35, 2008.
- Boehm C, Hayer S, Kilian A, Zaiss MM, Finger S, Hess A, Engelke K, Kollias G, Kroenke G, Zwerina J, Schett G, David JP. The alpha-isoform of p38 MAPK specifically regulates arthritic bone loss. *J Immunol* **183(9)**:5938–5947, 2009.
- Bours V, Bentires-Alj M, Hellin AC, Viatour P, Robe P, Delhalle S, Benoit V, Merville MP. Nuclear factor-kappa B, cancer, and apoptosis. *Biochem Pharmacol* **60(8)**:1085–9, 2000.
- Boyce BF, Yao Z, Xing L. Functions of nuclear factor kappaB in bone. *Ann N Y Acad Sci* **1192**:367–375, 2010.
- Bozec A, Bakiri L, Jimenez M, Schinke T, Amling M, Wagner EF. Fra-2/AP-1 controls bone formation by regulating osteoblast differentiation and collagen production. *J Cell Biol* **190(6)**:1093–1106, 2010.
- Bradham C, McClay DR. p38 MAPK in development and cancer. *Cell Cycle* **5(8)**:824–828, 2006.
- Bradley JR. TNF-mediated inflammatory disease. *J Pathol* **214(2)**:149–60, 2008.
- Bu R, Borysenko CW, Li Y, Cao L, Sabokbar A, Blair HC. Expression and function of TNF-family proteins and receptors in human osteoblasts. *Bone* **33(5)**:760–70, 2003.
- Bucay N, Sarosi I, Dunstan CR, Morony S, Tarpley J, Capparelli C, Scully S, Tan HL, Xu W, Lacey DL, Boyle WJ, Simonet WS. Osteoprotegerin-deficient mice develop early onset osteoporosis and arterial calcification. *Genes Dev* **12(9)**:1260–8, 1998.
- Carcamo-Orive I, Gaztelumendi A, Delgado J, Tejados N, Dorronsoro A, Fernandez-Rueda J, Pennington DJ, Trigueros C. Regulation of human bone marrow stromal cell proliferation and differentiation capacity by glucocorticoid receptor and AP-1 crosstalk. *J Bone Miner Res* **25(10)**:2115–2125, 2010.
- Carinci F, Pezzetti F, Spina AM, Palmieri A, Laino G, De Rosa A, Farina E, Illiano F, Stabellini G, Perrotti V, Piattelli A. Effect of Vitamin C on pre-osteoblast gene expression. *Arch Oral Biol* **50(5)**:481–96, 2005.
- Carswell EA, Old LJ, Kassel RL, Green S, Fiore N, Williamson B. An endotoxin-induced serum factor that causes necrosis of tumors. *Proc Natl Acad Sci U S A* **72(9)**:3666–3670, 1975.
- Carvalho PP, Wu X, Yu G, Dias IR, Gomes ME, Reis RL, Gimble JM. The effect of storage time on adipose-derived stem cell recovery from human lipoaspirates. *Cells Tissues Organs* **194(6)**:494–500, 2011.
- Celebi B, Elcin AE, Elcin YM. Proteome analysis of rat bone marrow mesenchymal stem cell differentiation. *J Proteome Res* **9(10)**:5217–27, 2010.
- Cell Signaling Technology. Immunofluorescence General Protocol. World Wide Web, 2011.
- Chaves Neto AH, Queiroz KC, Milani R, Paredes-Gamero EJ, Justo GZ, Peppelenbosch MP, Ferreira CV. Profiling the changes in signaling pathways in ascorbic acid/beta-glycerophosphate-induced osteoblastic differentiation. *J Cell Biochem* **112(1)**:71–7, 2011.
- Chen G, Goeddel DV. TNF-R1 signaling: a beautiful pathway. *Science* **296(5573)**:1634–1635, 2002.
- Cho HH, Shin KK, Kim YJ, Song JS, Kim JM, Bae YC, Kim CD, Jung JS. NF-kappaB activation stimulates osteogenic differentiation of mesenchymal stem cells derived from human adipose tissue by increasing TAZ expression. *J Cell Physiol* **223(1)**:168–77, 2010.
- Choi KM, Seo YK, Yoon HH, Song KY, Kwon SY, Lee HS, Park JK. Effect of ascorbic acid on bone marrow-derived mesenchymal stem cell proliferation and differentiation. *J Biosci Bioeng* **105(6)**:586–94, 2008.
- Chung CH, Golub EE, Forbes E, Tokuoka T, Shapiro IM. Mechanism of action of beta-glycerophosphate on bone cell mineralization. *Calcif Tissue Int* **51(4)**:305–11, 1992.

- Clark IA. How TNF was recognized as a key mechanism of disease. *Cytokine Growth Factor Rev* **18(3-4)**:335–343, 2007.
- Clark J, Vagenas P, Panesar M, Cope AP. What does tumour necrosis factor excess do to the immune system long term? *Ann Rheum Dis* **64 Suppl 4**:iv70–6, 2005.
- Cohen EBT, Hohensinner PJ, Kaun C, Maurer G, Huber K, Wojta J. Statins decrease TNF-alpha-induced osteoprotegerin production by endothelial cells and smooth muscle cells in vitro. *Biochem Pharmacol* **73(1)**:77–83, 2007.
- Cohen M, Lee KK, Wilson KL, Gruenbaum Y. Transcriptional repression, apoptosis, human disease and the functional evolution of the nuclear lamina. *Trends Biochem Sci* **26(1)**:41–47, 2001.
- Cooper GM, National Center for Biotechnology Information (US). *The Cell* (Sinauer Associates), 2nd edn., 2000.
- Corre J, Barreau C, Cousin B, Chavoïn JP, Caton D, Fournial G, Penicaud L, Casteilla L, Laharrague P. Human subcutaneous adipose cells support complete differentiation but not self-renewal of hematopoietic progenitors. *J Cell Physiol* **208(2)**:282–288, 2006.
- Costoya JA, Hobbs RM, Pandolfi PP. Cyclin-dependent kinase antagonizes promyelocytic leukemia zinc-finger through phosphorylation. *Oncogene* **27(27)**:3789–96, 2008.
- Cox WG, Singer VL. A high-resolution, fluorescence-based method for localization of endogenous alkaline phosphatase activity. *J Histochem Cytochem* **47(11)**:1443–1456, 1999.
- Crisan M, Yap S, Casteilla L, Chen CW, Corselli M, Park TS, Andriolo G, Sun B, Zheng B, Zhang L, Norotte C, Teng PN, Traas J, Schugar R, Deasy BM, Badyrak S, Buhning HJ, Giacobino JP, Lazzari L, Huard J, Peault B. A perivascular origin for mesenchymal stem cells in multiple human organs. *Cell Stem Cell* **3(3)**:301–13, 2008.
- Crop MJ, Baan CC, Korevaar SS, Ijzermans JN, Pescatori M, Stubbs AP, van Ijcken WF, Dahlke MH, Eggenhofer E, Weimar W, Hoogduijn MJ. Inflammatory conditions affect gene expression and function of human adipose tissue-derived mesenchymal stem cells. *Clin Exp Immunol* **162(3)**:474–86, 2010.
- da Silva Meirelles L, Caplan AI, Nardi NB. In search of the in vivo identity of mesenchymal stem cells. *Stem Cells* **26(9)**:2287–99, 2008.
- Dahlman JM, Wang J, Bakkar N, Guttridge DC. The RelA/p65 subunit of NF-kappaB specifically regulates cyclin D1 protein stability: implications for cell cycle withdrawal and skeletal myogenesis. *J Cell Biochem* **106(1)**:42–51, 2009.
- Datta HK, Ng WF, Walker JA, Tuck SP, Varanasi SS. The cell biology of bone metabolism. *J Clin Pathol* **61(5)**:577–587, 2008.
- Ding J, Ghali O, Lencel P, Broux O, Chauveau C, Devedjian JC, Hardouin P, Magne D. TNF-alpha and IL-1beta inhibit RUNX2 and collagen expression but increase alkaline phosphatase activity and mineralization in human mesenchymal stem cells. *Life Sci* **84(15-16)**:499–504, 2009.
- Discher DE, Mooney DJ, Zandstra PW. Growth factors, matrices, and forces combine and control stem cells. *Science* **324(5935)**:1673–1677, 2009.
- Douarin NML, Calloni GW, Dupin E. The stem cells of the neural crest. *Cell Cycle* **7(8)**:1013–1019, 2008.
- Duyao MP, Buckler AJ, Sonenshein GE. Interaction of an NF-kappa B-like factor with a site upstream of the c-myc promoter. *Proc Natl Acad Sci U S A* **87(12)**:4727–31, 1990.
- Fahnenstich J, Nandy A, Milde-Langosch K, Schneider-Merck T, Walther N, Gellersen B. Promyelocytic leukaemia zinc finger protein (PLZF) is a glucocorticoid- and progesterone-induced transcription factor in human endometrial stromal cells and myometrial smooth muscle cells. *Mol Hum Reprod* **9(10)**:611–23, 2003.
- Farkas LM, Huttner WB. The cell biology of neural stem and progenitor cells and its significance for their proliferation versus differentiation during mammalian brain development. *Curr Opin Cell Biol* **20(6)**:707–715, 2008.
- Faustman D, Davis M. TNF receptor 2 pathway: drug target for autoimmune diseases. *Nat Rev Drug Discov* **9(6)**:482–493, 2010.
- Fickert S, Schroter-Bobsin U, Gross AF, Hempel U, Wojciechowski C, Rentsch C, Corbeil D, Gunther KP. Human mesenchymal stem cell proliferation and osteogenic differentiation during long-term ex vivo cultivation is not age dependent. *J Bone Miner Metab* **29(2)**:224–235, 2011.
- Fischer S, Kohlhasse J, Bohm D, Schweiger B, Hoffmann D, Heitmann M, Horsthemke B, Wiczorek D. Biallelic loss of function of the promyelocytic leukaemia zinc finger (PLZF) gene causes severe skeletal defects and genital hypoplasia. *J Med Genet* **45(11)**:731–7, 2008.
- Frank O, Heim M, Jakob M, Barbero A, Schafer D, Bendik I, Dick W, Heberer M, Martin I. Real-time quantitative RT-PCR analysis of human bone marrow stromal cells during osteogenic differentiation in vitro. *J Cell Biochem* **85(4)**:737–46, 2002.

- Fukunaka A, Kurokawa Y, Teranishi F, Sekler I, Oda K, Ackland ML, Faundez V, Hiromura M, Masuda S, Nagao M, Enomoto S, Kambe T. Tissue nonspecific alkaline phosphatase is activated via a two-step mechanism by zinc transport complexes in the early secretory pathway. *J Biol Chem* **286**(18):16,363–16,373, 2011.
- Furness SGB, McNagny K. Beyond mere markers: functions for CD34 family of sialomucins in hematopoiesis. *Immunol Res* **34**(1):13–32, 2006.
- Gallagher SR, Desjardins PR. Quantitation of DNA and RNA with absorption and fluorescence spectroscopy. *Curr Protoc Protein Sci Appendix 3*:Appendix 4K, 2008.
- Gao L, McBeath R, Chen CS. Stem cell shape regulates a chondrogenic versus myogenic fate through Rac1 and N-cadherin. *Stem Cells* **28**(3):564–572, 2010.
- Gerstenfeld LC, Cho TJ, Kon T, Aizawa T, Cruceta J, Graves BD, Einhorn TA. Impaired intramembranous bone formation during bone repair in the absence of tumor necrosis factor- α signaling. *Cells Tissues Organs* **169**(3):285–94, 2001.
- Ghali O, Chauveau C, Hardouin P, Broux O, Devedjian JC. TNF- α 's effects on proliferation and apoptosis in human mesenchymal stem cells depend on RUNX2 expression. *J Bone Miner Res* **25**(7):1616–26, 2010.
- Giebel B, Bruns I. Self-renewal versus differentiation in hematopoietic stem and progenitor cells: a focus on asymmetric cell divisions. *Curr Stem Cell Res Ther* **3**(1):9–16, 2008.
- Gilbert L, He X, Farmer P, Boden S, Kozlowski M, Rubin J, Nanes MS. Inhibition of osteoblast differentiation by tumor necrosis factor- α . *Endocrinology* **141**(11):3956–64, 2000.
- Gilbert LC, Rubin J, Nanes MS. The p55 TNF receptor mediates TNF inhibition of osteoblast differentiation independently of apoptosis. *Am J Physiol Endocrinol Metab* **288**(5):E1011–E1018, 2005.
- Gilbert SF, National Center for Biotechnology Information (US). *Developmental Biology* (Sinauer Associates), 6th edn., 2000.
- Gillies RJ, Didier N, Denton M. Determination of cell number in monolayer cultures. *Anal Biochem* **159**(1):109–113, 1986.
- Gimble JM, Bunnell BA (Eds.). *Adipose-Derived Stem Cells* (SPRINGER, BERLIN; HUMANA PRESS), 1st edn., 2010.
- Giri S, Rattan R, Haq E, Khan M, Yasmin R, song Won J, Key L, Singh AK, Singh I. AICAR inhibits adipocyte differentiation in 3T3L1 and restores metabolic alterations in diet-induced obesity mice model. *Nutr Metab (Lond)* **3**:31, 2006.
- Glass GE, Chan JK, Freidin A, Feldmann M, Horwood NJ, Nanchahal J. TNF- α promotes fracture repair by augmenting the recruitment and differentiation of muscle-derived stromal cells. *Proc Natl Acad Sci U S A* **108**(4):1585–90, 2011.
- Goseki-Sone M, Sogabe N, Fukushi-Irie M, Mizoi L, Orimo H, Suzuki T, Nakamura H, Hosoi T. Functional analysis of the single nucleotide polymorphism (787T>C) in the tissue-nonspecific alkaline phosphatase gene associated with BMD. *J Bone Miner Res* **20**(5):773–82, 2005.
- Greenblatt MB, Shim JH, Zou W, Sitara D, Schweitzer M, Hu D, Lotinun S, Sano Y, Baron R, Park JM, Arthur S, Xie M, Schneider MD, Zhai B, Gygi S, Davis R, Glimcher LH. The p38 MAPK pathway is essential for skeletogenesis and bone homeostasis in mice. *J Clin Invest* **120**(7):2457–2473, 2010.
- Grell M, Douni E, Wajant H, Lohden M, Clauss M, Maxeiner B, Georgopoulos S, Lesslauer W, Kollias G, Pfizenmaier K, Scheurich P. The transmembrane form of tumor necrosis factor is the prime activating ligand of the 80 kDa tumor necrosis factor receptor. *Cell* **83**(5):793–802, 1995.
- Grimes BR, Steiner CM, Merfeld-Clauss S, Traktuev DO, Smith D, Reese A, Breman AM, Thurston VC, Vance GH, Johnstone BH, Slee RB, March KL. Interphase FISH demonstrates that human adipose stromal cells maintain a high level of genomic stability in long-term culture. *Stem Cells Dev* **18**(5):717–24, 2009.
- Gronthos S, Chen S, Wang CY, Robey PG, Shi S. Telomerase accelerates osteogenesis of bone marrow stromal stem cells by upregulation of CBFA1, osterix, and osteocalcin. *J Bone Miner Res* **18**(4):716–22, 2003.
- Gronthos S, Graves SE, Ohta S, Simmons PJ. The STRO-1+ fraction of adult human bone marrow contains the osteogenic precursors. *Blood* **84**(12):4164–4173, 1994.
- Guttridge DC, Albanese C, Reuther JY, Pestell RG, Baldwin J A S. NF- κ B controls cell growth and differentiation through transcriptional regulation of cyclin D1. *Mol Cell Biol* **19**(8):5785–99, 1999.
- Haridas V, Darnay BG, Natarajan K, Heller R, Aggarwal BB. Overexpression of the p80 TNF receptor leads to TNF-dependent apoptosis, nuclear factor- κ B activation, and c-Jun kinase activation. *J Immunol* **160**(7):3152–62, 1998.

- Hasselgren G. Alkaline phosphatase in developing teeth and bone of man and macaque monkey. *Acta Odontol Scand* **36(3)**:143–148, 1978.
- Hayes KC, Hull TCL, Delaney GA, Potter PJ, Sequeira KAJ, Campbell K, Popovich PG. Elevated serum titers of proinflammatory cytokines and CNS autoantibodies in patients with chronic spinal cord injury. *J Neurotrauma* **19(6)**:753–761, 2002.
- Heiland GR, Zwerina K, Baum W, Kireva T, Distler JH, Grisanti M, Asuncion F, Li X, Ominsky M, Richards W, Schett G, Zwerina J. Neutralisation of Dkk-1 protects from systemic bone loss during inflammation and reduces sclerostin expression. *Ann Rheum Dis* **69(12)**:2152–9, 2010.
- Helson L, Green S, Carswell E, Old LJ. Effect of tumour necrosis factor on cultured human melanoma cells. *Nature* **258(5537)**:731–732, 1975.
- Hess K, Ushmorov A, Fiedler J, Brenner RE, Wirth T. TNF α promotes osteogenic differentiation of human mesenchymal stem cells by triggering the NF-kappaB signaling pathway. *Bone* **45(2)**:367–76, 2009.
- Hinz M, Krappmann D, Eichten A, Heder A, Scheidereit C, Strauss M. NF-kappaB function in growth control: regulation of cyclin D1 expression and G0/G1-to-S-phase transition. *Mol Cell Biol* **19(4)**:2690–8, 1999.
- Hjortnaes J, Butcher J, Figueiredo JL, Riccio M, Kohler RH, Kozloff KM, Weissleder R, Aikawa E. Arterial and aortic valve calcification inversely correlates with osteoporotic bone remodelling: a role for inflammation. *Eur Heart J* **31(16)**:1975–1984, 2010.
- Hong D, Chen HX, Xue Y, Li DM, Wan XC, Ge R, Li JC. Osteoblastogenic effects of dexamethasone through upregulation of TAZ expression in rat mesenchymal stem cells. *J Steroid Biochem Mol Biol* **116(1-2)**:86–92, 2009.
- Hou LT, Li TI, Liu CM, Liu BY, Liu CL, Mi HW. Modulation of osteogenic potential by recombinant human bone morphogenic protein-2 in human periodontal ligament cells: effect of serum, culture medium, and osteoinductive medium. *J Periodontol Res* **42(3)**:244–252, 2007.
- Huang L, Qiu N, Zhang C, Wei HY, Li YL, Zhou HH, Xiao ZS. Nitroglycerin enhances proliferation and osteoblastic differentiation in human mesenchymal stem cells via nitric oxide pathway. *Acta Pharmacol Sin* **29(5)**:580–6, 2008.
- Hui TY, Cheung KM, Cheung WL, Chan D, Chan BP. In vitro chondrogenic differentiation of human mesenchymal stem cells in collagen microspheres: influence of cell seeding density and collagen concentration. *Biomaterials* **29(22)**:3201–12, 2008.
- Ichijo T, Voutetakis A, Cotrim AP, Bhattacharyya N, Fujii M, Chrousos GP, Kino T. The Smad6-histone deacetylase 3 complex silences the transcriptional activity of the glucocorticoid receptor: potential clinical implications. *J Biol Chem* **280(51)**:42,067–77, 2005.
- Ikeda R, Yoshida K, Tsukahara S, Sakamoto Y, Tanaka H, Furukawa K, Inoue I. The promyelotic leukemia zinc finger promotes osteoblastic differentiation of human mesenchymal stem cells as an upstream regulator of CBFA1. *J Biol Chem* **280(9)**:8523–30, 2005.
- Im GI, Shin YW, Lee KB. Do adipose tissue-derived mesenchymal stem cells have the same osteogenic and chondrogenic potential as bone marrow-derived cells? *Osteoarthritis Cartilage* **13(10)**:845–53, 2005.
- Imai S, Nishibayashi S, Takao K, Tomifuji M, Fujino T, Hasegawa M, Takano T. Dissociation of Oct-1 from the nuclear peripheral structure induces the cellular aging-associated collagenase gene expression. *Mol Biol Cell* **8(12)**:2407–2419, 1997.
- Imhoff BR, Hansen JM. Differential redox potential profiles during adipogenesis and osteogenesis. *Cell Mol Biol Lett* **16(1)**:149–161, 2011.
- Inoue I, Ikeda R, Tsukahara S. Current topics in pharmacological research on bone metabolism: Promyelotic leukemia zinc finger (PLZF) and tumor necrosis factor-alpha-stimulated gene 6 (TSG-6) identified by gene expression analysis play roles in the pathogenesis of ossification of the posterior longitudinal ligament. *J Pharmacol Sci* **100(3)**:205–10, 2006.
- Isakson P, Hammarstedt A, Gustafson B, Smith U. Impaired preadipocyte differentiation in human abdominal obesity: role of Wnt, tumor necrosis factor-alpha, and inflammation. *Diabetes* **58(7)**:1550–7, 2009.
- Jaeger M, Fischer J, Dohrn W, Li X, Ayers DC, Czibere A, Prall WC, Lensing-Hoehn S, Krauspe R. Dexamethasone modulates BMP-2 effects on mesenchymal stem cells in vitro. *J Orthop Res* **26(11)**:1440–1448, 2008.
- Jaiswal N, Haynesworth SE, Caplan AI, Bruder SP. Osteogenic differentiation of purified, culture-expanded human mesenchymal stem cells in vitro. *J Cell Biochem* **64(2)**:295–312, 1997.
- Janeway CAJ, Travers P, Walport M, Shlomchik MJ, National Center for Biotechnology Information (US). *Immunobiology* (Garland Science), 5th edn., 2001.

- Jeon EJ, Lee KY, Choi NS, Lee MH, Kim HN, Jin YH, Ryoo HM, Choi JY, Yoshida M, Nishino N, Oh BC, Lee KS, Lee YH, Bae SC. Bone morphogenetic protein-2 stimulates Runx2 acetylation. *J Biol Chem* **281**(24):16,502–11, 2006.
- Jovinge S, Hultgardh-Nilsson A, Regnstrom J, Nilsson J. Tumor necrosis factor-alpha activates smooth muscle cell migration in culture and is expressed in the balloon-injured rat aorta. *Arterioscler Thromb Vasc Biol* **17**(3):490–7, 1997.
- Jurgens WJ, Oedayrajsingh-Varma MJ, Helder MN, Zandiehoulabi B, Schouten TE, Kuik DJ, Ritt MJ, van Milligen FJ. Effect of tissue-harvesting site on yield of stem cells derived from adipose tissue: implications for cell-based therapies. *Cell Tissue Res* **332**(3):415–26, 2008.
- Kalbermatten DF, Schaakxs D, Kingham PJ, Wiberg M. Neurotrophic activity of human adipose stem cells isolated from deep and superficial layers of abdominal fat. *Cell Tissue Res* **344**(2):251–260, 2011.
- Kaneko R, Akita H, Shimauchi H, Sasano Y. Immunohistochemical localization of the STRO-1 antigen in developing rat teeth by light microscopy and electron microscopy. *J Electron Microscop (Tokyo)* **58**(6):363–373, 2009.
- Karamouzis MV, Konstantinopoulos PA, Papavassiliou AG. The activator protein-1 transcription factor in respiratory epithelium carcinogenesis. *Mol Cancer Res* **5**(2):109–120, 2007.
- Kearns AE, Khosla S, Kostenuik PJ. Receptor activator of nuclear factor kappaB ligand and osteoprotegerin regulation of bone remodeling in health and disease. *Endocr Rev* **29**(2):155–192, 2008.
- Keffer J, Probert L, Cazlaris H, Georgopoulos S, Kaslaris E, Kioussis D, Kollias G. Transgenic mice expressing human tumour necrosis factor: a predictive genetic model of arthritis. *EMBO J* **10**(13):4025–31, 1991.
- Kelly KA, Gimble JM. 1,25-Dihydroxy vitamin D3 inhibits adipocyte differentiation and gene expression in murine bone marrow stromal cell clones and primary cultures. *Endocrinology* **139**(5):2622–2628, 1998.
- Kim HH, Lee DE, Shin JN, Lee YS, Jeon YM, Chung CH, Ni J, Kwon BS, Lee ZH. Receptor activator of NF-kappaB recruits multiple TRAF family adaptors and activates c-Jun N-terminal kinase. *FEBS Lett* **443**(3):297–302, 1999.
- Kirton JP, Wilkinson FL, Canfield AE, Alexander MY. Dexamethasone downregulates calcification-inhibitor molecules and accelerates osteogenic differentiation of vascular pericytes: implications for vascular calcification. *Circ Res* **98**(10):1264–72, 2006.
- Kitaura H, Sands MS, Aya K, Zhou P, Hirayama T, Uthgenannt B, Wei S, Takeshita S, Novack DV, Silva MJ, Abu-Amer Y, Ross FP, Teitelbaum SL. Marrow stromal cells and osteoclast precursors differentially contribute to TNF-alpha-induced osteoclastogenesis in vivo. *J Immunol* **173**(8):4838–46, 2004.
- Komori T. Regulation of bone development and extracellular matrix protein genes by RUNX2. *Cell Tissue Res* **339**(1):189–95, 2010.
- Kong YY, Yoshida H, Sarosi I, Tan HL, Timms E, Capparelli C, Morony S, Oliveira-dos Santos AJ, Van G, Itie A, Khoo W, Wakeham A, Dunstan CR, Lacey DL, Mak TW, Boyle WJ, Penninger JM. OPGL is a key regulator of osteoclastogenesis, lymphocyte development and lymph-node organogenesis. *Nature* **397**(6717):315–23, 1999.
- Krens SFG, Spaink HP, Snaar-Jagalska BE. Functions of the MAPK family in vertebrate-development. *FEBS Lett* **580**(21):4984–4990, 2006.
- Kroeze RJ, Knippenberg M, Helder MN. Osteogenic differentiation strategies for adipose-derived mesenchymal stem cells. *Methods Mol Biol* **702**:233–248, 2011.
- Lacey DC, Simmons PJ, Graves SE, Hamilton JA. Proinflammatory cytokines inhibit osteogenic differentiation from stem cells: implications for bone repair during inflammation. *Osteoarthritis Cartilage* **17**(6):735–42, 2009.
- Lehmann JM, Lenhard JM, Oliver BB, Ringold GM, Kliewer SA. Peroxisome proliferator-activated receptors alpha and gamma are activated by indomethacin and other non-steroidal anti-inflammatory drugs. *J Biol Chem* **272**(6):3406–3410, 1997.
- Lencel P, Delplace S, Hardouin P, Magne D. TNF-alpha stimulates alkaline phosphatase and mineralization through PPARgamma inhibition in human osteoblasts. *Bone* **48**(2):242–249, 2011.
- Li B, Shi M, Li J, Zhang H, Chen B, Chen L, Gao W, Giuliani N, Zhao RC. Elevated tumor necrosis factor-alpha suppresses TAZ expression and impairs osteogenic potential of Flk-1+ mesenchymal stem cells in patients with multiple myeloma. *Stem Cells Dev* **16**(6):921–30, 2007.
- Lindroos B, Suuronen R, Miettinen S. The potential of adipose stem cells in regenerative medicine. *Stem Cell Rev* **7**(2):269–291, 2011.
- Liu D, He X, Wang K, He C, Shi H, Jian L. Biocompatible silica nanoparticles-insulin conjugates for mesenchymal stem cell adipogenic differentiation. *Bioconjug Chem* **21**(9):1673–1684, 2010.

- Lodish H, Berk A, Zipursky SL, Matsudaira P, Baltimore D, Darnell J, National Center for Biotechnology Information (US). *Molecular Cell Biology* (W. H. Freeman and Company), 4th edn., 1999.
- Lu X, Farmer P, Rubin J, Nanes MS. Integration of the NfκB p65 subunit into the vitamin D receptor transcriptional complex: identification of p65 domains that inhibit 1,25-dihydroxyvitamin D₃-stimulated transcription. *J Cell Biochem* **92**(4):833–48, 2004.
- Lukic IK, Grcevic D, Kovacic N, Katavic V, Ivcevic S, Kalajzic I, Marusic A. Alteration of newly induced endochondral bone formation in adult mice without tumour necrosis factor receptor 1. *Clin Exp Immunol* **139**(2):236–44, 2005.
- Lund P, Pilgaard L, Duroux M, Fink T, Zachar V. Effect of growth media and serum replacements on the proliferation and differentiation of adipose-derived stem cells. *Cytotherapy* **11**(2):189–97, 2009.
- MacEwan DJ. TNF receptor subtype signalling: differences and cellular consequences. *Cell Signal* **14**(6):477–92, 2002.
- Mahoney DJ, Mikecz K, Ali T, Mabileau G, Benayahu D, Plaas A, Milner CM, Day AJ, Sabokbar A. TSG-6 regulates bone remodeling through inhibition of osteoblastogenesis and osteoclast activation. *J Biol Chem* **283**(38):25,952–62, 2008.
- Mahoney DJ, Swales C, Athanasou NA, Bombardieri M, Pitzalis C, Kliskey K, Sharif M, Day AJ, Milner CM, Sabokbar A. TSG-6 inhibits osteoclast activity via an autocrine mechanism and is functionally synergistic with osteoprotegerin. *Arthritis Rheum* **63**(4):1034–1043, 2011.
- Mak W, Shao X, Dunstan CR, Seibel MJ, Zhou H. Biphasic glucocorticoid-dependent regulation of Wnt expression and its inhibitors in mature osteoblastic cells. *Calcif Tissue Int* **85**(6):538–45, 2009.
- Mansell PW, Ichinose H, Reed RJ, Kremenz ET, McNamee R, Luzio NRD. Macrophage-mediated destruction of human malignant cells in vivo. *J Natl Cancer Inst* **54**(3):571–580, 1975.
- Mathas S, Hinz M, Anagnostopoulos I, Krappmann D, Lietz A, Jundt F, Bommert K, Mehta-Grigoriou F, Stein H, Dörken B, Scheidereit C. Aberrantly expressed c-Jun and JunB are a hallmark of Hodgkin lymphoma cells, stimulate proliferation and synergize with NF-κB. *EMBO J* **21**(15):4104–4113, 2002.
- Matsuguchi T, Chiba N, Bandow K, Kakimoto K, Masuda A, Ohnishi T. JNK activity is essential for Atf4 expression and late-stage osteoblast differentiation. *J Bone Miner Res* **24**(3):398–410, 2009.
- Matsumoto D, Shigeura T, Sato K, Inoue K, Suga H, Kato H, Aoi N, Murase S, Gonda K, Yoshimura K. Influences of preservation at various temperatures on liposuction aspirates. *Plast Reconstr Surg* **120**(6):1510–1517, 2007.
- McBeath R, Pirone DM, Nelson CM, Bhadriraju K, Chen CS. Cell shape, cytoskeletal tension, and RhoA regulate stem cell lineage commitment. *Dev Cell* **6**(4):483–495, 2004.
- McConnell MJ, Chevallier N, Berkofsky-Fessler W, Giltane JM, Malani RB, Staudt LM, Licht JD. Growth suppression by acute promyelocytic leukemia-associated protein PLZF is mediated by repression of c-myc expression. *Mol Cell Biol* **23**(24):9375–88, 2003.
- Millan J, Cain RJ, Reglero-Real N, Bigarella C, Marcos-Ramiro B, Fernandez-Martin L, Correas I, Ridley AJ. Adherens junctions connect stress fibres between adjacent endothelial cells. *BMC Biol* **8**:11, 2010.
- Milner CM, Day AJ. TSG-6: a multifunctional protein associated with inflammation. *J Cell Sci* **116**(Pt 10):1863–73, 2003.
- Montalibet J, Skorey KI, Kennedy BP. Protein tyrosine phosphatase: enzymatic assays. *Methods* **35**(1):2–8, 2005.
- Moorehead WR, Biggs HG. 2-Amino-2-methyl-1-propanol as the alkalizing agent in an improved continuous-flow cresolphthalein complexone procedure for calcium in serum. *Clin Chem* **20**(11):1458–1460, 1974.
- Morin LG. Direct colorimetric determination of serum calcium with o-cresolphthalein complexon. *Am J Clin Pathol* **61**(1):114–117, 1974.
- Mountziaris PM, Tzouanas SN, Mikos AG. Dose effect of tumor necrosis factor-α on in vitro osteogenic differentiation of mesenchymal stem cells on biodegradable polymeric microfiber scaffolds. *Biomaterials* **31**(7):1666–75, 2010.
- Mukai T, Otsuka F, Otani H, Yamashita M, Takasugi K, Inagaki K, Yamamura M, Makino H. TNF-α inhibits BMP-induced osteoblast differentiation through activating SAPK/JNK signaling. *Biochem Biophys Res Commun* **356**(4):1004–10, 2007.
- Munday K. Vitamin C and bone markers: investigations in a Gambian population. *Proc Nutr Soc* **62**(2):429–36, 2003.
- Murata H, Tanaka H, Taguchi T, Shiigi E, Mizokami H, Sugiyama T, Kawai S. Dexamethasone induces human spinal ligament derived cells toward osteogenic differentiation. *J Cell Biochem* **92**(4):715–722, 2004.

- Myllyharju J. Prolyl 4-hydroxylases, key enzymes in the synthesis of collagens and regulation of the response to hypoxia, and their roles as treatment targets. *Ann Med* **40**:1–16, 2008.
- Nadra I, Mason JC, Philippidis P, Florey O, Smythe CDW, McCarthy GM, Landis RC, Haskard DO. Proinflammatory activation of macrophages by basic calcium phosphate crystals via protein kinase C and MAP kinase pathways: a vicious cycle of inflammation and arterial calcification? *Circ Res* **96**(12):1248–1256, 2005.
- Nakase T, Takaoka K, Masuhara K, Shimizu K, Yoshikawa H, Ochi T. Interleukin-1 beta enhances and tumor necrosis factor-alpha inhibits bone morphogenetic protein-2-induced alkaline phosphatase activity in MC3T3-E1 osteoblastic cells. *Bone* **21**(1):17–21, 1997.
- Nanes MS. Tumor necrosis factor-alpha: molecular and cellular mechanisms in skeletal pathology. *Gene* **321**:1–15, 2003.
- Nasir J, Speirs V. Rapid and irreversible loss of estrogen receptor in human osteoblast-like cells following culture in phenol red-free medium. *In Vitro Cell Dev Biol Anim* **33**(4):240–2, 1997.
- Natsume H, Tokuda H, Adachi S, Matsushima-Nishiwaki R, Kato K, Minamitani C, Otsuka T, Kozawa O. Wnt3a regulates tumor necrosis factor-alpha-stimulated interleukin-6 release in osteoblasts. *Mol Cell Endocrinol* **331**(1):66–72, 2011.
- Naumann M, Scheidereit C. Activation of NF-kappa B in vivo is regulated by multiple phosphorylations. *EMBO J* **13**(19):4597–607, 1994.
- Noble M, Mayer-Proeschel M, Proeschel C. Redox regulation of precursor cell function: insights and paradoxes. *Antioxid Redox Signal* **7**(11-12):1456–1467, 2005.
- Noble M, Smith J, Power J, Mayer-Proeschel M. Redox state as a central modulator of precursor cell function. *Ann N Y Acad Sci* **991**:251–271, 2003.
- Noeske K. [The binding of crystal violet on deoxyribonucleic acid. Cytophotometric studies on normal and tumor cell nuclei]. *Histochemie* **7**(3):273–287, 1966.
- Novack DV. Role of NF- κ B in the skeleton. *Cell Res* **21**(1):169–182, 2011.
- Oeckinghaus A, Ghosh S. The NF-kappaB family of transcription factors and its regulation. *Cold Spring Harb Perspect Biol* **1**(4):a000,034, 2009.
- Oedayrajsingh-Varma MJ, van Ham SM, Knippenberg M, Helder MN, Klein-Nulend J, Schouten TE, Ritt MJ, van Milligen FJ. Adipose tissue-derived mesenchymal stem cell yield and growth characteristics are affected by the tissue-harvesting procedure. *Cytotherapy* **8**(2):166–77, 2006.
- Office of the Surgeon General (US). *Bone Health and Osteoporosis* (National Center for Biotechnology Information (U.S.)), 1st edn., 2004.
- Ogasawara MA, Zhang H. Redox regulation and its emerging roles in stem cells and stem-like cancer cells. *Antioxid Redox Signal* **11**(5):1107–1122, 2009.
- Orimo H, Shimada T. The role of tissue-nonspecific alkaline phosphatase in the phosphate-induced activation of alkaline phosphatase and mineralization in SaOS-2 human osteoblast-like cells. *Mol Cell Biochem* **315**(1-2):51–60, 2008.
- Otto F, Kanegane H, Mundlos S. Mutations in the RUNX2 gene in patients with cleidocranial dysplasia. *Hum Mutat* **19**(3):209–16, 2002.
- Park JB. The Effects of Dexamethasone, Ascorbic Acid, and Beta-Glycerophosphate on Osteoblastic Differentiation by Regulating Estrogen Receptor and Osteopontin Expression. *J Surg Res* 2010.
- Parrado A, Robledo M, Moya-Quiles MR, Marin LA, Chomienne C, Padua RA, Alvarez-Lopez MR. The promyelocytic leukemia zinc finger protein down-regulates apoptosis and expression of the proapoptotic BID protein in lymphocytes. *Proc Natl Acad Sci U S A* **101**(7):1898–903, 2004.
- Pennica D, Nedwin GE, Hayflick JS, Seeburg PH, Derynck R, Palladino MA, Kohr WJ, Aggarwal BB, Goeddel DV. Human tumour necrosis factor: precursor structure, expression and homology to lymphotoxin. *Nature* **312**(5996):724–9, 1984.
- Peters K, Unger RE, Stumpf S, Schafer J, Tsaryk R, Hoffmann B, Eisenbarth E, Breme J, Ziegler G, Kirkpatrick CJ. Cell type-specific aspects in biocompatibility testing: the intercellular contact in vitro as an indicator for endothelial cell compatibility. *J Mater Sci Mater Med* **19**(4):1637–44, 2008.
- Petrescu F, Voican SC, Silosi I. Tumor necrosis factor-alpha serum levels in healthy smokers and nonsmokers. *Int J Chron Obstruct Pulmon Dis* **5**:217–222, 2010.

- Pietilae M, Palomaeki S, Lehtonen S, Ritamo I, Valmu L, Nystedt J, Laitinen S, Leskelae HV, Sormunen R, Pesaelae J, Nordstroem K, Vepsaelaeinen A, Lehenkari P. Mitochondrial function and energy metabolism in umbilical cord blood- and bone marrow-derived mesenchymal stem cells. *Stem Cells Dev* 2011.
- Potdar PD, D'Souza SB. Ascorbic acid induces in vitro proliferation of human subcutaneous adipose tissue derived mesenchymal stem cells with upregulation of embryonic stem cell pluripotency markers Oct4 and SOX 2. *Hum Cell* **23(4)**:152–5, 2010.
- Pradel W, Mai R, Gedrange T, Lauer G. Cell passage and composition of culture medium effects proliferation and differentiation of human osteoblast-like cells from facial bone. *J Physiol Pharmacol* **59 Suppl 5**:47–58, 2008.
- Promega. *CellTiter 96 Aqueous One Solution Cell Proliferation Assay*, 6/09 edn., 2009.
- Proudfoot D, Skepper JN, Hegyi L, Bennett MR, Shanahan CM, Weissberg PL. Apoptosis regulates human vascular calcification in vitro: evidence for initiation of vascular calcification by apoptotic bodies. *Circ Res* **87(11)**:1055–1062, 2000.
- Pruitt KD, Tatusova T, Klimke W, Maglott DR. NCBI Reference Sequences: current status, policy and new initiatives. *Nucleic Acids Res* **37(Database issue)**:D32–D36, 2009.
- QIAGEN. *QuantiTect Reverse Transcription Handbook*, 04/2005 edn., 2005.
- Rajgopal A, Young DW, Mujeeb KA, Stein JL, Lian JB, van Wijnen AJ, Stein GS. Mitotic control of RUNX2 phosphorylation by both CDK1/cyclin B kinase and PP1/PP2A phosphatase in osteoblastic cells. *J Cell Biochem* **100(6)**:1509–17, 2007.
- Raman M, Chen W, Cobb MH. Differential regulation and properties of MAPKs. *Oncogene* **26(22)**:3100–3112, 2007.
- Ratajczak MZ, Zuba-Surma EK, Wysoczynski M, Wan W, Ratajczak J, Wojakowski W, Kucia M. Hunt for pluripotent stem cell – regenerative medicine search for almighty cell. *J Autoimmun* **30(3)**:151–162, 2008.
- Rehman J. Empowering self-renewal and differentiation: the role of mitochondria in stem cells. *J Mol Med* **88(10)**:981–986, 2010.
- Reid A, Gould A, Brand N, Cook M, Strutt P, Li J, Licht J, Waxman S, Krumlauf R, Zelent A. Leukemia translocation gene, PLZF, is expressed with a speckled nuclear pattern in early hematopoietic progenitors. *Blood* **86(12)**:4544–52, 1995.
- Reuther T, Kettmann C, Scheer M, Kochel M, Iida S, Kubler AC. Cryopreservation of osteoblast-like cells: viability and differentiation with replacement of fetal bovine serum in vitro. *Cells Tissues Organs* **183(1)**:32–40, 2006.
- Roberta AP, Bird TD, Dolan CR, Stephens K. *GeneReviews [Internet]* (National Center for Biotechnology Information (U.S.) and University of Washington (Seattle)), 1st edn., 1993 - 2011.
- Roche Diagnostics. *CASY Model TT - Cell Counter and Analyzer*, 2010.
- Romas E, Gillespie MT, Martin TJ. Involvement of receptor activator of NFkappaB ligand and tumor necrosis factor-alpha in bone destruction in rheumatoid arthritis. *Bone* **30(2)**:340–6, 2002.
- Rosa AL, Beloti MM. Development of the osteoblast phenotype of serial cell subcultures from human bone marrow. *Braz Dent J* **16(3)**:225–30, 2005.
- Roura S, Farre J, Soler-Botija C, Llach A, Hove-Madsen L, Cairo JJ, Godia F, Cinca J, Bayes-Genis A. Effect of aging on the pluripotential capacity of human CD105+ mesenchymal stem cells. *Eur J Heart Fail* **8(6)**:555–563, 2006.
- Rozen S, Skaletsky H. Primer3 on the WWW for general users and for biologist programmers. *Methods Mol Biol* **132**:365–386, 2000.
- SABiosciences. Pathway Central. Website, 2011.
- Safranow K, Dziedziczko V, Rzeuski R, Czyzycka E, Wojtarowicz A, Binczak-Kuleta A, Jakubowska K, Olszewska M, Ciechanowicz A, Kornacewicz-Jach Z, Machalinski B, Pawlik A, Chlubek D. Plasma concentrations of TNF-alpha and its soluble receptors sTNFR1 and sTNFR2 in patients with coronary artery disease. *Tissue Antigens* **74(5)**:386–92, 2009.
- Saidenberg-Kermanac'h N, Corrado A, Lemeiter D, deVernejoul MC, Boissier MC, Cohen-Solal ME. TNF-alpha antibodies and osteoprotegerin decrease systemic bone loss associated with inflammation through distinct mechanisms in collagen-induced arthritis. *Bone* **35(5)**:1200–1207, 2004.
- Saksida A, Wraber B, Avsic-Zupanc T. Serum levels of inflammatory and regulatory cytokines in patients with hemorrhagic fever with renal syndrome. *BMC Infect Dis* **11(1)**:142, 2011.
- Sanggaard KW, Sonne-Schmidt CS, Krogager TP, Kristensen T, Wisniewski HG, Thogersen IB, Enghild JJ. TSG-6 transfers proteins between glycosaminoglycans via a Ser28-mediated covalent catalytic mechanism. *J Biol Chem* **283(49)**:33,919–26, 2008.

- Santee SM, Owen-Schaub LB. Human tumor necrosis factor receptor p75/80 (CD120b) gene structure and promoter characterization. *J Biol Chem* **271**(35):21,151–9, 1996.
- Sarkar BC, Chauhan UP. A new method for determining micro quantities of calcium in biological materials. *Anal Biochem* **20**(1):155–166, 1967.
- Sato N, Goto T, Haranaka K, Satomi N, Nariuchi H, Mano-Hirano Y, Sawasaki Y. Actions of tumor necrosis factor on cultured vascular endothelial cells: morphologic modulation, growth inhibition, and cytotoxicity. *J Natl Cancer Inst* **76**(6):1113–21, 1986.
- Shao JS, Cai J, Towler DA. Molecular mechanisms of vascular calcification: lessons learned from the aorta. *Arterioscler Thromb Vasc Biol* **26**(7):1423–1430, 2006.
- Shao JS, Cheng SL, Pingsterhaus JM, Charlton-Kachigian N, Loewy AP, Towler DA. Msx2 promotes cardiovascular calcification by activating paracrine Wnt signals. *J Clin Invest* **115**(5):1210–20, 2005.
- Shen R, Chen M, Wang YJ, Kaneki H, Xing L, O'Keefe R J, Chen D. Smad6 interacts with Runx2 and mediates Smad ubiquitin regulatory factor 1-induced Runx2 degradation. *J Biol Chem* **281**(6):3569–76, 2006.
- Shi J, Vogt PK. Posttranslational regulation of Myc by promyelocytic leukemia zinc finger protein. *Int J Cancer* **125**(7):1558–65, 2009.
- Shui C, Spelsberg TC, Riggs BL, Khosla S. Changes in Runx2/Cbfa1 expression and activity during osteoblastic differentiation of human bone marrow stromal cells. *J Bone Miner Res* **18**(2):213–21, 2003.
- Sigma-Aldrich. *BioFiles* (Sigma-Aldrich), 2008.
- Simonet WS, Lacey DL, Dunstan CR, Kelley M, Chang MS, Lacey R, Nguyen HQ, Wooden S, Bennett L, Boone T, Shimamoto G, DeRose M, Elliott R, Colombero A, Tan HL, Trail G, Sullivan J, Davy E, Bucay N, Renshaw-Gegg L, Hughes TM, Hill D, Pattison W, Campbell P, Sander S, Van G, Tarpley J, Derby P, Lee R, Boyle WJ. Osteoprotegerin: a novel secreted protein involved in the regulation of bone density. *Cell* **89**(2):309–319, 1997.
- Smith PJ, Wise LS, Berkowitz R, Wan C, Rubin CS. Insulin-like growth factor-I is an essential regulator of the differentiation of 3T3-L1 adipocytes. *J Biol Chem* **263**(19):9402–9408, 1988.
- Song IH, Caplan AI, Dennis JE. In vitro dexamethasone pretreatment enhances bone formation of human mesenchymal stem cells in vivo. *J Orthop Res* **27**(7):916–21, 2009.
- Sorisky A. From preadipocyte to adipocyte: differentiation-directed signals of insulin from the cell surface to the nucleus. *Crit Rev Clin Lab Sci* **36**(1):1–34, 1999.
- Spandl J, White DJ, Peychl J, Thiele C. Live cell multicolor imaging of lipid droplets with a new dye, LD540. *Traffic* **10**(11):1579–1584, 2009.
- Still K, Reading L, Scutt A. Effects of phenol red on CFU-f differentiation and formation. *Calcif Tissue Int* **73**(2):173–9, 2003.
- Talbot NC, Rexroad CE, Pursel VG, Powell AM. Alkaline phosphatase staining of pig and sheep epiblast cells in culture. *Mol Reprod Dev* **36**(2):139–147, 1993.
- Tat SK, Padrines M, Thammacharoen S, Heymann D, Fortun Y. IL-6, RANKL, TNF-alpha/IL-1: interrelations in bone resorption pathophysiology. *Cytokine Growth Factor Rev* **15**(1):49–60, 2004.
- Taylor PC. Anti-TNF therapy for rheumatoid arthritis and other inflammatory diseases. *Mol Biotechnol* **19**(2):153–168, 2001.
- Thomas CG, Vezyraki PE, Kalfakakou VP, Evangelou AM. Vitamin C transiently arrests cancer cell cycle progression in S phase and G2/M boundary by modulating the kinetics of activation and the subcellular localization of Cdc25C phosphatase. *J Cell Physiol* **205**(2):310–318, 2005.
- Thomas DM, Johnson SA, Sims NA, Trivett MK, Slavin JL, Rubin BP, Waring P, McArthur GA, Walkley CR, Holloway AJ, Diyagama D, Grim JE, Clurman BE, Bowtell DD, Lee JS, Gutierrez GM, Piscopo DM, Carty SA, Hinds PW. Terminal osteoblast differentiation, mediated by runx2 and p27KIP1, is disrupted in osteosarcoma. *J Cell Biol* **167**(5):925–34, 2004.
- Traktuev DO, Merfeld-Clauss S, Li J, Kolonin M, Arap W, Pasqualini R, Johnstone BH, March KL. A population of multipotent CD34-positive adipose stromal cells share pericyte and mesenchymal surface markers, reside in a periendothelial location, and stabilize endothelial networks. *Circ Res* **102**(1):77–85, 2008.
- Tsuboi M, Kawakami A, Nakashima T, Matsuoka N, Urayama S, Kawabe Y, Fujiyama K, Kiriya T, Aoyagi T, Maeda K, Eguchi K. Tumor necrosis factor-alpha and interleukin-1beta increase the Fas-mediated apoptosis of human osteoblasts. *J Lab Clin Med* **134**(3):222–31, 1999.

- Tsukahara S, Ikeda R, Goto S, Yoshida K, Mitsumori R, Sakamoto Y, Tajima A, Yokoyama T, Toh S, Furukawa K, Inoue I. Tumour necrosis factor alpha-stimulated gene-6 inhibits osteoblastic differentiation of human mesenchymal stem cells induced by osteogenic differentiation medium and BMP-2. *Biochem J* **398**(3):595–603, 2006.
- Udagawa N, Takahashi N, Akatsu T, Tanaka H, Sasaki T, Nishihara T, Koga T, Martin TJ, Suda T. Origin of osteoclasts: mature monocytes and macrophages are capable of differentiating into osteoclasts under a suitable microenvironment prepared by bone marrow-derived stromal cells. *Proc Natl Acad Sci U S A* **87**(18):7260–4, 1990.
- van Kooten TG, Klein CL, Wagner M, Kirkpatrick CJ. Focal adhesions and assessment of cytotoxicity. *J Biomed Mater Res* **46**(1):33–43, 1999.
- Varelas X, Sakuma R, Samavarchi-Tehrani P, Peerani R, Rao BM, Dembowy J, Yaffe MB, Zandstra PW, Wrana JL. TAZ controls Smad nucleocytoplasmic shuttling and regulates human embryonic stem-cell self-renewal. *Nat Cell Biol* **10**(7):837–48, 2008.
- Varfolomeev E, Vucic D. (Un)expected roles of c-IAPs in apoptotic and NFkappaB signaling pathways. *Cell Cycle* **7**(11):1511–21, 2008.
- Varki A, Cummings R, Esko J, Freeze H, Hart G, Marth J, National Center for Biotechnology Information (US). *Essentials of Glycobiology* (Cold Spring Harbor Laboratory Press), 2nd edn., 2009.
- Varum S, Rodrigues AS, Moura MB, Momcilovic O, Easley CA, Ramalho-Santos J, Houten BV, Schatten G. Energy metabolism in human pluripotent stem cells and their differentiated counterparts. *PLoS One* **6**(6):e20,914, 2011.
- Vasilopoulos Y, Gkretsi V, Armaka M, Aidinis V, Kollias G. Actin cytoskeleton dynamics linked to synovial fibroblast activation as a novel pathogenic principle in TNF-driven arthritis. *Ann Rheum Dis* **66** Suppl 3:iii23–8, 2007.
- Vernet D, Nolazco G, Cantini L, Magee TR, Qian A, Rajfer J, Gonzalez-Cadavid NF. Evidence that osteogenic progenitor cells in the human tunica albuginea may originate from stem cells: implications for peyronie disease. *Biol Reprod* **73**(6):1199–210, 2005.
- Viereck V, Siggelkow H, Tauber S, Raddatz D, Schutze N, Hufner M. Differential regulation of Cbfa1/Runx2 and osteocalcin gene expression by vitamin-D3, dexamethasone, and local growth factors in primary human osteoblasts. *J Cell Biochem* **86**(2):348–56, 2002.
- Vincent C, Findlay DM, Welldon KJ, Wijenayaka AR, Zheng TS, Haynes DR, Fazzalari NL, Evdokiou A, Atkins GJ. Pro-inflammatory cytokines TNF-related weak inducer of apoptosis (TWEAK) and TNFalpha induce the mitogen-activated protein kinase (MAPK)-dependent expression of sclerostin in human osteoblasts. *J Bone Miner Res* **24**(8):1434–1449, 2009.
- Voller A, Bidwell DE, Bartlett A. Enzyme immunoassays in diagnostic medicine. Theory and practice. *Bull World Health Organ* **53**(1):55–65, 1976.
- Wagner EF. Functions of AP1 (Fos/Jun) in bone development. *Ann Rheum Dis* **61** Suppl 2:ii40–ii42, 2002.
- Wagner EF, Nebreda AR. Signal integration by JNK and p38 MAPK pathways in cancer development. *Nat Rev Cancer* **9**(8):537–549, 2009.
- Wajant H, Scheurich P. TNFR1-induced activation of the classical NF- κ B pathway. *FEBS J* **278**(6):862–876, 2011.
- Walsh S, Jordan GR, Jefferiss C, Stewart K, Beresford JN. High concentrations of dexamethasone suppress the proliferation but not the differentiation or further maturation of human osteoblast precursors in vitro: relevance to glucocorticoid-induced osteoporosis. *Rheumatology (Oxford)* **40**(1):74–83, 2001.
- Wang Y, Singh A, Xu P, Pindrus MA, Blasioli DJ, Kaplan DL. Expansion and osteogenic differentiation of bone marrow-derived mesenchymal stem cells on a vitamin C functionalized polymer. *Biomaterials* **27**(17):3265–3273, 2006.
- Watson JV, Chambers SH, Smith PJ. A pragmatic approach to the analysis of DNA histograms with a definable G1 peak. *Cytometry* **8**(1):1–8, 1987.
- Weng LH, Wang CJ, Ko JY, Sun YC, Su YS, Wang FS. Inflammation induction of Dickkopf-1 mediates chondrocyte apoptosis in osteoarthritic joint. *Osteoarthritis Cartilage* **17**(7):933–43, 2009.
- Wheeler DL, Barrett T, Benson DA, Bryant SH, Canese K, Church DM, DiCuccio M, Edgar R, Federhen S, Helmberg W, Kenton DL, Khovayko O, Lipman DJ, Madden TL, Maglott DR, Ostell J, Pontius JU, Pruitt KD, Schuler GD, Schriml LM, Sequeira E, Sherry ST, Sirotkin K, Starchenko G, Suzek TO, Tatusov R, Tatusova TA, Wagner L, Yaschenko E. Database resources of the National Center for Biotechnology Information. *Nucleic Acids Res* **33**(Database issue):D39–45, 2005.
- Wikipedia. Metabolism. Website, 2011.
- Wong BR, Josien R, Choi Y. TRANCE is a TNF family member that regulates dendritic cell and osteoclast function. *J Leukoc Biol* **65**(6):715–24, 1999.

- Wright HL, McCarthy HS, Middleton J, Marshall MJ. RANK, RANKL and osteoprotegerin in bone biology and disease. *Curr Rev Musculoskelet Med* **2**(1):56–64, 2009.
- Wu L, Cai X, Dong H, Jing W, Huang Y, Yang X, Wu Y, Lin Y. Serum regulates adipogenesis of mesenchymal stem cells via MEK/ERK-dependent PPARgamma expression and phosphorylation. *J Cell Mol Med* **14**(4):922–932, 2010.
- Wu Z, Xie Y, Bucher NL, Farmer SR. Conditional ectopic expression of C/EBP beta in NIH-3T3 cells induces PPAR gamma and stimulates adipogenesis. *Genes Dev* **9**(19):2350–2363, 1995.
- Xu P, Derynck R. Direct activation of TACE-mediated ectodomain shedding by p38 MAP kinase regulates EGF receptor-dependent cell proliferation. *Mol Cell* **37**(4):551–566, 2010.
- Yanes O, Clark J, Wong DM, Patti GJ, Sanchez-Ruiz A, Benton HP, Trauger SA, Despons C, Ding S, Siuzdak G. Metabolic oxidation regulates embryonic stem cell differentiation. *Nat Chem Biol* **6**(6):411–7, 2010.
- Yokoyama M, Miwa H, Maeda S, Wakitani S, Takagi M. Influence of fetal calf serum on differentiation of mesenchymal stem cells to chondrocytes during expansion. *J Biosci Bioeng* **106**(1):46–50, 2008.
- Young DW, Hassan MQ, Yang XQ, Galindo M, Javed A, Zaidi SK, Furcinitti P, Lapointe D, Montecino M, Lian JB, Stein JL, van Wijnen AJ, Stein GS. Mitotic retention of gene expression patterns by the cell fate-determining transcription factor Runx2. *Proc Natl Acad Sci U S A* **104**(9):3189–94, 2007.
- Yuan JS, Reed A, Chen F, Stewart J C N. Statistical analysis of real-time PCR data. *BMC Bioinformatics* **7**:85, 2006.
- Zhao L, Huang J, Zhang H, Wang Y, Matesic LE, Takahata M, Awad H, Chen D, Xing L. Tumor necrosis factor inhibits mesenchymal stem cell differentiation into osteoblasts via the ubiquitin E3 ligase Wwp1. *Stem Cells* **29**(10):1601–1610, 2011.
- Zhu H, Jiang XX, Guo ZK, Li H, Su YF, Yao HY, Wang XY, Li XS, Wu Y, Liu YL, Zhang Y, Mao N. Tumor necrosis factor-alpha alters the modulatory effects of mesenchymal stem cells on osteoclast formation and function. *Stem Cells Dev* **18**(10):1473–1484, 2009.
- Zuk P, Chou YF, Mussano F, Benhaim P, Wu BM. Adipose-derived stem cells and BMP2: part 2. BMP2 may not influence the osteogenic fate of human adipose-derived stem cells. *Connect Tissue Res* **52**(2):119–132, 2011.
- Zuk PA, Zhu M, Ashjian P, De Ugarte DA, Huang JI, Mizuno H, Alfonso ZC, Fraser JK, Benhaim P, Hedrick MH. Human adipose tissue is a source of multipotent stem cells. *Mol Biol Cell* **13**(12):4279–95, 2002.
- Zuk PA, Zhu M, Mizuno H, Huang J, Futrell JW, Katz AJ, Benhaim P, Lorenz HP, Hedrick MH. Multilineage cells from human adipose tissue: implications for cell-based therapies. *Tissue Eng* **7**(2):211–28, 2001.

Selbstständigkeitserklärung

Ich versichere hiermit an Eides statt, dass ich die vorliegende Arbeit selbstständig angefertigt und ohne fremde Hilfe verfasst habe. Dazu habe ich keine außer den von mir angegebenen Hilfsmitteln und Quellen verwendet, und die den benutzten Werken inhaltlich oder wörtlich entnommenen Stellen habe ich als solche kenntlich gemacht.

Rostock, den 02.03.2012

Achim Salamon

Curriculum Vitae

Personal Information

Name, First Name SALAMON, Achim
E-Mail achim.salamon@med.uni-rostock.de
Citizenship German
Date and Place of Birth 26.07.1979 in Berlin-Neukölln

Professional Experience

since November 2006
Research Fellow at Rostock University Medical Center, Department of Cell Biology, Schillingallee 69, D-18057 Rostock
Topic of PhD Thesis: *The Impact of Tumor Necrosis Factor on Osteogenic Differentiation of Human Adipose Tissue-Derived Stem Cells In Vitro*
Graduation *magna cum laude* as *Doctor rerum naturalium* (ISCED Level 6)

Vocational Education

October 2000 to November 2006
Academic Studies of Medical Biotechnology at the Technische Universität Berlin, Straße des 17. Juni 135, D-10623 Berlin
Diploma Thesis at the Max Planck Institute of Molecular Genetics, Department of Human Molecular Genetics, Ihnestraße 63-73, D-14195 Berlin
Topic of Diploma Thesis: *Functional Aspects of a Mutation in the PLP2 Promoter Region of Patients with Non-Syndromic X-Linked Mental Retardation*
Graduation with distinction as *Diplom-Ingenieur* (ISCED Level 5)

Additional Information

Scientific Publications
Peters K, Prinz C, **Salamon A**, Rychly J, Neumann HG. In vitro evaluation of cytocompatibility of shellac as coating for intravascular devices. *Trends Biomater Artif Organs* 26(2):110-113 (2012)

Jonitz A, Lochner K, Peters K, **Salamon A**, Pasold J, Mueller-Hilke B, Hansmann D, Bader R. Differentiation capacity of human chondrocytes embedded in alginate matrix. *Connect Tissue Res* 52(6):503-511 (2011)

Salamon A, Adam S, Neumann HG, Rychly J, Peters K. Changed expression of stem cell markers and cadherins in differentiation of adipose tissue-derived stem cells in vitro. *Hum Gene Ther* 20(11):1492 (2009)

Peters K, **Salamon A**, van Vlierberghe S, Rychly J, Neumann HG, Schacht E, Dubrue P. A new approach for adipose tissue regeneration based on human mesenchymal stem cells and hydrogels - An in vitro study. *Adv Eng Mater* 11(10):B155-B161 (2009)

Peters K, Kamp G, Berz A, Unger RE, Barth S, **Salamon A**, Rychly J, Kirkpatrick CJ. Changes in human endothelial cell energy metabolic capacities during in vitro cultivation. The role of "aerobic glycolysis" and proliferation. *Cell Physiol Biochem* 24(5-6):483-492 (2009)

Talks on International Conferences

Jahrestagung der Deutschen Gesellschaft für Biomaterialien, 01.-03.11.2012, Hamburg (DE)

World Biomaterials Congress, 01.-05.06.2012, Chengdu (CN)

TERMIS-EU Chapter Meeting, 07.-10.06.2011, Granada (ES)

Jahrestagung der Deutschen Gesellschaft für Biomaterialien, 08.-10.10.2009, Tübingen (DE)

European Conference on Biomaterials, 07.-11.09.2009, Lausanne (CH)

TERMIS-EU Chapter Meeting, 04.-07.09.2007, London (UK)

Poster Presentations on International Conferences

Jahrestagung der Deutschen Gesellschaft für Biomaterialien, 01.-03.11.2012, Hamburg (DE)

International Symposium Interface Biology of Implants, 09.-11.05.2012, Rostock (DE)

Jahrestagung der Deutschen Gesellschaft für Biomaterialien, 10.-12.11.2011, Giessen (DE)

Joint Meeting European Society of Microcirculation (ESM) and German Society of Microcirculation and Vascular Biology (GfMVB), 13.-16.10.2011, München (DE)

TERMIS-EU Chapter Meeting, 07.-10.06.2011, Granada (ES)

International Meeting of the Stem Cell Network North-Rhine Westphalia, 05.-06.04.2011, Essen (DE)

Jahrestagung der Deutschen Gesellschaft für Biomaterialien, 18.-20.11.2010, Heilbad Heiligenstadt (DE)

TERMIS-EU Chapter Meeting, 13.-17.06.2010, Galway (IE)

Jahrestagung der Deutschen Gesellschaft für Zellbiologie, 10.-13.03.2010, Regensburg (DE)

International Symposium Interface Biology of Implants, 13.-15.05.2009, Rostock (DE)

International Meeting of the Stem Cell Network North-Rhine Westphalia, 24.-25.03.2009, Aachen (DE)

Jahrestagung der Deutschen Gesellschaft für Biomaterialien, 20.-22.11.2008, Hamburg (DE)

Congress on Regenerative Biology and Medicine - BioStar, 09.-11.10.2008, Stuttgart (DE)

World Biomaterials Congress, 28.05.-01.06.2008, Amsterdam (NL)

Jahrestagung der Deutschen Gesellschaft für Zellbiologie, 12.-15.03.2008, Marburg (DE)

Jahrestagung der Deutschen Gesellschaft für Biomaterialien, 22.-24.11.2007, Hannover (DE)

International Meeting of the European Life Scientist Organization, 01.-04.09.2007, Dresden (DE)

Rostock, 19.11.2012

Achim Salamon

Danksagung

Abschließend muß ich mich bei einer Reihe von Menschen bedanken, die in unterschiedlicher Weise mit zur Entstehung dieser Arbeit beigetragen haben.

Mein wissenschaftlicher Dank gilt zuvörderlichst meiner Betreuerin Kirsten Peters, zum einen für die Bereitstellung des bearbeiteten Themas und die wissenschaftlichen Diskussionen im Zusammenhang mit diesem, insbesondere aber dafür, daß sie mir wiederholt die Möglichkeit eingeräumt hat, für das schmale Budget unserer Nachwuchsgruppe sehr teure Assays durchzuführen und an einer für Doktoranden weitaus überdurchschnittlichen Anzahl internationaler Kongresse teilzunehmen. Daß ich meine Arbeit trotz der desaströsen Forschungsförderung des Landes Mecklenburg-Vorpommern überhaupt beenden konnte, ist ihrem unentwegten und erfolgreichen Einwerben verschiedenster Drittmittel zu verdanken.

Bei Joachim Rychly möchte ich mich dafür bedanken, daß ich in seiner Abteilung für Zellbiologie meine Doktorarbeit anfertigen durfte und daß er außerordentliches Bemühen in das Halten seiner Mitarbeiter in finanziell unsicheren Zeiten investiert hat und nicht die in der Wissenschaft üblichen befristeten Arbeitsverträge unbeeindruckt den unausweichlichen Gang ihrer Dinge hat gehen lassen.

In diesem Zusammenhang gilt mein besonderer Dank auch Hans-Georg Neumann von der DOT GmbH, der, ohne daß er davon einen wirtschaftlich relevanten Vorteil gehabt hätte, durch mehrere Bürgschaften seiner Firma das Ausscheiden von fünf Mitarbeitern der Abteilung Zellbiologie, darunter auch ich, in die Arbeitslosigkeit verhindert und so den langen Zeitraum bis zur weit überfälligen Bewilligung des Syntero-Projektes durch das Wirtschaftsministerium überbrückt hat.

Ich muß mich bei Dieter Weiss für das bereitwillige Begutachten und für konstruktive Hinweise zu meiner Dissertation bedanken.

Bei Roland Lauster muß ich mich für die unkomplizierte und äußerst kurzentschlossene Zusage, als Gutachter der Dissertation zur Verfügung zu stehen, bedanken.

Mein Dank gilt auch Günter Kamp für das Lesen und die Hinweise zu den Ergebnissen und Überlegungen zum Energiestoffwechsel der Stammzellen.

Großer Dank gebührt Marcel Adler für sein ausdauerndes Korrekturlesen und seine sachverständigen Hinweise. Selbstredend möchte ich mich dabei auch bei Regina Arlt bedanken, die mit ihrer Geduld dieses erst ermöglicht hat und Marcel dabei sicherlich ein ganzes Stück weit von seinen umfangreichen Haushaltsdiensten wird haben freistellen müssen!

Bei Stefanie Adam möchte ich mich für ihre äußerst zuverlässige und engagierte Arbeit sowie ihre derben Frotzeleien und ausufernden Sarkasmus bedanken, die zum Charme der Arbeitsatmosphäre erheblich beigetragen haben.

Den Mitarbeitern der Abteilung Zellbiologie gilt mein Dank für die langjährige und angenehme Zusammenarbeit.

Jürgen Weber (und seinen Patientinnen) gilt größter Dank für die kontinuierliche Bereitstellung sterilen Liposuktionsgewebes, die Grundlage aller Arbeiten.

Mein besonderer Dank gilt meinem alten Freund Florian von Langsdorff, dafür, daß er durch den fruchtbaren Wechsel an die Hochschule Wismar die Voraussetzung für unzählige gesellige Abende geschaffen hat, aber auch für sein Angebot des Korrekturlesens der Dissertation, welches letztlich von der zu-Guttenbergschen Erkenntnis der Unvereinbarkeit von Beruf und Familie mit der Promotion torpediert wurde!

Bei meinem (noch weitaus älteren) Freund Christian von Langsdorff möchte ich mich für die zahlreichen und äußerst angenehmen Übernachtungsmöglichkeiten anlässlich von Kongressen und sonstigen Dienstreisen bedanken, die mich an Stätten führten, an denen er zufälligerweise seine chirurgische Kompetenz auf ein solides Fundament zu stellen trachtet(e).

So nicht oben schon geschehen, möchte ich mich noch bei meinen zahlreichen Freunden aus Rostock und Umgebung für die schöne gemeinsam verbrachte Zeit bedanken, darunter die Gestalten Tomas Fiedler, Enrico Eisert, Gregor Fiedler, Wiebke Demasius, Ellen Schmuhl, Jasmin Althaus, Marcus Waser, Dario Furlani, Evgenya Delyagina, Roman Tsaryk, Verena Benecke, Sandra Kern, Janine Wetzels, Juliane Meyer, Kristina Henschel, Susanne Thümecke, Frank Baudisch und Alexander Ustorp.

Bei meiner Familie möchte ich mich aufrichtig für die stete Unterstützung nicht nur während der Promotion, sondern auch schon während Schulzeit und Studium bedanken.

Schlußendlich möchte ich der Person, die als einzige der vorgenannten während der Zeit meiner Promotion ein Opfer bringen mußte, meinen allergrößten Dank aussprechen: meiner lieben Kathi! –, dafür, daß, obwohl Du von den zehn gemeinsamen Jahren fünf allein verbringen mußtest, Du mir all die Zeit die Treue gehalten hast, damit nun endlich das gemeinsame Leben beginnen kann!